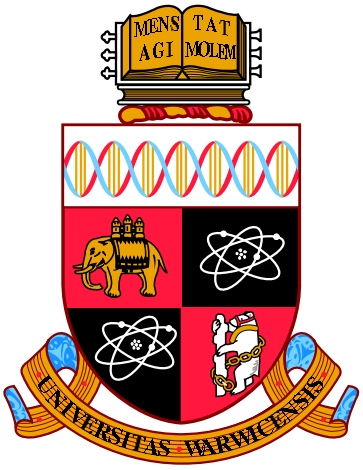

Analysis of Discontinuous Galerkin Methods on Surfaces

by

Pravin Madhavan

Thesis

Submitted to the University of Warwick

for the degree of

Doctor of Philosophy

Warwick Mathematics Institute

September 2014

THE UNIVERSITY OF WARWICK

Contents

List of Tables

List of Figures

Acknowledgments

First and foremost, I would like to thank my supervisor Dr Andreas Dedner and my co-supervisor Dr Björn Stinner for all their help and guidance during the writing of this thesis, as well as providing well-written lecture notes on finite element methods that have allowed me to quickly get to grips with the field. I am also grateful to Professor Charlie Elliott and Professor Christoph Ortner for their insights and advice on many problems I had. I would also like to thank the Engineering and Physical Sciences Research Council (EPSRC) for funding my position in MASDOC.

Last but not least, I would like to thank friends and family who have supported me throughout my PhD. In particular, my parents, Nadathur and Anuradha; my sister, Preeta; my grandparents, Neela Patti and Chary Thatha; and my girlfriend, Vandita.

Declarations

The results presented in Chapters 4, 5, 6 and 7 are, to the best of the author's knowledge, entirely new. Much of these results have either now been published (see Dedner et al. [2013]), are currently under review for publication (see Dedner and Madhavan [2014a] and Antonietti et al. [2014]) or in preparation (see Dedner and Madhavan [2014b]). Chapter 4 is based on work done in collaboration with Simone Stangalino and his supervisors Dr Paola Antonietti and Dr Marco Verani from Politecnico di Milano. The numerics in this thesis are performed using the Distributed and Unified Numerics Environment (DUNE) software package (see Bastian et al. [2012] for more details) with the DUNE-FEM module (see Dedner et al. [2012]).

In memory of my grandmother Sulo Patti and my uncle Dr Padmanabhan Mukundan.

Abstract

In this thesis, we extend the discontinuous Galerkin framework to surface partial differential equations. This is done by deriving both a priori and a posteriori error estimates for model elliptic problems posed on compact smooth and oriented surfaces in $\mathbb{R}^3$, and investigating both theoretical estimates and several generalisations numerically.

Chapter 1

Introduction

1.1 Surface PDEs and surface FEM

Partial differential equations (PDEs) on manifolds have become an active area of research in recent years due to the fact that, in many applications, models have to be formulated not on a flat Euclidean domain but on a curved surface. For example, they arise naturally in fluid dynamics (e.g. surface active agents on the interface between two fluids, James and Lowengrub [2004] and Garcke et al. [2014]) and material science (e.g. diffusion of species along grain boundaries, Deckelnick et al. [2001]) but have also emerged in areas as diverse as image processing and cell biology (e.g. cell motility involving processes on the cell membrane, Neilson et al. [2011], Amarasinghe et al. [2012] and Elliott et al. [2012] or phase separation on biomembranes, Elliott and Stinner [2010]).

Finite element methods (FEM) for elliptic problems and their a priori error analysis have been successfully applied to problems on surfaces via the intrinsic approach in Dziuk [1988] using piecewise linear ansatz functions and approximations of the surface. This approach has subsequently been extended to parabolic problems in Dziuk and Elliott [2007b] as well as evolving surfaces in Dziuk and Elliott [2007a]. Higher order error estimates, which require higher order surface approximations, have been derived in Demlow [2009] for the Laplace-Beltrami operator. The literature on the application of FEM to various surface PDEs and geometric flows is now quite extensive, reviews of which can be found in Dziuk and Elliott [2013] and Deckelnick et al. [2005].

The literature on a posteriori error estimation and adaptivity on surfaces is sig-

nificantly less extensive than its a priori counterpart. Demlow and Dziuk [2008] derived an a posteriori error estimator for the finite element discretisation of the Laplace-Beltrami operator on surfaces, showing that the error can be split into a residual indicator term and a geometric error term. Mekchay et al. [2011] have also considered an adaptive finite element method for the Laplace-Beltrami operator posed on C^1 graphs.

However, there are a number of situations where FEM may not be the appropriate numerical method; for instance, problems which lead to steep gradients or even discontinuities in the solution. Such issues can arise for problems posed on surfaces, as in Sokolov et al. [2012], where the authors analyse a model for bacteria/cell aggregation posed on the surface of organs, which are inherently curved surfaces. Without an appropriate stabilisation mechanism artificially added to the surface FEM scheme, the solution may exhibit spurious oscillatory behaviour which, in the context of the above problem, may lead to negative densities of on-surface living cells. The literature on alternative numerical methods for such problems are very limited: to date, we are only aware of the works of Ju and Du [2009], Ju et al. [2009], Lenz et al. [2011] and Giesselmann and Müller [2014] which considered finite volume methods on (evolving) surfaces via the intrinsic approach, and Olshanskii et al. [2013] which considered a volume mesh FEM with an SUPG-type stabilisation.

1.2 Discontinuous Galerkin methods

Discontinuous Galerkin (DG) methods are a class of numerical methods that have been succesfully applied to hyperbolic, elliptic and parabolic PDEs arising from a wide range of applications. Some of its main advantages compared to conforming finite element methods include

- local, element-wise mass conservation;
- applicability to problems with discontinuous coefficients and ability to capture solution discontinuities, namely those arising in advection dominated problems;
- less restriction on grid structure and basis functions, making them ideal for hp-adaptive refinement strategies;
- easily parallelisable due to (relatively) local data communications.

The main idea of DG methods is not to require continuity of the solution between elements. Instead, inter-element behaviour has to be prescribed carefully in such

a way that the resulting scheme has adequate consistency, stability and accuracy properties. A short introduction to DG methods for both ODEs and PDEs is given in Cockburn [2003]. A history of the development of DG methods can be found in Cockburn et al. [2000] and Arnold et al. [2002]. Arnold et al. [2002] provides an in-depth analysis of a large class of discontinuous Galerkin methods for linear second-order elliptic problems, Ortner and Süli [2007] perform a detailed a priori error analysis for nonlinear second-order elliptic problems and Georgoulis et al. [2007] derive both a priori and a posteriori error estimates for advection-diffusion-reaction problems.

1.3 Thesis motivation and contributions

Given the many advantageous properties that DG methods possess, it is natural to extend the DG framework for PDEs posed on surfaces. The motivation for this thesis has thus been to investigate the issues arising when attempting to apply DG methods to problems on surfaces, both in the derivation of a priori and a posteriori error estimates. Although we have restricted our attention to analysing model second-order elliptic problems, we expect that much of the analysis will follow through for parabolic PDEs on evolving surfaces, along the lines of Dziuk and Elliott [2007a]. To the best of our knowledge, we have been the first to look at DG methods posed on surfaces from a rigorous mathematical perspective.

Our first contribution to the field, which has been published in Dedner et al. [2013], involved extending the DG framework to a linear second-order elliptic problem on a compact smooth and oriented surface in $\mathbb{R}^3$. A (symmetric) surface interior penalty (IP) method is introduced on a piecewise linear discrete surface and we derived a priori error estimates by relating the latter to the original surface via the lift introduced in Dziuk [1988]. The estimates suggested that the geometric error terms arising from the surface discretisation do not affect the overall convergence rate of the surface IP method when using linear ansatz functions and surface approximations. This was then verified numerically for a number of challenging test problems. An intricate issue was the approximation of the surface conormal required in the surface IP formulation, choices of which were investigated numerically. Numerical tests involving nonconforming grids and higher order ansatz functions (but still with linear surface approximations) have also been considered. Furthermore, we presented a generic implementation of test problems on surfaces.

Since then, a continuous/discontinuous Galerkin method for a fourth order

elliptic PDE on surfaces and its error analysis have been considered in Larsson and Larson [2013] and an isogeometric analysis of a DG method for elliptic PDEs on surfaces has been considered in Langer and Moore [2014].

Our second contribution, which is currently under review for publication (a preprint of which can be found in Dedner and Madhavan [2014a]), has been to derive and analyse an a posteriori error estimator for the surface IP method considered in Dedner et al. [2013]. Following the work done in Demlow and Dziuk [2008] and Houston et al. [2007], we showed that the estimator for the error in the DG norm may be split into a residual term, a "DG" term and a geometric term. Upper and lower bounds for the resulting a posteriori error estimator were rigorously proven and we considered a number of challenging test problems to demonstrate the reliability and efficiency of the estimator. We also presented a novel "geometric" driven refinement strategy for PDEs on surfaces which considerably improved the performance of the method on complicated surfaces.

Our third contribution, which is currently under review for publication (a preprint of which can be found in Antonietti et al. [2014]), has been to generalise the results of Dedner et al. [2013] by considering both a larger class of DG methods as well as deriving higher order estimates for this class. This was done by carefully adapting the unified DG approach of Arnold et al. [2002] onto piecewise polynomial discrete surfaces, the theory of which was first considered in Demlow [2009]. Optimal error estimates were proven in both the DG and L^2 norms provided that the surface approximations are of high enough order compared to the DG space order.

Our fourth contribution, which is currently under preparation (see Dedner and Madhavan [2014b]), has been to extend the surface DG analysis to advection-diffusion problems posed on surfaces. This was done by discretising the diffusive term along the lines of Antonietti et al. [2014] and using a "discrete surface" upwind flux for the discretisation of the advective term. A key issue arising in the analysis (which does not appear in the planar setting) was the treatment of the discrete velocity field, choices of which play an important role in the stability of the scheme. We then proved optimal error estimates in the DG norm given a number of assumptions on the discrete velocity field, and verified the estimates numerically for test problems exhibiting advection-dominated behaviour.

1.4 Outline of thesis

This thesis is organised in the following way. In Chapter 2, we introduce the general setup of surface PDEs and their finite element approximation based on the approach considered in Dziuk [1988]. For simplicity, we consider the model second-order elliptic problem

$$-\Delta_\Gamma u + u = f \quad \text{on } \Gamma \tag{1.1}$$

where Γ is a compact smooth and oriented (hyper)surface in $\mathbb{R}^3$ and Δ_Γ is the Laplace-Beltrami operator on Γ. We introduce some elementary differential geometry required to derive the variational formulation of the surface PDE, defining Sobolev spaces on manifolds and citing regularity results along the way. We then approximate Γ by a piecewise linear discrete surface Γ_h and define a linear finite element space on the discrete surface. A priori error esimates are then derived in the H^1 norm and in the L^2 norm by relating the discrete surface to the original surface via the surface lift operator introduced in Dziuk [1988]. We then show that the geometric error terms arising from the discretisation of the surface converge fast enough as to not influence the overall convergence rate of the approximation. Finally, we give a brief overview of a posteriori error estimation for FEM on surfaces, as considered in Demlow and Dziuk [2008].

In Chapter 3, we introduce a unified approach for the analysis of DG methods for second-order elliptic problems on planar domains, following the framework introduced in Arnold et al. [2002]. We first rewrite the problem as a first-order system and obtain its flux formulation by multiplying each equation by test functions in appropriate spaces (which do not assume continuity across elements). Introducing jump and averaging operators on edges of elements allows us to derive the general form of a DG method for the equation, known as the primal formulation. We then introduce the notions of consistency and conservativity and give examples of DG methods with such properties. Next, we derive a priori error estimates for the IP method (although much of the analysis may be applied to a wider range of DG methods) in the DG norm as well as in the L^2 norm. This is done by making use of the classical properties of consistency, boundedness and stability similarly as for a typical finite element error analysis. Finally, we briefly look into DG methods for first-order hyperbolic as detailed in Brezzi et al. [2004]. In particular, we derive stability estimates when considering an upwind flux discretisation of the advection term and state a priori error estimates for the resulting scheme.

In Chapter 4, which is based on work we have done in Dedner et al. [2013] and Antonietti et al. [2014], we again consider the model second-order elliptic problem (1.1) posed on a compact smooth and oriented (hyper)surface $\Gamma \subset \mathbb{R}^3$. Following the framework given in Demlow [2009] (which extends to higher order the surface FEM analysis considered in Dziuk [1988] for linear ansatz functions/suface approximation), we approximate Γ by a piecewise polynomial discrete surface Γ_h^k of order $k \geq 1$. Following the unified DG framework of Arnold et al. [2002], we then derive the primal formulation of the surface PDE on Γ_h^k. The derivation requires an integration by parts formula which makes use of "discrete surface" trace operators that differ from the conventional ones used in the planar case. Our choice for the trace operators is later shown to play a key part in making the analysis possible. Finally, by choosing the numerical fluxes of the primal formulation appropriately, we derive "discrete surface" counter-parts of the planar DG bilinear forms stated in Chapter 3. A priori error esimates are derived in the DG norm and in the L^2 norm using the surface lift operator introduced in Chapter 2, and we show that the geometric error terms arising from the discretisation of the surface converge fast enough as to not influence the overall convergence rate of the approximation provided that the surface approximation order is at least of the same order as that of the DG space. The geometric error terms involve those arising from surface FEM given in Chapter 2 as well as additional terms arising from those present in the surface DG methods. Assuming that the exact solution $u \in H^{k+1}(\Gamma)$, the estimates are given by

$$\|u - u_h^\ell\|_{L^2(\Gamma)} + h^\eta \|u - u_h^\ell\|_{DG} \lesssim h^{k+\eta}(\|f\|_{L^2(\Gamma)} + \|u\|_{H^{k+1}(\Gamma)})$$

where u_h^l is the surface lift of the surface DG approximation u_h, f is the right-hand side of our model problem and $\eta = 0, 1$ depending on the choice of surface DG method.

We then present some numerical results, making use of the Distributed and Unified Numerics Environment (DUNE) software package (see Bastian et al. [2008a], Bastian et al. [2008b]) and, in particular, the DUNE-FEM module described in Dedner et al. [2010] (also see dune.mathematik.uni-freiburg.de for more details on this module). We consider a number of test problems, for which we compute experimental orders of convergence (EOCs) in both the L^2 norm and the DG norm, and show that these coincide with the theoretical error estimates derived previously. In the process, we present a generic implementation of test problems on surfaces which follows as a direct application of implicit surface lift algorithms considered in Demlow

and Dziuk [2008].

In Chapter 5, which is based on work we have done in Dedner and Madhavan [2014a], we derive a dual weighted residual-based a posteriori error estimate for the surface IP method considered in Chapter 4, restricting ourselves to the piecewise linear surface approximation setting for simplicity. We prove both reliability and efficiency of the error estimator in the DG norm and show that the error may be split into a "residual part", made up of an element residual term along with the jump of the DG approximation, and a higher order "geometric part" which arises from the surface approximation. The geometric residual terms involve those present for the surface FEM geometric residual given in Chapter 2 as well as additional terms arising from those present in the surface IP method. We conclude by verifying the reliability and efficiency estimates numerically for a number of challenging test problems.

In Chapter 6, which is based on work we have done in Dedner and Madhavan [2014b], we extend the analysis considered in Chapter 4 to advection-diffusion problems posed on surfaces, following the lines of Brezzi et al. [2004]. The model problem we consider takes the form

$$-\Delta_\Gamma u + u + w \cdot \nabla_\Gamma u = f \quad \text{on } \Gamma,$$

where the velocity field w is purely tangential to the surface and divergence-free. The fluxes considered in Chapter 4 are used for the discretisation of the diffusion term and we use a "discrete surface" upwind flux to deal with the advection term. A number of challenging issues which do not appear in the planar setting arise when attempting to prove stability of the numerical scheme, related to the treatment of the velocity field on the discrete surface. We then derive optimal a priori error estimates for the scheme given a number of assumptions on the discrete velocity field. We then attempt to justify these assumptions by choosing the discrete velocity field to be a Raviart-Thomas-type interpolant of the velocity field. Numerical results are then presented for test problems exhibiting advection-dominated behaviour, suggesting that our surface DG method is stable and free of spurious oscillations in contrast to the unstabilised surface FEM.

In Chapter 7, which is based on work we have done in both Dedner et al. [2013] and Dedner and Madhavan [2014a], we look into a variety of topics which fall beyond the theory discussed in Chapters 4, 5 and 6. We first consider several alternative

but intuitive ways of approximating the surface conormal for the surface interior penalty (IP) method derived in Chapter 4, and investigate the resulting schemes numerically. It is worth noting that this is a feature which appears exclusively for DG methods posed on discrete surfaces.

Next, we will look into issues arising when attempting to derive a priori error estimates on nonconforming grids, discuss a way of tackling the issue and present numerical results which suggest that the convergence rates derived in Chapter 4 appear to hold for nonconforming grids in the piecewise linear surface approximation setting. In addition, we show numerical results involving different conormal choices for nonconforming grids.

Finally, we show the benefits of using adaptive refinement for problems posed on complicated surfaces which, when discretised, poorly resolves regions of high curvature. We then describe and test a new adaptive refinement strategy which is based on the "geometric part" of the residual and show that we may obtain similar errors to the standard adaptive refinement strategy for a fraction of the computational cost, making it a significantly better adaptive refinement strategy for such problems.

We finish off with Chapter 8 in which we give the conclusions of this thesis, dwell into some of the key issues we came across to derive the results of the previous chapters and outline further research that can be done in this field.

Chapter 2

Surface Finite Elements

In this chapter, we will introduce the general setup of surface PDEs and their surface finite element approximation based on the approach considered in Dziuk [1988] and Dziuk and Elliott [2013].

2.1 Notation and setting

Let Γ be a compact smooth and oriented surface in $\mathbb{R}^3$ given by the zero level-set of a signed distance function $|d(x)| = dist(x, \Gamma)$ defined in an open subset U of $\mathbb{R}^3$. For simplicity we assume that $\partial\Gamma = \emptyset$ and that $d < 0$ in the interior of Γ and $d > 0$ in the exterior. The orientation of Γ is set by taking the normal ν of Γ to be pointing in the direction of increasing d whence

$$\nu(\xi) = \nabla d(\xi), \ \xi \in \Gamma.$$

With a slight abuse of notation we also denote the projection to Γ by ξ, i.e. $\xi : U \to \Gamma$ is given by

$$\xi(x) = x - d(x)\nu(x) \quad \text{where } \nu(x) := \nu(\xi(x)). \tag{2.1}$$

It is worth noting that such a projection is (locally) unique provided that the width $\delta_U > 0$ of U satisfies

$$\delta_U < \left[\max_{i=1,2} \|\kappa_i\|_{L^\infty(\Gamma)}\right]^{-1}$$

where κ_i denotes the ith principle curvature of the Weingarten map $\mathbf{H}$, given by

$$\mathbf{H}(x) := \nabla^2 d(x). \tag{2.2}$$

Later on, we will consider a triangulated surface $\Gamma_h \subset U$ approximating Γ such that there is a one-to-one relation between points $x \in \Gamma_h$ and $\xi \in \Gamma$ so that, in particular, the above relation (2.1) can be inverted. Throughout this thesis, we denote by

$$\mathbf{P}(\xi) := \mathbf{I} - \nu(\xi) \otimes \nu(\xi), \ \xi \in \Gamma,$$

the projection onto the tangent space $T_\xi\Gamma$ on Γ at a point $\xi \in \Gamma$. Here $\otimes$ denotes the usual tensor product.

Remark 2.1.1. It is easy to see that

$$\nabla\xi = \mathbf{P} - d\mathbf{H}. \tag{2.3}$$

Definition 2.1.2. For any function η defined on an open subset of U containing Γ we can define its *tangential gradient* on Γ by

$$\nabla_\Gamma\eta := \nabla\eta - (\nabla\eta \cdot \nu)\,\nu = \mathbf{P}\nabla\eta$$

and then the *Laplace-Beltrami* operator on Γ by

$$\Delta_\Gamma\eta := \nabla_\Gamma \cdot (\nabla_\Gamma\eta).$$

Definition 2.1.3. We define the surface Sobolev spaces

$$H^m(\Gamma) := \{u \in L^2(\Gamma) \ : \ \nabla^\alpha u \in L^2(\Gamma) \ \forall |\alpha| \le m\}, \quad m \in \mathbb{N} \cup \{0\},$$

with corresponding Sobolev seminorm and norm respectively given by

$$|u|_{H^m(\Gamma)} := \left(\sum_{|\alpha|=m} \|\nabla^\alpha u\|^2_{L^2(\Gamma)} \right)^{1/2}, \quad \|u\|_{H^m(\Gamma)} := \left(\sum_{k=0}^{m} |u|^2_{H^k(\Gamma)} \right)^{1/2}.$$

We refer to Wloka [1987] for a proper discussion of Sobolev spaces on manifolds.

Throughout this thesis, we write $x \lesssim y$ to signify $x < Cy$, where C is a generic positive constant whose value, possibly different at any occurrence, does not depend on the grid size. Moreover, we use $x \sim y$ to state the equivalence between x and y, i.e., $C_1 y \le x \le C_2 y$, for $C_1,\ C_2$ independent of the grid size.

The problem that we consider in this chapter is the following second-order elliptic equation:

$$-\Delta_\Gamma u + u = f \ \text{ on } \Gamma \tag{2.4}$$

for a given $f \in L^2(\Gamma)$. In order to derive a weak formulation for such a PDE, we need the following generalisation, taken from Theorem 2.10 in Dziuk and Elliott [2013], of the integration by parts formula to surfaces.

Theorem 2.1.4. *Let $\eta \in H^1(\Gamma)$ and $\xi \in [H^1(\Gamma)]^3$. Then we have that*

$$\int_\Gamma \eta \nabla_\Gamma \cdot \xi \; dA = -\int_\Gamma \xi \cdot \nabla_\Gamma \eta + \eta \xi \cdot \kappa \; dA + \int_{\partial\Gamma} \eta \xi \cdot \mu \; ds \tag{2.5}$$

where μ denotes the outer conormal of Γ on $\partial\Gamma$ and $\kappa(x) = tr(\mathbf{H}(x))\nu$ is the mean curvature vector, with $tr(\mathbf{H}(x))$ denoting the trace of the Weingarten map (2.2). Here dA and ds denote respectively the two and one dimensional surface measures over Γ.

Remark 2.1.5. The integration by parts formula on surfaces (2.5) differs from its planar counterpart through the presence of the additional term involving the mean curvature vector κ.

Multiplying (2.4) by a test function $v \in H^1(\Gamma)$, integrating by parts using (2.5), making use of the fact that $\partial\Gamma = \emptyset$ and that $\nabla_\Gamma u \perp \nu$, the weak problem reads:

($\mathbf{P}_\Gamma$) Find $u \in H^1(\Gamma)$ such that

$$a_\Gamma(u, v) = \int_\Gamma f v \; \mathrm{dA} \quad \forall v \in H^1(\Gamma) \tag{2.6}$$

where

$$a_\Gamma(u, v) = \int_\Gamma \nabla_\Gamma u \cdot \nabla_\Gamma v + uv \; \mathrm{dA}.$$

Existence and uniqueness of a solution u follow from standard arguments. In addition, we assume that $u \in H^2(\Gamma)$ and satisfies

$$\|u\|_{H^2(\Gamma)} \lesssim \|f\|_{L^2(\Gamma)} \tag{2.7}$$

where we refer to Aubin [1982] and Wloka [1987] for more details on elliptic regularity on surfaces.

2.2 Surface FEM approximation

To obtain a discretisation of u, the smooth surface Γ is approximated by a polyhedral surface $\Gamma_h \subset U$, with outward unit normal ν_h, composed of planar triangles. Let $\mathcal{T}_h$

be the associated regular, conforming triangulation of Γ_h i.e.

$$\Gamma_h = \bigcup_{K_h \in \mathcal{T}_h} K_h.$$

The vertices of $\{K_h\}_{K_h \in \mathcal{T}_h}$ are taken to sit on Γ so that Γ_h is its linear interpolant. As mentioned before, we assume that the projection map ξ defined in (2.1) is a bijection when restricted to Γ_h, thus avoiding multiple coverings of Γ by Γ_h, and that $\nu \cdot \nu_h \geq 0$ everywhere on Γ_h.

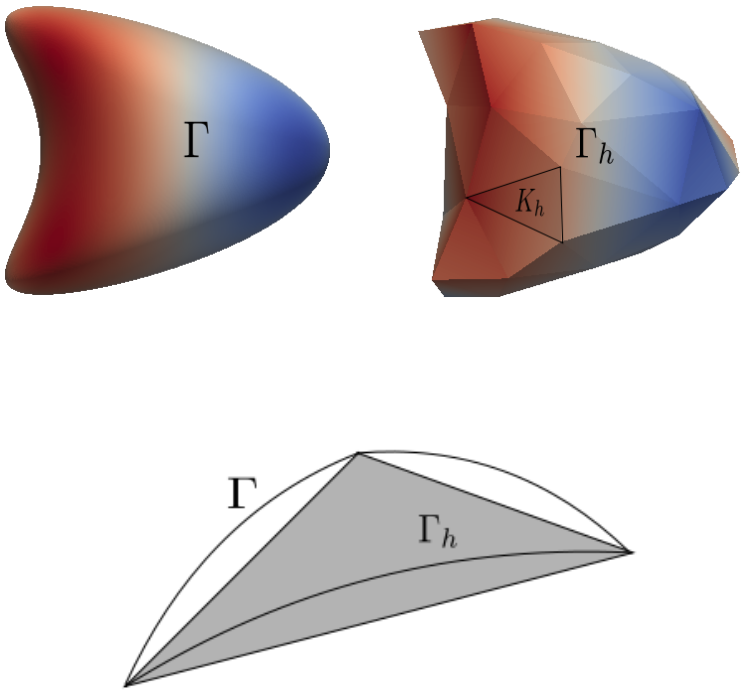

Figure 2.1: Example of smooth surface Γ and its linear interpolant $\Gamma_h = \bigcup_{K_h \in \mathcal{T}_h} K_h$ (top) and a situation showing that $\Gamma_h \not\subset \Gamma$ (bottom).

A discrete finite element space associated with Γ_h is given by

$$V_h := \{v_h \in C^0(\Gamma_h) \ : \ v_h|_{K_h} \in \mathbb{P}^1(K_h) \ \forall K_h \in \mathcal{T}_h\}$$

i.e. the space of piecewise linear functions which are globally in $C^0(\Gamma_h)$. Note that $V_h \subset H^1(\Gamma_h)$, more details on the smoothness requirements on manifolds when defining Sobolev spaces can be found in Wloka [1987]. We can now define a discrete finite element formulation on Γ_h for a given function $f_h \in L^2(\Gamma_h)$ (note that, in

general, this is not a finite element function, it will be related to the function f given in problem $(\mathbf{P}_\Gamma)$ later on, see (2.9) below):

$(\mathbf{P}_{\Gamma_h})$ Find $u_h \in V_h$ such that

$$a_{\Gamma_h}(u_h, v_h) = \int_{\Gamma_h} f_h v_h \, \mathrm{dA_h} \; \forall v_h \in V_h \tag{2.8}$$

where

$$a_{\Gamma_h}(u_h, v_h) := \int_{\Gamma_h} \nabla_{\Gamma_h} u_h \cdot \nabla_{\Gamma_h} v_h + u_h v_h \, \mathrm{dA_h}.$$

Here $\mathrm{dA_h}$ denotes the two dimensional surface measure over Γ_h. Our goal is to now compare the solution $u \in H^2(\Gamma)$ of $(\mathbf{P}_\Gamma)$ with the solution $u_h \in V_h$ of $(\mathbf{P}_{\Gamma_h})$. However, as can be seen in Figure 2.1, these two functions live on different domains (since $\Gamma_h \not\subset \Gamma$) and hence cannot be compared to each other directly. It is also worth noting that, by approximating the surface, we are introducing what is known as a *variational crime*: plugging the exact solution u of $(\mathbf{P}_\Gamma)$ into (2.8) does not yield the right-hand side of (2.6) tested with v_h. In other words, Galerkin orthogonality does not hold in our setting. In order to deal with this issue, we need to intoduce some extra tools.

2.3 Technical tools

In this section we introduce the necessary tools and geometric relations needed to work on discrete domains, following the framework introduced in Dziuk [1988].

2.3.1 Surface lift

Definition 2.3.1. For any function w defined on Γ_h we define the *surface lift* onto Γ by

$$w^l(\xi) := w(x(\xi)), \; \xi \in \Gamma,$$

where by (2.1) and the non-overlapping of the triangular elements, $x(\xi)$ is defined as the unique solution of

$$x = \xi + d(x)\nu(\xi).$$

Extending w^l constantly along the lines $s \mapsto \xi + s\nu(\xi)$ we obtain a function

defined on U. In particular, we

$$\text{define } f_h \text{ such that } f_h^l = f \text{ on } \Gamma. \tag{2.9}$$

By (2.1), for every $K_h \in \mathcal{T}_h$, there is a unique curved triangle $K_h^l := \xi(K_h) \subset \Gamma$. Note that we assumed $\xi(x)$ is a bijection so multiple coverings are in fact not permitted. We now define the regular, conforming triangulation $\mathcal{T}_h^l$ of Γ such that

$$\Gamma = \bigcup_{K_h^l \in \mathcal{T}_h^l} K_h^l.$$

The triangulation $\mathcal{T}_h^l$ of Γ is thus induced by the triangulation $\mathcal{T}_h$ of Γ_h via the surface lift.

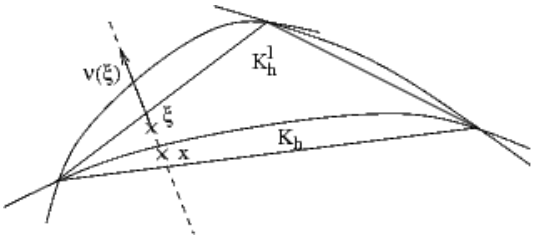

Figure 2.2: Surface lift of $K_h \in \mathcal{T}_h$ to $K_h^l \in \mathcal{T}_h^l$.

The appropriate function space for surface lifted functions is given by

$$V_h^l := \{v_h^l \in C^0(\Gamma) \ : \ v_h^l(\xi) = v_h(x(\xi)) \text{ with some } v_h \in V_h\}.$$

We define, for $x \in \Gamma_h$,

$$\mathbf{P}_h(x) = \mathbf{I} - \nu_h(x) \otimes \nu_h(x)$$

so that, for v_h defined on Γ_h and $x \in \Gamma_h$,

$$\nabla_{\Gamma_h} v_h(x) = \mathbf{P}_h \nabla v_h(x).$$

Note that this projection is well defined in the interior of triangles only, as ν_h jumps between elements. Finally, by applying the chain rule for differentiation on (2.1), one can show that for $x \in \Gamma_h$ and v_h defined on Γ_h, we have that

$$\nabla_{\Gamma_h} v_h(x) = \mathbf{P}_h(x)(\mathbf{I} - d\mathbf{H})(x)\mathbf{P}(x)\nabla_\Gamma v_h^l(\xi(x)). \tag{2.10}$$

See Dziuk [1988] or Dziuk and Elliott [2013] for further details. From this and the smoothness of Γ, we see that $u_h^l \in H^1(\Gamma)$ and so $V_h^l \subset H^1(\Gamma)$. Next we state integral equalities which we shall use repeatedly. For $x \in \Gamma_h$, we denote the local area deformation when transforming Γ_h to Γ by $\delta_h(x)$ i.e.

$$\delta_h(x)\ \mathrm{dA_h}(x) = \ \mathrm{dA}(\xi(x)). \tag{2.11}$$

Note that, by construction, $\delta_h(x) > 1$. Also, let

$$\mathbf{R}_h(x) = \mathbf{R}_h^l(\xi(x)) = \delta_h^{-1}(x)\mathbf{P}(x)(\mathbf{I} - d\mathbf{H})(x)\mathbf{P}_h(x)(\mathbf{I} - d\mathbf{H})(x)\mathbf{P}(x). \tag{2.12}$$

Then, for every $K_h \in \mathcal{T}_h$, one can show that

$$\begin{aligned}\int_{K_h} \nabla_{\Gamma_h} u_h \cdot \nabla_{\Gamma_h} v_h\ \mathrm{dA_h} &= \int_{K_h^l} (\mathbf{P}_h(\mathbf{I} - d\mathbf{H})\mathbf{P}\nabla_\Gamma u_h^l \cdot \mathbf{P}_h(\mathbf{I} - d\mathbf{H})\mathbf{P}\nabla_\Gamma v_h^l)\delta_h^{-1}\ \mathrm{dA} \\ &= \int_{K_h^l} \mathbf{R}_h^l \nabla_\Gamma u_h^l \cdot \nabla_\Gamma v_h^l\ \mathrm{dA}. \end{aligned} \tag{2.13}$$

Summing over all elements and proceeding similarly with the other terms of (2.8), we obtain

$$\int_\Gamma \mathbf{R}_h^l \nabla_\Gamma u_h^l \cdot \nabla_\Gamma v_h^l + \delta_h^{-1} u_h^l v_h^l\ \mathrm{dA} = \int_\Gamma f v_h^l \delta_h^{-1}\ \mathrm{dA} \tag{2.14}$$

which holds for every $v_h^l \in V_h^l$.

2.3.2 Geometric estimates

We next prove some geometric estimates relating Γ to Γ_h.

Lemma 2.3.2. *Let Γ be a compact smooth and oriented surface in $\mathbb{R}^3$ and let Γ_h be its linear interpolation. Then, omitting the surface lift symbols, we have that*

$$\|d\|_{L^\infty(\Gamma_h)} \lesssim h^2, \tag{2.15}$$

$$\|1 - \delta_h\|_{L^\infty(\Gamma_h)} \lesssim h^2, \tag{2.16}$$

$$\|\nu - \nu_h\|_{L^\infty(\Gamma_h)} \lesssim h, \tag{2.17}$$

$$\|\mathbf{P} - \mathbf{R}_h\|_{L^\infty(\Gamma_h)} \lesssim h^2. \tag{2.18}$$

Proof. The first and second inequalities follow from standard interpolation theory (we linearly interpolate a smooth surface Γ). The third one as well because normals are related to derivatives of local parametrisations. See the proof of Lemma 4.1 in

Dziuk and Elliott [2013] for further details.
The last estimate follows by observing that

$$\mathbf{P} - \mathbf{R}_h = \delta_h^{-1}(\mathbf{P} - \delta_h \mathbf{R}_h) + \left(1 - \delta_h^{-1}\right)\mathbf{P}$$

and so, by (2.16), the only term we have to deal with is $\mathbf{P} - \delta_h \mathbf{R}_h$. Since d is C^2, we have that $\mathbf{H} = \nabla^2 d$ is bounded and so, using (2.15), we have that

$$\begin{aligned}
\mathbf{P} - \delta_h \mathbf{R}_h &= \mathbf{P}(\mathbf{I} - d\mathbf{H})\mathbf{P}_h(\mathbf{I} - d\mathbf{H})\mathbf{P} \\
&= \mathbf{P} - \mathbf{P}\mathbf{P}_h\mathbf{P} + O(h^2) \\
&= \mathbf{P} - \mathbf{P}\mathbf{I}\mathbf{P} + \mathbf{P}\nu_h \otimes \nu_h \mathbf{P} + O(h^2) \quad = \mathbf{P}(\nu_h - \nu) \otimes (\nu_h - \nu)\mathbf{P} + O(h^2)
\end{aligned}$$

since $\mathbf{P}\nu = 0$. The result follows by applying (2.17). □

2.3.3 Stability

We finally prove some stability estimates satisfied by the finite element approximation u_h on both Γ_h and Γ.

Theorem 2.3.3. *There is a unique weak solution $u_h \in V_h$ to (2.8) which satisfies*

$$\|u_h\|_{H^1(\Gamma_h)} \lesssim \|f_h\|_{L^2(\Gamma_h)}. \tag{2.19}$$

Proof. This follows straightforwardly from applying the Lax-Milgram theorem. □

Theorem 2.3.4. *Let $u_h \in V_h$ satisfy (2.8). Then $u_h^l \in V_h^l$ satisfies*

$$\|u_h^l\|_{H^1(\Gamma)} \lesssim \|f\|_{L^2(\Gamma)} \tag{2.20}$$

for h small enough.

Proof. Using the geometric estimate (2.16), we have that

$$\int_{\Gamma_h} |f_h|^2 \, \mathrm{dA_h} = \int_\Gamma |f|^2 \delta_h^{-1} \, \mathrm{dA} = \int_\Gamma |f|^2 \, \mathrm{dA} + \int_\Gamma |f|^2 \left(\delta_h^{-1} - 1\right) \, \mathrm{dA} \lesssim \|f\|^2_{L^2(\Gamma)}$$

for h small enough. Similarly, using (2.14), the fact that $\mathbf{P}\nabla_\Gamma u_h^l = \nabla_\Gamma u_h^l$ and the

geometric estimate (2.18), we have that

$$\begin{aligned}
&\int_{\Gamma_h} |\nabla_{\Gamma_h} u_h|^2 + |u_h|^2 \, \mathrm{dA_h} = \int_{\Gamma} \mathbf{R}_h \nabla_\Gamma u_h^l \cdot \nabla_\Gamma u_h^l + \delta_h^{-1} |u_h^l|^2 \, \mathrm{dA} \\
&= \int_{\Gamma} |\nabla_\Gamma u_h^l|^2 + |u_h^l|^2 \, \mathrm{dA} + \int_{\Gamma} (\mathbf{R}_h - \mathbf{P}) \nabla_\Gamma u_h^l \cdot \nabla_\Gamma u_h^l + \left(\delta_h^{-1} - 1\right) |u_h^l|^2 \, \mathrm{dA} \\
&\gtrsim \|u_h^l\|_{H^1(\Gamma)}
\end{aligned}$$

for h small enough. Hence we obtain the desired estimate. □

2.4 A priori error estimates

Theorem 2.4.1. *Let $u \in H^2(\Gamma)$ and $u_h \in V_h$ denote the solutions to $(\mathbf{P}_\Gamma)$ and $(\mathbf{P}_{\Gamma_h})$, respectively. Denote by $u_h^l \in V_h^l$ the lift of u_h onto Γ. Then*

$$\|u - u_h^l\|_{L^2(\Gamma)} + h\|u - u_h^l\|_{H^1(\Gamma)} \lesssim h^2 \|f\|_{L^2(\Gamma)}.$$

The proof of Theorem 2.4.1 will, for the most part, follow the standard a priori error analysis framework. We have that

$$\|\phi_h^l - u_h^l\|_{H^1(\Gamma)}^2 = a_\Gamma(\phi_h^l - u_h^l, \phi_h^l - u_h^l) = a_\Gamma(\phi_h^l - u, \phi_h^l - u_h^l) + a_\Gamma(u - u_h^l, \phi_h^l - u_h^l) \tag{2.21}$$

where $\phi_h^l \in V_h^l$. Dealing with the first term will require an interpolation estimate. The presence of the second term marks the departure from standard error analysis as this term would be identically equal to zero in the planar setting due to Galerkin orthogonality. It can be thought of as quantifying the variational crime caused by the geometric error arising from approximating the smooth surface Γ by Γ_h. These terms are addressed by the following lemmas:

Lemma 2.4.2. *For a given $\eta \in H^2(\Gamma)$ there exists an interpolant $I_h^l \eta \in V_h^l$ such that*

$$\|\eta - I_h^l \eta\|_{L^2(\Gamma)} + h\|\nabla_\Gamma(\eta - I_h^l \eta)\|_{L^2(\Gamma)} \lesssim h^2 \left(\|\nabla_\Gamma^2 \eta\|_{L^2(\Gamma)} + h\|\nabla_\Gamma \eta\|_{L^2(\Gamma)}\right)$$

Proof. See Lemma 4.3 in Dziuk and Elliott [2013]. □

Lemma 2.4.3. *Let u and u_h^l be given as in Theorem 2.4.1 and define the functional E_h^{FEM} on V_h^l by*

$$E_h^{FEM}(v_h^l) := a_\Gamma(u - u_h^l, v_h^l)$$

for every $v_h^l \in V_h^l$. *Then* E_h^{FEM} *can be written as*

$$E_h^{FEM}(v_h^l) = \sum_{K_h^l \in \mathcal{T}_h^l} \int_{K_h^l} (\mathbf{R}_h - \mathbf{P}) \nabla_\Gamma u_h^l \cdot \nabla_\Gamma v_h^l + \left(\delta_h^{-1} - 1\right) u_h^l v_h^l + \left(1 - \delta_h^{-1}\right) f v_h^l \; dA$$

where $\mathbf{R}_h$ *is defined in (2.12). Furthermore,* E_h^{FEM} *scales quadratically in* h *i.e.*

$$|E_h^{FEM}(v_h^l)| \lesssim h^2 \|f\|_{L^2(\Gamma)} \|v_h^l\|_{H^1(\Gamma)}. \tag{2.22}$$

Before we give the full proof of Lemma 2.4.3, we will complete that of Theorem 2.4.1 assuming this result. Using the equality (2.21) given at the start of the proof of Theorem 2.4.1 and the quadratic scaling of E_h^{FEM} given in (2.22), we have that

$$\begin{aligned}
\|\phi_h^l - u_h^l\|_{H^1(\Gamma)}^2 &= E_h^{\text{FEM}}(\phi_h^l - u_h^l) + a_\Gamma(\phi_h^l - u, \phi_h^l - u_h^l) \\
&\leq E_h^{\text{FEM}}(\phi_h^l - u_h^l) + \|\phi_h^l - u\|_{H^1(\Gamma)} \|\phi_h^l - u_h^l\|_{H^1(\Gamma)} \\
&\lesssim h^2 \|f\|_{L^2(\Gamma)} \|\phi_h^l - u_h^l\|_{H^1(\Gamma)} + \|\phi_h^l - u\|_{H^1(\Gamma)} \|\phi_h^l - u_h^l\|_{H^1(\Gamma)},
\end{aligned}$$

thus

$$\|\phi_h^l - u_h^l\|_{H^1(\Gamma)} \lesssim h^2 \|f\|_{L^2(\Gamma)} + \|\phi_h^l - u\|_{H^1(\Gamma)}.$$

Now taking the continuous interpolant $\phi_h^l = I_h^l u$ and using Lemma 2.4.2 we obtain

$$\begin{aligned}
\|u - u_h^l\|_{H^1(\Gamma)} &\leq \|u - \phi_h^l\|_{H^1(\Gamma)} + \|\phi_h^l - u_h^l\|_{H^1(\Gamma)} \\
&\lesssim \|u - \phi_h^l\|_{H^1(\Gamma)} + h^2 \|f\|_{L^2(\Gamma)} + \|\phi_h^l - u\|_{H^1(\Gamma)} \\
&\lesssim h \|f\|_{L^2(\Gamma)}
\end{aligned}$$

as required. A standard duality argument and the Aubin-Nitsche trick yield an estimate of the error in the L^2 norm as detailed in Dziuk [1988]. The proof will be discussed in more detail in Chapter 4 in the context of higher order surface DG methods. This concludes the proof of Theorem 2.4.1.

Proof of Lemma 2.4.3. The expression for the error functional E_h^{FEM} given in Lemma 2.4.3 is obtained by considering the difference between the two equations (2.6) and (2.8). Making use of (2.13) and (2.14), we have that

$$\begin{aligned}
0 &= a_\Gamma(u, v_h^l) - \sum_{K_h^l \in \mathcal{T}_h^l} \int_{K_h^l} f v_h^l \; \mathrm{dA} - a_{\Gamma_h}(u_h, v_h) + \sum_{K_h \in \mathcal{T}_h} \int_{K_h} f_h v_h \; \mathrm{dA_h} \\
&= a_\Gamma(u - u_h^l, v_h^l) - E_h^{\text{FEM}}(v_h^l)
\end{aligned}$$

as required. Finally, using the stability estimate (2.20) and Lemma 2.3.2, we can estimate the error functional E_h^{FEM} as follows:

$$\begin{aligned}|E_h^{\mathrm{FEM}}(v_h^l)| &\leq \|\mathbf{R}_h - \mathbf{P}\|_{L^\infty(\Gamma)}\|\nabla_\Gamma u_h^l\|_{L^2(\Gamma)}\|\nabla_\Gamma v_h^l\|_{L^2(\Gamma)} \\ &+ \|\delta_h^{-1} - 1\|_{L^\infty(\Gamma)}\|u_h^l\|_{L^2(\Gamma)}\|v_h^l\|_{L^2(\Gamma)} \\ &+ \|1 - \delta_h^{-1}\|_{L^\infty(\Gamma)}\|f\|_{L^2(\Gamma)}\|v_h^l\|_{L^2(\Gamma)} \\ &\lesssim h^2\|u_h^l\|_{H^1(\Gamma)}\|v_h^l\|_{H^1(\Gamma)} + h^2\|f\|_{L^2(\Gamma)}\|v_h^l\|_{H^1(\Gamma)} \\ &\lesssim h^2\|f\|_{L^2(\Gamma)}\|v_h^l\|_{H^1(\Gamma)}\end{aligned}$$

for every $v_h^l \in V_h^l$, which concludes the proof. □

2.5 A posteriori error estimates

In this section we state the main results for surface FEM a posteriori error estimation, as first considered in Demlow and Dziuk [2008].

2.5.1 A posteriori upper bound (reliability)

Theorem 2.5.1. *Suppose that $\mathcal{T}_h$ is shape-regular. Denote by h_{K_h} the largest edge of $K_h \in \mathcal{T}_h$. For any given vertex p of $\{K_h\}_{K_h\in\mathcal{T}_h}$, let the patch $w_p = \mathrm{interior}(\cup_{K_h|p\in\bar{K}_h}\bar{K}_h)$. Furthermore, let*

$$\eta_{K_h} = h_{K_h}\|f_h\delta_h + \Delta_{\Gamma_h}u_h - u_h\delta_h\|_{L^2(K_h)} + h_{K_h}^{1/2}\|[\nabla_{\Gamma_h}u_h]\|_{L^2(\partial K_h)} \tag{2.23}$$

be the sum of the scaled element and jump residuals, then

$$\|u - u_h^l\|_{H^1(\Gamma)} \leq C\left(\sum_{K_h\in\mathcal{T}_h}\mathcal{R}_{K_h}^2 + \mathcal{G}_{K_h}^2\right)^{\frac{1}{2}}$$

with

$$\mathcal{R}_{K_h}^2 := \|\mathbf{R}_h\|_{l^2,L^\infty(w_{K_h})}\eta_{K_h}^2, \tag{2.24}$$

$$\mathcal{G}_{K_h}^2 := \|\mathbf{B}_h\nabla_{\Gamma_h}u_h\|_{L^2(K_h)}^2 + \|(1-\delta_h)(u_h - f_h)\|_{L^2(K_h)}^2, \tag{2.25}$$

where C depends only on the shape regularity of the grid and $w_{K_h} = \bigcup_{p\in K_h} w_p$. The operators $\mathbf{R}_h, \mathbf{B}_h$ are defined in (2.12) and (5.4), respectively. Here $\|\mathbf{R}_h\|_{l^2,L^\infty(w_{K_h})} :=$

$\|\|\mathbf{R}_h\|_{l^2\to l^2}\|_{L^\infty(w_{K_h})}$.

2.5.2 A posteriori lower bound (efficiency)

Theorem 2.5.2. *Suppose that $\mathcal{T}_h$ is shape-regular and let $R := f_h\delta_h + \Delta_{\Gamma_h} u_h - u_h\delta_h$. Then for each $K_h \in \mathcal{T}_h$, we have*

$$\begin{aligned}\eta_{K_h} \le{}& C\|\mathbf{R}_h\|^{1/2}_{l^2,L^\infty(w_{K_h})}\left(\|u-u_h^l\|_{H^1(w^l_{K_h})} + \|\mathbf{B}_h\nabla_{\Gamma_h}u_h\|_{L^2(w_{K_h})}\right)\\ &+ Ch_{K_h}\|R-\bar{R}\|_{L^2(w_{K_h})}.\end{aligned}$$

where η_{K_h} is given in Theorem 2.5.1. Here C depends on the number of elements in w_{K_h}, the minimum angle of the elements in w_{K_h}. $\bar{R}$ is a piecewise linear approximation of R.

Chapter 3

Discontinuous Galerkin Methods

In this chapter, we introduce a unified approach for the analysis of DG methods for second-order elliptic problems on planar domains, following the framework introduced in Arnold et al. [2002].

3.1 Flux formulation

For the sake of simplicity we restrict ourselves to the model problem

$$-\Delta u + u = f \quad \text{in } \Omega\ ,\ u = 0 \quad \text{on } \partial\Omega \tag{3.1}$$

where $\Omega \subset \mathbb{R}^2$ is assumed to be a convex polygonal domain and f a given function in $L^2(\Omega)$. In addition, we assume throughout this chapter that there exists a weak solution $u \in H^2(\Omega)$ to (3.1) satisfying

$$\|u\|_{H^2(\Omega)} \lesssim \|f\|_{L^2(\Omega)}. \tag{3.2}$$

As done in Arnold et al. [2002], the first step towards deriving a class of DG methods for (3.1) is to introduce an auxiliary variable σ and rewrite (3.1) as a first-order system, given by

$$\sigma = \nabla u\ ,\ -\nabla \cdot \sigma + u = f \quad \text{in } \Omega\ ,\ u = 0 \quad \text{on } \partial\Omega.$$

Multiplying these equations by respectively the vector-valued test function τ and the scalar test function v, and integrating by parts over a subset $\widetilde{K}_h$ of Ω, we obtain

$$\int_{\widetilde{K}_h} \sigma \cdot \tau \, \mathrm{dx} = -\int_{\widetilde{K}_h} u \nabla \cdot \tau \, \mathrm{dx} + \int_{\partial \widetilde{K}_h} u \, n_{\widetilde{K}_h} \cdot \tau \, \mathrm{ds},$$
$$\int_{\widetilde{K}_h} \sigma \cdot \nabla v + uv \, \mathrm{dx} = \int_{\widetilde{K}_h} fv \, \mathrm{dx} + \int_{\partial \widetilde{K}_h} \sigma \cdot n_{\widetilde{K}_h} \, v \, \mathrm{ds},$$

where $n_{\widetilde{K}_h}$ is the unit outward normal to $\partial \widetilde{K}_h$.
Let $\widetilde{\mathcal{T}}_h$ be a triangulation of Ω i.e.

$$\Omega = \bigcup_{\widetilde{K}_h \in \widetilde{\mathcal{T}}_h} \widetilde{K}_h.$$

Given our assumptions on the domain, Ω can be triangulated exactly by taking $\widetilde{K}_h$ to be triangles (the domain is not approximated). We define the corresponding finite element spaces as follows:

$$\tilde{S}_h := \{v \in L^2(\Omega) \ : \ v|_{\widetilde{K}_h} \in \mathbb{P}^1(\widetilde{K}_h) \ \ \forall \widetilde{K}_h \in \widetilde{\mathcal{T}}_h\},$$
$$\tilde{\Sigma}_h := \{v \in [L^2(\Omega)]^2 \ : \ v|_{\widetilde{K}_h} \in [\mathbb{P}^1(\widetilde{K}_h)]^2 \ \ \forall \widetilde{K}_h \in \widetilde{\mathcal{T}}_h\},$$

where $\mathbb{P}^1(\widetilde{K}_h)$ is the space of piecewise linear functions on $\widetilde{K}_h$. We can now derive the flux formulation for (3.1): find $u_h \in \tilde{S}_h$ and $\sigma_h \in \tilde{\Sigma}_h$ such that for all $\widetilde{K}_h \in \widetilde{\mathcal{T}}_h$ we have that

$$\int_{\widetilde{K}_h} \sigma_h \cdot \tau \, \mathrm{dx} = -\int_{\widetilde{K}_h} u_h \nabla \cdot \tau \, \mathrm{dx} + \int_{\partial \widetilde{K}_h} \hat{u}_{\widetilde{K}_h} \, n_{\widetilde{K}_h} \cdot \tau \, \mathrm{ds} \ \ \forall \tau \in [\mathbb{P}^k(\widetilde{K}_h)]^2, \tag{3.3}$$
$$\int_{\widetilde{K}_h} \sigma_h \cdot \nabla v \, \mathrm{dx} + \int_{\widetilde{K}_h} u_h v \, \mathrm{dx} = \int_{\widetilde{K}_h} fv \, \mathrm{dx} + \int_{\partial \widetilde{K}_h} \hat{\sigma}_{\widetilde{K}_h} \cdot n_{\widetilde{K}_h} \, v \, \mathrm{ds} \ \ \forall v \in \mathbb{P}^k(\widetilde{K}_h), \tag{3.4}$$

where the numerical fluxes $\hat{\sigma}_{\widetilde{K}_h}$ and $\hat{u}_{\widetilde{K}_h}$ are approximations to $\sigma = \nabla u$ and to u on $\partial \widetilde{K}_h$, respectively. The choice of the numerical fluxes is key to deriving an appropriate DG method. We will now show how to go from the flux formulation (3.3)–(3.4) to a typical finite element formulation, called the primal formulation, which is obtained by eliminating the auxiliary variable σ_h.

3.2 Primal formulation

We begin by introducing an appropriate functional setting. We denote by $H^m(\widetilde{\mathcal{T}}_h)$ the space of functions in Ω whose restriction to each element $\widetilde{K}_h$ belongs to $H^m(\widetilde{K}_h)$. Thus, the finite element spaces $\tilde{S}_h$ and $\tilde{\Sigma}_h$ are subsets of $H^m(\widetilde{\mathcal{T}}_h)$ and $[H^l(\widetilde{\mathcal{T}}_h)]^2$, respectively, for any m. The traces of functions in $H^1(\widetilde{\mathcal{T}}_h)$ belong to $T(\widetilde{\mathcal{E}}_h) := \prod_{\widetilde{K}_h \in \widetilde{\mathcal{T}}_h} L^2(\partial \widetilde{K}_h)$, where $\widetilde{\mathcal{E}}_h$ denotes the union of the boundaries of elements $\widetilde{K}_h$ of $\widetilde{\mathcal{T}}_h$. Note that $L^2(\widetilde{\mathcal{E}}_h)$ is a subspace of $T(\widetilde{\mathcal{E}}_h)$.

Now let $\widetilde{K}_h^1$, $\widetilde{K}_h^2$ and $\widetilde{K}_h^3$ be the neighbouring elements of $\widetilde{K}_h$. Let $e_1 = \partial \widetilde{K}_h \cap \partial \widetilde{K}_h^1$, $e_2 = \partial \widetilde{K}_h \cap \partial \widetilde{K}_h^2$ and $e_3 = \partial \widetilde{K}_h \cap \partial \widetilde{K}_h^3$, then

$$\partial \widetilde{K}_h = e_1 \cup e_2 \cup e_3.$$

Definition 3.2.1. The *scalar* numerical flux $\hat{u} = \left(\hat{u}_{\widetilde{K}_h}\right)_{\widetilde{K}_h \in \widetilde{\mathcal{T}}_h}$ and the *vector* numerical flux $\hat{\sigma} = \left(\hat{\sigma}_{\widetilde{K}_h}\right)_{\widetilde{K}_h \in \widetilde{\mathcal{T}}_h}$ are defined to be linear mappings

$$\hat{u} : H^2(\widetilde{\mathcal{T}}_h) \to T(\widetilde{\mathcal{E}}_h), \quad \hat{\sigma} : H^2(\widetilde{\mathcal{T}}_h) \times [H^1(\widetilde{\mathcal{T}}_h)]^2 \to [T(\widetilde{\mathcal{E}}_h)]^2.$$

To be more specific, for $u_h \in H^2(\widetilde{\mathcal{T}}_h)$, each component of the numerical fluxes, given by

$$\hat{u}_{\widetilde{K}_h}(u_h)(x) = \begin{cases} \hat{u}(u_h)|_{e_1}(x) & \text{if } x \in e_1; \\ \hat{u}(u_h)|_{e_2}(x) & \text{if } x \in e_2; \\ \hat{u}(u_h)|_{e_3}(x) & \text{if } x \in e_3; \end{cases}$$

and

$$\hat{\sigma}_{\widetilde{K}_h}(u_h, \nabla u_h)(x) = \begin{cases} \hat{\sigma}(u_h, \nabla u_h)|_{e_1}(x) & \text{if } x \in e_1; \\ \hat{\sigma}(u_h, \nabla u_h)|_{e_2}(x) & \text{if } x \in e_2; \\ \hat{\sigma}(u_h, \nabla u_h)|_{e_3}(x) & \text{if } x \in e_3. \end{cases}$$

is in $L^2(\partial \widetilde{K}_h)$.

Definition 3.2.2. Numerical fluxes are said to be *consistent* if

$$\hat{u}(v) = v|_{\widetilde{\mathcal{E}}_h}, \quad \hat{\sigma}(v, \nabla v) = \nabla v|_{\widetilde{\mathcal{E}}_h},$$

for every $v \in H^2(\Omega) \cap H_0^1(\Omega)$.

Definition 3.2.3. Numerical fluxes $\hat{u}$ and $\hat{\sigma}$ are said to be *conservative* if

$$\hat{u} : H^2(\widetilde{\mathcal{T}}_h) \to L^2(\widetilde{\mathcal{E}}_h), \quad \hat{\sigma} : H^2(\widetilde{\mathcal{T}}_h) \times [H^1(\widetilde{\mathcal{T}}_h)]^2 \to [L^2(\widetilde{\mathcal{E}}_h)]^2.$$

We now introduce some trace operators that will allow us to manipulate the numerical fluxes and obtain the primal formulation. Let $\widetilde{e}_h$ be an edge shared by elements $\widetilde{K}_h^+$ and $\widetilde{K}_h^-$ and define $n_{\widetilde{K}_h^+}$ and $n_{\widetilde{K}_h^-}$ to be respectively the outward unit normals to $\widetilde{K}_h^+$ and $\widetilde{K}_h^-$ on $\widetilde{e}_h$ (we say that $n_{\widetilde{K}_h^+}$ and $n_{\widetilde{K}_h^-}$ are respectively conormals to $\widetilde{K}_h^+$ and $\widetilde{K}_h^-$). In addition, let $q^{+/-} := q|_{\partial \widetilde{K}_h^{+/-}}$.

Definition 3.2.4. For $q \in T(\widetilde{\mathcal{E}}_h)$, the *average* $\{\{q\}\}$ and the *jump* $[\![q]\!]$ of q are given by

$$\{\{q\}\} = \frac{1}{2}(q^+ + q^-), \quad [\![q]\!] = q^+ n_{\widetilde{K}_h^+} + q^- n_{\widetilde{K}_h^-} \quad \text{on } \widetilde{e}_h \in \widetilde{\mathcal{E}}_h,$$

where $\widetilde{\mathcal{E}}_h$ is the set of interior edges. For $\varphi \in [T(\widetilde{\mathcal{E}}_h)]^2$, $\{\{\varphi\}\}$ and $[\![\varphi]\!]$ are given by

$$\{\{\varphi\}\} = \frac{1}{2}(\varphi^+ + \varphi^-), \quad [\![\varphi]\!] = \varphi^+ \cdot n_{\widetilde{K}_h^+} + \varphi^- \cdot n_{\widetilde{K}_h^-} \quad \text{on } \widetilde{e}_h \in \widetilde{\mathcal{E}}_h.$$

Notice that the jump $[\![q]\!]$ of the scalar q is a vector quantity, and the jump $[\![\varphi]\!]$ of the vector φ is a scalar quantity. For $\widetilde{e}_h \in \widetilde{\mathcal{E}}_h^\partial$, the set of boundary edges, each $q \in T(\widetilde{\mathcal{E}}_h)$ and $\varphi \in [T(\widetilde{\mathcal{E}}_h)]^2$ has a uniquely defined retriction on $\widetilde{e}_h$. We set

$$[\![q]\!] = q\nu, \quad \{\{\varphi\}\} = \varphi \quad \text{on } \widetilde{e}_h \in \widetilde{\mathcal{E}}_h^\partial \subset \partial\Omega$$

where ν is the outward unit normal to Ω. Note that both the average and jump operators map functions in $T(\widetilde{\mathcal{E}}_h)$ to functions in $L^2(\widetilde{\mathcal{E}}_h)$. In short,

$$\begin{aligned}
&\{\{\cdot\}\} : T(\widetilde{\mathcal{E}}_h) \to L^2(\widetilde{\mathcal{E}}_h), \quad [\![\cdot]\!] : T(\widetilde{\mathcal{E}}_h) \to [L^2(\widetilde{\mathcal{E}}_h)]^2, \\
&\{\{\cdot\}\} : [T(\widetilde{\mathcal{E}}_h)]^2 \to [L^2(\widetilde{\mathcal{E}}_h)]^2, \quad [\![\cdot]\!] : [T(\widetilde{\mathcal{E}}_h)]^2 \to L^2(\widetilde{\mathcal{E}}_h).
\end{aligned}$$

Summing (3.3)–(3.4) over all the elements $\widetilde{K}_h \in \widetilde{\mathcal{T}}_h$, we obtain

$$\begin{aligned}
\int_\Omega \sigma_h \cdot \tau \, \mathrm{dx} &= -\int_\Omega u_h \nabla_h \cdot \tau \, \mathrm{dx} + \sum_{\widetilde{K}_h \in \widetilde{\mathcal{T}}_h} \int_{\partial \widetilde{K}_h} \hat{u}_{\widetilde{K}_h} \, n_{\widetilde{K}_h} \cdot \tau \, \mathrm{ds} \quad \forall \tau \in \tilde{\Sigma}_h, \\
\int_\Omega \sigma_h \cdot \nabla_h v + u_h v \, \mathrm{dx} &= \int_\Omega f v \, \mathrm{dx} + \sum_{\widetilde{K}_h \in \widetilde{\mathcal{T}}_h} \int_{\partial \widetilde{K}_h} \hat{\sigma}_{\widetilde{K}_h} \cdot n_{\widetilde{K}_h} \, v \, \mathrm{ds} \quad \forall v \in \tilde{S}_h,
\end{aligned}$$

where $\nabla_h v$ and $\nabla_h \cdot \tau$ are the functions whose restrictions to each element $\widetilde{K}_h \in \widetilde{\mathcal{T}}_h$ are equal to ∇v and $\nabla \cdot \tau$, respectively. We may rewrite sums of the form $\sum_{\widetilde{K}_h \in \widetilde{\mathcal{T}}_h} \int_{\partial \widetilde{K}_h} q_{\widetilde{K}_h} \varphi_{\widetilde{K}_h} \cdot n_{\widetilde{K}_h} \, \mathrm{ds}$ using the average and jump operators introduced

previously: for all $q \in T(\widetilde{\mathcal{E}}_h)$ and $\varphi \in [T(\widetilde{\mathcal{E}}_h)]^2$, we have that

$$\sum_{\widetilde{K}_h \in \widetilde{\mathcal{T}}_h} \int_{\partial \widetilde{K}_h} q_{\widetilde{K}_h} \varphi_{\widetilde{K}_h} \cdot n_{\widetilde{K}_h} \, \mathrm{ds} = \sum_{\widetilde{e}_h \in \widetilde{\mathcal{E}}_h \cup \widetilde{\mathcal{E}}_h^\partial} \int_{\widetilde{e}_h} [\![q]\!] \cdot \{\!\{\varphi\}\!\} + \{\!\{q\}\!\} [\![\varphi]\!] \, \mathrm{ds}. \tag{3.5}$$

After a simple application of this identity, we get that

$$\int_\Omega \sigma_h \cdot \tau \, \mathrm{dx} = -\int_\Omega u_h \nabla_h \cdot \tau \, \mathrm{dx} + \sum_{\widetilde{e}_h \in \widetilde{\mathcal{E}}_h \cup \widetilde{\mathcal{E}}_h^\partial} \int_{\widetilde{e}_h} [\![\hat{u}]\!] \cdot \{\!\{\tau\}\!\} + \{\!\{\hat{u}\}\!\} [\![\tau]\!] \, \mathrm{ds}, \tag{3.6}$$

$$\int_\Omega \sigma_h \cdot \nabla_h v + u_h v \, \mathrm{dx} - \sum_{\widetilde{e}_h \in \widetilde{\mathcal{E}}_h \cup \widetilde{\mathcal{E}}_h^\partial} \int_{\widetilde{e}_h} \{\!\{\hat{\sigma}\}\!\} \cdot [\![v]\!] + [\![\hat{\sigma}]\!] \{\!\{v\}\!\} \, \mathrm{ds} = \int_\Omega f v \, \mathrm{dx}, \tag{3.7}$$

respectively for all $\tau \in \tilde{\Sigma}_h$ and $v \in \tilde{S}_h$. Taking q equal to the trace of v and φ equal to the trace of τ in (3.5), we obtain the integration by parts formula

$$-\int_\Omega \nabla_h \cdot \tau \; v \, \mathrm{dx} = \int_\Omega \tau \cdot \nabla_h v \, \mathrm{dx} - \sum_{\widetilde{e}_h \in \widetilde{\mathcal{E}}_h \cup \widetilde{\mathcal{E}}_h^\partial} \int_{\widetilde{e}_h} \{\!\{\tau\}\!\} \cdot [\![v]\!] + [\![\tau]\!] \{\!\{v\}\!\} \, \mathrm{ds}. \tag{3.8}$$

Taking $v = u_h$ in the above identity and inserting the resulting right-hand side into (3.6), we get that for every $\tau \in \tilde{\Sigma}_h$,

$$\int_\Omega \sigma_h \cdot \tau \, \mathrm{dx} = \int_\Omega \nabla_h u_h \cdot \tau \, \mathrm{dx} + \sum_{\widetilde{e}_h \in \widetilde{\mathcal{E}}_h \cup \widetilde{\mathcal{E}}_h^\partial} \int_{\widetilde{e}_h} [\![\hat{u} - u_h]\!] \cdot \{\!\{\tau\}\!\} + \{\!\{\hat{u} - u_h\}\!\} [\![\tau]\!] \, \mathrm{ds}. \tag{3.9}$$

Let the DG lifting operators $r : [L^2(\widetilde{\mathcal{E}}_h)]^2 \to \tilde{\Sigma}_h$ and $l : L^2(\widetilde{\mathcal{E}}_h) \to \tilde{\Sigma}_h$ be given by

$$\int_\Omega r(\varphi) \cdot \tau \, \mathrm{dx} := -\sum_{\widetilde{e}_h \in \widetilde{\mathcal{E}}_h \cup \widetilde{\mathcal{E}}_h^\partial} \int_{\widetilde{e}_h} \varphi \cdot \{\!\{\tau\}\!\} \, \mathrm{ds} \quad \forall \tau \in \tilde{\Sigma}_h,$$

$$\int_\Omega l(q) \cdot \tau \, \mathrm{dx} := -\sum_{\widetilde{e}_h \in \widetilde{\mathcal{E}}_h \cup \widetilde{\mathcal{E}}_h^\partial} \int_{\widetilde{e}_h} q [\![\tau]\!] \, \mathrm{ds} \quad \forall \tau \in \tilde{\Sigma}_h.$$

Using the DG lifting operators r and l, we can write σ_h solely in terms of u_h:

$$\sigma_h = \sigma_h(u_h) := \nabla_h u_h - r([\![\hat{u}(u_h) - u_h]\!]) - l(\{\!\{\hat{u}(u_h) - u_h\}\!\}). \tag{3.10}$$

Taking $\tau = \nabla_h v$ in (3.9), we may then rewrite (3.7) as follows:

$$a^{DG}(u_h, v) = \int_\Omega f v \, \mathrm{dx} \quad \forall v \in \tilde{S}_h, \tag{3.11}$$

where

$$a^{DG}(u_h, v) := \int_\Omega \nabla_h u_h \cdot \nabla_h v + u_h v \, \mathrm{dx} + \sum_{\widetilde{e}_h \in \widetilde{\mathcal{E}}_h \cup \widetilde{\mathcal{E}}_h^\partial} \int_{\widetilde{e}_h} (\llbracket \hat{u} - u_h \rrbracket \cdot \{\{\nabla_h v\}\} - \{\{\hat{\sigma}\}\} \cdot \llbracket v \rrbracket) \, \mathrm{ds} + \sum_{\widetilde{e}_h \in \widetilde{\mathcal{E}}_h \cup \widetilde{\mathcal{E}}_h^\partial} \int_{\widetilde{e}_h} (\{\{\hat{u} - u_h\}\} \llbracket \nabla_h v \rrbracket - \llbracket \hat{\sigma} \rrbracket \{\{v\}\}) \, \mathrm{ds}. \tag{3.12}$$

For any functions $u_h \in H^2(\widetilde{\mathcal{T}}_h)$ and $v \in H^2(\widetilde{\mathcal{T}}_h)$, (3.12) defines $a^{DG}(u_h, v)$, with the understanding that $\hat{u} = \hat{u}(u_h)$ and $\hat{\sigma}(u_h, \sigma_h(u_h))$, where the map $u_h \mapsto \sigma_h(u_h)$ is given by (3.10). $a^{DG} : H^2(\widetilde{\mathcal{T}}_h) \times H^2(\widetilde{\mathcal{T}}_h) \to \mathbb{R}$ is a bilinear form, and if $(u_h, \sigma_h) \in \tilde{S}_h \times \tilde{\Sigma}_h$ solves (3.3)–(3.4), then u_h solves (3.11) and σ_h is given by (3.10). We call (3.11) the *primal formulation* of the method.

3.3 Consistency and Galerkin orthogonality

Plugging the solution u of (3.1) into the bilinear form (3.12) and using the integration by parts formula (3.8), we have for any $v \in H^2(\widetilde{\mathcal{T}}_h)$ that

$$\int_\Omega \nabla_h u \cdot \nabla_h v \, \mathrm{dx} = -\int_\Omega \Delta u v \, \mathrm{dx} + \sum_{\widetilde{e}_h \in \widetilde{\mathcal{E}}_h \cup \widetilde{\mathcal{E}}_h^\partial} \int_{\widetilde{e}_h} \{\{\nabla_h u\}\} \cdot \llbracket v \rrbracket + \llbracket \nabla_h u \rrbracket \{\{v\}\} \, \mathrm{ds}.$$

Now by assumption $u \in H^2(\Omega)$, so we have that $\{\{u\}\} = u$, $\llbracket u \rrbracket = 0$, $\{\{\nabla_h u\}\} = \nabla u$, $\llbracket \nabla_h u \rrbracket = 0$ on $\widetilde{\mathcal{E}}_h$, and $-\Delta u + u = f$. Furthermore if the numerical flux $\hat{u}$ is consistent, i.e. $\hat{u}(u) = u|_{\widetilde{\mathcal{E}}_h}$, then $\llbracket \hat{u} \rrbracket = 0$ and $\{\{\hat{u}\}\} = u$ on $\widetilde{\mathcal{E}}_h$ which implies by (3.10) that $\sigma_h(u) = \nabla u$. If the numerical flux $\hat{\sigma}$ is also consistent, we have $\llbracket \hat{\sigma} \rrbracket = 0$, $\{\{\hat{\sigma}\}\} = \nabla u$ on $\widetilde{\mathcal{E}}_h$. We thus conclude that

$$a^{DG}(u, v) = \int_\Omega f v \, \mathrm{dx}.$$

Thus if the numerical fluxes are consistent, the primal formulation itself is consistent and hence we must have *Galerkin orthogonality* i.e.

$$a^{DG}(u - u_h, v) = 0 \quad \forall v \in \tilde{S}_h. \tag{3.13}$$

Now consider the dual problem given by

$$-\Delta \psi + \psi = g \ \text{ in } \Omega \ , \ \psi = 0 \ \text{ on } \partial\Omega.$$

Definition 3.3.1. We say that the primal form is *adjoint consistent* if

$$a^{DG}(v,\psi) = \int_\Omega vg \ \mathrm{dx} \tag{3.14}$$

for all $v \in H^2(\widetilde{\mathcal{T}}_h)$.

Since by assumption $\psi \in H^2(\Omega)$ we have that $\{\{\psi\}\} = \psi$, $[\![\psi]\!] = 0$, $\{\{\nabla\psi\}\} = \nabla\psi$ and $[\![\nabla\psi]\!] = 0$. Hence from (3.11) we have that

$$a^{DG}(v,\psi) = \int_\Omega vg \ \mathrm{dx} + \sum_{\widetilde{e}_h \in \widetilde{\mathcal{E}}_h \cup \widetilde{\mathcal{E}}_h^\partial} \int_{\widetilde{e}_h} [\![\hat{u}(v)]\!] \cdot \nabla\psi - [\![\hat{\sigma}(v,\sigma_h(v))]\!]\psi \ \mathrm{ds}.$$

Now if we choose the numerical fluxes to be conservative (i.e. $\hat{u}(\cdot) \in L^2(\widetilde{\mathcal{E}}_h)$ and $\hat{\sigma}(\cdot,(\cdot,\cdot)) \in [L^2(\widetilde{\mathcal{E}}_h)]^2)$, then $[\![\hat{u}]\!] = 0$ and $[\![\hat{\sigma}]\!] = 0$ on $\widetilde{\mathcal{E}}_h$. Thus conservativity of the numerical fluxes implies adjoint consistency.

3.4 Examples of DG methods

Bassi-Rebay method

Let $\widetilde{e}_h$ be an interior edge shared by $\widetilde{K}_h^+$ and $\widetilde{K}_h^-$, then a simple choice for the numerical fluxes is given by

$$\hat{u}|_{\partial\widetilde{K}_h^{+/-}} = \{\{u_h\}\}|_{\widetilde{e}_h} \quad \text{for} \quad \widetilde{e}_h \in \widetilde{\mathcal{E}}_h, \quad \hat{u} = 0 \quad \text{for} \quad \widetilde{e}_h \in \widetilde{\mathcal{E}}_h^\partial,$$
$$\hat{\sigma}|_{\partial\widetilde{K}_h^{+/-}} = \{\{\sigma_h\}\}|_{\widetilde{e}_h} \quad \text{for} \quad \widetilde{e}_h \in \widetilde{\mathcal{E}}_h.$$

Plugging these choices into (3.12) and (3.10), we obtain the method of *Bassi-Rebay*, first considered in Bassi and Rebay [1997]:

$$a^{BR}(u_h,v) := \int_\Omega \nabla_h u_h \cdot \nabla_h v + u_h v + r([\![u_h]\!]) \cdot r([\![v]\!]) \ \mathrm{dx}$$
$$- \sum_{\widetilde{e}_h \in \widetilde{\mathcal{E}}_h \cup \widetilde{\mathcal{E}}_h^\partial} \int_{\widetilde{e}_h} \{\{\nabla_h u_h\}\} \cdot [\![v]\!] + [\![u_h]\!] \cdot \{\{\nabla_h v\}\} \ \mathrm{ds}.$$

along with

$$\sigma_h = \nabla_h u_h + r([\![u_h]\!]).$$

Interior penalty (IP) method

As a second example, we derive the classical *interior penalty (IP) method*, first considered in Douglas and Dupont [1976]; Arnold [1982], for which the numerical fluxes are given by

$$\hat{u}|_{\partial \widetilde{K}_h^{+/-}} = \{\{u_h\}\}|_{\widetilde{e}_h} \text{ for } \widetilde{e}_h \in \widetilde{\mathcal{E}}_h, \quad \hat{u} = 0 \text{ for } \widetilde{e}_h \in \widetilde{\mathcal{E}}_h^{\partial},$$

$$\hat{\sigma}|_{\partial \widetilde{K}_h^{+/-}} = \{\{\nabla_h u_h\}\}|_{\widetilde{e}_h} - \beta_{\widetilde{e}_h} [\![u_h]\!]|_{\widetilde{e}_h} \text{ for } \widetilde{e}_h \in \widetilde{\mathcal{E}}_h$$

where $\beta_{\widetilde{e}_h} := \alpha h_{\widetilde{e}_h}^{-1}$ with $h_{\widetilde{e}_h}$ being a length scale associated with the edge $\widetilde{e}_h$ and α is some positive parameter. For such a choice we have σ_h as for the *Bassi-Rebay* method, but the bilinear form now looks like

$$\begin{aligned} a^{IP}(u_h, v) &:= \int_\Omega \nabla_h u_h \cdot \nabla_h v + u_h v \, \mathrm{dx} \\ &- \sum_{\widetilde{e}_h \in \widetilde{\mathcal{E}}_h \cup \widetilde{\mathcal{E}}_h^{\partial}} \int_{\widetilde{e}_h} [\![u_h]\!] \cdot \{\{\nabla_h v\}\} + \{\{\nabla_h u_h\}\} \cdot [\![v]\!] \, \mathrm{ds} + \sum_{\widetilde{e}_h \in \widetilde{\mathcal{E}}_h \cup \widetilde{\mathcal{E}}_h^{\partial}} \int_{\widetilde{e}_h} \beta_{\widetilde{e}_h} [\![u_h]\!] \cdot [\![v]\!] \, \mathrm{ds} \\ &= I_1(u_h, v) + I_2(u_h, v) + I_3(u_h, v). \end{aligned} \tag{3.15}$$

LDG method

A third example is the *LDG method*, first considered in Cockburn and Shu [1998], for which the numerical fluxes are now chosen to be

$$\hat{u}|_{\partial \widetilde{K}_h^{+/-}} = \{\{u_h\}\}|_{\widetilde{e}_h} - \mu \cdot [\![u_h]\!]|_{\widetilde{e}_h} \text{ for } \widetilde{e}_h \in \widetilde{\mathcal{E}}_h, \quad \hat{u} = 0 \text{ for } \widetilde{e}_h \in \widetilde{\mathcal{E}}_h^{\partial},$$

$$\hat{\sigma}|_{\partial \widetilde{K}_h^{+/-}} = \{\{\sigma_h\}\}|_{\widetilde{e}_h} + \mu [\![\sigma_h]\!]|_{\widetilde{e}_h} - \beta_{\widetilde{e}_h} [\![u_h]\!]|_{\widetilde{e}_h} \text{ for } \widetilde{e}_h \in \widetilde{\mathcal{E}}_h, \;\; \hat{\sigma} = \{\{\sigma_h\}\} - \beta_{\widetilde{e}_h} [\![u_h]\!] \text{ for } \widetilde{e}_h \in \widetilde{\mathcal{E}}_h^{\partial}$$

where $\mu \in [L^2(\widetilde{\mathcal{E}}_h)]^2$ is a vector-valued function which is constant on each edge. The bilinear from for the LDG method is now given by

$$\begin{aligned} a^{LDG}(u_h, v) := &\int_\Omega \nabla_h u_h \cdot \nabla_h v + u_h v \ \mathrm{dx} - \sum_{\widetilde{e}_h \in \widetilde{\mathcal{E}}_h \cup \widetilde{\mathcal{E}}_h^\partial} \int_{\widetilde{e}_h} [\![u_h]\!] \cdot \{\!\{\nabla_h v\}\!\} + \{\!\{\nabla_h u_h\}\!\} \cdot [\![v]\!] \ \mathrm{ds} \\ &+ \sum_{\widetilde{e}_h \in \widetilde{\mathcal{E}}_h \cup \widetilde{\mathcal{E}}_h^\partial} \int_{\widetilde{e}_h} \mu \cdot [\![u_h]\!][\![\nabla_h v]\!] + [\![u_h]\!]\beta_{\widetilde{e}_h} \cdot [\![v]\!] \ \mathrm{ds} \\ &+ \int_\Omega (r([\![u_h]\!]) + l(\mu \cdot [\![u_h]\!])) \cdot (r([\![v]\!]) + l(\mu \cdot [\![v]\!])) \ \mathrm{dx} \\ &+ \sum_{\widetilde{e}_h \in \widetilde{\mathcal{E}}_h \cup \widetilde{\mathcal{E}}_h^\partial} \int_{\widetilde{e}_h} \beta_{\widetilde{e}_h} [\![u_h]\!] \cdot [\![v]\!] \ \mathrm{ds}. \end{aligned}$$

We note that both the scalar flux $\hat{u}$ and the vector flux $\hat{\sigma}$ are consistent for all the DG methods that have been mentioned. Hence, as discussed previously, their corresponding bilinear forms are also consistent and Galerkin orthogonality holds. Furthermore both the scalar and numerical fluxes are conservative, hence these DG methods are also adjoint consistent.

3.5 Boundedness, stability and interpolation

For simplicity, we will focus our analysis on the interior penalty (IP) method whose bilinear form is given in (3.15), although much of what follows can be directly applied to other DG methods.

To analyse this DG method we cannot directly use the H^1 norm because $H^2(\widetilde{\mathcal{T}}_h)$ is not a subset of $H^1(\Omega)$. Also, a piecewise version of the H^1 norm would not produce a suitable norm on $H^2(\widetilde{\mathcal{T}}_h)$. We thus introduce a DG norm, which will be the norm of choice in the error analysis.

Definition 3.5.1. For $u \in H^2(\widetilde{\mathcal{T}}_h)$ we define

$$|u|_{1,h}^2 := \sum_{\widetilde{K}_h \in \widetilde{\mathcal{T}}_h} \|u\|_{H^1(\widetilde{K}_h)}^2 \quad , \quad |u|_{*,h}^2 := \sum_{\widetilde{e}_h \in \widetilde{\mathcal{E}}_h} h_{\widetilde{e}_h}^{-1} \|[\![u]\!]\|_{L^2(\widetilde{e}_h)}^2.$$

Now it can be shown that the following provides a norm on $H^2(\widetilde{\mathcal{T}}_h)$:

$$\|u\|_{DG}^2 := |u|_{1,h}^2 + |u|_{*,h}^2.$$

First we prove a boundedness estimate of a^{IP}:

Lemma 3.5.2. *Let $u \in H^2(\Omega)$ and $v, w \in \widetilde{S}_h$. If $\beta_{\widetilde{e}_h} = \alpha h_{\widetilde{e}_h}^{-1}$ with $\alpha = O(1)$ then*

$$|a^{IP}(u+w,v)| \lesssim \left(\|u+w\|_{DG} + h^2\|u\|_{H^2(\Omega)}\right)\|v\|_{DG}. \tag{3.16}$$

Proof. From (3.15), it can be easily seen that $I_1(u+w,v) \leq |u+w|_{1,h}|v|_{1,h}$ and $I_3(u+w,v) \lesssim |u+w|_{*,h}|v|_{*,h}$. It remains to bound $I_2(u+w,v) = -\sum_{\widetilde{e}_h \in \widetilde{\mathcal{E}}_h \cup \widetilde{\mathcal{E}}_h^{\partial}} \int_{\widetilde{e}_h} [\![u+w]\!] \cdot \{\{\nabla_h v\}\} + \{\{\nabla_h (u+w)\}\} \cdot [\![v]\!]$ ds. It suffices to show that the first term is bounded by $\|u+w\|_{DG}\|v\|_{DG}$.
Using Cauchy-Schwartz we can estimate

$$\left|\sum_{\widetilde{e}_h \in \widetilde{\mathcal{E}}_h \cup \widetilde{\mathcal{E}}_h^{\partial}} \int_{\widetilde{e}_h} \{\{\nabla_h (u+w)\}\} \cdot [\![v]\!] \text{ ds}\right| = \left|\sum_{\widetilde{e}_h \in \widetilde{\mathcal{E}}_h \cup \widetilde{\mathcal{E}}_h^{\partial}} \int_{\widetilde{e}_h} h_{\widetilde{e}_h}^{\frac{1}{2}} \{\{\nabla (u+w)\}\} \cdot h_{\widetilde{e}_h}^{-\frac{1}{2}} [\![v]\!] \text{ ds}\right|$$

$$\leq \left(\sum_{\widetilde{e}_h \in \widetilde{\mathcal{E}}_h \cup \widetilde{\mathcal{E}}_h^{\partial}} \int_{\widetilde{e}_h} h_{\widetilde{e}_h}^{-1} |[\![v]\!]|^2 \text{ ds}\right)^{\frac{1}{2}} \left(\sum_{\widetilde{e}_h \in \widetilde{\mathcal{E}}_h \cup \widetilde{\mathcal{E}}_h^{\partial}} \int_{\widetilde{e}_h} h_{\widetilde{e}_h} |\{\{\nabla (u+w)\}\}|^2 \text{ ds}\right)^{\frac{1}{2}}.$$

Now clearly the first part can be estimated by $\|v\|_{DG}$. For the second part we make use of Cauchy-Schwartz and Young's inequality to show that for interior intersections, we have that

$$\begin{aligned}\|\{\{\nabla (u+w)\}\}\|_{L^2(\widetilde{e}_h)}^2 &\lesssim \| \nabla (u+w)|_{\widetilde{K}_h^+} \cdot n_{\widetilde{K}_h^+}\|_{L^2(\widetilde{e}_h)}^2 + \| \nabla (u+w)|_{\widetilde{K}_h^-} \cdot n_{\widetilde{K}_h^-}\|_{L^2(\widetilde{e}_h)}^2 \\ &\leq \| \nabla (u+w)|_{\widetilde{K}_h^+} \|_{L^2(\widetilde{e}_h)}^2 + \| \nabla (u+w)|_{\widetilde{K}_h^-} \|_{L^2(\widetilde{e}_h)}^2,\end{aligned}$$

while on boundary interesections,

$$\|\{\{\nabla (u+w)\}\}\|_{L^2(\widetilde{e}_h)}^2 \leq \| \nabla (u+w)|_{\widetilde{K}_h} \|_{L^2(\widetilde{e}_h)}^2.$$

Putting this together, we get

$$\sum_{\widetilde{e}_h \in \widetilde{\mathcal{E}}_h \cup \widetilde{\mathcal{E}}_h^{\partial}} \int_{\widetilde{e}_h} h_{\widetilde{e}_h} |\{\{\nabla (u+w)\}\}|^2 \text{ ds} \leq 2 \sum_{\widetilde{K}_h \in \widetilde{\mathcal{T}}_h} \sum_{\widetilde{e}_h \subset \partial \widetilde{K}_h} h_{\widetilde{e}_h} \| \nabla (u+w)|_{\widetilde{K}_h} \|_{L^2(\widetilde{e}_h)}^2.$$

Finally, applying the trace theorem as in (2.5) in Arnold [1982] followed by an inverse inequality as in Brezzi et al. [1999] gives

$$\| \nabla (u+w)|_{\widetilde{K}_h} \|_{L^2(\widetilde{e}_h)}^2 \lesssim h_{\widetilde{e}_h}^{-1} \|\nabla (u+w)\|_{L^2(\widetilde{K}_h)}^2 + h_{\widetilde{e}_h} \|\nabla^2 u\|_{L^2(\widetilde{K}_h)}^2,$$

hence

$$\sum_{\widetilde{e}_h \in \widetilde{\mathcal{E}}_h \cup \widetilde{\mathcal{E}}_h^\partial} \int_{\widetilde{e}_h} h_{\widetilde{e}_h} |\{\{\nabla(u+w)\}\}|^2 \, \mathrm{ds} \lesssim \sum_{\widetilde{K}_h \in \widetilde{\mathcal{T}}_h} |u+w|^2_{H^1(\widetilde{K}_h)} + h^2 |u|^2_{H^2(\widetilde{K}_h)}$$

which concludes the proof. □

We now move on to proving stability of a^{IP}:

Lemma 3.5.3. *Let $v \in \widetilde{S}_h$. If $\beta_{\widetilde{e}_h} = \alpha h_{\widetilde{e}_h}^{-1}$ with $\alpha = O(1)$ then*

$$|a^{IP}(v,v)| \gtrsim \|v\|^2_{DG} \tag{3.17}$$

if α is chosen large enough.

Proof. Using the arguments found in the proof of the boundedness lemma with $w = v$ and $u \equiv 0$, we have that $|I_2(v,v)| \geq -C|v|_{1,h}|v|_{*,h}$ where C depends on the grid (angle condition) but not on the penalty coefficients α. Using Young's inequality with δ we obtain $|I_2(v,v)| \geq -\delta|v|^2_{1,h} - C\frac{1}{4\delta}|v|^2_{*,h}$. Therefore

$$\begin{aligned}
|a^{IP}(v,v)| &\geq |I_1(v,v)| + |I_2(v,v)| + |I_3(v,v)| \\
&\geq |v|^2_{1,h} + \alpha|v|^2_{*,h} - C\delta|v|^2_{1,h} - C\frac{1}{4\delta}|v|^2_{*,h} \\
&= (1 - C\delta)|v|^2_{1,h} + \left(\alpha - \frac{C}{4\delta}\right)|v|^2_{*,h}.
\end{aligned}$$

Now if we take $\delta = \frac{1}{2C}$ then

$$\begin{aligned}
|a^{IP}(v,v)| &\geq \frac{1}{2}|v|^2_{1,h} + \left(\alpha - \frac{C^2}{2}\right)|v|^2_{*,h} \\
&\geq C\|v\|^2_{DG}
\end{aligned}$$

where $C > 0$ if α is sufficiently large. □

The last ingredient required for the error analysis is a bound on the interpolation error $\|u - \widetilde{I}_h u\|_{DG}$ when $\widetilde{I}_h u \in \tilde{S}_h$ is the linear interpolant of the exact solution u. If $\widetilde{I}_h u$ is chosen to be a continuous interpolant, then the jump of $u - \widetilde{I}_h u$ will be zero at the inter-element boundaries. Standard interpolation theory then yields the interpolation estimate

$$\|u - \widetilde{I}_h u\|_{DG} = |u - \widetilde{I}_h u|_{1,h} \lesssim h|u|_{H^2(\Omega)}. \tag{3.18}$$

3.6 Error estimates

We now derive a priori error estimates for the IP method. More generally, the proof presented below applies to DG methods with are completely consistent (consistent and adjoint consistent), bounded and stable in the appropriate norms.

Theorem 3.6.1. *Let $u \in H^2(\Gamma)$ denote the solution to (3.1) and $u_h \in \widetilde{S}_h$ its interior penalty (IP) approximation, given by (3.15). We then have that*

$$\|u - u_h\|_{L^2(\Omega)} + h\|u - u_h\|_{DG} \lesssim h\|f\|_{L^2(\Omega)}. \tag{3.19}$$

Proof. Using the stability of a^{IP} given in (3.17), the Galerkin orthogonality condition (3.13), the boundedness estimate (3.16), the stability estimate (3.2) and the interpolation estimate (3.18) with $\widetilde{I}_h u$ chosen to be the continuous interpolant of u, we have that

$$\begin{aligned}
\|\widetilde{I}_h u - u_h\|_{DG}^2 &\lesssim a^{IP}(\widetilde{I}_h u - u_h, \widetilde{I}_h u - u_h) = a^{IP}(\widetilde{I}_h u - u, \widetilde{I}_h u - u_h) \\
&\lesssim \left(\|\widetilde{I}_h u - u\|_{DG} + h^2\|u\|_{H^2(\Omega)}\right)\|\widetilde{I}_h u - u_h\|_{DG} \\
&\lesssim h\|f\|_{L^2(\Omega)}\|\widetilde{I}_h u - u_h\|_{DG}.
\end{aligned}$$

Using this, we then have that

$$\begin{aligned}
\|u - u_h\|_{DG} &\leq \|u - \widetilde{I}_h u\|_{DG} + \|\widetilde{I}_h u - u_h\|_{DG} \\
&\lesssim \|u - \widetilde{I}_h u\|_{DG} + h\|f\|_{L^2(\Gamma)} \\
&\lesssim h\|f\|_{L^2(\Gamma)}
\end{aligned}$$

as required. A standard duality argument and the Aubin-Nitsche trick yield an estimate of the error in the L^2 norm as detailed in Arnold et al. [2002]. □

3.7 DG methods for first order hyperbolic problems

In this section we will briefly outline some key aspects of the a priori error analysis of DG methods for first order hyperbolic problems, following the lines of Brezzi et al. [2004]. Aspects of its analysis will be combined with that of the elliptic case to derive a priori error estimates for advection-diffusion problems on surfaces in Chapter 6. We make use of the same notation as in the previous section and, in addition, let $c \in C(\bar{\Omega})$ and let the velocity field $w = (w_1, w_2)^T$ be a vector-valued function defined on $\bar{\Omega}$ with $w_i \in C^1(\bar{\Omega}), i = 1, 2$. As a model problem we will consider the hyperbolic

boundary value problem

$$\nabla \cdot (wu) + cu = f \quad \text{in } \Omega \tag{3.20}$$

$$u = 0 \quad \text{on } \partial\Omega. \tag{3.21}$$

We shall assume the existence of a positive constant c_0 such that

$$c(x) + \frac{1}{2}\nabla \cdot w(x) \geq c_0 \ \forall x \in \bar{\Omega}.$$

3.7.1 Upwind flux DG discretisation

A DG discretisation of (3.20) based on a jump-stabilisation discretisation of the advection term is given as follows: find $u_h \in \tilde{S}_h$ such that

$$a^{UP}(u_h, v_h) = \sum_{\widetilde{K}_h \in \widetilde{\mathcal{T}}_h} \int_{\widetilde{K}_h} f v_h \ \mathrm{dx} \ \forall \varphi_h \in \tilde{S}_h \tag{3.22}$$

where

$$\begin{aligned} a^{UP}(u_h, v_h) := & \sum_{\widetilde{K}_h \in \widetilde{\mathcal{T}}_h} \int_{\widetilde{K}_h} -u_h w \cdot \nabla v_h + c u_h v_h \ \mathrm{dx} \\ & + \sum_{\widetilde{e}_h \in \widetilde{\mathcal{E}}_h} \int_{\widetilde{e}_h} \{\{w u_h\}\}_{up} \cdot [\![v_h]\!] \ \mathrm{ds} \end{aligned} \tag{3.23}$$

with $\{\{wu_h\}\}_{up} \cdot n_{\widetilde{K}_h} := \left(\{\{wu_h\}\} + \xi_{\widetilde{e}_h}[\![u_h]\!]\right) \cdot n_{\widetilde{K}_h}$ where $\xi_{\widetilde{e}_h} = \frac{\left|w \cdot n_{\widetilde{K}_h}\right|}{2}$ for each $\widetilde{e}_h \subset \partial \widetilde{K}_h$.

Remark 3.7.1. Note that the jump-stabilisation term $\{\{wu_h\}\}_{up}$ is exactly equivalent to the classical upwind flux. However, as we will see later on, there are distinct advantages of writing the upwing flux in this jump-satbilisation form.

3.7.2 Stability

We shall prove stability in the norm

$$|||\cdot|||^2 := \|\cdot\|^2_{L^2(\Omega)} + \sum_{\widetilde{e}_h \in \widetilde{\mathcal{E}}_h} \|\xi^{1/2}_{\widetilde{e}_h}[\![\cdot]\!]\|^2_{L^2(\widetilde{e}_h)}.$$

We proceed along the lines of Brezzi et al. [2004] by testing (3.23) with $v_h = u_h$ and integrating by parts on each $\widetilde{K}_h \in \widetilde{\mathcal{T}}_h$. By doing so, we obtain

$$\begin{aligned} a^{UP}(u_h, u_h) := & \sum_{\widetilde{K}_h \in \widetilde{\mathcal{T}}_h} \int_{\widetilde{K}_h} \left(c + \frac{1}{2} \nabla \cdot w \right) u_h^2 \, \mathrm{dx} \\ & + \sum_{\widetilde{e}_h \in \widetilde{\mathcal{E}}_h} \int_{\widetilde{e}_h} \xi_{\widetilde{e}_h} |[\![u_h]\!]|^2 + \{\{w u_h\}\} \cdot [\![u_h]\!] \, \mathrm{ds} \\ & - \frac{1}{2} \sum_{\widetilde{K}_h \in \widetilde{\mathcal{T}}_h} \int_{\partial \widetilde{K}_h} \left(w \cdot n_{\widetilde{K}_h} \right) u_h^2 \, \mathrm{ds}. \end{aligned} \tag{3.24}$$

Using formula (3.5) for DG functions and the fact that $[\![w]\!] = 0$, we have that

$$\sum_{\widetilde{K}_h \in \widetilde{\mathcal{T}}_h} \int_{\partial \widetilde{K}_h} \left(w \cdot n_{\widetilde{K}_h} \right) u_h^2 \, \mathrm{ds} = \sum_{\widetilde{e}_h \in \widetilde{\mathcal{E}}_h} \int_{\widetilde{e}_h} [\![w u_h^2]\!] \, \mathrm{ds} \tag{3.25}$$

$$= \sum_{\widetilde{e}_h \in \widetilde{\mathcal{E}}_h} \int_{\widetilde{e}_h} \{\{w\}\} \cdot [\![u_h^2]\!] \, \mathrm{ds}. \tag{3.26}$$

On the other hand, using the continuity of w and the definitions of the planar jump and average, we have that

$$\{\{w u_h\}\} \cdot [\![u_h]\!] \equiv \frac{1}{2} \{\{w\}\} \cdot [\![u_h^2]\!]. \tag{3.27}$$

As noted in Brezzi et al. [2004], formula (3.27) is straightforward yet crucial for providing a simple treatment of the jump-stabilisation given in (3.23), compared with the classical upwind stabilisation. Plugging (3.25) and (3.27) into (3.24) yields

$$\begin{aligned} a^{UP}(u_h, u_h) := & \sum_{\widetilde{K}_h \in \widetilde{\mathcal{T}}_h} \int_{\widetilde{K}_h} \left(\frac{1}{2} \nabla \cdot w + c \right) u_h^2 \, \mathrm{dx} + \frac{1}{2} \sum_{\widetilde{e}_h \in \widetilde{\mathcal{E}}_h} \int_{\widetilde{e}_h} \{\{w\}\} \cdot [\![u_h^2]\!] \, \mathrm{ds} \\ & - \frac{1}{2} \sum_{\widetilde{e}_h \in \widetilde{\mathcal{E}}_h} \int_{\widetilde{e}_h} \{\{w\}\} \cdot [\![u_h^2]\!] \, \mathrm{ds} + \sum_{\widetilde{e}_h \in \widetilde{\mathcal{E}}_h} \int_{\widetilde{e}_h} \xi_{\widetilde{e}_h} |[\![u_h]\!]|^2 \, \mathrm{ds} \\ & \geq c_0 \|u_h\|_{L^2(\Omega)}^2 + \sum_{\widetilde{e}_h \in \widetilde{\mathcal{E}}_h} \|\xi_{\widetilde{e}_h}^{1/2} [\![u_h]\!]\|_{L^2(\widetilde{e}_h)}^2 \gtrsim |||u_h|||^2 \end{aligned} \tag{3.28}$$

which gives the desired result.

3.7.3 Error estimates

Optimal a priori error estimates for the solution u_h to (3.22) follow standard arguments, details of which can be found in Brezzi et al. [2004]. The estimate takes the

form

$$\|u-u_h\|^2_{L^2(\Omega)}+\sum_{\widetilde{e}_h\in\widetilde{\mathcal{E}}_h}\|\xi^{1/2}_{\widetilde{e}_h}[\![u-u_h]\!]\|^2_{L^2(\widetilde{e}_h)}\lesssim h^3\|u\|^2_{H^2(\Omega)}.$$

Chapter 4

A Priori Error Analysis of DG Methods on Surfaces

In this chapter, we will derive and analyse a large class of surface DG methods posed on piecewise polynomial discrete surfaces, extending on the a priori error analysis done for surface FEM and the planar DG method. As such, we urge the reader to first consider reading through Chapter 2 and Chapter 3, which give an outline of the latter two and introduce much of the notation found in this chapter, before reading through this chapter and subsequent ones.

4.1 Notation and setting

Recall from Chapter 2 the model weak problem (2.6), given as follows: let $f \in L^2(\Gamma)$ be a given function, find $u \in H^1(\Gamma)$ such that

$$a_\Gamma(u, v) = \int_\Gamma fv \ \mathrm{dA} \quad \forall v \in H^1(\Gamma) \tag{4.1}$$

where

$$a_\Gamma(u, v) = \int_\Gamma \nabla_\Gamma u \cdot \nabla_\Gamma v + uv \ \mathrm{dA}.$$

As before, Γ is a compact smooth oriented surface in $\mathbb{R}^3$ with $\partial\Gamma = \emptyset$. In addition, for this chapter, we assume that $u \in H^s(\Gamma)$, $s \geq 2$. Existence, uniqueness and regularity of such a solution are shown in Aubin [1982].

4.2 Higher order surface DG approximation

4.2.1 Surface approximation

Following the surface approximation framework discussed in Chapter 2, we approximate Γ by a piecewise linear surface approximation Γ_h composed of planar triangles $\{K_h\}_{K_h \in \mathcal{T}_h}$ whose vertices lie on Γ, and denote by $\mathcal{T}_h$ the associated regular, conforming triangulation of Γ_h, i.e., $\Gamma_h = \bigcup_{K_h \in \mathcal{T}_h} K_h$. We now describe a family Γ_h^k of polynomial approximations to Γ which are of degree k (with the convention that $\Gamma_h^1 = \Gamma_h$), as introduced in Demlow [2009]. For a given element $K_h \in \mathcal{T}_h$, let $\{\phi_i^k\}_{1 \le i \le n_k}$ be the Lagrange basis functions of degree k defined on K_h corresponding to a set of nodal points $x_1, ..., x_{n_k}$. For $x \in K_h$, we define the discrete projection $\xi_k : \Gamma_h \to U$ by

$$\xi_k(x) = \sum_{j=1}^{n_k} \xi(x_j)\phi_j^k(x).$$

Recall from (2.1) that the map $\xi(x)$ is given by

$$\xi(x) = x - d(x)\nu(x) \quad \text{where } \nu(x) := \nu(\xi(x))$$

with d and ν being respectively the signed distance function and the outward unit normal to Γ. By constructing ξ_k elementwise we obtain a continuous piecewise polynomial map on Γ_h. We then define the corresponding discrete surface $\Gamma_h^k = \{\xi_k(x) : x \in \Gamma_h\}$ and the corresponding regular, conforming triangulation $\widehat{\mathcal{T}}_h = \{\xi_k(K_h)\}_{K_h \in \mathcal{T}_h}$. We denote by $\widehat{\mathcal{E}}_h$ the set of all (codimension one) intersections $\widehat{e}_h$ of elements in $\widehat{\mathcal{T}}_h$, i.e., the edges $\widehat{e}_h = \widehat{K}_h^+ \cap \widehat{K}_h^-$, for some elements $\widehat{K}_h^\pm \in \widehat{\mathcal{T}}_h$. Furthermore, we denote by $h_{\widehat{e}_h}$ the length of the edge $\widehat{e}_h \in \widehat{\mathcal{E}}_h$. For any $\widehat{e}_h \in \widehat{\mathcal{E}}_h$, the conormal $\widehat{n}_h^+$ to a point $x \in \widehat{e}_h$ is the unique unit vector that belongs to $T_x\widehat{K}_h^+$ and satisfies

$$\widehat{n}_h^+(x) \cdot (x - y) \ge 0 \quad \forall y \in \widehat{K}_h^+ \cap B_\epsilon(x).$$

Analogously, one can define the conormal $\widehat{n}_h^-$ on $\widehat{e}_h$ by exchanging $\widehat{K}_h^+$ with $\widehat{K}_h^-$. It is important to notice that, with the above definition,

$$\widehat{n}_h^+ \neq -\widehat{n}_h^-$$

in general and independently of the surface approximation order k (see Figure 4.1), in contrast to the planar setting. Finally, we will denote by $\widehat{\nu}_h$ the outward unit normal to Γ_h^k and define for each $\widehat{K}_h \in \widehat{\mathcal{T}}_h$ the discrete projection $\mathbf{P}_{hk}$ onto the

tangential space of Γ_h^k by

$$\mathbf{P}_{hk}(x) = \mathbf{I} - \widehat{\nu}_h(x) \otimes \widehat{\nu}_h(x), \ x \in \widehat{K}_h,$$

so that, for v_h defined on Γ_h^k,

$$\nabla_{\Gamma_h^k} v_h = \mathbf{P}_{hk} \nabla v_h.$$

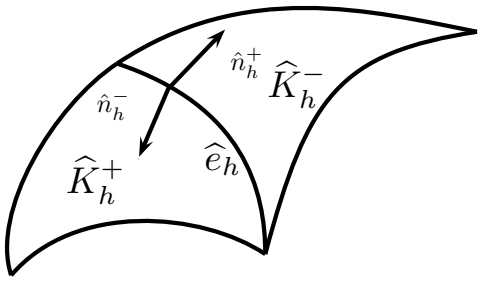

Figure 4.1: Example of two elements in $\widehat{\mathcal{T}}_h$ and their respective conormals on the common edge $\widehat{e}_h$. Notice that $\widehat{n}_h^+ \neq -\widehat{n}_h^-$.

Let $K \subset \mathbb{R}^2$ be the (flat) reference element and let $F_{\widehat{K}_h} : K \to \widehat{K}_h \subset \mathbb{R}^3$ for $\widehat{K}_h \in \widehat{\mathcal{T}}_h$. We define the DG space associated to Γ_h^k by

$$\widehat{S}_{hk} = \{\widehat{\chi} \in L^2(\Gamma_h^k) : \widehat{\chi}|_{\widehat{K}_h} = \chi \circ F_{\widehat{K}_h}^{-1}, \ \chi \in \mathbb{P}^k(K) \quad \forall \widehat{K}_h \in \widehat{\mathcal{T}}_h\}.$$

For $v_h \in \widehat{S}_{hk}$ we adopt the convention that $v_h^\pm$ is the trace of v_h on $\widehat{e}_h = \widehat{K}_h^+ \cap \widehat{K}_h^-$ taken within the interior of $\widehat{K}_h^\pm$, respectively. In addition, we define the vector-valued function space

$$\widehat{\Sigma}_{hk} = \{\widehat{w} \in [L^2(\Gamma_h^k)]^3 : \widehat{w}|_{\widehat{K}_h} = \nabla F_{\widehat{K}_h}^{-T} \left(w \circ F_{\widehat{K}_h}^{-1} \right), \ w \in [\mathbb{P}^k(K)]^2 \quad \forall \widehat{K}_h \in \widehat{\mathcal{T}}_h\}.$$

Here, $\nabla F_{\widehat{K}_h}^{-1}$ refers to the (left) *pseudo-inverse* of $\nabla F_{\widehat{K}_h}$, i.e.,

$$\nabla F_{\widehat{K}_h}^{-1} = \left(\nabla F_{\widehat{K}_h}^T \nabla F_{\widehat{K}_h} \right)^{-1} \nabla F_{\widehat{K}_h}^T.$$

Note that $\mathbf{P}_{hk} \nabla F_{\widehat{K}_h}^{-T} = \nabla F_{\widehat{K}_h}^{-T}$, i.e., $\widehat{\tau} \in \widehat{\Sigma}_{hk} \Rightarrow \widehat{\tau} \in T_x \Gamma_h^k$ almost everywhere. This result straightforwardly implies that $\widehat{\chi} \in \widehat{S}_{hk} \Rightarrow \nabla_{\Gamma_h^k} \widehat{\chi} \in \widehat{\Sigma}_{hk}$.

Remark 4.2.1. This follows by noting that since the columns of $\nabla F_{\widehat{K}_h}^T$ span the tangential space of Γ_h^k, we have $\nabla F_{\widehat{K}_h}^T \widehat{\nu}_h = 0$. Combining this with the definition of

the (left) pseudo-inverse, we straighforwardly have that $\nabla F_{\widehat{K}_h}^{-1}\widehat{\nu}_h = 0$ which can be rewritten as $\widehat{\nu}_h^T \nabla F_{\widehat{K}_h}^{-T} = 0$. Now $\mathbf{P}_{hk}\nabla F_{\widehat{K}_h}^{-T}\eta = \nabla F_{\widehat{K}_h}^{-T}\eta - (\widehat{\nu}_h^T \nabla F_{\widehat{K}_h}^{-T}\eta)\widehat{\nu}_h = \nabla F_{\widehat{K}_h}^{-T}\eta$ for all η.

4.2.2 Primal formulation

Following the lines of Arnold et al. [2002] as outlined in Chapter 3, we wish to find $(u_h, \sigma_h) \in \widehat{S}_{hk} \times \widehat{\Sigma}_{hk}$ such that

$$\int_{\widehat{K}_h} \sigma_h \cdot w_h \ \mathrm{dA_{hk}} = -\int_{\widehat{K}_h} u_h \nabla_{\Gamma_h^k} \cdot w_h \ \mathrm{dA_{hk}} + \int_{\partial \widehat{K}_h} \widehat{u}\ w_h \cdot n_{\widehat{K}_h} \ \mathrm{ds_{hk}},$$
$$\int_{\widehat{K}_h} \sigma_h \cdot \nabla_{\Gamma_h^k} v_h + u_h v_h \ \mathrm{dA_{hk}} = \int_{\widehat{K}_h} f_h v_h \ \mathrm{dA_{hk}} + \int_{\partial \widehat{K}_h} \widehat{\sigma} \cdot n_{\widehat{K}_h}\ v_h \ \mathrm{ds_{hk}},$$

for all $w_h \in \widehat{\Sigma}_{hk}$, $v_h \in \widehat{S}_{hk}$, where $\mathrm{dA_{hk}}$ and $\mathrm{ds_{hk}}$ denote respectively the two and one dimensional surface measures over Γ_h^k and the discrete right-hand side $f_h \in L^2(\Gamma_h^k)$ will be related to f in Section 4.3.1. Here $\widehat{u} = \widehat{u}(u_h)$ and $\widehat{\sigma} = \widehat{\sigma}(u_h, \sigma_h(u_h))$ are the so called numerical fluxes which determine the inter-element behaviour of the solution and will be prescribed later on.

In order to deal with these terms, we need to introduce the following discrete surface trace operators:

Definition 4.2.2. Suppose there is an element numbering for all $\widehat{K}_h \in \widehat{\mathcal{T}}_h$. For $q \in \Pi_{\widehat{K}_h \in \widehat{\mathcal{T}}_h} L^2(\partial \widehat{K}_h)$, $\{q\}$ and $[q]$ are given by

$$\{q\} := \frac{1}{2}(q^+ + q^-), \ [q] := q^+ - q^- \text{ on } \widehat{e}_h \in \widehat{\mathcal{E}}_h.$$

For $\phi, \tilde{n} \in [\Pi_{\widehat{K}_h \in \widehat{\mathcal{T}}_h} L^2(\partial \widehat{K}_h)]^3$, $\{\phi; \tilde{n}\}$ and $[\phi; \tilde{n}]$ are given by

$$\{\phi; \tilde{n}\} := \frac{1}{2}(\phi^+ \cdot \tilde{n}^+ - \phi^- \cdot \tilde{n}^-), \quad [\phi; \tilde{n}] := \phi^+ \cdot \tilde{n}^+ + \phi^- \cdot \tilde{n}^- \quad \text{on } \widehat{e}_h \in \widehat{\mathcal{E}}_h.$$

We now state and prove a useful formula which holds for functions in

$$H^1(\widehat{\mathcal{T}}_h) := \{v|_{\widehat{K}_h} \in H^1(\widehat{K}_h) \ : \ \forall \widehat{K}_h \in \widehat{\mathcal{T}}_h\}.$$

Lemma 4.2.3. *Let $\phi \in [H^1(\widehat{\mathcal{T}}_h)]^3$ and $\psi \in H^1(\widehat{\mathcal{T}}_h)$. Then we have that*

$$\sum_{\widehat{K}_h \in \widehat{\mathcal{T}}_h} \int_{\partial \widehat{K}_h} \psi \phi \cdot n_{\widehat{K}_h} \ ds_{hk} = \sum_{\widehat{e}_h \in \widehat{\mathcal{E}}_h} \int_{\widehat{e}_h} [\phi; \widehat{n}_h]\{\psi\} + \{\phi; \widehat{n}_h\}[\psi] \ ds_{hk}.$$

Proof. The result follows straightforwardly by noting that

$$\begin{aligned}\sum_{\widehat{K}_h\in\widehat{\mathcal{T}}_h}\int_{\partial\widehat{K}_h}\psi\phi\cdot n_{\widehat{K}_h}\,\mathrm{dS_{hk}} &= \sum_{\widehat{e}_h\in\widehat{\mathcal{E}}_h}\int_{\widehat{e}_h}[\psi\phi;\widehat{n}_h]\,\mathrm{dS_{hk}}\\ &= \sum_{\widehat{e}_h\in\widehat{\mathcal{E}}_h}\int_{\widehat{e}_h}[\phi;\widehat{n}_h]\{\psi\}+\{\phi;\widehat{n}_h\}[\psi]\,\mathrm{dS_{hk}}.\end{aligned}$$

□

Remark 4.2.4. Note that the way we have defined our trace operators is in line with the classical approach to DG methods, considered for example in Arnold [1982], rather than the modern approach considered in Arnold et al. [2002], in which the analogue of Lemma 4.2.3 (given in (3.5)) requires that $\widehat{n}_h^+ = -\widehat{n}_h^-$.

Applying the above lemma, summing over all elements and proceeding in a similar fashion to the planar case setting outlined in Chapter 3, we obtain

$$\begin{aligned}\sum_{\widehat{K}_h\in\widehat{\mathcal{T}}_h}\int_{\widehat{K}_h}\sigma_h\cdot w_h\,\mathrm{dA_{hk}} &= \sum_{\widehat{K}_h\in\widehat{\mathcal{T}}_h}\int_{\widehat{K}_h}\nabla_{\Gamma_h^k}u_h\cdot w_h\,\mathrm{dA_{hk}}\\ &\quad+\sum_{\widehat{e}_h\in\widehat{\mathcal{E}}_h}\int_{\widehat{e}_h}[\widehat{u}-u_h]\{w_h;\widehat{n}_h\}+\{\widehat{u}-u_h\}[w_h;\widehat{n}_h]\,\mathrm{dS_{hk}},\end{aligned}\tag{4.2}$$

$$\begin{aligned}\sum_{\widehat{K}_h\in\widehat{\mathcal{T}}_h}\int_{\widehat{K}_h}\sigma_h\cdot\nabla_{\Gamma_h^k}v_h+u_hv_h\,\mathrm{dA_{hk}} &= \sum_{\widehat{K}_h\in\widehat{\mathcal{T}}_h}\int_{\widehat{K}_h}f_hv_h\,\mathrm{dA_{hk}}\\ &\quad+\sum_{\widehat{e}_h\in\widehat{\mathcal{E}}_h}\int_{\widehat{e}_h}\Big(\{\widehat{\sigma};\widehat{n}_h\}[v_h]+[\widehat{\sigma};\widehat{n}_h]\{v_h\}\Big)\,\mathrm{dS_{hk}},\end{aligned}\tag{4.3}$$

for every $w_h\in\widehat{\Sigma}_{hk}$ and $v_h\in\widehat{S}_{hk}$.

We now introduce the DG lift operators $r_{\widehat{e}_h}:L^2(\widehat{\mathcal{E}}_h)\to\widehat{\Sigma}_{hk}$ and $l_{\widehat{e}_h}:L^2(\widehat{\mathcal{E}}_h)\to\widehat{\Sigma}_{hk}$ which satisfy

$$\int_{\Gamma_h^k}r_{\widehat{e}_h}(\phi)\cdot\tau_h\,\mathrm{dA_{hk}} = -\int_{\widehat{e}_h}\phi\{\tau_h;\widehat{n}_h\}\,\mathrm{dS_{hk}}\quad\forall\tau_h\in\widehat{\Sigma}_{hk},$$

$$\int_{\Gamma_h^k}l_{\widehat{e}_h}(q)\cdot\tau_h\,\mathrm{dA_{hk}} = -\int_{\widehat{e}_h}q[\tau_h;\widehat{n}_h]\,\mathrm{dS_{hk}}\quad\forall\tau_h\in\widehat{\Sigma}_{hk},$$

and $r_h : L^2(\widehat{\mathcal{E}}_h) \to \widehat{\Sigma}_{hk}$ and $l_h : L^2(\widehat{\mathcal{E}}_h) \to \widehat{\Sigma}_{hk}$, given by

$$r_h(\phi) = \sum_{\widehat{e}_h \in \widehat{\mathcal{E}}_h} r_{\widehat{e}_h}(\phi), \qquad l_h(\phi) = \sum_{\widehat{e}_h \in \widehat{\mathcal{E}}_h} l_{\widehat{e}_h}(\phi).$$

Existence of such operators follow standard arguments. Using these, we can write σ_h solely in terms of u_h. Indeed, on each element $\widehat{K}_h \in \widehat{\mathcal{T}}_h$ we obtain from (4.2) that

$$\sigma_h = \sigma_h(u_h) = \nabla_{\Gamma_h^k} u_h - r_h([\widehat{u}(u_h) - u_h]) - l_h(\{\widehat{u}(u_h) - u_h\}). \tag{4.4}$$

Note that (4.4) does in fact imply that $\sigma_h \in \widehat{\Sigma}_{hk}$ as $\nabla_{\Gamma_h^k} u_h \in \widehat{\Sigma}_{hk}$ and $r_h, l_h \in \widehat{\Sigma}_{hk}$ by construction. Taking $w_h = \nabla_{\Gamma_h^k} v_h$ in (4.2), substituting the resulting expression into (4.3) and using (4.4), we obtain the primal formulation: find $(u_h, \sigma_h) \in \widehat{S}_{hk} \times \widehat{\Sigma}_{hk}$ such that

$$\mathcal{A}_h^k(u_h, v_h) = \sum_{\widehat{K}_h \in \widehat{\mathcal{T}}_h} \int_{\widehat{K}_h} f_h v_h \ \mathrm{dA_{hk}} \quad \forall v_h \in \widehat{S}_{hk}, \tag{4.5}$$

where

$$\begin{aligned}
\mathcal{A}_h^k(u_h, v_h) = &\sum_{\widehat{K}_h \in \widehat{\mathcal{T}}_h} \int_{\widehat{K}_h} \nabla_{\Gamma_h^k} u_h \cdot \nabla_{\Gamma_h^k} v_h + u_h v_h \ \mathrm{dA_{hk}} \\
&+ \sum_{\widehat{e}_h \in \widehat{\mathcal{E}}_h} \int_{\widehat{e}_h} \Big([\widehat{u} - u_h]\{\nabla_{\Gamma_h^k} v_h; \widehat{n}_h\} - \{\widehat{\sigma}; \widehat{n}_h\}[v_h] \Big) \ \mathrm{ds_{hk}} \\
&+ \sum_{\widehat{e}_h \in \widehat{\mathcal{E}}_h} \int_{\widehat{e}_h} \Big(\{\widehat{u} - u_h\}[\nabla_{\Gamma_h^k} v_h; \widehat{n}_h] - [\widehat{\sigma}; \widehat{n}_h]\{v_h\} \Big) \ \mathrm{ds_{hk}}.
\end{aligned} \tag{4.6}$$

4.2.3 Examples of surface DG methods

For the following methods we introduce the penalization coefficients $\eta_{\widehat{e}_h}$ and $\beta_{\widehat{e}_h}$, given by

$$\eta_{\widehat{e}_h} := \alpha, \quad \beta_{\widehat{e}_h} := \alpha k^2 h_{\widehat{e}_h}^{-1}, \tag{4.7}$$

where $\alpha > 0$ is a parameter at our disposal.

Surface Bassi-Rebay method

To derive the surface Bassi-Rebay method, based on Bassi and Rebay [1997], we choose

$$\begin{aligned} \widehat{u}^+ &= \{u_h\}, & \widehat{u}^- &= \{u_h\}, \\ \widehat{\sigma}^+ &= \{\sigma_h; \widehat{n}_h\}\widehat{n}_h^+, & \widehat{\sigma}^- &= -\{\sigma_h; \widehat{n}_h\}\widehat{n}_h^-. \end{aligned}$$

From (4.4) we obtain $\sigma_h = \nabla_{\Gamma_h^k} u_h + r_h([u_h])$ and

$$\begin{aligned} &\sum_{\widehat{e}_h \in \widehat{\mathcal{E}}_h} \int_{\widehat{e}_h} \{\widehat{\sigma}; \widehat{n}_h\}[v_h] \, \mathrm{ds_{hk}} \\ &\qquad = \sum_{\widehat{e}_h \in \widehat{\mathcal{E}}_h} \int_{\widehat{e}_h} \{\sigma_h; \widehat{n}_h\}[v_h] \, \mathrm{ds_{hk}} \\ &\qquad = \sum_{\widehat{e}_h \in \widehat{\mathcal{E}}_h} \int_{\widehat{e}_h} \{\nabla_{\Gamma_h^k} u_h; \widehat{n}_h\}[v_h] \, \mathrm{ds_{hk}} + \sum_{\widehat{e}_h \in \widehat{\mathcal{E}}_h} \int_{\widehat{e}_h} \{r_h([u_h]); \widehat{n}_h\}[v_h] \, \mathrm{ds_{hk}} \\ &\qquad = \sum_{\widehat{e}_h \in \widehat{\mathcal{E}}_h} \int_{\widehat{e}_h} \{\nabla_{\Gamma_h^k} u_h; \widehat{n}_h\}[v_h] \, \mathrm{ds_{hk}} - \sum_{\widehat{K}_h \in \widehat{\mathcal{T}}_h} \int_{\widehat{K}_h} r_h([u_h]) \cdot r_h([v_h]) \, \mathrm{dA_{hk}}. \end{aligned}$$

Therefore, making use of the fact that $\{\widehat{u} - u_h\} = 0$, $[\widehat{u} - u_h] = [u_h]$ and $[\widehat{\sigma}; \widehat{n}_h] = 0$, we have that

$$\begin{aligned} \mathcal{A}_h^k(u_h, v_h) = &\sum_{\widehat{K}_h \in \widehat{\mathcal{T}}_h} \int_{\widehat{K}_h} \left(\nabla_{\Gamma_h^k} u_h \cdot \nabla_{\Gamma_h^k} v_h + u_h v_h + r_h([u_h]) \cdot r_h([v_h]) \right) \mathrm{dA_{hk}} \\ &- \sum_{\widehat{e}_h \in \widehat{\mathcal{E}}_h} \int_{\widehat{e}_h} \left(\{\nabla_{\Gamma_h^k} u_h; \widehat{n}_h\}[v_h] + \{\nabla_{\Gamma_h^k} v_h; \widehat{n}_h\}[u_h] \right) \mathrm{ds_{hk}}. \end{aligned} \tag{4.8}$$

Surface Brezzi et al. method

For the surface Brezzi et al. method, based on Brezzi et al. [1999], we choose

$$\begin{aligned} \widehat{u}^+ &= \{u_h\}, & \widehat{u}^- &= \{u_h\}, \\ \widehat{\sigma}^+ &= \{\sigma_h + \eta_{\widehat{e}_h} r_{\widehat{e}_h}([u_h]); \widehat{n}_h\}\widehat{n}_h^+, & \widehat{\sigma}^- &= -\{\sigma_h + \eta_{\widehat{e}_h} r_{\widehat{e}_h}([u_h]); \widehat{n}_h\}\widehat{n}_h^-, \end{aligned}$$

The method is similar to that of Bassi-Rebay, but with an additional term. Indeed,

$$
\begin{aligned}
&\sum_{\widehat{e}_h\in\widehat{\mathcal{E}}_h}\int_{\widehat{e}_h}\{\widehat{\sigma};\widehat{n}_h\}[v_h]\ \mathrm{ds_{hk}}\\
&\quad=\sum_{\widehat{e}_h\in\widehat{\mathcal{E}}_h}\int_{\widehat{e}_h}\{\sigma_h+\eta_{\widehat{e}_h}r_{\widehat{e}_h}([u_h]);\widehat{n}_h\}[v_h]\ \mathrm{ds_{hk}}\\
&\quad=\sum_{\widehat{e}_h\in\widehat{\mathcal{E}}_h}\int_{\widehat{e}_h}\{\nabla_{\Gamma_h^k}u_h;\widehat{n}_h\}[v_h]+\{r_h([u_h])+\eta_{\widehat{e}_h}r_{\widehat{e}_h}([u_h]);\widehat{n}_h\}[v_h]\ \mathrm{ds_{hk}}\\
&\quad=\sum_{\widehat{e}_h\in\widehat{\mathcal{E}}_h}\int_{\widehat{e}_h}\{\nabla_{\Gamma_h^k}u_h;\widehat{n}_h\}[v_h]\ \mathrm{ds_{hk}}-\sum_{\widehat{K}_h\in\widehat{\mathcal{T}}_h}\int_{\widehat{K}_h}r_h([u_h])\cdot r_h([v_h])\ \mathrm{dA_{hk}}\\
&\qquad-\sum_{\widehat{K}_h\in\widehat{\mathcal{T}}_h}\int_{\widehat{K}_h}\eta_{\widehat{e}_h}r_{\widehat{e}_h}([u_h])\cdot r_{\widehat{e}_h}([v_h])\ \mathrm{dA_{hk}}.
\end{aligned}
$$

Then

$$
\begin{aligned}
\mathcal{A}_h^k(u_h,v_h)=&\sum_{\widehat{K}_h\in\widehat{\mathcal{T}}_h}\int_{\widehat{K}_h}\nabla_{\Gamma_h^k}u_h\cdot\nabla_{\Gamma_h^k}v_h+u_hv_h\ \mathrm{dA_{hk}}\\
&-\sum_{\widehat{e}_h\in\widehat{\mathcal{E}}_h}\int_{\widehat{e}_h}\{\nabla_{\Gamma_h^k}u_h;\widehat{n}_h\}[v_h]+\{\nabla_{\Gamma_h^k}v_h;\widehat{n}_h\}[u_h]\ \mathrm{ds_{hk}}\\
&+\sum_{\widehat{K}_h\in\widehat{\mathcal{T}}_h}\int_{\widehat{K}_h}r_h([u_h])\cdot r_h([v_h])+\eta_{\widehat{e}_h}r_{\widehat{e}_h}([u_h])\cdot r_{\widehat{e}_h}([v_h])\ \mathrm{dA_{hk}}.
\end{aligned}
\tag{4.9}
$$

Surface IP method

To derive the surface IP method, based on Douglas and Dupont [1976]; Baker [1977]; Arnold [1982], we choose the numerical fluxes $\widehat{u}$ and $\widehat{\sigma}$ as follows:

$$
\begin{aligned}
\widehat{u}^+&=\{u_h\}, & \widehat{u}^-&=\{u_h\},\\
\widehat{\sigma}^+&=\Big(\{\nabla_{\Gamma_h^k}u_h;\widehat{n}_h\}-\beta_{\widehat{e}_h}[u_h]\Big)\widehat{n}_h^+, & \widehat{\sigma}^-&=-\Big(\{\nabla_{\Gamma_h^k}u_h;\widehat{n}_h\}-\beta_{\widehat{e}_h}[u_h]\Big)\widehat{n}_h^-.
\end{aligned}
$$

Substituting them into (4.6), we obtain

$$
\begin{aligned}
\mathcal{A}_h^k(u_h,v_h)=&\sum_{\widehat{K}_h\in\widehat{\mathcal{T}}_h}\int_{\widehat{K}_h}\nabla_{\Gamma_h^k}u_h\cdot\nabla_{\Gamma_h^k}v_h+u_hv_h\ \mathrm{dA_{hk}}+\sum_{\widehat{e}_h\in\widehat{\mathcal{E}}_h}\int_{\widehat{e}_h}\beta_{\widehat{e}_h}[u_h][v_h]\ \mathrm{ds_{hk}}\\
&-\sum_{\widehat{e}_h\in\widehat{\mathcal{E}}_h}\int_{\widehat{e}_h}\big([u_h]\{\nabla_{\Gamma_h^k}v_h;\widehat{n}_h\}+[v_h]\{\nabla_{\Gamma_h^k}u_h;\widehat{n}_h\}\big)\ \mathrm{ds_{hk}}.
\end{aligned}
\tag{4.10}
$$

Surface NIPG method

For the surface NIPG method, based on Rivière et al. [1999] (or equivalently the Baumann-Oden method in Baumann and Oden [1998] with $\beta_{\widehat{e}_h} = 0$), we choose

$$\begin{aligned} \widehat{u}^+ &= \{u_h\} + [u_h], & \widehat{u}^- &= \{u_h\} - [u_h], \\ \widehat{\sigma}^+ &= \Big(\{\nabla_{\Gamma_h^k} u_h; \widehat{n}_h\} - \beta_{\widehat{e}_h}[u_h]\Big)\widehat{n}_h^+, & \widehat{\sigma}^- &= -\Big(\{\nabla_{\Gamma_h^k} u_h; \widehat{n}_h\} - \beta_{\widehat{e}_h}[u_h]\Big)\widehat{n}_h^-. \end{aligned}$$

We may derive the surface NIPG bilinear form in a similar way as for the surface IP method.

Surface IIPG method

For the surface IIPG method, based on Dawson et al. [2004], we choose the numerical fluxes $\widehat{u}$ and $\widehat{\sigma}$ as follows:

$$\begin{aligned} \widehat{u}^+ &= u_h^+, & \widehat{u}^- &= u_h^-, \\ \widehat{\sigma}^+ &= \Big(\{\nabla_{\Gamma_h^k} u_h; \widehat{n}_h\} - \beta_{\widehat{e}_h}[u_h]\Big)\widehat{n}_h^+, & \widehat{\sigma}^- &= -\Big(\{\nabla_{\Gamma_h^k} u_h; \widehat{n}_h\} - \beta_{\widehat{e}_h}[u_h]\Big)\widehat{n}_h^-. \end{aligned}$$

Here again, we may derive the surface IIPG bilinear form in a similar way as for the surface IP method.

Surface Bassi et al. method

For the surface Bassi et al. method, based on Bassi et al. [1997], we choose

$$\begin{aligned} \widehat{u}^+ &= \{u_h\}, & \widehat{u}^- &= \{u_h\}, \\ \widehat{\sigma}^+ &= \Big(\{\nabla_{\Gamma_h^k} u_h + \eta_{\widehat{e}_h} r_{\widehat{e}_h}([u_h]); \widehat{n}_h\}\Big)\widehat{n}_h^+, & \widehat{\sigma}^- &= -\Big(\{\nabla_{\Gamma_h^k} u_h + \eta_{\widehat{e}_h} r_{\widehat{e}_h}([u_h]); \widehat{n}_h\}\Big)\widehat{n}_h^-. \end{aligned}$$

The resulting bilinear form can be easily obtained in a similar way as for the surface IP and surface Brezzi et al. bilinear forms.

Surface LDG method

Finally for the surface LDG method, based on Cockburn and Shu [1998], the numerical fluxes are chosen as follows:

$$\begin{aligned}
\widehat{u}^{+} &= \{u_h\} - \beta \cdot \widehat{n}_h^{+}[u_h], \quad \widehat{u}^{-} = \{u_h\} - \beta \cdot \widehat{n}_h^{+}[u_h], \\
\widehat{\sigma}^{+} &= \Big(\{\sigma_h; \widehat{n}_h\} - \beta_{\widehat{e}_h}[u_h] + \beta \cdot \widehat{n}_h^{+}[\sigma_h; \widehat{n}_h]\Big)\widehat{n}_h^{+}, \\
\widehat{\sigma}^{-} &= -\Big(\{\sigma_h; \widehat{n}_h\} - \beta_{\widehat{e}_h}[u_h] + \beta \cdot \widehat{n}_h^{+}[\sigma_h; \widehat{n}_h]\Big)\widehat{n}_h^{-},
\end{aligned}$$

where $\beta \in [L^{\infty}(\Gamma_h^k)]^3$ is a (possibly null) constant on each edge $\widehat{e}_h \in \widehat{\mathcal{E}}_h$. We see that $\{\widehat{u} - u_h\} = -\beta \cdot \widehat{n}_h^{+}[u_h]$ and $[\widehat{u} - u_h] = -[u_h]$. So, from (4.4), we obtain:

$$\begin{aligned}
\widehat{\sigma}^{+} = \Big(&\{\nabla_{\Gamma_h^k} u_h; \widehat{n}_h\} + \{r_h([u_h]); \widehat{n}_h\} + \{\beta \cdot \widehat{n}_h^{+} l_h([u_h]); \widehat{n}_h\} - \beta_{\widehat{e}_h}[u_h] \\
&+ \beta \cdot \widehat{n}_h^{+}\Big([\nabla_{\Gamma_h^k} u_h; \widehat{n}_h] + [r_h([u_h]); \widehat{n}_h] + [\beta \cdot \widehat{n}_h^{+} l_h([u_h]); \widehat{n}_h]\Big)\Big)\widehat{n}_h^{+},
\end{aligned}$$

and in a similar way $\widehat{\sigma}^{-}$. Then

$$\begin{aligned}
&\sum_{\widehat{e}_h \in \widehat{\mathcal{E}}_h^k} \int_{\widehat{e}_h} \{\widehat{\sigma}; \widehat{n}_h\}[v_h] \, \mathrm{ds_{hk}} \\
&\quad = \sum_{\widehat{e}_h \in \widehat{\mathcal{E}}_h^k} \int_{\widehat{e}_h} \Big(\{\nabla_{\Gamma_h^k} u_h; \widehat{n}_h\}[v_h] + [\nabla_{\Gamma_h^k} u_h; \widehat{n}_h]\beta \cdot \widehat{n}_h^{+}[v_h] - \beta_{\widehat{e}_h}[u_h][v_h]\Big) \, \mathrm{ds_{hk}} \\
&\quad - \sum_{\widehat{K}_h \in \widehat{\mathcal{T}}_h} \int_{\widehat{K}_h} \Big(r_h([u_h]) + \beta \cdot \widehat{n}_h^{+} l_h\big([u_h]\big)\Big) \cdot \Big(r_h([v_h]) + \beta \cdot \widehat{n}_h^{+} l_h\big([v_h]\big)\Big) \, \mathrm{dA_{hk}},
\end{aligned}$$

and the surface LDG form can be written as

$$\begin{aligned}
\mathcal{A}_h^k(u_h, v_h) = &\sum_{\widehat{K}_h \in \widehat{\mathcal{T}}_h} \int_{\widehat{K}_h} \nabla_{\Gamma_h^k} u_h \cdot \nabla_{\Gamma_h^k} v_h + u_h v_h \, \mathrm{dA_{hk}} \\
&- \sum_{\widehat{e}_h \in \widehat{\mathcal{E}}_h} \int_{\widehat{e}_h} [u_h]\{\nabla_{\Gamma_h^k} v_h; \widehat{n}_h\} - \{\nabla_{\Gamma_h^k} u_h; \widehat{n}_h\}[v_h] \, \mathrm{ds_{hk}} \\
&+ \sum_{\widehat{e}_h \in \widehat{\mathcal{E}}_h} \int_{\widehat{e}_h} \Big(- [\nabla_{\Gamma_h^k} u_h; \widehat{n}_h]\beta \cdot \widehat{n}_h^{+}[v_h] - \beta \cdot \widehat{n}_h^{+}[u_h][\nabla_{\Gamma_h^k} v_h; \widehat{n}_h] + \beta_{\widehat{e}_h}[u_h][v_h]\Big) \, \mathrm{ds_{hk}} \\
&+ \sum_{\widehat{K}_h \in \widehat{\mathcal{T}}_h} \int_{\widehat{K}_h} \Big(r_h([u_h]) + \beta \cdot \widehat{n}_h^{+} l_h\big([u_h]\big)\Big) \cdot \Big(r_h([v_h]) + \beta \cdot \widehat{n}_h^{+} l_h\big([v_h]\big)\Big) \, \mathrm{dA_{hk}}. \quad (4.11)
\end{aligned}$$

Remark 4.2.5. Notice that for all of our choices of the numerical fluxes $\widehat{u}$ and $\widehat{\sigma}$, we have that $[\![\widehat{u}]\!] = 0$ and $[\![\widehat{\sigma}; \widehat{n}_h]\!] = 0$. In addition, they are consistent with the corresponding fluxes in the flat case given in Chapter 3 and Arnold et al. [2002], with the exception of the fluxes for the surface LDG method which cannot be combined in the same way to obtain the corresponding LDG fluxes in the flat case due to the fact that the trace operators are scalars. On the other hand, in the flat case (for which we have $\widehat{n}_h^+ = -\widehat{n}_h^-$), all of the surface DG methods yield the corresponding ones found in Chapter 3 and Arnold et al. [2002]. This can be seen by noticing that $\{\cdot; n_h\}[\cdot] = \{\{\cdot\}\} \cdot [\![\cdot]\!]$ and that $[\cdot][\cdot] = [\![\cdot]\!] \cdot [\![\cdot]\!]$ in the flat case, where the operators $[\![\cdot]\!]$ and $\{\{\cdot\}\}$ are defined in Chapter 3. On discrete surfaces however, these equalities no longer hold.

4.3 Technical tools

In this section we recall from Chapter 2 some of the tools and geometric relations required to work on discrete surfaces, applying them to the new setting of surface DG methods posed on higher order discrete surface approximations. In addition, we prove boundedness and stability of the surface DG bilinear forms.

4.3.1 Surface lift

Recall from Chapter 2 that for any function w defined on Γ_h^k we define the surface *lift* onto Γ by

$$w^\ell(\xi) = w(x(\xi)), \ \xi \in \Gamma$$

with $\xi = \xi(x)$ given by (2.1) and where, as before, $x(\xi)$ is defined as the unique solution of

$$x(\xi) = \xi(x) + d(x)\nu(\xi).$$

In particular, for every $\widehat{K}_h \in \widehat{\mathcal{T}}_h$, there is a unique curved triangle $\widehat{K}_h^\ell = \xi(\widehat{K}_h) \subset \Gamma$. We may then define a regular, conforming triangulation $\widehat{\mathcal{T}}_h^\ell$ of Γ, given by

$$\Gamma = \bigcup_{\widehat{K}_h^\ell \in \widehat{\mathcal{T}}_h^\ell} \widehat{K}_h^\ell.$$

The triangulation $\widehat{\mathcal{T}}_h^\ell$ of Γ is thus induced by the triangulation $\widehat{\mathcal{T}}_h$ of Γ_h^k via the surface lift operator. Similarly, we denote by $\widehat{e}_h^\ell = \xi(\widehat{e}_h) \in \widehat{\mathcal{E}}_h^\ell$ the unique curved edge associated to $\widehat{e}_h$. The function space for surface lifted functions is chosen to

be given by

$$\widehat{S}_{hk}^{\ell} = \{\chi \in L^2(\Gamma) : \chi = \widehat{\chi}^{\ell} \text{ for some } \widehat{\chi} \in \widehat{S}_{hk}\}.$$

As in (2.9), we define the discrete right-hand side f_h of (4.5) such that $f_h^{\ell} = f$. We also denote by $w^{-\ell} \in \widehat{S}_{hk}$ the *inverse* surface lift of some function $w \in \widehat{S}_{hk}^{\ell}$, satisfying $(w^{-\ell})^{\ell} = w$.

One can show that for v_h defined on Γ_h^k, we have that

$$\nabla_{\Gamma_h^k} v_h = \mathbf{P}_{hk}(x)(\mathbf{I} - d\mathbf{H})(x)\mathbf{P}(x)\nabla_{\Gamma} v_h^{\ell}(\xi(x)).$$

Furthermore, let δ_{hk} be the local area deformation when transforming $\widehat{K}_h$ to $\widehat{K}_h^{\ell}$, i.e.,

$$\delta_{hk}(x)\ \mathrm{dA_{hk}}(x) = \ \mathrm{dA}(\xi(x)),$$

and finally, let $\delta_{\widehat{e}_h}$ be the local edge deformation when transforming $\widehat{e}_h$ to $\widehat{e}_h^{\ell}$, i.e.,

$$\delta_{\widehat{e}_h}(x)\ \mathrm{ds_{hk}}(x) = \ \mathrm{ds}(\xi(x)).$$

Finally, let

$$\mathbf{R}_{hk}(x) = \mathbf{R}_{hk}^{l}(\xi(x)) = \delta_{hk}^{-1}(x)\mathbf{P}(x)(\mathbf{I} - d\mathbf{H})(x)\mathbf{P}_{hk}(x)(\mathbf{I} - d\mathbf{H})(x)\mathbf{P}(x). \tag{4.12}$$

Then one can show that

$$\int_{\Gamma_h^k} \nabla_{\Gamma_h^k} u_h \cdot \nabla_{\Gamma_h^k} v_h + u_h v_h \ \mathrm{dA_{hk}} = \int_{\Gamma} \mathbf{R}_{hk}\nabla_{\Gamma} u_h^{\ell} \cdot \nabla_{\Gamma} v_h^{\ell} + \delta_{hk}^{-1} u_h^{\ell} v_h^{\ell} \ \mathrm{dA}. \tag{4.13}$$

4.3.2 Geometric estimates

We next prove some geometric error estimates relating Γ to Γ_h^k. Given the importance of the following lemma, we restate it in Appendix A for the convenience of the reader.

Lemma 4.3.1. *Let Γ be a compact smooth and oriented surface in $\mathbb{R}^3$ and let Γ_h^k be its Lagrange interpolant of degree k. Furthermore, we denote by $n^{+/-}$ the unit (surface) conormals to respectively $\widehat{e}_h^{l+/-}$. Then, omitting the surface lift symbols,*

we have that

$$\|d\|_{L^\infty(\Gamma_h^k)} \lesssim h^{k+1}, \tag{4.14a}$$

$$\|1-\delta_{hk}\|_{L^\infty(\Gamma_h^k)} \lesssim h^{k+1}, \tag{4.14b}$$

$$\|\nu-\widehat{\nu}_h\|_{L^\infty(\Gamma_h^k)} \lesssim h^{k}, \tag{4.14c}$$

$$\|\mathbf{P}-\mathbf{R}_{hk}\|_{L^\infty(\Gamma_h^k)} \lesssim h^{k+1}, \tag{4.14d}$$

$$\|1-\delta_{\widehat{e}_h}\|_{L^\infty(\widehat{\mathcal{E}}_h)} \lesssim h^{k+1}, \tag{4.14e}$$

$$\sup_{\widehat{K}\in\widehat{\mathcal{T}}_h} \|\mathbf{P}-\mathbf{R}_{\widehat{e}_h}\|_{L^\infty(\partial\widehat{K}_h)} \lesssim h^{k+1}, \tag{4.14f}$$

$$\|n^{+/-}-\mathbf{P}\widehat{n}_h^{+/-}\|_{L^\infty(\widehat{\mathcal{E}}_h)} \lesssim h^{k+1}, \tag{4.14g}$$

for sufficiently small h, where $\mathbf{R}_{\widehat{e}_h}=\delta_{\widehat{e}_h}^{-1}\mathbf{P}(\mathbf{I}-d\mathbf{H})\mathbf{P}_{hk}(\mathbf{I}-d\mathbf{H})$.

Proof of Lemma 4.3.1. Proofs of (4.14a)-(4.14d) can be found in Proposition 2.3 and Proposition 4.1 in Demlow [2009]. The proof of (4.14f) will follow exactly the same lines as (4.14d) once we have proven (4.14e). Let e, K be the reference segment [0,1] and the (flat) reference element, respectively, and let K_h, $\widehat{K}_h$ and $\widehat{K}_h^\ell$ be elements in Γ_h, Γ_h^k and Γ, respectively, such that $\xi_k(K_h)=\widehat{K}_h$ and $\xi(\widehat{K}_h)=\widehat{K}_h^\ell$. Let also L_e be the inclusion operator that maps e into an edge of K and let $L_{K_h}(K)=K_h$. In what follows, all geometric operators and quantities are implicitely considered

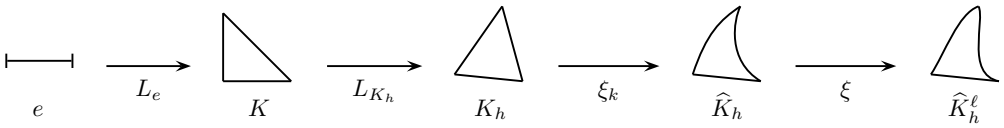

Figure 4.2: Mappings used in the proof of Lemma 4.3.1.

as being evaluated either at a point $\widehat{x}\in\widehat{e}_h\subset\partial\widehat{K}_h$ (if on the discrete surface Γ_h^k) or at a point $\widehat{x}^l:=\xi(\widehat{x})\in\widehat{e}_h^l\subset\partial\widehat{K}_h^l$ (if on the smooth surface Γ), omitting the evaluation operator for notational simplicity. A tangent on such an edge $\widehat{e}_h$ is given by $\widehat{\tau}_h=\nabla(\xi_k\circ L_{K_h}\circ L_e)$. Analogously, a tangent on the corresponding surface lifted edge $\widehat{e}_h^\ell$ is given by $\tau=\nabla\xi\widehat{\tau}_h$. We denote by $\underline{\widehat{\tau}}_h$ and $\underline{\tau}$ respectively the unit tangents of $\widehat{e}_h$ and $\widehat{e}_h^\ell$, and let $\lambda=\|\widehat{\tau}_h\|_{l^2}$. We will now prove estimate (4.14e). Let dx be the

Lebesgue measure on the reference interval e. We then have that

$$\begin{aligned}\mathrm{ds_{hk}} &= \lambda \ \mathrm{dx},\\ \mathrm{ds} &= \sqrt{\|(\nabla\xi\widehat{\tau}_h)^T\cdot\nabla\xi\widehat{\tau}_h\|_{l^2}}\ \mathrm{dx} = \lambda\sqrt{\|(\nabla\xi\widehat{\underline{\tau}}_h)^T\cdot\nabla\xi\widehat{\underline{\tau}}_h\|_{l^2}}\ \mathrm{dx} = \underbrace{\|\nabla\xi\widehat{\underline{\tau}}_h\|_{l^2}}_{\delta_{\widehat{e}_h}}\ \mathrm{ds_{hk}}.\end{aligned}$$

Having characterised $\delta_{\widehat{e}_h}$, we wish to show that

$$1 - Ch^{k+1} \leq \|\nabla\xi\widehat{\underline{\tau}}_h\|_{l^2} \leq 1 + Ch^{k+1}.$$

Making use of (2.3) and (4.14a), we have that

$$\|\nabla\xi\widehat{\underline{\tau}}_h\|_{l^2} \leq \|\nabla\xi\|_{l^2}\|\widehat{\underline{\tau}}_h\|_{l^2} \leq \|\mathbf{P} - d\mathbf{H}\|_{l^2} \leq 1 + Ch^{k+1}. \tag{4.15}$$

Next, to provide a lower bound for $\|\nabla\xi\widehat{\underline{\tau}}_h\|_{l^2}$, we consider

$$\tau - \widehat{\tau}_h = (\nabla\xi - \mathbf{P}_{hk})\widehat{\tau}_h = \lambda(\nabla\xi - \mathbf{P}_{hk})\widehat{\underline{\tau}}_h.$$

Recalling the definition of the projection matrices $\mathbf{P}$ and $\mathbf{P}_{hk}$, we have that

$$\|\tau - \widehat{\tau}_h\|_{l^2} \leq \lambda\|(\mathbf{P} - \mathbf{P}_{hk}) - d\mathbf{H}\|_{l^2}\|\widehat{\underline{\tau}}_h\|_{l^2} \leq \lambda Ch^k.$$

Using the reverse triangle inequality, we obtain

$$\lambda\|\nabla\xi\widehat{\underline{\tau}}_h\|_{l^2} = \|\tau\|_{l^2} \geq \|\widehat{\tau}_h\|_{l^2} - \|\tau - \widehat{\tau}_h\|_{l^2} \geq \lambda(1 - Ch^k) \tag{4.16}$$

and, dividing by λ and using (4.15), we obtain the sub-optimal estimate

$$1 - Ch^k \leq \|\nabla\xi\widehat{\underline{\tau}}_h\|_{l^2} \leq 1 + Ch^{k+1}. \tag{4.17}$$

The lower bound (4.17) can be improved in an iterative way as follows. We consider

$$\lambda\|\nabla\xi\widehat{\underline{\tau}}_h\|_{l^2} = \|\tau\|_{l^2} \geq \|\mathbf{P}\widehat{\tau}_h\|_{l^2} - \|\mathbf{P}\widehat{\tau}_h - \tau\|_{l^2}. \tag{4.18}$$

Then, using again the reverse triangular inequality, we have that

$$\|\mathbf{P}\widehat{\tau}_h\|_{l^2} = \lambda\|\mathbf{P}\widehat{\underline{\tau}}_h\|_{l^2} \geq \lambda(\|\underline{\tau}\|_{l^2} - \|\underline{\tau} - \mathbf{P}\widehat{\underline{\tau}}_h\|_{l^2}) = \lambda(1 - \|\underline{\tau} - \mathbf{P}\widehat{\underline{\tau}}_h\|_{l^2}). \tag{4.19}$$

Since $\underline{\tau}, n, \nu$ form an orthonormal basis of $\mathbb{R}^3$ and recalling that $\mathbf{P}$ maps vectors into

the tangential space of Γ (hence have null normal component), we get

$$\begin{aligned}\lambda(1-\|\underline{\tau}-\mathbf{P}\widehat{\underline{\tau}}_h\|_{l^2}) &= \lambda(1-\|1-(\underline{\tau},\mathbf{P}\widehat{\underline{\tau}}_h)\underline{\tau}-(n,\mathbf{P}\widehat{\underline{\tau}}_h)n\|_{l^2})\\ &\geq \lambda(1-\|(1-(\underline{\tau},\widehat{\underline{\tau}}_h))\|_{l^2}-\|(n,\widehat{\underline{\tau}}_h)\|_{l^2})\\ &\geq \lambda(1-\|\underline{\tau}-\widehat{\underline{\tau}}_h\|_{l^2}^2-\|(n,\widehat{\underline{\tau}}_h)\|_{l^2}).\end{aligned} \tag{4.20}$$

Now

$$\widehat{\underline{\tau}}_h-\underline{\tau}=(\mathbf{P}_{hk}-\frac{\nabla\xi}{\|\nabla\xi\widehat{\underline{\tau}}_h\|_{l^2}})\widehat{\underline{\tau}}_h,$$

so using (4.17) and a Taylor expansion argument, it is easy to see that

$$\|\widehat{\underline{\tau}}_h-\underline{\tau}\|_{l^2}\lesssim h^k. \tag{4.21}$$

To deal with the last term of (4.20) we note that

$$(n,\widehat{\underline{\tau}}_h)=(\underline{\tau}\times\nu,\widehat{\underline{\tau}}_h)=(\nu,\widehat{\underline{\tau}}_h\times\underline{\tau})=(\nu,\widehat{\underline{\tau}}_h\times\frac{\nabla\xi\widehat{\underline{\tau}}_h}{\|\nabla\xi\widehat{\underline{\tau}}_h\|_{l^2}}).$$

Then, using the sub-optimal lower bound (4.17) and a Taylor expansion argument, we get

$$(\nu,\widehat{\underline{\tau}}_h\times\frac{\nabla\xi\widehat{\underline{\tau}}_h}{\|\nabla\xi\widehat{\underline{\tau}}_h\|_{l^2}})=\frac{1}{\|\nabla\xi\widehat{\underline{\tau}}_h\|_{l^2}}(\nu,\widehat{\underline{\tau}}_h\times\nabla\xi\widehat{\underline{\tau}}_h)\lesssim\left|(\nu,\widehat{\underline{\tau}}_h\times\nabla\xi\widehat{\underline{\tau}}_h)\right|.$$

Using the definition of $\mathbf{P}$ and (2.3), we have that

$$\nabla\xi\widehat{\underline{\tau}}_h=(\mathbf{P}-d\mathbf{H})\widehat{\underline{\tau}}_h=\widehat{\underline{\tau}}_h-(\nu\cdot\widehat{\underline{\tau}}_h)\nu-d\mathbf{H}\widehat{\underline{\tau}}_h. \tag{4.22}$$

Now, using (4.22), we can write

$$(\nu,\widehat{\underline{\tau}}_h\times\nabla\xi\widehat{\underline{\tau}}_h)=\left(\nu,\widehat{\underline{\tau}}_h\times(\widehat{\underline{\tau}}_h-(\widehat{\underline{\tau}}_h\cdot\nu)\nu-d\mathbf{H}\widehat{\underline{\tau}}_h)\right)=-(\nu,\widehat{\underline{\tau}}_h\times d\mathbf{H}\widehat{\underline{\tau}}_h).$$

Hence,

$$\|(n,\widehat{\underline{\tau}}_h)\|_{l^2}\lesssim\|d\|_{L^\infty}\|(\nu,\widehat{\underline{\tau}}_h\times\mathbf{H}\widehat{\underline{\tau}}_h)\|_{l^2}\lesssim h^{k+1}. \tag{4.23}$$

Combining (4.23) and (4.21) with (4.20) we obtain that

$$\|\mathbf{P}\widehat{\tau}_h\|_{l^2}\geq\lambda(1-\|(1-(\underline{\tau},\mathbf{P}\widehat{\underline{\tau}}_h))\underline{\tau}-(n,\mathbf{P}\widehat{\underline{\tau}}_h)n\|_{l^2})\geq\lambda(1-Ch^{k+1}). \tag{4.24}$$

For the second term in the right-hand side of (4.18), notice that

$$\|\tau - \mathbf{P}\widehat{\tau}_h\|_{l^2} = \|\nabla\xi\widehat{\tau}_h - \mathbf{P}\widehat{\tau}_h\|_{l^2} = \|d\mathbf{H}\widehat{\tau}_h\|_{l^2} \leq \lambda C h^{k+1}. \tag{4.25}$$

We are now ready to improve the lower bound in (4.17). By making use of (4.25) and (4.24) in (4.18), we get

$$\|\nabla\xi\widehat{\underline{\tau}}_h\|_{l^2} \geq 1 - Ch^{k+1} \tag{4.26}$$

which proves (4.14e).

To prove (4.14g), we need to first prove the following auxiliary estimates:

$$|(\underline{\tau}, \widehat{n}_h)| \lesssim h^{k+1}, \tag{4.27}$$

$$|1 - (n, \widehat{n}_h)| \lesssim h^{2k}. \tag{4.28}$$

We start showing (4.27). Using the property of the cross product, we get

$$(\underline{\tau}, \widehat{n}_h) = (\underline{\tau}, \widehat{\nu}_h \times \widehat{\underline{\tau}}_h) = (\widehat{\nu}_h, \widehat{\underline{\tau}}_h \times \underline{\tau}) = (\widehat{\nu}_h, \widehat{\underline{\tau}}_h \times \nabla\xi\widehat{\underline{\tau}}_h). \tag{4.29}$$

Replacing (4.22) in (4.29), we obtain

$$(\underline{\tau}, \widehat{n}_h) = [\nu \cdot (\widehat{\underline{\tau}}_h - \underline{\tau})](\widehat{\underline{\tau}}_h, \nu \times \widehat{\nu}_h) - (\widehat{\nu}_h, \widehat{\underline{\tau}}_h \times dH\widehat{\underline{\tau}}_h).$$

Taking the absolute value and using (4.14a), (4.14c) and (4.21), we find

$$|(\underline{\tau}, \widehat{n}_h)| \lesssim h^{2k+1} + Ch^{k+1} \lesssim h^{k+1}.$$

In order to prove (4.28), we start showing that the following holds

$$|(\nu, \widehat{n}_h)| \lesssim h^k. \tag{4.30}$$

Indeed, using again the properties of the cross and scalar products, we obtain:

$$|(\nu, \widehat{n}_h)| = |(\nu, \widehat{\nu}_h \times \widehat{\underline{\tau}}_h)| = |(\widehat{\nu}_h, \widehat{\underline{\tau}}_h \times \nu)| = |(\widehat{\nu}_h, \widehat{\underline{\tau}}_h \times (\nu - \widehat{\nu}_h))| \lesssim h^k.$$

Since the vector $\widehat{n}_h$ is of unit length, there exist $a(x), b(x), c(x) \in \mathbb{R}$ satisfying $a^2 + b^2 + c^2 = 1$ such that

$$\widehat{n}_h = a\underline{\tau} + bn + c\nu,$$

where $a = (\underline{\tau}, \widehat{n}_h)$, $b = (n, \widehat{n}_h)$ and $c = (\nu, \widehat{n}_h)$. Hence, using (4.27), (4.30) and a

Taylor expansion argument, we get

$$b = \pm\sqrt{1 - a^2 - c^2} = \pm\sqrt{1 + Ch^{2k}} = \pm 1 + Ch^{2k}.$$

The inequality (4.28) follows by assuming that the grid size h of $\widehat{\mathcal{T}}_h$ is chosen small enough so that $b = 1 + Ch^{2k}$. Finally, writing $\mathbf{P}\widehat{n}_h = (\underline{\tau}, \mathbf{P}\widehat{n}_h)\underline{\tau} + (n, \mathbf{P}\widehat{n}_h)n$, we obtain (4.14g), i.e.,

$$\begin{aligned} |n - \mathbf{P}\widehat{n}_h| &= |n - (\underline{\tau}, \mathbf{P}\widehat{n}_h)\underline{\tau} + (n, \mathbf{P}\widehat{n}_h)n| \\ &\leq |1 - (n, \mathbf{P}\widehat{n}_h)| + |(\underline{\tau}, \mathbf{P}\widehat{n}_h)| \\ &= |1 - (n, \widehat{n}_h)| + |(\underline{\tau}, \widehat{n}_h)| \lesssim h^{k+1}. \end{aligned}$$

□

4.3.3 Boundedness and stability

Lemma 4.3.2. *Let $\widehat{v} \in H^j(\widehat{K}_h)$, $j \geq 2$, and let $\widetilde{v} = \widehat{v} \circ \xi_k$. Then, for h small enough, we have that*

$$\|\widehat{v}^\ell\|_{L^2(\widehat{K}_h^\ell)} \sim \|\widehat{v}\|_{L^2(\widehat{K}_h)} \sim \|\widetilde{v}\|_{L^2(K_h)}, \tag{4.31a}$$

$$\|\nabla_\Gamma \widehat{v}^\ell\|_{L^2(\widehat{K}_h^\ell)} \sim \|\nabla_{\Gamma_h^k} \widehat{v}\|_{L^2(\widehat{K}_h)} \sim \|\nabla_{\Gamma_h} \widetilde{v}\|_{L^2(K_h)}, \tag{4.31b}$$

$$\|D^j_{\Gamma_h^k} \widehat{v}\|_{L^2(\widehat{K}_h)} \lesssim \sum_{1 \leq m \leq j} \|D^m_\Gamma \widehat{v}^\ell\|_{L^2(\widehat{K}_h^\ell)}, \tag{4.31c}$$

$$\|D^j_{\Gamma_h} \widetilde{v}\|_{L^2(K_h)} \lesssim \sum_{1 \leq m \leq j} \|D^m_{\Gamma_h^k} \widehat{v}\|_{L^2(\widehat{K}_h)}. \tag{4.31d}$$

Proof. The proof of these relations is discussed in Demlow [2009]. □

We next prove the following trace inequality:

Lemma 4.3.3. *For sufficiently small h, we have that*

$$\|\nabla_{\Gamma_h^k} \widehat{w}_h\|^2_{L^2(\partial \widehat{K}_h)} \lesssim h^{-1} \|\nabla_{\Gamma_h^k} \widehat{w}_h\|^2_{L^2(\widehat{K}_h)} \qquad \forall \widehat{w}_h \in \widehat{S}_{hk}.$$

Proof. Defining $\delta_{e_h} := \mathrm{ds}/\,\mathrm{ds}_{\mathrm{h1}}$ and $\delta_{e_h \to \widehat{e}_h} := \mathrm{ds}_{\mathrm{hk}}/\,\mathrm{ds}_{\mathrm{h1}}$, using (4.14e) and a Taylor expansion argument, we have that

$$|1 - \delta_{e_h \to \widehat{e}_h}| = \left|1 - \frac{\delta_{e_h}}{\delta_{\widehat{e}_h}}\right| = \left|1 - \frac{1 + O(h^2)}{1 + O(h^{k+1})}\right| \lesssim h^2.$$

Now let $\widetilde{w}_h$ be defined such that $\widetilde{w}_h = \widehat{w}_h \circ \xi_k$. From (2.21) and (2.22) in Demlow

[2009] we have that

$$\left|\nabla_{\Gamma_h^k}\widehat{w}_h(\xi_k(\tilde{x}))\right| \lesssim |\nabla_{\Gamma_h}\widetilde{w}_h(\tilde{x})| \tag{4.32}$$

for each $\tilde{x} \in \Gamma_h$, provided h is sufficiently small. Applying classical inverse estimates on each $K_h \in \mathcal{T}_h$ (which can be done given that $\widetilde{w}_h$ is a finite-dimensional function living on the flat triangle K_h), we get

$$\int_{\partial K_h} |\nabla_{\Gamma_h}\widetilde{w}_h|^2 \, \mathrm{ds_{h1}} \lesssim \frac{1}{h}\|\nabla_{\Gamma_h}\widetilde{w}_h\|^2_{L^2(K_h)}.$$

Surface lifting the left-hand side to Γ_h^k, making use of (4.32) and using (4.31b) for the right-hand side we have that

$$\int_{\partial \widehat{K}_h} |\nabla_{\Gamma_h^k}\widehat{w}_h|^2 \delta^{-1}_{e_h \to \widehat{e}_h} \, \mathrm{ds_{hk}} \lesssim \frac{1}{h}\|\nabla_{\Gamma_h^k}\widehat{w}_h\|^2_{L^2(\widehat{K}_h)}.$$

We thus obtain, using (4.14e),

$$(1 - Ch^2)\|\nabla_{\Gamma_h^k}\widehat{w}_h\|^2_{L^2(\partial\widehat{K}_h)} \lesssim \frac{1}{h}\|\nabla_{\Gamma_h^k}\widehat{w}_h\|^2_{L^2(\widehat{K}_h)},$$

which yields the desired result for h small enough. □

In order to perform a unified analysis of the surface DG methods presented in Section 4.2.3, we introduce the stabilisation function

$$S_h(u_h, v_h) = \begin{cases} \displaystyle\sum_{\widehat{e}_h \in \widehat{\mathcal{E}}_h} \beta_{\widehat{e}_h} \int_{\widehat{e}_h} [u_h][v_h] \, \mathrm{ds_{hk}}, & \text{(4.33a)} \\ \displaystyle\sum_{\widehat{e}_h \in \widehat{\mathcal{E}}_h} \eta_{\widehat{e}_h} \int_{\Gamma_h^k} r_{\widehat{e}_h}([u_h]) \cdot r_{\widehat{e}_h}([v_h]) \, \mathrm{dA_{hk}}, & \text{(4.33b)} \end{cases}$$

for $u_h,\ v_h \in \widehat{S}_{hk}$, cf. also Table 4.1.

Finally, we define the DG norm $\|\cdot\|_{DG}$ to be given by

$$\|u_h\|^2_{\mathrm{DG}} = \|u_h\|^2_{1,h} + |u_h|^2_{*,h} \quad \forall u_h \in \widehat{S}_{hk}, \tag{4.34}$$

with

$$\|u_h\|^2_{1,h} = \sum_{\widehat{K}_h \in \widehat{\mathcal{T}}_h} \|u_h\|^2_{H^1(\widehat{K}_h)},$$

and

$$|u_h|^2_{*,h} = S_h(u_h, u_h),$$

Method	Stabilisation function $S_h(\cdot,\cdot)$
Surface IP Surface NIPG Surface IIPG Surface LDG	(4.33a)
Surface Brezzi et al. Surface Bassi et al.	(4.33b)

Table 4.1: Stabilisation function of the DG methods considered in our unified analysis.

where $S_h(\cdot,\cdot)$ depends on the method under investigation and is defined as in (4.33a)-(4.33b).

We will now prove boundedness and stability (in the DG norm) of the bilinear forms $\mathcal{A}_h^k(\cdot,\cdot)$ corresponding to the surface DG methods given in Table 4.1. We first state some estimates required for the analysis of the surface LDG method.

Lemma 4.3.4. *For any $v_h \in \widehat{S}_{hk}$,*

$$\alpha\|r_{\widehat{e}_h}([v_h])\|^2_{L^2(\Gamma_h^k)} \lesssim \beta_{\widehat{e}_h}\|[v_h]\|^2_{L^2(\widehat{e}_h)},$$
$$\alpha\|l_{\widehat{e}_h}([v_h])\|^2_{L^2(\Gamma_h^k)} \lesssim \beta_{\widehat{e}_h}\|[v_h]\|^2_{L^2(\widehat{e}_h)},$$

on each $\widehat{e}_h \in \widehat{\mathcal{E}}_h$.

Proof. The proof is the same as that of Lemma 2.3 in Antonietti and Houston [2011] provided proper definition of the DG lift operators. □

Lemma 4.3.5. *The bilinear forms $\mathcal{A}_h^k(\cdot,\cdot)$ corresponding to the surface DG methods given in Table 4.1 are bounded and stable in the DG norm (4.34), i.e.,*

$$\mathcal{A}_h^k(u_h,v_h) \lesssim \|u_h\|_{DG}\|v_h\|_{DG}, \quad \mathcal{A}_h^k(u_h,u_h) \gtrsim \|u_h\|^2_{DG},$$

for every $u_h, v_h \in \widehat{S}_{hk}$.

For the surface IP, Bassi et al. and IIPG methods, stability holds provided the penalty parameter α appearing in the definition of $\beta_{\widehat{e}_h}$ or $\eta_{\widehat{e}_h}$ in (4.7) is chosen sufficiently large.

Proof. For all the methods stabilized with $S_h(\cdot,\cdot)$ defined as in (4.33a), Lemma 4.3.3

implies that

$$\sum_{\widehat{e}_h\in\widehat{\mathcal{E}}_h}\int_{\widehat{e}_h}[u_h]\{\nabla_{\Gamma_h^k}v_h;\widehat{n}_h\}\,\mathrm{ds_{hk}} \leq \sum_{\widehat{e}_h\in\widehat{\mathcal{E}}_h}\left\|\beta_{\widehat{e}_h}^{1/2}[u_h]\right\|_{L^2(\widehat{e}_h)}\left\|\beta_{\widehat{e}_h}^{-1/2}\{\nabla_{\Gamma_h^k}v_h;\widehat{n}_h\}\right\|_{L^2(\widehat{e}_h)}$$
$$\lesssim \sum_{\widehat{K}_h\in\widehat{\mathcal{T}}_h}\alpha^{-\frac{1}{2}}|u_h|_{*,h}\|\nabla_{\Gamma_h^k}v_h\|_{L^2(\widehat{K}_h)}$$
$$\lesssim \alpha^{-\frac{1}{2}}|u_h|_{*,h}\|v_h\|_{1,h}, \tag{4.35}$$

where the hidden constant depends on the degree of the polynomial approximation but not on the penalty parameter $\beta_{\widehat{e}_h}$. Otherwise, if $S_h(\cdot,\cdot)$ is given as in (4.33b), we observe that for $u_h, v_h \in \widehat{S}_{hk}$ we have that

$$\sum_{\widehat{e}_h\in\widehat{\mathcal{E}}_h}\int_{\widehat{e}_h}[u_h]\{\nabla_{\Gamma_h^k}v_h;\widehat{n}_h\}\,\mathrm{ds_{hk}} = \sum_{\widehat{K}_h\in\widehat{\mathcal{T}}_h}\int_{\widehat{K}_h} r_h([u_h])\cdot\nabla_{\Gamma_h^k}v_h\,\mathrm{dA_{hk}}$$

and, making use of the fact that $r_{\widehat{e}_h}$ only has support on $\widehat{K}_h^+\bigcup\widehat{K}_h^-$ where $\partial\widehat{K}_h^+\bigcap\partial\widehat{K}_h^- = \widehat{e}_h$,

$$\|r_h(\phi)\|^2_{L^2(\widehat{K}_h)} = \left\|\sum_{\widehat{e}_h\subset\partial\widehat{K}_h} r_{\widehat{e}_h}(\phi)\right\|^2_{L^2(\widehat{K}_h)} \lesssim \sum_{\widehat{e}_h\subset\partial\widehat{K}_h}\|r_{\widehat{e}_h}(\phi)\|^2_{L^2(\widehat{K}_h)}. \tag{4.36}$$

Hence, applying Cauchy-Schwarz, we obtain

$$\sum_{\widehat{K}_h\in\widehat{\mathcal{T}}_h}\|\eta_{\widehat{e}_h}^{1/2}r_h([u_h])\|_{L^2(\widehat{K}_h)}\|\eta_{\widehat{e}_h}^{-1/2}\nabla_{\Gamma_h^k}v_h\|_{L^2(\widehat{K}_h)} \lesssim \alpha^{-\frac{1}{2}}|u_h|_{*,h}\|v_h\|_{1,h}, \tag{4.37}$$

where the hidden constant depends on the degree of the polynomial approximation but not on the penalty parameter $\eta_{\widehat{e}_h}$. For the surface LDG method, using Lemma 4.3.4, Lemma 4.3.3 and the $L^\infty(\Gamma_h^k)$ bound on β, we obtain

$$\left|\int_{\widehat{e}_h}[\nabla_{\Gamma_h^k}u_h;\widehat{n}_h]\beta\cdot\widehat{n}_h^+[v_h]\,\mathrm{ds_{hk}}\right| \lesssim \alpha^{-\frac{1}{2}}\|\beta\|_{L^\infty(\Gamma_h^k)}\|\nabla_{\Gamma_h^k}u_h\|_{L^2(\widehat{K}_h)}|v_h|_{*,h},$$

$$\left|\int_{\widehat{K}_h} r_h([u_h])\cdot l_h(\beta\cdot\widehat{n}_h^+[u_h])\,\mathrm{ds_{hk}}\right| \lesssim \alpha^{-1}\|\beta\|_{L^\infty(\Gamma_h^k)}|u_h|_{*,h}|v_h|_{*,h},$$

and, in a similar way, the remaining quantities. Boundedness then follows from Cauchy-Schwarz and the above estimates.

We next show stability of the DG bilinear forms. For the surface NIPG

method, stability follows straightforwardly from the Cauchy-Schwarz inequality. For the surface LDG method, we have that

$$\begin{aligned}\mathcal{A}_h^k(u_h,u_h) \geq &\|u_h\|_{1,h}^2 - 2\sum_{\widehat{e}_h\in\widehat{\mathcal{E}}_h^k}\int_{\widehat{e}_h}\left|[u_h]\{\nabla_{\Gamma_h^k}u_h;\widehat{n}_h\}\right|\ \mathrm{ds_{hk}}\\ &- 2\|\beta\|_{L^\infty(\Gamma_h^k)}\sum_{\widehat{e}_h\in\widehat{\mathcal{E}}_h^k}\int_{\widehat{e}_h}\left|[u_h][\nabla_{\Gamma_h^k}u_h;\widehat{n}_h]\right|\ \mathrm{ds_{hk}} + |u_h|_{*,h}^2.\end{aligned}$$

For the other methods involving $S_h(\cdot,\cdot)$ defined as in (4.33a) we obtain

$$\mathcal{A}_h^k(u_h,u_h) \geq \|u_h\|_{1,h}^2 - 2\sum_{\widehat{e}_h\in\widehat{\mathcal{E}}_h^k}\int_{\widehat{e}_h}\left|[u_h]\{\nabla_{\Gamma_h^k}u_h;\widehat{n}_h\}\right|\ \mathrm{ds_{hk}} + |u_h|_{*,h}^2,$$

otherwise, if $S_h(\cdot,\cdot)$ is given as in (4.33b), we have that

$$\mathcal{A}_h^k(u_h,u_h) \geq \|u_h\|_{1,h}^2 - 2\sum_{\widehat{K}_h\in\widehat{\mathcal{T}}_h^k}\int_{\widehat{K}_h}\left|r_h([u_h])\cdot\nabla_{\Gamma_h^k}u_h\right|\ \mathrm{dA_{hk}} + |u_h|_{*,h}^2.$$

The result follows by making use of the corresponding boundedness estimates, using using Cauchy-Schwarz inequality and Young's inequalities and choosing the penalty parameter α sufficiently large. □

Lemma 4.3.5, together with Lax-Milgram, guarantees that there exists a unique solution $u_h \in \widehat{S}_{hk}$ of (4.6) that satisfies the stability estimate

$$\|u_h\|_{\mathrm{DG}} \lesssim \|f_h\|_{L^2(\Gamma_h^k)}, \tag{4.38}$$

Remark 4.3.6. It is worth noting that one would run into issues when trying to prove h independent boundedness/stability of the planar DG methods (considered in Chapter 3) when posed on Γ_h^k. Recall the planar jump and average operators $[\![\cdot]\!]$ and $\{\!\{\cdot\}\!\}$ defined in Chapter 3. On discrete surfaces, since $\widehat{n}_h^+ \neq -\widehat{n}_h^-$, $[\![u_h]\!] = 0 \not\Rightarrow u_h = 0$ and thus cannot constitute a part of a DG norm. If, on the other hand, we kept the DG norm as it is defined in (4.34) but chose to use the planar operators $[\![\cdot]\!]$ and $\{\!\{\cdot\}\!\}$ instead of respectively the discrete surface operators $[\cdot]$ and $\{\cdot;\widehat{n}_h\}$ in the surface DG bilinear forms, we would not be able to write the planar operators in terms of the discrete surface operators independently of h. As such, we would not obtain boundedness/stability independently of h.

We now define the DG norm for functions in $\widehat{S}_{hk}^{\ell}$ as follows:

$$\|u_h^\ell\|_{\mathrm{DG}}^2 = \|u_h^\ell\|_{1,h}^2 + |u_h^\ell|_{*,h}^2 \quad \forall u_h^\ell \in \widehat{S}_{hk}^{\ell}, \tag{4.39}$$

with

$$\|u_h^\ell\|_{1,h}^2 = \sum_{\widehat{K}_h^\ell \in \widehat{\mathcal{T}}_h^\ell} \|u_h^\ell\|_{H^1(\widehat{K}_h^\ell)}^2,$$

and

$$|u_h^\ell|_{*,h}^2 = S_h^\ell(u_h^\ell, u_h^\ell),$$

where $S_h^\ell(\cdot,\cdot)$ is given by

$$S_h^\ell(u_h^\ell, v_h^\ell) = \begin{cases} \displaystyle\sum_{\widehat{e}_h^l \in \widehat{\mathcal{E}}_h^l} \beta_{\widehat{e}_h} \int_{\widehat{e}_h^\ell} \delta_{\widehat{e}_h}^{-1} [u_h^\ell][v_h^\ell] \ \mathrm{ds}, & \text{(4.40a)} \\ \displaystyle\sum_{\widehat{e}_h^l \in \widehat{\mathcal{E}}_h^l} \eta_{\widehat{e}_h} \int_{\Gamma} \delta_{hk}^{-1} \left(r_{\widehat{e}_h}([u_h])\right)^\ell \cdot \left(r_{\widehat{e}_h}([v_h])\right)^\ell \ \mathrm{dA}, & \text{(4.40b)} \end{cases}$$

for $u_h^\ell,\ v_h^\ell \in \widehat{S}_{hk}^{\ell}$.

Lemma 4.3.7. *Let $u_h \in \widehat{S}_{hk}$ satisfy (4.38). Then $u_h^\ell \in \widehat{S}_{hk}^{\ell}$ satisfies*

$$\|u_h^\ell\|_{DG} \lesssim \|f\|_{L^2(\Gamma)}, \tag{4.41}$$

for h small enough.

Proof. We first show that for any function $v_h \in \widehat{S}_{hk}$, for sufficiently small h,

$$\|v_h^\ell\|_{DG} \lesssim \|v_h\|_{\mathrm{DG}}. \tag{4.42}$$

The $\|\cdot\|_{1,h}^2$ component of the DG norm is dealt with in exactly the same way as in Demlow [2009]. For the $|\cdot|_{*,h}^2$ component of the DG norm we have that

$$\int_{\widehat{e}_h} [v_h]^2 \ \mathrm{ds_{hk}} = \int_{\widehat{e}_h^\ell} \delta_{\widehat{e}_h}^{-1} [v_h^\ell]^2 \ \mathrm{ds} \quad \text{and} \quad \int_{\Gamma_h^k} |r_h([v_h])|^2 \ \mathrm{dA_{hk}} = \int_{\Gamma} \delta_{hk}^{-1} |r_h([v_h])^\ell|^2 \ \mathrm{dA},$$

which straightforwardly yields (4.42). Making use of the discrete stability estimate (4.38) and noting that, by Lemma 4.3.4, $\|f_h\|_{L^2(\Gamma_h^k)} \lesssim \|f_h^\ell\|_{L^2(\Gamma)} = \|f\|_{L^2(\Gamma)}$, we get the desired result. □

For each of the surface DG bilinear forms given in Table 4.1, we define a corresponding bilinear form on Γ induced by the surface lifted triangulation $\widehat{\mathcal{T}}_h^\ell$

which is well defined for functions $w, v \in H^2(\Gamma) + \widehat{S}_{hk}^{\ell}$. For the surface IP bilinear form (4.10), we define

$$\begin{aligned}\mathcal{A}(w,v) = &\sum_{\widehat{K}_h^\ell \in \widehat{\mathcal{T}}_h^\ell} \int_{\widehat{K}_h^\ell} \nabla_\Gamma w \cdot \nabla_\Gamma v + wv \ \mathrm{dA} - \sum_{\widehat{e}_h^\ell \in \widehat{\mathcal{E}}_h^\ell} \int_{\widehat{e}_h^\ell} [w]\{\nabla_\Gamma v; n\} + [v]\{\nabla_\Gamma w; n\} \ \mathrm{ds} \\ &+ \sum_{\widehat{e}_h^\ell \in \widehat{\mathcal{E}}_h^\ell} \int_{\widehat{e}_h^\ell} \delta_{\widehat{e}_h}^{-1} \beta_{\widehat{e}_h} [w][v] \ \mathrm{ds}, \end{aligned} \tag{4.43}$$

where n^+ and n^- are respectively the unit surface conormals to $\widehat{K}_h^{\ell+}$ and $\widehat{K}_h^{\ell-}$ on $\widehat{e}_h^\ell \in \widehat{\mathcal{E}}_h^\ell$. For the Brezzi et al. bilinear form (4.9), we define

$$\begin{aligned}\mathcal{A}(w,v) = &\sum_{\widehat{K}_h^\ell \in \widehat{\mathcal{T}}_h^\ell} \int_{\widehat{K}_h^\ell} \nabla_\Gamma w \cdot \nabla_\Gamma v + wv \ \mathrm{dA} \\ &+ \sum_{\widehat{K}_h^\ell \in \widehat{\mathcal{T}}_h^\ell} \int_{\widehat{K}_h^\ell} \delta_{hk}^{-1} \eta_{\widehat{e}_h} r_{\widehat{e}_h}([w^{-\ell}])^\ell \cdot r_{\widehat{e}_h}([v^{-\ell}])^\ell + \delta_{hk}^{-1} \big(r_h([w^{-\ell}])\big)^\ell \cdot \big(r_h([v^{-\ell}])\big)^\ell \ \mathrm{dA} \\ &- \sum_{\widehat{e}_h^\ell \in \widehat{\mathcal{E}}_h^\ell} \int_{\widehat{e}_h^\ell} [w]\{\nabla_\Gamma v; n\} + [v]\{\nabla_\Gamma w; n\} \ - \delta_{\widehat{e}_h}^{-1} \beta_{\widehat{e}_h} [w][v] \ \mathrm{ds}. \end{aligned} \tag{4.44}$$

For the surface LDG bilinear form (4.11), we define

$$\begin{aligned}\mathcal{A}(w,v) = &\sum_{\widehat{K}_h^\ell \in \widehat{\mathcal{T}}_h^\ell} \int_{\widehat{K}_h^\ell} \nabla_\Gamma w \cdot \nabla_\Gamma v + wv \ \mathrm{dA} - \sum_{\widehat{e}_h^\ell \in \widehat{\mathcal{E}}_h^\ell} \int_{\widehat{e}_h^\ell} [w]\{\nabla_\Gamma v; n\} - \{\nabla_\Gamma w; n\}[v] \ \mathrm{ds} \\ &+ \sum_{\widehat{e}_h^\ell \in \widehat{\mathcal{E}}_h^\ell} \int_{\widehat{e}_h^\ell} \Big(- \delta_{\widehat{e}_h}^{-1} [\nabla_\Gamma w; n] \beta \cdot \widehat{n}_h^{\ell+}[v] - \delta_{\widehat{e}_h}^{-1} \beta \cdot \widehat{n}_h^{\ell+}[w][\nabla_\Gamma v; n] + \delta_{\widehat{e}_h}^{-1} \beta_{\widehat{e}_h}[w][v] \Big) \ \mathrm{ds} \\ &+ \sum_{\widehat{K}_h^\ell \in \widehat{\mathcal{T}}_h^\ell} \int_{\widehat{K}_h^\ell} \Big(r_h([w^{-\ell}]) + \beta \cdot \widehat{n}_h^{\ell+} l_h([w^{-\ell}]) \Big)^\ell \cdot \Big(r_h([v^{-\ell}]) + \beta \cdot \widehat{n}_h^{\ell+} l_h([v^{-\ell}]) \Big)^\ell \ \mathrm{dA}. \end{aligned} \tag{4.45}$$

The corresponding bilinear forms for the other surface DG methods can be derived in a similar manner. Since we assumed that the weak solution u of (4.1) belongs to $H^s(\Gamma)$, $s \geq 2$, they all satisfy

$$\mathcal{A}(u,v) = \sum_{\widehat{K}_h^\ell \in \widehat{\mathcal{T}_h}^{\ell}} \int_{\widehat{K}_h^\ell} fv \ \mathrm{dA}, \qquad \forall v \in H^2(\Gamma) + \widehat{S}_{hk}^{\ell}. \tag{4.46}$$

Finally, we require the following boundedness/stability estimates for $\mathcal{A}(\cdot,\cdot)$, which follow by applying similar arguments as those found in the proof of Lemma

4.3.5.

Lemma 4.3.8. *The bilinear forms $\mathcal{A}(\cdot,\cdot)$ induced by the surface DG methods given in Table 4.1 are bounded and stable in the DG norm (4.39), i.e.,*

$$\mathcal{A}(u_h^l, v_h^l) \lesssim \|u_h^\ell\|_{DG}\|v_h^\ell\|_{DG}, \quad \mathcal{A}(u_h^l, u_h^l) \gtrsim \|u_h^\ell\|_{DG}^2,$$

for all $u_h^\ell, v_h^\ell \in \widehat{S}_{hk}^\ell$ if, for the surface IP, Bassi et al. and IIPG methods, the penalty parameter α appearing in the definition of $\beta_{\widehat{e}_h}$ or $\eta_{\widehat{e}_h}$ in (4.7) is chosen sufficiently large.

4.4 Convergence

We now state the main result of this chapter.

Theorem 4.4.1. *Let $u \in H^{k+1}(\Gamma)$ and $u_h \in \widehat{S}_{hk}$ denote the solutions to (4.1) and (4.5), respectively. Let $\eta = 0$ for IIPG, NIPG formulations and let $\eta = 1$ otherwise. Then,*

$$\|u - u_h^\ell\|_{L^2(\Gamma)} + h^\eta \|u - u_h^\ell\|_{DG} \lesssim h^{k+\eta}(\|f\|_{L^2(\Gamma)} + \|u\|_{H^{k+1}(\Gamma)}),$$

provided the grid size h is small enough and the penalty parameter α is large enough for the surface IP, Bassi et al. and IIPG methods. Here the hidden constant depends, in particular, on the signed distance function d and its first/second derivatives.

The proof will follow an argument similar to the one outlined in Arnold et al. [2002]. Using the stability result given in Lemma 4.3.8, we have that

$$\|\phi_h^\ell - u_h^\ell\|_{DG}^2 \lesssim \mathcal{A}(\phi_h^\ell - u_h^\ell, \phi_h^\ell - u_h^\ell) = \mathcal{A}(u - u_h^\ell, \phi_h^\ell - u_h^\ell) + \mathcal{A}(\phi_h^\ell - u, \phi_h^\ell - u_h^\ell), \quad (4.47)$$

where $\phi_h^\ell \in \widehat{S}_{hk}^\ell$. Since we do not directly have Galerkin orthogonality the first term on the right-hand side of (4.47) is not zero and its estimation will be the main part of this section. The second term is dealt with in the following way: following Demlow [2009], for $\widehat{w} \in H^2(\Gamma_h^k)$, we define the interpolant $\widehat{I}_h^k : C^0(\Gamma_h^k) \to \widehat{S}_{hk}$ by

$$\widehat{I}_h^k \widehat{w} = \widetilde{I}_h^k(\widehat{w} \circ \xi_k),$$

where $\widetilde{I}_h^k$ is the standard Lagrange interpolant of degree k on the piecewise linear surface Γ_h. We also define the interpolant $I_h^k : C^0(\Gamma) \to \widehat{S}_{hk}^\ell$ by

$$I_h^k w = \widehat{I}_h^k(w \circ \xi).$$

Lemma 4.4.2. *Let $w \in H^m(\Gamma)$ with $2 \leq m \leq k+1$. Then for $i = 0, 1$,*

$$|w - I_h^k w|_{H^i(\widehat{K}_h^\ell)} \lesssim h^{m-i} \|w\|_{H^m(\widehat{K}_h^\ell)}.$$

Proof. The proof follows easily by combining standard estimates for the Lagrange interpolant on Γ_h with Lemma 4.3.2. See Demlow [2009] for further details. □

Lemma 4.4.3. *Let $w \in H^m(\Gamma)$ with $2 \leq m \leq k+1$. Then, for sufficiently small h, we have that*

$$\|w - I_h^k w\|^2_{L^2(\partial \widehat{K}_h^\ell)} + h^2 \|\nabla_\Gamma (w - I_h^k w)\|^2_{L^2(\partial \widehat{K}_h^\ell)} \lesssim h^{2m-1} \|w\|^2_{H^m(\widehat{K}_h^\ell)}.$$

Proof. Fix an arbitrary element $\widehat{K}_h^\ell \in \widehat{\mathcal{T}}_h^\ell$. We then define $\widehat{w} \in H^m(\widehat{K}_h)$ and $\widetilde{w} \in H^m(K_h)$ such that $w = \widehat{w} \circ \xi$ and $\widetilde{w} = \widehat{w} \circ \xi_k$.

Applying the trace theorem on $K_h \in \mathcal{T}_h$ we get

$$\int_{\partial K_h} |\nabla_{\Gamma_h} (\widetilde{w} - \widetilde{I}_h^k \widetilde{w})|^2 \, \mathrm{ds_{h1}} \lesssim \int_{K_h} \frac{1}{h} |\nabla_{\Gamma_h} (\widetilde{w} - \widetilde{I}_h^k \widetilde{w})|^2 + h |\nabla^2_{\Gamma_h} (\widetilde{w} - \widetilde{I}_h^k \widetilde{w})|^2 \, \mathrm{dA_{h1}}.$$

Applying a classical interpolation result for the right-hand side of the above (see, for example, Theorem 6.4 in Braess [2001]), we obtain

$$\int_{\partial K_h} |\nabla_{\Gamma_h} (\widetilde{w} - \widetilde{I}_h^k \widetilde{w})|^2 \, \mathrm{ds_{h1}} \lesssim h^{2m-3} |\widetilde{w}|^2_{H^m(K_h)}.$$

Then, lifting the left-hand side onto Γ_h^k as in Lemma 4.3.3 and using (4.31b) with (4.31d), we get

$$(1 - Ch^2) \int_{\partial \widehat{K}_h} |\nabla_{\Gamma_h^k} (\widehat{w} - \widehat{I}_h^k \widehat{w})|^2 \, \mathrm{ds_{hk}} \lesssim h^{2m-3} \|\widehat{w}\|^2_{H^m(\widehat{K}_h)}.$$

In the same way, we lift the left-hand side onto Γ and use (4.31b) with (4.31d) to obtain

$$(1 - Ch^{k+1})(1 - Ch^2) \|\nabla_\Gamma (w - I_h^k w)\|^2_{L^2(\partial \widehat{K}_h^\ell)} \lesssim h^{2m-3} \|w\|^2_{H^m(\widehat{K}_h^\ell)}.$$

Then, proceeding similarly with $\|w - I_h^k w\|^2_{L^2(\partial \widehat{K}_h^\ell)}$, we get the desired result for h small enough. □

These interpolation estimates allow us to derive the following boundedness estimates for $\mathcal{A}(\cdot, \cdot)$:

Lemma 4.4.4. *Let $u \in H^m(\Gamma)$ and $w \in H^n(\Gamma)$ with $2 \leq m, n \leq k+1$. Then, for all $v_h^\ell \in \widehat{S}_{hk}^\ell$, we have that*

$$\mathcal{A}(u - I_h^k u, v_h^\ell) \lesssim h^{m-1} \|u\|_{H^m(\Gamma)} \|v_h^\ell\|_{DG}, \tag{4.48}$$

$$\mathcal{A}(u - I_h^k u, w - I_h^k w) \lesssim h^{m+n-2} \|u\|_{H^m(\Gamma)} \|w\|_{H^n(\Gamma)}. \tag{4.49}$$

Proof. Since $u \in H^m(\Gamma) \subset C^0(\Gamma)$ for $m \geq 2$ and $I_h^k u \in C^0(\Gamma)$, we have that $[u - I_h^k u] = 0$ on each $\widehat{e}_h^l \in \widehat{\mathcal{E}}_h^l$. Than, using Cauchy-Schwarz in the definition of $r_{\widehat{e}_h}$ and $l_{\widehat{e}_h}$, we have that

$$\|r_{\widehat{e}_h}([(u - I_h^k u)^{-l}])\|_{L^2(\Gamma_h^k)}^2 = 0, \quad \|l_{\widehat{e}_h}((u - I_h^k u)^{-l}])\|_{L^2(\Gamma_h^k)}^2 = 0.$$

Then, following the proof of Lemma 4.3.5, it is easy to obtain (4.48) and (4.49) from Lemma 4.4.2 and Lemma 4.4.3. □

For the first term on the right-hand side of (4.47), we require the following *perturbed* Galerkin orthogonality result:

Lemma 4.4.5. *Let $u \in H^s(\Gamma)$, $s \geq 2$, and $u_h \in \widehat{S}_{hk}$ denote the solutions to (4.1) and (4.5), respectively. We define the functional E_{hk} on $\widehat{S}_{hk}^\ell$ by*

$$E_{hk}(v_h^\ell) = \mathcal{A}(u - u_h^\ell, v_h^\ell).$$

Then, for all surface DG methods apart from LDG, E_{hk} can be written as

$$\begin{aligned} E_{hk}(v_h^\ell) = &\sum_{\widehat{K}_h^\ell \in \widehat{\mathcal{T}}_h^\ell} \int_{\widehat{K}_h^\ell} (\mathbf{R}_{hk} - \mathbf{P}) \nabla_\Gamma u_h^\ell \cdot \nabla_\Gamma v_h^\ell + \left(\delta_{hk}^{-1} - 1\right) u_h^\ell v_h^\ell + \left(1 - \delta_{hk}^{-1}\right) f v_h^\ell \, dA \\ &+ \sum_{\widehat{e}_h^\ell \in \widehat{\mathcal{E}}_h^\ell} \int_{\widehat{e}_h^\ell} [u_h^\ell] \left(\{\nabla_\Gamma v_h^\ell; n\} - \{\delta_{\widehat{e}_h}^{-1} \mathbf{P}_{hk} (\mathbf{I} - d\mathbf{H}) \mathbf{P} \nabla_\Gamma v_h^\ell; \widehat{n}_h^\ell\} \right) \, ds \\ &+ \sum_{\widehat{e}_h^\ell \in \widehat{\mathcal{E}}_h^\ell} \int_{\widehat{e}_h^\ell} [v_h^\ell] \left(\{\nabla_\Gamma u_h^\ell; n\} - \{\delta_{\widehat{e}_h}^{-1} \mathbf{P}_{hk} (\mathbf{I} - d\mathbf{H}) \mathbf{P} \nabla_\Gamma u_h^\ell; \widehat{n}_h^\ell\} \right) \, ds \end{aligned} \tag{4.50}$$

where $\mathbf{R}_{hk}$ is given in (4.12). The functional corresponding to the surface LDG

method can be written as

$$
\begin{aligned}
E_{hk}(v_h^\ell) =& (4.50) \\
&+ \sum_{\widehat{e}_h^\ell \in \widehat{\mathcal{E}}_h^\ell} \int_{\widehat{e}_h^\ell} \delta_{\widehat{e}_h}^{-1} \beta \cdot \widehat{n}_h^{\ell+} [v_h^\ell] \left([\nabla_\Gamma u_h^\ell; n] - [\mathbf{P}_{hk}(\mathbf{I} - d\mathbf{H})\mathbf{P}\nabla_\Gamma u_h^\ell; \widehat{n}_h^\ell] \right) \, ds \\
&+ \sum_{\widehat{e}_h^\ell \in \widehat{\mathcal{E}}_h^\ell} \int_{\widehat{e}_h^\ell} \delta_{\widehat{e}_h}^{-1} \beta \cdot \widehat{n}_h^{\ell+} [u_h^\ell] \left([\nabla_\Gamma v_h^\ell; n] - [\mathbf{P}_{hk}(\mathbf{I} - d\mathbf{H})\mathbf{P}\nabla_\Gamma v_h^\ell; \widehat{n}_h^\ell] \right) \, ds.
\end{aligned}
\tag{4.51}
$$

Furthermore,

$$
|E_{hk}(v_h^\ell)| \lesssim h^{k+1} \|f\|_{L^2(\Gamma)} \|v_h^\ell\|_{DG}. \tag{4.52}
$$

The proof of Lemma 4.4.5 will be the main part of this section. Before we give its full proof, we will complete that of Theorem 4.4.1 assuming this result.

Proof of Theorem 4.4.1. Choosing the continuous interpolant $\phi_h^\ell = I_h^k u$, using the boundedness estimate (4.48) and the error functional estimate (4.52), (4.47) can be bounded by

$$
\begin{aligned}
\|I_h^k u - u_h^\ell\|_{DG}^2 &\lesssim E_{hk}(I_h^k u - u_h^\ell) + \mathcal{A}(I_h^k u - u, I_h^k u - u_h^\ell) \\
&\lesssim h^{k+1} \|f\|_{L^2(\Gamma)} \|I_h^k u - u_h^\ell\|_{DG} + h^k \|u\|_{H^{k+1}(\Gamma)} \|I_h^k u - u_h^\ell\|_{DG},
\end{aligned}
$$

which implies

$$
\|I_h^k u - u_h^\ell\|_{DG} \lesssim h^k (\|f\|_{L^2(\Gamma)} + \|u\|_{H^{k+1}(\Gamma)}).
$$

Recalling that $u - I_h^k u \in C^0(\Gamma)$, using Lemma 4.4.2 we obtain

$$
\|u - u_h^\ell\|_{DG} \leq \|u - I_h^k u\|_{DG} + \|I_h^k u - u_h^\ell\|_{DG} \lesssim h^k (\|f\|_{L^2(\Gamma)} + \|u\|_{H^{k+1}(\Gamma)}).
$$

This concludes the first part of the proof. In the case of $\eta = 1$, to derive the L^2 estimate, we first observe that the solution $z \in H^2(\Gamma)$ to the dual problem

$$
-\Delta_\Gamma z + z = u - u_h^\ell \tag{4.53}
$$

satisfies

$$
\|z\|_{H^2(\Gamma)} \lesssim \|u - u_h^\ell\|_{L^2(\Gamma)}. \tag{4.54}
$$

Then, using the symmetry of the bilinear form $\mathcal{A}(\cdot,\cdot)$, we have that

$$\begin{aligned}\|u-u_h^\ell\|_{L^2(\Gamma)}^2 &= (u-u_h^\ell, u-u_h^\ell)_\Gamma = \mathcal{A}(z, u-u_h^\ell)\\ &= \mathcal{A}(u-u_h^\ell, z) = \mathcal{A}(u-u_h^\ell, z-I_h^k z) + E_{hk}(I_h^k z). \end{aligned} \tag{4.55}$$

Using (4.52), a triangle inequality and the interpolation estimate in Lemma 4.4.2, we obtain

$$|E_{hk}(I_h^k z)| \lesssim h^{k+1}\|f\|_{L^2(\Gamma)}\|I_h^k z\|_{H^1(\Gamma)} \lesssim h^{k+1}\|f\|_{L^2(\Gamma)}\|z\|_{H^2(\Gamma)}.$$

Hence, using (4.54),

$$|E_{hk}(I_h^k z)| \lesssim h^{k+1}\|f\|_{L^2(\Gamma)}\|u-u_h^\ell\|_{L^2(\Gamma)}$$

Making use of the continuity of $I_h^k z - z$ and $I_h^k u - u$, the symmetry of the bilinear form $\mathcal{A}(\cdot,\cdot)$, Lemma 4.4.4 and the stability estimate (4.54) we get

$$\begin{aligned}\mathcal{A}(u-u_h^\ell, z-I_h^k z) &= \mathcal{A}(z-I_h^k z, u-u_h^\ell)\\ &\lesssim \mathcal{A}(z-I_h^k z, I_h^k u-u_h^\ell) + \mathcal{A}(z-I_h^k z, u-I_h^k u)\\ &\lesssim h\|z\|_{H^2(\Gamma)}\|I_h^k u-u_h^\ell\|_{DG} + h^{k+1}\|z\|_{H^2(\Gamma)}\|u\|_{H^{k+1}(\Gamma)}\\ &\lesssim h\|z\|_{H^2(\Gamma)}(\|I_h^k u-u\|_{DG} + \|u-u_h^\ell\|_{DG}) + h^{k+1}\|z\|_{H^2(\Gamma)}\|u\|_{H^{k+1}(\Gamma)}\\ &\lesssim (h^{k+1}\|u\|_{H^{k+1}(\Gamma)} + h\|u-u_h^\ell\|_{DG})\|u-u_h^\ell\|_{L^2(\Gamma)}.\end{aligned}$$

Combining these estimates with (4.55) yields

$$\|u-u_h^\ell\|_{L^2(\Gamma)}^2 \lesssim \left(h\|u-u_h^\ell\|_{DG} + h^{k+1}(\|f\|_{L^2(\Gamma)} + \|u\|_{H^{k+1}(\Gamma)})\right)\|u-u_h^\ell\|_{L^2(\Gamma)},$$

which gives us the desired L^2 estimate and concludes the proof. In the case of $\eta = 0$, we can trivially obtain the (sub-optimal) bound for the error in the L^2 norm from bounding it by the error in the DG norm. □

Proof of Lemma 4.4.5. The expression for the error functional E_{hk} given in Lemma 4.4.5 is obtained by considering the difference between the two equations (4.46) and (4.5). In order to do this, the integrals of (4.5) have to first be lifted onto Γ. Recall that, for every $\widehat{K}_h \in \widehat{\mathcal{T}}_h$, we have that

$$\int_{\widehat{K}_h} \nabla_{\Gamma_h^k} u_h \cdot \nabla_{\Gamma_h^k} v_h + u_h v_h \ \mathrm{dA_{hk}} = \int_{\widehat{K}_h^l} \mathbf{R}_{hk}\nabla_\Gamma u_h^l \cdot \nabla_\Gamma v_h^l + \delta_{hk}^{-1} u_h^l v_h^l \ \mathrm{dA}.$$

Furthermore, for every $\widehat{e}_h \in \widehat{\mathcal{E}}_h$, we have that

$$\begin{aligned}
&\int_{\widehat{e}_h} [u_h]\{\nabla_{\Gamma_h^k} v_h; \widehat{n}_h\} + [v_h]\{\nabla_{\Gamma_h^k} u_h; \widehat{n}_h\} \ \mathrm{ds_{hk}} \\
&= \int_{\widehat{e}_h^l} [u_h^l]\{\mathbf{P}_{hk}(\mathbf{I} - d\mathbf{H})\mathbf{P}\nabla_\Gamma v_h^l; \widehat{n}_h^l\}\delta_{\widehat{e}_h}^{-1} + [v_h^l]\{\mathbf{P}_{hk}(\mathbf{I} - d\mathbf{H})\mathbf{P}\nabla_\Gamma u_h^l; \widehat{n}_h^l\}\delta_{\widehat{e}_h}^{-1} \ \mathrm{ds}.
\end{aligned}$$

And finally, we have that

$$\int_{\widehat{e}_h} \beta_{\widehat{e}_h}[u_h][v_h] \ \mathrm{ds_{hk}} = \int_{\widehat{e}_h^l} \delta_{\widehat{e}_h}^{-1}\beta_{\widehat{e}_h}[u_h^l][v_h^l] \ \mathrm{ds}.$$

The right-hand side of (4.5) gets transformed in a similar way:

$$\sum_{\widehat{K}_h \in \widehat{\mathcal{T}}_h} \int_{\widehat{K}_h} f_h v_h \ \mathrm{dA_{hk}} = \sum_{\widehat{K}_h^l \in \widehat{\mathcal{T}}_h^l} \int_{\widehat{K}_h^l} f v_h^l \delta_{hk}^{-1} \ \mathrm{dA}.$$

Making use of the above, the difference between the two equations (4.46) and (4.5) yields

$$\begin{aligned}
0 &= \mathcal{A}(u, v_h^l) - \sum_{\widehat{K}_h^l \in \widehat{\mathcal{T}}_h^l} \int_{\widehat{K}_h^l} f v_h^l \ \mathrm{dA} - \mathcal{A}_h^k(u_h, v_h) + \sum_{\widehat{K}_h \in \widehat{\mathcal{T}}_h} \int_{\widehat{K}_h} f_h v_h \ \mathrm{dA_{hk}} \\
&= \mathcal{A}(u - u_h^l, v_h^l) - E_{hk}(v_h^l)
\end{aligned}$$

as required.

Finally we need to show that the error functional E_{hk} scales appropriately i.e.

$$|E_{hk}(v_h^l)| \lesssim h^{k+1}\|f\|_{L^2(\Gamma)}\|v_h^l\|_{DG}.$$

To this end we need to show that the additional terms arising in the error functional E_{hk} do not affect the convergence rates expressed in Demlow [2009]. The first term of the error functional E_{hk} (the element integral) is the one resulting from the standard (higher order) surface FEM approach. By Lemma 4.3.1, this term scales like h^{k+1} and making use of the stability estimate (4.41) this term scales like the right-hand side of (4.52). We will now get a bound for the third term of E_{hk}, for

which we have the following:

$$\begin{aligned}
&\sum_{\widehat{e}_h^l \in \widehat{\mathcal{E}}_h} \int_{\widehat{e}_h^l} [v_h^l]\{\nabla_\Gamma u_h^l; n\}\left(1 + \delta_{\widehat{e}_h}^{-1} - \delta_{\widehat{e}_h}^{-1}\right) - [v_h^l]\{\mathbf{P}_{hk}(\mathbf{I} - d\mathbf{H})\mathbf{P}\nabla_\Gamma u_h^l; \widehat{n}_h^l\}\delta_{\widehat{e}_h}^{-1}\ \mathrm{ds} \\
&= \sum_{\widehat{e}_h^l \in \widehat{\mathcal{E}}_h^l} \int_{\widehat{e}_h^l} [v_h^l]\{\nabla_\Gamma u_h^l; n\}\left(1 - \delta_{\widehat{e}_h}^{-1}\right) \\
&\qquad + \delta_{\widehat{e}_h}^{-1}[v_h^l]\Big(\{\nabla_\Gamma u_h^l; n\} - \{\mathbf{P}_{hk}(\mathbf{I} - d\mathbf{H})\mathbf{P}\nabla_\Gamma u_h^l; \widehat{n}_h^l\}\Big)\ \mathrm{ds}.
\end{aligned}$$

Making use of Lemma 4.3.8, Lemma 4.3.1 and the stability estimate (4.41) it is clear that the first component in the above scales appropriately, so all we have to deal with is the second component. We first note that since $\mathbf{PH} = \mathbf{HP} = \mathbf{H}$, we have that

$$\begin{aligned}
&\nabla_\Gamma u_h^{l+} \cdot n^+ - \mathbf{P}_{hk}^+(\mathbf{I} - d\mathbf{H})\mathbf{P}\nabla_\Gamma u_h^{l+} \cdot \widehat{n}_h^{l+} = \nabla_\Gamma u_h^{l+} \cdot n^+ - \nabla_\Gamma u_h^{l+} \cdot \mathbf{P}(\mathbf{I} - d\mathbf{H})\mathbf{P}_{hk}^+\widehat{n}_h^{l+} \\
&\quad = \nabla_\Gamma u_h^{l+} \cdot n^+ - \nabla_\Gamma u_h^{l+} \cdot \mathbf{P}(\mathbf{I} - d\mathbf{H})\widehat{n}_h^{l+} = \nabla_\Gamma u_h^{l+} \cdot (n^+ - \mathbf{P}\widehat{n}_h^{l+}) + d\nabla_\Gamma u_h^{l+} \cdot \mathbf{H}\widehat{n}_h^{l+}
\end{aligned}$$

where we have used the fact that the Hessian $\mathbf{H}$ is symmetric. Hence

$$\begin{aligned}
&\sum_{\widehat{e}_h^l \in \widehat{\mathcal{E}}_h^l} \int_{\widehat{e}_h^l} \delta_{\widehat{e}_h}^{-1}[v_h^l]\left(\{\nabla_\Gamma u_h^l; n\} - \{\mathbf{P}_{hk}(\mathbf{I} - d\mathbf{H})\mathbf{P}\nabla_\Gamma u_h^l; \widehat{n}_h^l\}\right)\ \mathrm{ds} \\
&= \sum_{\widehat{e}_h^l \in \widehat{\mathcal{E}}_h^l} \int_{\widehat{e}_h^l} \delta_{\widehat{e}_h}^{-1}[v_h^l]\left(\{\nabla_\Gamma u_h^l; n - \mathbf{P}\widehat{n}_h^l\} + d\{\nabla_\Gamma u_h^l; \mathbf{H}\widehat{n}_h^l\}\right)\ \mathrm{ds}.
\end{aligned}$$

For the first component of the above, we have that

$$\begin{aligned}
&\sum_{\widehat{e}_h^l \in \widehat{\mathcal{E}}_h^l} \int_{\widehat{e}_h^l} \delta_{\widehat{e}_h}^{-1}[v_h^l]\{\nabla_\Gamma u_h^l; n - \mathbf{P}\widehat{n}_h^l\}\ \mathrm{ds} \\
&\lesssim \|v_h^l\|_{DG}\left(\sum_{\widehat{e}_h^l \in \widehat{\mathcal{E}}_h^l} \int_{\widehat{e}_h^l} \delta_{\widehat{e}_h}^{-1} h_{\widehat{e}_h^l} |\{\nabla_\Gamma u_h^l; n - \mathbf{P}\widehat{n}_h^l\}|^2\ \mathrm{ds}\right)^{\frac{1}{2}}
\end{aligned}$$

after applying Cauchy-Schwartz. Using similar arguments as done in the proof of

Lemma 4.3.8, we have that

$$\begin{aligned}
&\sum_{\widehat{e}_h^l \in \widehat{\mathcal{E}}_h^l} \int_{\widehat{e}_h^l} \delta_{\widehat{e}_h}^{-1} h_{\widehat{e}_h^l} \left| (n^+ - \mathbf{P}\widehat{n}_h^{l+}) \cdot \nabla_\Gamma u_h^{l+} \right|^2 \, \mathrm{ds} \\
&\leq \sum_{\widehat{e}_h^l \in \widehat{\mathcal{E}}_h^l} \int_{\widehat{e}_h^l} \delta_{\widehat{e}_h}^{-1} h_{\widehat{e}_h^l} |n^+ - \mathbf{P}\widehat{n}_h^{l+}|^2 |\nabla_\Gamma u_h^{l+}|^2 \, \mathrm{ds} \\
&\lesssim \|n^+ - \mathbf{P}\widehat{n}_h^{l+}\|^2_{L^\infty(\widehat{\mathcal{E}}_h^l)} \sum_{\widehat{K}_h^l \in \widehat{\mathcal{T}}_h^l} \sum_{\widehat{e}_h^l \in \partial \widehat{K}_h^l} h_{\widehat{e}_h^l} \| \nabla_\Gamma u_h^l \Big|_{\widehat{K}_h^l} \|^2_{L^2(\widehat{e}_h^l)} \\
&\lesssim \|n^+ - \mathbf{P}\widehat{n}_h^{l+}\|^2_{L^\infty(\widehat{\mathcal{E}}_h^l)} \|u_h^l\|^2_{DG}.
\end{aligned}$$

For the second component, we have that

$$\begin{aligned}
&\sum_{\widehat{e}_h^l \in \widehat{\mathcal{E}}_h^l} \int_{\widehat{e}_h^l} \delta_{\widehat{e}_h}^{-1} [v_h^l] d \{ \nabla_\Gamma u_h^l ; \mathbf{H}\widehat{n}_h^l \} \, \mathrm{ds} \\
&\lesssim \|v_h^l\|_{DG} \left(\sum_{\widehat{e}_h^l \in \widehat{\mathcal{E}}_h^l} \int_{\widehat{e}_h^l} \delta_{\widehat{e}_h}^{-1} h_{\widehat{e}_h^l} d^2 \left| \{ \nabla_\Gamma u_h^l ; \mathbf{H}\widehat{n}_h^l \} \right|^2 \, \mathrm{ds} \right)^{\frac{1}{2}}.
\end{aligned}$$

Pursuing the analysis as before and using the fact that the Hessian $\mathbf{H}$ is bounded, we have that

$$\begin{aligned}
&\sum_{\widehat{e}_h^l \in \widehat{\mathcal{E}}_h^l} \int_{\widehat{e}_h^l} \delta_{\widehat{e}_h}^{-1} h_{\widehat{e}_h^l} d^2 |\nabla_\Gamma u_h^{l+} \cdot \mathbf{H}\widehat{n}_h^{l+}|^2 \, \mathrm{ds} \leq \sum_{\widehat{e}_h^l \in \widehat{\mathcal{E}}_h^l} \int_{\widehat{e}_h^l} \delta_{\widehat{e}_h}^{-1} h_{\widehat{e}_h^l} d^2 |\nabla_\Gamma u_h^{l+}|^2 |\mathbf{H}\widehat{n}_h^{l+}|^2 \, \mathrm{ds} \\
&\lesssim \|d\|^2_{L^\infty(\Gamma)} \sum_{\widehat{K}_h^l \in \widehat{\mathcal{T}}_h^l} \sum_{\widehat{e}_h^l \in \partial \widehat{K}_h^l} h_{\widehat{e}_h^l} \| \nabla_\Gamma u_h^l \Big|_{\widehat{K}_h^l} \|^2_{L^2(\widehat{e}_h^l)} \lesssim \|d\|^2_{L^\infty(\Gamma)} \|u_h^l\|^2_{DG}
\end{aligned}$$

where again the last inequality follows from applying similar arguments as in the proof of Lemma 4.3.8.

We can now estimate the error functional E_{hk}:

$$\begin{aligned}
|E_{hk}(v_h^l)| &\lesssim \|\mathbf{R}_{hk} - \mathbf{P}\|_{L^\infty(\Gamma)} \|u_h^l\|_{DG} \|v_h^l\|_{DG} + \|\delta_{hk}^{-1} - 1\|_{L^\infty(\Gamma)} \|u_h^l\|_{DG} \|v_h^l\|_{DG} \\
&+ \|1 - \delta_{hk}^{-1}\|_{L^\infty(\Gamma)} \|f\|_{L^2(\Gamma)} \|v_h^l\|_{DG} + \|1 - \delta_{\widehat{e}_h}^{-1}\|_{L^\infty(\widehat{\mathcal{E}}_h^l)} \|u_h^l\|_{DG} \|v_h^l\|_{DG} \\
&+ \|n^+ - \mathbf{P}\widehat{n}_h^{l+}\|_{L^\infty(\widehat{\mathcal{E}}_h^l)} \|u_h^l\|_{DG} \|v_h^l\|_{DG} + \|n^- - \mathbf{P}\widehat{n}_h^{l-}\|_{L^\infty(\widehat{\mathcal{E}}_h^l)} \|u_h^l\|_{DG} \|v_h^l\|_{DG} \\
&+ \|d\|_{L^\infty(\Gamma)} \|u_h^l\|_{DG} \|v_h^l\|_{DG}.
\end{aligned}$$

So by Lemma 4.3.1 and the stability estimate (4.41) we have

$$|E_{hk}(v_h^l)| \lesssim h^{k+1}\|f\|_{L^2(\Gamma)}\|v_h^l\|_{DG}$$

for every $v_h^l \in V_h^l$ as required. □

Remark 4.4.6. Note that the error functional E_{hk} in Lemma 4.4.5 includes all of the terms present in the higher order surface FEM setting (see Demlow [2009]) as well as additional terms arising from the surface DG methods.

4.5 Numerical tests

4.5.1 Implementation aspects

In the following numerical tests we will restrict our attention to the (symmetric) surface IP method (4.10) with the penalty parameter α chosen to be equal to 10. This surface DG method has been implemented using DUNE-FEM, a discretisation module based on the Distributed and Unified Numerics Environment (DUNE), (further information about DUNE can be found in Bastian et al. [2008b], Bastian et al. [2008a] and Bastian et al. [2012]). DG methods are well tested for the DUNE-FEM module, as shown in Dedner et al. [2010], Brdar et al. [2012], but only simple schemes have been tested for surface PDEs (further information about the DUNE-FEM module can be found in Dedner et al. [2010] and Dedner et al. [2012]). The initial grid generation for each test case is performed using the 3D surface grid generation module of the Computational Geometry and Algorithms Library (CGAL) (see Rineau and Yvinec [2009]).

The efficient computation of the surface lifting ξ and the signed distance function d are central to implementing the surface DG methods analysed in the previous sections; namely for performing grid refinements, as newly created nodes have to be surface lifted onto Γ. However, only in a very few cases is d available explicitely (for example, $d(x) = |x| - R$ for a sphere of radius R). Even for relatively simple surfaces such as ellipsoids, an explicit expression for d is not available and so both ξ and d must be approximated. Since d is assumed to be smooth and we need to be concerned only about starting points sufficiently close to Γ, standard methods of nonlinear optimisation (based on the more general/available *level-set* description ϕ of the surface) to approximate d are, in principle, applicable.

Two different algorithms, developed and discussed in Demlow and Dziuk [2008], have been tested for such problems: one being Newton's method and the other being an ad-hoc first-order method. Before describing the methods, we note a

relationship which we shall use in our algorithms. For $x \in U$, $\phi(x) = \int_0^{d(x)} \nabla\phi(\xi(x) + t\nu(x)) \cdot \nu(x)\ \mathrm{d}t = d|\nabla\phi(x)| + O(d^2)$. Thus,

$$d(x) \approx \frac{\phi(x)}{|\nabla\phi(x)|}. \tag{4.56}$$

Next, we describe the implementation of Newton's method. Assume that $x_0 \in U$ and that we wish to compute $\xi(x_0)$. The Newton method seeks to find a stationary point of the function $F(x, \lambda) = |x - x_0|^2 + \lambda\phi(x)$ where ϕ is the level-set function of Γ (and not necessarily a signed distance function). Note that $\nabla F(x, \lambda) = (2(x - x_0) + \lambda\nabla\phi(x), \phi(x))$. Thus $\nabla F(x, \lambda) = 0$ implies that $x \in \Gamma$ and $(x - x_0)$ is parallel to $\nabla\phi(x)$, that is, $x = \xi(x_0)$. In order to choose a starting point, we note that $2(x - x_0) + \lambda\nabla\phi(x) = 0$ implies that $\lambda = \frac{2d(x_0)}{|\nabla\phi(x_0)|}$. Using (4.56), we thus choose the starting value $(x_0, \lambda_0) = (x_0, 2\phi(x_0)/|\nabla\phi(x_0)|^2)$. Given a tolerance *tol*, we iterate Newton's method until

$$\left(\frac{\phi(x)^2}{|\nabla\phi(x)|^2} + \left| \frac{\nabla\phi(x)}{|\nabla\phi(x)|} + sign(\phi(x_0)) \frac{x - x_0}{|x - x_0|} \right|^2 \right)^{1/2} < tol \tag{4.57}$$

is reached. Fulfillment of this stopping criteria guarantees that the returned value $x \approx \xi(x_0)$ lies in the correct direction from x_0 to within *tol* and that, because of (4.56), $d(x) < tol$ up to higher-order terms.

The first-order algorithm detailed in Demlow and Dziuk [2008] may be described as follows: since $\xi(x) = x - d(x)\nu(x)$, we may use (4.56) and $\nu(x) \approx \frac{\nabla\phi(x)}{|\nabla\phi(x)|}$ to approximate ξ by $\xi(x) \approx x - \frac{\phi(x)\nabla\phi(x)}{|\nabla\phi(x)|^2}$. Iterating this relationship leads to an algorithm which converges to some point on Γ but no generally to $\xi(x)$. We thus correct the direction $x - x_0$ at each step, yielding the following algorithm.

1. Stipulate *tol* and x_0 and initialise $x = x_0$.
2. While (4.57) is not satisfied, iterate the following steps:
   (a) Calculate $\tilde{x} = x - \frac{\phi(x)\nabla\phi(x)}{|\nabla\phi(x)|^2}$ and $dist = sign(\phi(x_0))|\tilde{x} - x_0|$.
   (b) Set $x = x_0 - dist\frac{\nabla\phi(\tilde{x})}{|\nabla\phi(\tilde{x})|}$.

For both algorithms, we additionally choose to approximate the entries of $\nabla\phi(x)$ via second order finite difference approximations for a more generic implementation. It was observed in Demlow and Dziuk [2008] that in practice the second of the two algorithms was more efficient due to the fact that each step of Newton's method is relatively expensive. This was observed in practice and, as such, the numerical tests discussed below make use of the first-order algorithm.

In addition, we make use of this algorithm to provide a generic implementa-

tion of test problems on surfaces. Computing the Laplace-Beltrami operator of some given function over an arbitrary compact smooth and oriented surface in $\mathbb{R}^3$ given by the zero level-set of some function is tedious and requires changing the implementation for every such surface. In particular, we would need to explicitly compute the outward unit normal of the surface and its gradient whenever we consider a new surface. For any $u \in C^2(\mathbb{R}^3)$, we have that

$$\Delta_\Gamma u = \Delta u - \nu \cdot \nabla^2 u \nu - \mathrm{tr}(\nabla \nu) \nabla u \cdot \nu \tag{4.58}$$

where Δ is the usual Euclidean Laplace operator in $\mathbb{R}^3$, $\nabla^2 u \in \mathbb{R}^{3\times 3}$ the (Euclidean) Hessian of u, ∇u the (Euclidean) gradient of u and finally $\mathrm{tr}(\nabla \nu)$ the trace of $\nabla \nu$ where $\nabla \nu \in \mathbb{R}^{3\times 3}$ whose entries are the (Euclidean) partial derivatives of each component of the normal. We can make use of the ad-hoc first-order algorithm described previously to approximate the outward unit normal ν of Γ in (4.58): this is done by computing $\nu(\xi(x_0)) \approx sign(\phi(x_0)) \frac{\tilde{\xi}(x_0)-x_0}{|\tilde{\xi}(x_0)-x_0|}$ where $\tilde{\xi}(x_0)$ is the approximation of $\xi(x_0)$ resulting from the algorithm . We may also approximate the (diagonal) entries of $\nabla \nu$ via second-order finite difference approximations as done for the approximation of $\nabla \phi$ in the first-order algorithm. Such a generic implementation has the benefit of only requiring input of the level-set function for the surface and nothing more, significantly facilitating numerical tests. Although we omit a rigorous error analysis of such an approximation of the Laplace-Beltrami operator, the error caused by such an approximation appears not to affect the resulting convergence orders for all of the test cases considered below.

4.5.2 Test problem on the sphere

We first consider the simple test problem

$$-\Delta_\Gamma u + u = f \tag{4.59}$$

on the unit sphere

$$\Gamma = \{x \in \mathbb{R}^3 \ : \ |x| = 1\}$$

whose exact solution is chosen to be given by
$u(x_1, x_2, x_3) = \cos(2\pi x_1)\cos(2\pi x_2)\cos(2\pi x_3)$. Table 4.2 shows the L^2 and DG errors/EOCs for linear ($k = 1$) DG/surface approximation order. As expected, the experimental orders of convergence (EOCs) match up well with the theoretical convergence rates.

Elements	h	L_2-error	L_2-eoc	DG-error	DG-eoc
632	0.223929	0.171459		5.07662	
2528	0.112141	0.0528817	1.70	2.64273	0.94
10112	0.0560925	0.0146074	1.86	1.3151	1.01
40448	0.028049	0.00378277	1.95	0.653612	1.01
161792	0.0140249	0.000957472	1.98	0.325961	1.00
647168	0.00701247	0.000240483	1.99	0.162822	1.00

Table 4.2: Errors and convergence orders for the DG approximation of (4.59) on the unit sphere with $k = 1$.

4.5.3 Test problem on Dziuk surface

Our second test problem, taken from Dziuk [1988], considers (4.59) on the Dziuk surface

$$\Gamma = \{x \in \mathbb{R}^3 \ : \ (x_1 - x_3^2)^2 + x_2^2 + x_3^2 = 1\}$$

whose exact solution is chosen to be given by $u(x) = x_1 x_2$. The outward unit normal to this surface is given by $\nu(x) = (x_1 - x_3^2, x_2, x_3(1 - 2(x_1 - x_3^2)))/(1 + 4x_3^2(1 - x_1 - x_2^2))^{1/2}$. There is no explicit projection map for mapping newly created nodes to Γ so $\xi(x)$ has to be approximated via the ad-hoc first order algorithm described in Section 4.5.1.

Elements	h	L_2-error	L_2-eoc	DG-error	DG-eoc
92	0.704521	0.243493		0.894504	
368	0.353599	0.0842372	1.53	0.490805	0.87
1472	0.176993	0.0268596	1.65	0.263808	0.90
5888	0.0885231	0.00637826	2.07	0.135162	0.97
23552	0.0442651	0.00171047	1.90	0.0685366	0.98
94208	0.022133	0.000416366	2.04	0.0343677	1.00
376832	0.0110666	0.000104274	2.00	0.0171891	1.00
1507328	0.0055333	2.60734e-05	2.00	0.0085935	1.00

Table 4.3: Errors and convergence orders for the DG approximation of (4.59) on the Dziuk surface with $k = 1$.

Table 4.3 shows the L^2 and DG errors/EOCs for linear ($k = 1$) DG/surface approximation order. As before, the experimental orders of convergence (EOCs) match up well with the theoretical convergence rates. Figure 4.3 shows the resulting DG approximation to (4.59) on the Dziuk surface.

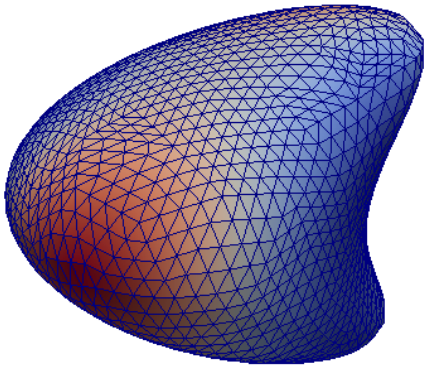

(a)

Figure 4.3: DG approximation of (4.59) on the Dziuk surface with $k = 1$.

4.5.4 Test problem on Enzensberger-Stern surface

Our next test problem considers (4.59) on the Enzensberger-Stern surface

$$\Gamma = \{x \in \mathbb{R}^3 \ : \ 400(x^2y^2 + y^2z^2 + x^2z^2) - (1 - x^2 - y^2 - z^2)^3 - 40 = 0\}$$

whose exact solution is again chosen to be given by $u(x) = x_1x_2$. As for the previous test problem, there is no explicit projection map so we make use of the first order ad-hoc algorithm. In this test problem, the computation of $\Delta_\Gamma u$ to derive the right-hand side of (4.59) is done via our approximation of the Laplace-Beltrami operator described in Section 4.5.1.

Elements	h	L_2-error	L_2-eoc	DG-error	DG-eoc
2358	0.163789	0.476777		0.998066	
9432	0.0817973	0.175293	1.44	0.472241	1.08
37728	0.040885	0.0160606	3.45	0.150144	1.65
150912	0.0204411	0.00139698	3.52	0.0703901	1.09
603648	0.0102204	0.00033846	2.04	0.03473453	1.02
2414592	0.00511	7.86713e-05	2.10	0.0172348	1.01

Table 4.4: Errors and convergence orders for the DG approximation of (4.59) on the Enzensberger-Stern surface with $k = 1$.

Table 4.4 shows the L^2 and DG errors/EOCs for linear ($k = 1$) DG/surface approximation order. Although the EOCs are more erratic than for the previous test problem, partly due to our approximation of the Laplace-Beltrami operator, they

nevertheless match up well with theoretical convergence rates. Figure 4.4 shows the resulting DG approximation to (4.59) on this surface.

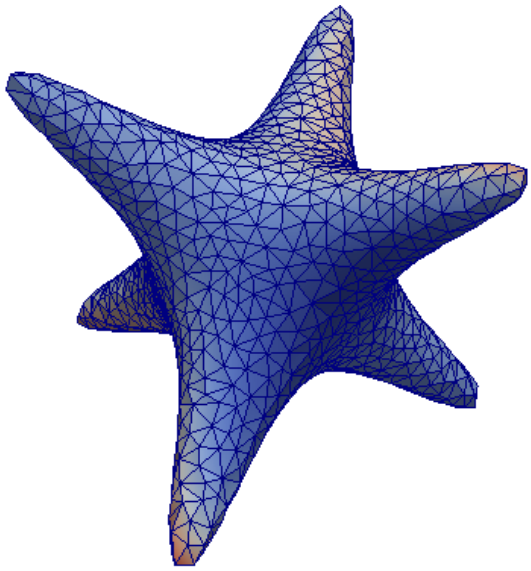

(a)

Figure 4.4: DG approximation of (4.59) on the Enzensberger-Stern surface with $k = 1$.

4.5.5 Higher order numerics

Table 4.5 and Table 4.6 show the L^2 and DG errors/EOCs for respectively *quadratic* ($k = 2$) and *quartic* ($k = 4$) DG/surface approximation order for the sphere test problem. As expected, we observe higher order optimal convergence rates which coincide with those that were derived theoretically.

Elements	h	L_2-error	L_2-eoc	DG-error	DG-eoc
632	0.223929	0.0369759		1.42052	
2528	0.112141	0.00490374	2.91	0.386962	1.88
10112	0.0560925	0.000609787	3.00	0.0986477	1.97
40448	0.028049	7.58558e-05	3.01	0.0247951	1.99
161792	0.0140249	9.45978e-06	3.00	0.00620871	2.00

Table 4.5: Errors and convergence orders for the DG approximation of (4.59) on the unit sphere with $k = 2$.

Next, we look at the case when the surface approximation order k and the DG space order r do not coincide. In this case, one can show that, for symmetric

Elements	h	L_2-error	L_2-eoc	DG-error	DG-eoc
632	0.223929	0.000776829		0.0471208	
2528	0.112141	2.68079e-05	4.86	0.00325848	3.85
10112	0.0560925	8.48343e-07	4.98	0.000207653	3.97
40448	0.028049	2.65819e-08	5.00	1.30507e-05	4.00

Table 4.6: Errors and convergence orders for the DG approximation of (4.59) on the unit sphere with $k = 4$.

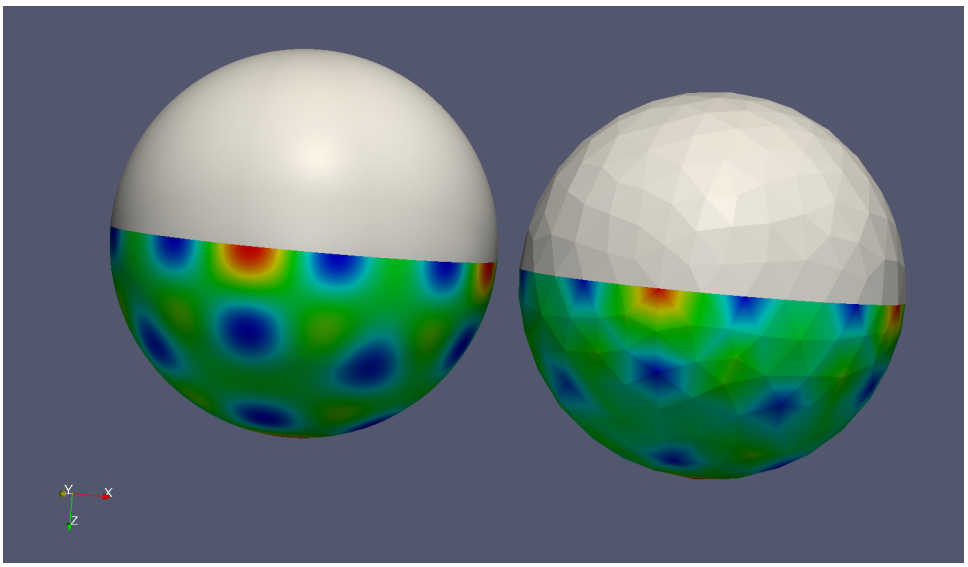

Figure 4.5: Paraview plots of the linear ($k = 1$) (right) and quartic ($k = 4$) (left) DG approximation of (4.59) on the unit sphere (623 elements).

surface DG methods, if $u \in H^{r+1}(\Gamma)$, the estimates given in Theorem 4.4.1 are now given by

$$\|u - u_h^l\|_{DG} \lesssim h^r \|u\|_{H^{r+1}(\Gamma)} + h^{k+1} \|f\|_{L^2(\Gamma)},$$
$$\|u - u_h^l\|_{L^2(\Gamma)} \lesssim h^{r+1} \|u\|_{H^{r+1}(\Gamma)} + h^{k+1} \|f\|_{L^2(\Gamma)}.$$

These estimates indicate that one could obtain optimal higher order convergence rates in the DG norm by choosing the ansatz space order to be one order higher than the surface approximation order. This is shown in Table 4.7 for the Dziuk test problem.

Elements	h	L_2-error	L_2-eoc	DG-error	DG-eoc
92	0.704521	0.136442		0.322416	
368	0.353599	0.0551454	1.31	0.150303	1.10
1472	0.176993	0.0215041	1.36	0.0601722	1.32
5888	0.0885231	0.00448861	2.26	0.0182412	1.72
23552	0.0442651	0.00120287	1.90	0.00513161	1.83
94208	0.022133	0.00029651	2.02	0.00130482	1.98
376832	0.0110666	7.41044e-05	2.00	0.00032728	2.00

Table 4.7: Errors and convergence orders for the DG approximation of (4.59) on the Dziuk surface with $k = 1$ and $r = 2$.

Chapter 5

A Posteriori Error Analysis of DG Methods on Surfaces

In this chapter, we will derive and analyse an a posteriori error estimator for the (symmetric) surface IP method (4.10). For simplicity we will restrict our a posteriori analysis to piecewise linear surface approximations/DG spaces, rather than higher order surface approximations/DG spaces which was considered in Chapter 4 for the a priori analysis. To highlight this, all Γ_h geometric objects and derived quantities (functions spaces, change of measures, etc.) defined in Chapter 4 will appear without hats (e.g. $e_h \in \mathcal{E}_h$ instead of $\widehat{e}_h \in \widehat{\mathcal{E}}_h$ and δ_{e_h} instead of $\delta_{\widehat{e}_h}$) and without the surface approximation order ("k") subscripts (e.g. S_h instead of $\widehat{S}_{h1}$). Much of the analysis presented in this chapter can be straightforwardly applied to both a larger class of surface DG methods and higher order surface approximations, as in Chapter 4. It is also worth comparing the main results in this chapter (Theorem 5.5.1 and Theorem 5.6.1) with those for surface FEM given in Section 2.5.

5.1 Notation and setting

Recall from Chapter 2 the model problem (2.6): given $f \in L^2(\Gamma)$, find $u \in H^1(\Gamma)$ such that

$$a_\Gamma(u,v) = \int_\Gamma fv \ \mathrm{dA} \quad \forall v \in H^1(\Gamma) \tag{5.1}$$

where

$$a_\Gamma(u,v) = \int_\Gamma \nabla_\Gamma u \cdot \nabla_\Gamma v + uv \ \mathrm{dA}.$$

Here Γ is still a compact smooth and oriented surface in $\mathbb{R}^3$. In this chapter, we will only assume that $u \in H^1(\Gamma)$: no higher (elliptic) regularity results will be assumed.

5.2 Surface IP approximation

As in Chapter 2, we approximate Γ by a piecewise linear surface approximation Γ_h composed of planar triangles $\{K_h\}_{K_h \in \mathcal{T}_h}$ whose vertices lie on Γ, and denote by $\mathcal{T}_h$ the associated regular, conforming triangulation of Γ_h, i.e., $\Gamma_h = \bigcup_{K_h \in \mathcal{T}_h} K_h$. In addition, let $\mathcal{N}$ denote the set of nodes of triangles in $\mathcal{T}_h$ (note that $\mathcal{N} \subset \Gamma$). We also denote by h_{K_h} the largest edge of $K_h \in \mathcal{T}_h$. Given $p \in \mathcal{N}$, we define the patch $w_p = interior(\cup_{K_h | p \in \bar{K}_h} \bar{K}_h)$ and let $h_p = \max_{K_h \subset w_p} h_{K_h}$. The discrete problem reads: find $u_h \in S_h$ such that

$$\mathcal{A}_h^{IP}(u_h, v_h) = \sum_{K_h \in \mathcal{T}_h} \int_{K_h} f_h v_h \, \mathrm{dA_h} \; \forall v_h \in S_h \tag{5.2}$$

where

$$\begin{aligned} \mathcal{A}_h^{IP}(u_h, v_h) := & \sum_{K_h \in \mathcal{T}_h} \int_{K_h} \nabla_{\Gamma_h} u_h \cdot \nabla_{\Gamma_h} v_h + u_h v_h \, \mathrm{dA_h} \\ & - \sum_{e_h \in \mathcal{E}_h} \int_{e_h} [u_h]\{\nabla_{\Gamma_h} v_h; n_h\} + [v_h]\{\nabla_{\Gamma_h} u_h; n_h\} \, \mathrm{ds_h} \\ & + \sum_{e_h \in \mathcal{E}_h} \int_{e_h} \beta_{e_h} [u_h][v_h] \, \mathrm{ds_h} \end{aligned}$$

where β_{e_h} is given by (4.7) with $k = 1$.

5.3 Technical tools

5.3.1 Surface lift

The surface lift is defined as in Section 2.3.1. As before, for every $K_h \in \mathcal{T}_h$, there is a unique curved triangle $K_h^l := \xi(K_h) \subset \Gamma$ and these lifted triangles induce a (lifted) regular, conforming triangulation $\mathcal{T}_h^l$ of Γ. Similarly, $e_h^l := \xi(e_h) \in \mathcal{E}_h^l$ are the unique curved edges. The surface lift S_h^l of the scalar function space S_h is given in the usual way. As in (2.9), we define the discrete right-hand side f_h such that $f_h^\ell = f$. Recall that we denote by $w^{-\ell} \in S_h$ the *inverse* surface lift of some function $w \in S_h^\ell$ satisfying $(w^{-\ell})^\ell = w$.

In addition to (2.10), which provides a formula for moving from gradients on

Γ_h to gradients on Γ, one can show that for $x \in \Gamma_h$ and v_h defined on Γ_h, we have that

$$\nabla_\Gamma v_h^l(\xi(x)) = \mathbf{F}_h(x)\nabla_{\Gamma_h} v_h(x) \tag{5.3}$$

where

$$\mathbf{F}_h(x) := (\mathbf{I} - d\mathbf{H})(x)^{-1}\left(\mathbf{I} - \frac{\nu_h \otimes \nu}{\nu_h \cdot \nu}\right).$$

See Demlow and Dziuk [2008] for further details. We will also require the surface lift Σ_h^l of the vector-valued function space Σ_h, which is given by

$$\Sigma_h^l := \{w_h^l \in [L^2(\Gamma)]^3 : \ w_h^l(\xi) = \mathbf{F}_h w_h(x(\xi)), \ \text{ for some } w_h \in \Sigma_h\}.$$

Remark 5.3.1. Note that the definition of Σ_h^l also implies that $w_h = \mathbf{P}_h(\mathbf{I} - d\mathbf{H})\mathbf{P}w_h^l$ for $w_h^l \in \Sigma_h^l$. This can be seen by noting that since w_h^l is tangential to Γ, we have that

$$\mathbf{F}_h\mathbf{P}_h(\mathbf{I} - d\mathbf{H})\mathbf{P}w_h^l = (\mathbf{I} - d\mathbf{H})^{-1}(\mathbf{I} - \frac{\nu_h \otimes \nu}{\nu_h \cdot \nu})(\mathbf{I} - \nu_h \otimes \nu_h)(\mathbf{I} - d\mathbf{H})w_h^l.$$

Now $\frac{(\nu_h \otimes \nu)(\nu_h \otimes \nu_h)}{\nu_h \cdot \nu} = \frac{(\nu \cdot \nu_h)\nu_h \otimes \nu_h}{\nu \cdot \nu_h} = \nu_h \otimes \nu_h$ so

$$\begin{aligned}\mathbf{F}_h\mathbf{P}_h(\mathbf{I} - d\mathbf{H})\mathbf{P}w_h^l &= (\mathbf{I} - d\mathbf{H})^{-1}(\mathbf{I} - \frac{\nu_h \otimes \nu}{\nu_h \cdot \nu})(\mathbf{I} - d\mathbf{H})w_h^l \\ &= w_h^l - \frac{1}{\nu_h \cdot \nu}(\mathbf{I} - d\mathbf{H})^{-1}(\nu_h \otimes \nu)(\mathbf{I} - d\mathbf{H})w_h^l.\end{aligned}$$

Now we define $\tilde{w}_h^l := (\mathbf{I} - d\mathbf{H})w_h^l$ and note that this is still tangential to Γ. As such, we have that $(\nu_h \otimes \nu)\tilde{w}_h^l = (\nu \cdot \tilde{w}_h^l)\nu_h = 0$. And so,

$$\mathbf{F}_h\mathbf{P}_h(\mathbf{I} - d\mathbf{H})\mathbf{P}w_h^l = w_h^l.$$

Finally, we define

$$\mathbf{B}_h := \sqrt{\delta_h}(\mathbf{P} - \mathbf{R}_h)\mathbf{F}_h \tag{5.4}$$

where, as before, $\mathbf{R}_h$ is given by (2.12). Next, we derive explicit formulas for the change of measures δ_h and δ_{e_h}, which will be useful to obtain a computable a posteriori error estimator.

Lemma 5.3.2. *Assume that $x \in \Gamma_h$. Then*

$$\delta_h(x) = (1 - d(x)\kappa_1(x))(1 - d(x)\kappa_2(x))\nu \cdot \nu_h, \tag{5.5}$$

$$\delta_{e_h}(x) = |\nabla\xi(x)\tau_h(x)| \tag{5.6}$$

where τ_h is the unit tangent of e_h.

Proof. See Proposition 2.1 in Demlow and Dziuk [2008] for the first expression. To prove the second expression, we do the following: let $e \subset \mathbb{R}$ be the reference edge for codimension one entities. Let $f : e \to e_h \subset \Gamma_h$ be the linear transformation from the reference edge to some fixed edge $e_h \in \mathcal{E}_h$. $F := f' \in \mathbb{R}^{3\times 1}$ is tangent to e_h and so $F = \lambda\tau_h$ where $\lambda \in \mathbb{R}$ and τ_h is the unit tangent of e_h. Hence we have that $\mathrm{ds} = \sqrt{|F^T\nabla\xi^T\nabla\xi F|}\ \mathrm{dx} = |\lambda||\nabla\xi\tau_h|\ \mathrm{dx}$ where $\nabla\xi \in \mathbb{R}^{3\times 3}$ is the gradient of the projection mapping ξ given in (2.1) and dx is the Lebesgue measure on e. Similarly, we have that $\mathrm{ds_h} = |\lambda|\ \mathrm{dx}$ and the second expression follows. □

5.3.2 Clément interpolation

We now define a quasi-interpolant and state some estimates that it must satisfy. Given $z \in L^1(\Gamma)$ and $p \in \mathcal{N}$, we let

$$z_p^{-l} := \frac{1}{\int_{w_p} \varphi_p \ \mathrm{dA_h}} \int_{w_p} \varphi_p z^{-l} \ \mathrm{dA_h} \tag{5.7}$$

where $\varphi_p \in S_h \cap H^1(\Gamma_h)$ denotes the Lagrange nodal basis function associated with p, and define

$$I_h z^{-l} := \sum_{p\in\mathcal{N}} z_p^{-l}\varphi_p. \tag{5.8}$$

We note a useful property that the weights z_p^{-l} satisfy (see (2.2.33) in Demlow and Dziuk [2008]):

$$\|z_p^{-l}\|_{L^2(w_p)} \le \sqrt{\frac{3}{2}}\|z^{-l}\|_{L^2(w_p)} \le \sqrt{\frac{3}{2}}\|\sqrt{\delta_h}\|_{L^\infty(w_p)}\|z\|_{L^2(w_p^l)}. \tag{5.9}$$

Since $\{\varphi_p\}$ is a partition of unity i.e. $\sum_{p\in\mathcal{N}} \varphi_p = 1$, we also have the following:

$$\int_{\Gamma_h} (z^{-l} - I_h z^{-l}) \ \mathrm{dA_h} = \sum_{p\in\mathcal{N}} \int_{w_p} (z^{-l} - z_p^{-l})\varphi_p \ \mathrm{dA_h} = 0. \tag{5.10}$$

The Clément interpolant satisfies the following estimates.

Lemma 5.3.3. *Let $z \in H^1(\Gamma)$. Assume that the grid $\mathcal{T}_h$ is shape-regular and that the number of elements sharing the node p is bounded. Let w_p^l be the surface lift of the patch w_p onto Γ. Then for each $p \in \mathcal{N}$, we have that*

$$\|z^{-l} - z_p^{-l}\|_{L^2(w_p)} \leq Ch_p \|\mathbf{R}_h\|_{l^2,L^\infty(w_p)}^{\frac{1}{2}} \|\nabla_\Gamma z\|_{L^2(w_p^l)}. \tag{5.11}$$

Let also $p \in \bar{e}_h \subset \mathcal{E}_h$. Then

$$\|z^{-l} - z_p^{-l}\|_{L^2(e_h)} \leq Ch_p^{\frac{1}{2}} \|\mathbf{R}_h\|_{l^2,L^\infty(w_p)}^{\frac{1}{2}} \|\nabla_\Gamma z\|_{L^2(w_p^l)} \tag{5.12}$$

where $\mathbf{R}_h$ is given by (2.12). Note that C does not depend on any essential quantities. Here $\|\mathbf{R}_h\|_{l^p,L^q(w_p)} := \|\|\mathbf{R}_h\|_{l^p \to l^p}\|_{L^q(w_p)}$ and, if $p = q$, we omit the first index.

Proof. See Lemma 2.2 in Demlow and Dziuk [2008]. □

5.4 Dual weighted residual equation

We derive a residual equation for some quantity of interest $J(u - u_h^l)$ where J is some bounded, linear functional acting on $H^1(\Gamma) + S_h^l$.

5.4.1 Bilinear form on Γ

Before we state the bilinear form we consider on Γ, we require the following DG lift operators.

Definition 5.4.1. Let $w \in H^1(\Gamma) + S_h^l$. Define the operators $\mathbf{L} : H^1(\Gamma) + S_h^l \to \Sigma_h^l$ and, for every $e_h^l \in \mathcal{E}_h^l$, $\mathbf{L}_{e_h^l} : H^1(\Gamma) + S_h^l \to \Sigma_h^l$ by respectively

$$\sum_{K_h^l \in \mathcal{T}_h^l} \int_{K_h^l} \mathbf{L}(w) \cdot \phi_h^l \, \mathrm{dA} = \sum_{e_h^l \in \mathcal{E}_h^l} \int_{e_h^l} [w]\{\phi_h^l; n\} \, \mathrm{ds},$$
$$\sum_{K_h^l \in \mathcal{T}_h^l} \int_{K_h^l} \mathbf{L}_{e_h^l}(w) \cdot \phi_h^l \, \mathrm{dA} = \int_{e_h^l} [w]\{\phi_h^l; n\} \, \mathrm{ds}$$

for all $\phi_h^l \in \Sigma_h^l$, where n^+ and n^- are respectively the unit surface conormals to K_h^{l+} and K_h^{l-} on $e_h^l \in \mathcal{E}_h^l$, satisfying $n^+ = -n^-$.

Remark 5.4.2. Note that $w \in H^1(\Gamma) \Rightarrow \mathbf{L}(w) = 0$ and $\mathbf{L}_{e_h^l}(w) = 0$ for all $e_h \in \mathcal{E}_h$.

Remark 5.4.3. Note that, for each $e_h^l \in \mathcal{E}_h^l$, $\mathbf{L}_{e_h^l}(w)$ vanishes outside the union of the two triangles containing e_h^l and that $\mathbf{L}(w) = \sum_{e_h^l \in \mathcal{E}_h^l} \mathbf{L}_{e_h^l}(w)$ for all $w \in H^1(\Gamma) + S_h^l$.

The DG lifting operator $\mathbf{L}_{e_h^l}$ satisfies the following stability estimate:

Lemma 5.4.4. *Let $w_{e_h} = K_h^+ \cup K_h^-$ and $w_{e_h}^\partial = \partial K_h^+ \cup \partial K_h^-$. Then there exists a constant $C_L > 0$ such that, for each $e_h^l = K_h^{l+} \cap K_h^{l-} \in \mathcal{E}_h^l$,*

$$\|\mathbf{L}_{e_h^l}(w)\|_{L^2(\Gamma)} \lesssim \|\mathbf{F}_h\|_{L^\infty(w_{e_h}^\partial)} \|\mathbf{P}_h(\mathbf{I} - d\mathbf{H})\mathbf{P}\|_{L^\infty(w_{e_h})} \|\delta_{e_h}\|_{L^\infty(e_h)} \|\sqrt{\beta_{e_h}}[w^{-l}]\|_{L^2(e_h)}$$

for every $w \in S_h^l + H^1(\Gamma)$. The constant C_L depends solely on the shape-regularity of the mesh and on the penalty parameter α.

Proof. The proof will follow a similar argument to the one found in Schötzau et al. [2003]. Let $\Sigma_h^l(w_{e_h}^l)$ denote the space of all functions in Σ_h^l restricted to $w_{e_h}^l$. For $w \in S_h^l + H^1(\Gamma)$, making use of Remark 5.4.3 and the definition of Σ_h^l, we have that

$$\begin{aligned}
\|\mathbf{L}_{e_h^l}(w)\|_{L^2(w_{e_h}^l)} &= \sup_{\phi_h^l \in \Sigma_h^l(w_{e_h}^l)} \frac{\int_{w_{e_h}^l} \mathbf{L}_{e_h^l}(w) \cdot \phi_h^l \, \mathrm{dA}}{\|\phi_h^l\|_{L^2(w_{e_h}^l)}} = \sup_{\phi_h^l \in \Sigma_h^l(w_{e_h}^l)} \frac{\int_{e_h^l} [w]\{\phi_h^l; n\} \, \mathrm{ds}}{\|\phi_h^l\|_{L^2(w_{e_h}^l)}} \\
&\leq \sup_{\phi_h^l \in \Sigma_h^l(w_{e_h}^l)} \frac{\left(\int_{e_h^l} \delta_{e_h} \beta_{e_h} |[w]|^2 \, \mathrm{ds}\right)^{\frac{1}{2}} \left(\int_{e_h^l} \delta_{e_h}^{-1} \beta_{e_h}^{-1} |\{\phi_h^l; n\}|^2 \, \mathrm{ds}\right)^{\frac{1}{2}}}{\|\phi_h^l\|_{L^2(w_{e_h}^l)}}.
\end{aligned}$$

Now, by definition of Σ_h^l, there exists a $\phi_h \in \Sigma_h$ such that $\phi_h^l(\xi) = \mathbf{F}_h \phi_h(x(\xi))$. Therefore

$$\begin{aligned}
&\frac{\left(\int_{e_h^l} \delta_{e_h} \beta_{e_h} |[w]|^2 \, \mathrm{ds}\right)^{\frac{1}{2}} \left(\int_{e_h^l} \delta_{e_h}^{-1} \beta_{e_h}^{-1} |\{\phi_h^l; n\}|^2 \, \mathrm{ds}\right)^{\frac{1}{2}}}{\|\phi_h^l\|_{L^2(w_{e_h}^l)}} \\
&\leq \frac{\left(\int_{e_h} \delta_{e_h}^2 \beta_{e_h} |[w^{-l}]|^2 \, \mathrm{ds_h}\right)^{\frac{1}{2}} \left(\int_{w_{e_h}^\partial} \beta_{e_h}^{-1} |\mathbf{F}_h \phi_h|^2 \, \mathrm{ds_h}\right)^{\frac{1}{2}}}{\|\phi_h^l\|_{L^2(w_{e_h}^l)}}
\end{aligned}$$

Applying the trace theorem on Γ_h and lifting back onto Γ, we obtain

$$\begin{aligned}
\int_{\partial K_h^+} \beta_{e_h}^{-1} |\mathbf{F}_h \phi_h|^2 \, \mathrm{ds_h} &\leq \|\mathbf{F}_h\|_{L^\infty(\partial K_h^+)}^2 \int_{\partial K_h^+} \beta_{e_h}^{-1} |\phi_h|^2 \, \mathrm{ds_h} \\
&\leq C \|\mathbf{F}_h\|_{L^\infty(\partial K_h^+)}^2 \int_{K_h^+} \alpha^{-1} |\phi_h|^2 \, \mathrm{dA_h} \\
&\leq C \|\mathbf{F}_h\|_{L^\infty(\partial K_h^+)}^2 \|\mathbf{P}_h(\mathbf{I} - d\mathbf{H})\mathbf{P}\|_{L^\infty(K_h^+)}^2 \|\phi_h^l\|_{L^2(K_h^{l+})}^2
\end{aligned}$$

where we have used that $\delta_h^{-1} < 1$. Here C depends on the shape-regularity of the mesh and on the penalty parameter α but not on any other essential quantity like h. This provides the desired estimate. □

We can now define a bilinear form on Γ which is well-defined in the space

$(H^1(\Gamma) + S_h^l) \times (H^1(\Gamma) + S_h^l)$ by making use of the DG lift. Let

$$\mathcal{A}^{IP}(v,z) := \sum_{K_h^l \in \mathcal{T}_h^l} \int_{K_h^l} \nabla_\Gamma v \cdot \nabla_\Gamma z + vz \text{ dA} - \sum_{K_h^l \in \mathcal{T}_h^l} \int_{K_h^l} \mathbf{L}(v) \cdot \nabla_\Gamma z + \mathbf{L}(z) \cdot \nabla_\Gamma v \text{ dA}$$
$$+ \sum_{e_h^l \in \mathcal{E}_h^l} \int_{e_h^l} \delta_{e_h}^{-1} \beta_{e_h} [v][z] \text{ ds}. \tag{5.13}$$

The bilinear form $\mathcal{A}^{IP}$ is related to the original problem (5.1) in the following way:

Lemma 5.4.5. *Let $u_h \in S_h$ denote the solution to (5.2) and $u_h^l \in S_h^l$ its surface lift onto Γ. Let $z_h^l \in S_h^{c,l} := S_h^l \cap H^1(\Gamma)$. Then we have that*

$$\mathcal{A}^{IP}(u_h^l, z_h^l) = \sum_{K_h^l \in \mathcal{T}_h^l} \int_{K_h^l} f z_h^l \ dA - E_h(z_h^l)$$

where

$$E_h(z_h^l) := \sum_{K_h^l \in \mathcal{T}_h^l} \int_{K_h^l} (\mathbf{R}_h^l - \mathbf{P}) \nabla_\Gamma u_h^l \cdot \nabla_\Gamma z_h^l + \left(\delta_h^{-1} - 1\right) u_h^l z_h^l + \left(1 - \delta_h^{-1}\right) f z_h^l \ dA$$
$$+ \sum_{e_h^l \in \mathcal{E}_h^l} \int_{e_h^l} [u_h^l] \left(\{\nabla_\Gamma z_h^l; n\} - \left\{ \mathbf{P}_h^l (\mathbf{I} - d\mathbf{H}) \mathbf{P} \nabla_\Gamma z_h^l; n_h^l \right\} \delta_{e_h}^{-1} \right) \ ds.$$

Proof. We notice that $\mathcal{A}^{IP}(u_h^l, z_h^l) = \mathcal{A}^{IP}(u_h^l - u, z_h^l) + \mathcal{A}^{IP}(u, z_h^l)$. Since $u, z_h^l \in H^1(\Gamma)$ we have that $\mathcal{A}^{IP}(u, z_h^l) = a_\Gamma(u, z_h^l) = \sum_{K_h^l \in \mathcal{T}_h^l} \int_{K_h^l} f z_h^l \text{ dA}$ by Remark 5.4.2 and (5.1). Also, we have that $\mathcal{A}^{IP}(u - u_h^l, z_h^l) = E_h(z_h^l)$ by Lemma 4.4.5. □

5.4.2 Residual equation

In order to derive the residual equation, we consider the following dual problem: find $z \in H^1(\Gamma)$ such that

$$\mathcal{A}^{IP}(v,z) = J(v) \ \forall v \in H^1(\Gamma). \tag{5.14}$$

In a similar fashion to Karakashian and Pascal [2003] and Houston et al. [2007], we decompose the error $\mathrm{e}_h := u - u_h^l$ using $u_h = u_h^c + u_h^\perp$ (hence $u_h^l = u_h^{c,l} + u_h^{\perp,l}$) with $u_h^{c,l} \in S_h^{c,l}$ (which will be constructed explicitely in the proof of Lemma 5.5.3) and $u_h^{\perp,l} \in S_h^{\perp,l}$ where $S_h^{\perp,l}$ denotes the orthogonal complement in S_h^l of $S_h^{c,l}$ with respect to the DG norm. Thus $\mathrm{e}_h^c = u - u_h^{c,l} \in H^1(\Gamma)$. Let $z_h^l \in S_h^{c,l}$, then from the dual

problem (5.14) we have that

$$\begin{aligned} J(\mathrm{e}_h) &= J(\mathrm{e}_h^c) - J(u_h^{\perp,l}) = \mathcal{A}^{IP}(\mathrm{e}_h^c, z) - J(u_h^{\perp,l}) \\ &= \mathcal{A}^{IP}(\mathrm{e}_h, z) + \mathcal{A}^{IP}(u_h^{\perp,l}, z) - J(u_h^{\perp,l}) \\ &= \mathcal{A}^{IP}(u, z) - \mathcal{A}^{IP}(u_h^l, z - z_h^l) - \mathcal{A}^{IP}(u_h^l, z_h^l) + \mathcal{A}^{IP}(u_h^{\perp,l}, z) - J(u_h^{\perp,l}) \end{aligned}$$

Using the fact that $\mathcal{A}^{IP}(u, z) = a_\Gamma(u, z)$ (by Remark 5.4.2), (5.1) and Lemma 5.4.5, we get

$$J(\mathrm{e}_h) = \sum_{K_h^l \in \mathcal{T}_h^l} \int_{K_h^l} f(z - z_h^l) \,\mathrm{dA} - \mathcal{A}^{IP}(u_h^l, z - z_h^l) + \mathcal{A}^{IP}(u_h^{\perp,l}, z) - J(u_h^{\perp,l}) + E_h(z_h^l).$$

Using the fact that $z - z_h^l \in H^1(\Gamma)$ so that $[z - z_h^l] = 0$ holds, we have that

$$\begin{aligned} J(\mathrm{e}_h) = &\sum_{K_h^l \in \mathcal{T}_h^l} \int_{K_h^l} f(z - z_h^l) \,\mathrm{dA} - \sum_{K_h^l \in \mathcal{T}_h^l} \int_{K_h^l} \nabla_\Gamma u_h^l \cdot \nabla_\Gamma (z - z_h^l) + u_h^l (z - z_h^l) \,\mathrm{dA} \\ &+ \sum_{K_h^l \in \mathcal{T}_h^l} \int_{K_h^l} \mathbf{L}(u_h^l) \cdot \nabla_\Gamma (z - z_h^l) \,\mathrm{dA} + \mathcal{A}^{IP}(u_h^{\perp,l}, z) - J(u_h^{\perp,l}) + E_h(z_h^l). \end{aligned}$$

Moving the first two integrals in the above onto Γ_h and integrating by parts, we get

$$\begin{aligned} J(\mathrm{e}_h) = &\sum_{K_h \in \mathcal{T}_h} \left(\int_{K_h} (f_h \delta_h + \Delta_{\Gamma_h} u_h - u_h \delta_h)(z^{-l} - z_h) \,\mathrm{dA_h} - \int_{\partial K_h} \nabla_{\Gamma_h} u_h \cdot n_{K_h} (z^{-l} - z_h) \,\mathrm{ds_h} \right) \\ &- \sum_{K_h^l \in \mathcal{T}_h^l} \int_{K_h^l} (\mathbf{P} - \mathbf{R}_h^l) \nabla_\Gamma u_h^l \cdot \nabla_\Gamma z \,\mathrm{dA} + \sum_{K_h^l \in \mathcal{T}_h^l} \int_{K_h^l} \left(\delta_h^{-1} - 1 \right) (u_h^l - f) z_h^l \,\mathrm{dA} \\ &+ \sum_{K_h^l \in \mathcal{T}_h^l} \int_{K_h^l} \mathbf{L}(u_h^l) \cdot \nabla_\Gamma (z - z_h^l) \,\mathrm{dA} \\ &+ \sum_{e_h^l \in \mathcal{E}_h^l} \int_{e_h^l} [u_h^l] \left(\{ \nabla_\Gamma z_h^l ; n \} - \left\{ \mathbf{P}_h^l (\mathbf{I} - d\mathbf{H}) \mathbf{P} \nabla_\Gamma z_h^l ; n_h^l \right\} \delta_{e_h}^{-1} \right) \,\mathrm{ds} + \mathcal{A}^{IP}(u_h^{\perp,l}, z) - J(u_h^{\perp,l}). \end{aligned}$$

We now wish to move all the terms in the above onto the discrete surface. Making use of (5.3), we have the following:

$$- \int_{K_h^l} (\mathbf{P} - \mathbf{R}_h^l) \nabla_\Gamma u_h^l \cdot \nabla_\Gamma z \,\mathrm{ds} = - \int_{K_h} \delta_{e_h} \mathbf{F}_h^T (\mathbf{P}^{-l} - \mathbf{R}_h) \mathbf{F}_h \nabla_{\Gamma_h} u_h \cdot \nabla_{\Gamma_h} z^{-l} \,\mathrm{ds_h}$$

and

$$\sum_{K_h^l \in \mathcal{T}_h^l} \int_{K_h^l} \mathbf{L}(u_h^l) \cdot \nabla_\Gamma (z - z_h^l) \,\mathrm{dA} = \sum_{K_h \in \mathcal{T}_h} \int_{K_h} \mathbf{L}^{-l}(u_h^l) \cdot \delta_h \mathbf{F}_h \nabla_{\Gamma_h} (z^{-l} - z_h) \,\mathrm{dA_h}.$$

Furthermore, making use of the fact that $\mathbf{P}_h^{l+/-} n_h^{l+/-} = n_h^{l+/-}$ on each $e_h^l \in \mathcal{E}_h^l$ and $\mathbf{HP} = \mathbf{H}$, we have that

$$\begin{aligned}
&\sum_{e_h^l \in \mathcal{E}_h^l} \int_{e_h^l} [u_h^l] \left(\left\{ \nabla_\Gamma z_h^l; n \right\} - \left\{ \mathbf{P}_h^l (\mathbf{I} - d\mathbf{H}) \mathbf{P} \nabla_\Gamma z_h^l; n_h^l \right\} \delta_{e_h}^{-1} \right) \, \mathrm{ds} \\
&= \sum_{e_h^l \in \mathcal{E}_h^l} \int_{e_h^l} [u_h^l] \left(\left\{ \nabla_\Gamma z_h^l; n \right\} - \left\{ \nabla_\Gamma z_h^l; \delta_{e_h}^{-1} \mathbf{P} (\mathbf{I} - d\mathbf{H}) n_h^l \right\} \right) \, \mathrm{ds} \\
&= \sum_{e_h^l \in \mathcal{E}_h^l} \int_{e_h^l} [u_h^l] \left(\left\{ \nabla_\Gamma z_h^l; (n - \delta_{e_h}^{-1} \mathbf{P} n_h^l) \right\} + \delta_{e_h}^{-1} d \left\{ \nabla_\Gamma z_h^l; \mathbf{H} n_h^l \right\} \right) \, \mathrm{ds} \\
&= \sum_{e_h \in \mathcal{E}_h} \int_{e_h} [u_h] \left(\left\{ \mathbf{F}_h \nabla_{\Gamma_h} z_h; (\delta_{e_h} n^{-l} - \mathbf{P}^{-l} n_h) \right\} + d \left\{ \mathbf{F}_h \nabla_{\Gamma_h} z_h; \mathbf{H} n_h \right\} \right) \, \mathrm{ds_h}.
\end{aligned}$$

Making use of the above and writing all terms as element-wise computations, we derive the following residual equation:

$$\begin{aligned}
J(\mathrm{e}_h) = &\underbrace{\sum_{K_h \in \mathcal{T}_h} \int_{K_h} (f_h \delta_h + \Delta_{\Gamma_h} u_h - u_h \delta_h)(z^{-l} - z_h) \, \mathrm{dA_h}}_{I} \underbrace{- \frac{1}{2} \sum_{K_h \in \mathcal{T}_h} \int_{\partial K_h} [\nabla_{\Gamma_h} u_h; n_h](z^{-l} - z_h) \, \mathrm{ds_h}}_{II} \\
&\underbrace{- \sum_{K_h \in \mathcal{T}_h} \int_{K_h} \delta_{e_h} \mathbf{F}_h^T (\mathbf{P}^{-l} - \mathbf{R}_h) \mathbf{F}_h \nabla_{\Gamma_h} u_h \cdot \nabla_{\Gamma_h} z^{-l} \, \mathrm{dA_h}}_{III} + \underbrace{\sum_{K_h \in \mathcal{T}_h} \int_{K_h} (1 - \delta_h)(u_h - f_h) z_h \, \mathrm{dA_h}}_{IV} \\
&+ \underbrace{\sum_{K_h \in \mathcal{T}_h} \int_{K_h} \mathbf{L}^{-l}(u_h^l) \cdot \delta_h \mathbf{F}_h \nabla_{\Gamma_h} (z^{-l} - z_h) \, \mathrm{dA_h}}_{V} \\
&+ \underbrace{\sum_{K_h \in \mathcal{T}_h} \frac{1}{2} \int_{\partial K_h} [u_h] \left(\left\{ \mathbf{F}_h \nabla_{\Gamma_h} z_h; (\delta_{e_h} n^{-l} - \mathbf{P}^{-l} n_h) \right\} + d \left\{ \mathbf{F}_h \nabla_{\Gamma_h} z_h; \mathbf{H} n_h \right\} \right) \, \mathrm{ds_h}}_{VI} \\
&+ \underbrace{\mathcal{A}^{IP}(u_h^{\perp,l}, z) - J(u_h^{\perp,l})}_{VII}. \qquad (5.15)
\end{aligned}$$

Remark 5.4.6. The residual equation (5.15) may be used to estimate an *arbitrary* bounded linear functional J in $H^1 + S_h^l$ of the error e_h. In particular, one may use it to derive a posteriori error estimates in the L^2 or L^∞ norm, which will be the subject of future work. In this paper, we will only focus on deriving estimates in the DG norm and will do so by bounding all of the terms in the residual equation (5.15), approximating the dual weights $z^{-l} - z_h$ using interpolation estimates. It is worth mentioning that instead of using interpolation estimates, one may also deal with the weights by approximating the dual solution z of (5.14) by a fine mesh approximation (thus requiring an additional solve step for each iteration), and computing the resulting terms in the residual directly. Such an approach was considered in Georgoulis et al. [2009] for example, and typically leads to very accurate estimators

(with efficiency indices close to 1).

5.5 A posteriori upper bound (reliability)

In this section we derive a reliable estimator for the error in the DG norm.

Theorem 5.5.1. *Suppose that $\mathcal{T}_h$ is shape-regular and let*

$$\eta_{K_h} = h_{K_h}\|f_h\delta_h + \Delta_{\Gamma_h}u_h - u_h\delta_h\|_{L^2(K_h)} + h_{K_h}^{1/2}\|[\nabla_{\Gamma_h}u_h; n_h]\|_{L^2(\partial K_h)} \tag{5.16}$$

be the sum of the scaled element and jump residuals, then

$$\|u - u_h^l\|_{DG(\Gamma)} \leq C\left(\sum_{K_h\in\mathcal{T}_h} \mathcal{R}_{K_h}^2 + \mathcal{R}_{DG_{K_h}}^2 + \mathcal{G}_{K_h}^2 + \mathcal{G}_{DG_{K_h}}^2\right)^{\frac{1}{2}}$$

with

$$\mathcal{R}_{K_h}^2 := \|\mathbf{R}_h\|_{l^2,L^\infty(w_{K_h})}\eta_{K_h}^2, \tag{5.17}$$

$$\begin{aligned}\mathcal{R}_{DG_{K_h}}^2 := \Big(1 + \|\mathbf{F}_h\|_{L^\infty(w_{\partial K_h}^\partial)}^2\|\mathbf{P}_h(\mathbf{I}-d\mathbf{H})\mathbf{P}\|_{L^\infty(w_{\partial K_h})}^2\|\delta_{e_h}\|_{L^\infty(\partial K_h)}^2 + \|\mathbf{R}_h\|_{l^2,L^\infty(w_{K_h})}\\ \|\delta_h\|_{L^\infty(w_{K_h})}\|\mathbf{F}_h\|_{L^\infty(w_{\partial K_h}^\partial)}^2\|\mathbf{P}_h(\mathbf{I}-d\mathbf{H})\mathbf{P}\|_{L^\infty(w_{\partial K_h})}^2\|\delta_{e_h}\|_{L^\infty(\partial K_h)}^2\Big)\|\sqrt{\beta_{e_h}}[u_h]\|_{L^2(\partial K_h)}^2,\end{aligned} \tag{5.18}$$

$$\mathcal{G}_{K_h}^2 := \|\mathbf{B}_h\nabla_{\Gamma_h}u_h\|_{L^2(K_h)}^2 + \|(1-\delta_h)(u_h - f_h)\|_{L^2(K_h)}^2, \tag{5.19}$$

$$\begin{aligned}\mathcal{G}_{DG_{K_h}}^2 := \|\delta_h\|_{L^\infty(w_{K_h})}h_{K_h}^{-2}\Big(\|\sqrt{\beta_{e_h}}[u_h]\left\{|\left(\mathbf{F}_h\mathbf{P}_h\right)^T\left(\delta_{e_h}n^{-l} - \mathbf{P}^{-l}n_h\right)|\right\}\|_{L^2(\partial K_h)}^2\\ + \|d\sqrt{\beta_{e_h}}[u_h]\left\{|\left(\mathbf{F}_h\mathbf{P}_h\right)^T\mathbf{H}n_h|\right\}\|_{L^2(\partial K_h)}^2\Big),\end{aligned} \tag{5.20}$$

where C depends only on the shape regularity of the grid, $w_{K_h} = \bigcup_{p\in K_h} w_p$, $w_{\partial K_h} = \bigcup_{e_h\subset\partial K_h} w_{e_h}$ and $w_{\partial K_h}^\partial = \bigcup_{e_h\subset\partial K_h} w_{e_h}^\partial$. The operators $\mathbf{R}_h, \mathbf{B}_h$ are defined in (2.12) and (5.4), respectively.

Remark 5.5.2. The geometric estimates given in Lemma A.0.1 (applied to the piecewise linear surface approximation setting $k = 1$) make it clear that, if Γ is sufficiently

smooth, the geometric residuals $\mathcal{G}_{K_h}$ and $\mathcal{G}_{DG_{K_h}}$ defined in Theorem 5.5.1 are of higher order compared to $\mathcal{R}_{K_h}$ and $\mathcal{R}_{DG_{K_h}}$ i.e.

$$\left(\sum_{K_h\in\mathcal{T}_h}\mathcal{R}_{K_h}^2+\mathcal{R}_{DG_{K_h}}^2\right)^{1/2}\leq Ch \quad\text{and}\quad \left(\sum_{K_h\in\mathcal{T}_h}\mathcal{G}_{K_h}^2+\mathcal{G}_{DG_{K_h}}^2\right)^{1/2}\leq Ch^2.$$

In addition, the scaling terms for $\eta_{K_h}^2$ and $\|\sqrt{\beta_{e_h}}[u_h]\|_{L^2(\partial K_h)}^2$ given in respectively (5.17) and (5.18) scale like $O(1)+h$ and can thus be omitted from the local estimator computation for small enough h.

The proof of Theorem 5.5.1 will require the following approximation result:

Lemma 5.5.3. *Suppose $\mathcal{T}_h$ is a conforming grid. Then for any $v_h\in S_h$, there exists $v_h^c\in S_h^c$ such that*

$$\|v_h^l-v_h^{c,l}\|_{DG}\leq C_\perp\left(\sum_{e_h^l\in\mathcal{E}_h^l}\int_{e_h^l}\delta_{e_h}^{-1}\beta_{e_h}|[v_h^l]|^2\ ds\right)^{1/2}$$

for some constant $C_\perp$ independent of h but which may depend on the shape-regularity of the grid.

Proof. We construct $v_h^c\in S_h^c$ in such a way that, at every node of $\mathcal{T}_h$ corresponding to a Lagrangian-type degree of freedom for S_h^c, the value of v_h^c is set to the average of the values of v_h at that node. Its surface lift, $v_h^{c,l}\in S_h^{c,l}$, simply lifts the resulting function onto $\mathcal{T}_h^l$ in the usual way. The proof then follows along the lines of Theorem 2.2 in Karakashian and Pascal [2003]. □

To prove Theorem 5.5.1, we begin by bounding term I of (5.15). Let $z_h=I_hz^{-l}$, $R:=f_h\delta_h+\Delta_{\Gamma_h}u_h-u_h\delta_h$, $r:=[\nabla_{\Gamma_h}u_h;n_h]$. Recalling that $\{\varphi_p\}_{p\in\mathcal{N}}$ is a partition of unity, recalling (5.10) and applying (5.11), we then have that

$$I=\sum_{p\in\mathcal{N}}\int_{w_p}R(z^{-l}-z_p^{-l})\varphi_p\ \mathrm{ds_h}\leq C\sum_{p\in\mathcal{N}}h_p\|\mathbf{R}_h\|_{l^2,L^\infty(w_p)}^{\frac{1}{2}}\|R\varphi_p\|_{L^2(w_p)}\|\nabla_\Gamma z\|_{L^2(w_p^l)}. \tag{5.21}$$

Next we turn to bounding term II. Applying (5.12), we get

$$\begin{aligned} II &= -\sum_{p\in\mathcal{N}}\sum_{\bar{e}_h\ni p}\int_{e_h} r(z^{-l}-z_p^{-l})\varphi_p \ \mathrm{ds_h} \\ &\le C\sum_{p\in\mathcal{N}}\sum_{\bar{e}_h\ni p} h_p^{\frac{1}{2}}\|\mathbf{R}_h\|_{l^2,L^\infty(w_p)}^{\frac{1}{2}}\|r\varphi_p\|_{L^2(e_h)}\|\nabla_\Gamma z\|_{L^2(w_p^l)}. \end{aligned} \tag{5.22}$$

Let

$$\eta_p = h_p\|R\varphi_p\|_{L^2(w_p)} + \sum_{\bar{e}_h\ni p} h_p^{\frac{1}{2}}\|r\varphi_p\|_{L^2(e_h)}.$$

Combining (5.21) and (5.22) and noting that each element K_h has only three nodes, we thus find that

$$\begin{aligned} I+II &\le C\sum_{p\in\mathcal{N}}\|\mathbf{R}_h\|_{l^2,L^\infty(w_p)}^{\frac{1}{2}}\eta_p\|\nabla_\Gamma z\|_{L^2(w_p^l)} \\ &\le C\left(\sum_{p\in\mathcal{N}}\|\mathbf{R}_h\|_{l^2,L^\infty(w_p)}\eta_p^2\right)^{\frac{1}{2}}\|z\|_{H^1(\Gamma)}, \end{aligned} \tag{5.23}$$

where C does not depend on $\mathcal{T}_h$ or any other essential quantities.

In order to bound term III in (5.15) we first surface lift the integral back to Γ, and making use of (5.3) and (5.4) we get

$$\begin{aligned} III &= -\sum_{K_h^l\in\mathcal{T}_h^l}\int_{K_h^l}(\mathbf{P}-\mathbf{R}_h^l)\nabla_\Gamma u_h^l\cdot\nabla_\Gamma z \ \mathrm{ds} \\ &\le \left(\sum_{K_h\in\mathcal{T}_h}\|\mathbf{B}_h\nabla_{\Gamma_h}u_h\|_{L^2(K_h)}^2\right)^{1/2}\|z\|_{H^1(\Gamma)}. \end{aligned}$$

Next we bound term IV. First we note that, for $p\in\mathcal{N}$ and with z_p^{-l} defined as in (5.7), we have that

$$\|\sqrt{\varphi_p}z_p^{-l}\|_{L^2(w_p)} = \sqrt{\int_{w_p}\varphi_p \ \mathrm{ds_h}}\frac{1}{\int_{w_p}\varphi_p \ \mathrm{ds_h}}\left|\int_{w_p}\varphi_p z_p^{-l} \ \mathrm{ds_h}\right| \le \|\sqrt{\varphi_p}z^{-l}\|_{L^2(w_p)}.$$

Making use of the above, we have the following:

$$\begin{aligned}
IV &= \sum_{K_h \in \mathcal{T}_h} \int_{K_h} (1-\delta_h)(u_h - f_h) z_h \ \mathrm{dA_h} \\
&\leq \sum_{p \in \mathcal{N}} \|\sqrt{\varphi_p}(1-\delta_h)(u_h - f_h)\|_{L^2(w_p)} \|\sqrt{\varphi_p} z_p^{-l}\|_{L^2(w_p)} \\
&\leq \sum_{p \in \mathcal{N}} \|\delta_h^{-1}\|^{1/2}_{L^\infty(w_p)} \|\sqrt{\varphi_p}(1-\delta_h)(u_h - f_h)\|_{L^2(w_p)} \|\sqrt{\varphi_p^l} z\|_{L^2(w_p^l)} \\
&\leq \left(\sum_{p \in \mathcal{N}} \|\sqrt{\varphi_p}(1-\delta_h)(u_h - f_h)\|^2_{L^2(w_p)} \right)^{1/2} \|z\|_{H^1(\Gamma)}.
\end{aligned}$$

Making use of Remark 5.4.3, we may bound term V in the following way:

$$\begin{aligned}
V &= \sum_{p \in \mathcal{N}} \int_{w_p} \mathbf{L}^{-l}(u_h^l) \cdot \delta_h \mathbf{F}_h \nabla_{\Gamma_h}((z^{-l} - z_p^{-l})\varphi_p) \ \mathrm{dA_h} \\
&= \sum_{p \in \mathcal{N}} \int_{w_p} \mathbf{L}^{-l}(u_h^l) \cdot \left(\delta_h \mathbf{F}_h \nabla_{\Gamma_h} z^{-l} \varphi_p + \delta_h \mathbf{F}_h (z^{-l} - z_p^{-l}) \nabla_{\Gamma_h} \varphi_p \right) \ \mathrm{dA_h} \\
&= \sum_{p \in \mathcal{N}} \int_{w_p^l} \mathbf{L}(u_h^l) \cdot \nabla_\Gamma z \varphi_p^l + \mathbf{L}(u_h^l) \cdot \nabla_\Gamma \varphi_p^l (z - z_p) \ \mathrm{dA} \\
&\leq \sum_{p \in \mathcal{N}} \|\mathbf{L}(u_h^l)\sqrt{\varphi_p^l}\|_{L^2(w_p^l)} \|\nabla_\Gamma z \sqrt{\varphi_p^l}\|_{L^2(w_p^l)} \\
&+ \sum_{p \in \mathcal{N}} \|\mathbf{L}(u_h^l) \cdot \nabla \varphi_p^l\|_{L^2(w_p^l)} \|\delta_h\|^{1/2}_{L^\infty(w_p)} \|z - z_p\|_{L^2(w_p)} \\
&\leq \left(\sum_{p \in \mathcal{N}} \int_{w_p^l} \left(\sum_{e_h^l \subset \bar{w}_p^l} \mathbf{L}_{e_h^l}(u_h^l) \right)^2 \varphi_p^l \ \mathrm{dA} \right)^{1/2} \left(\sum_{p \in \mathcal{N}} \|\nabla_\Gamma z \sqrt{\varphi_p^l}\|^2_{L^2(w_p^l)} \right)^{1/2} \\
&+ C\sqrt{2} \sum_{p \in \mathcal{N}} h_p^{-1} \|\mathbf{L}(u_h^l)\|_{L^2(w_p^l)} \|\delta_h\|^{1/2}_{L^\infty(w_p)} h_p \|\mathbf{R}_h\|^{\frac{1}{2}}_{l^2, L^\infty(w_p)} \|\nabla_\Gamma z\|_{L^2(w_p^l)} \\
&\leq C \left(\sum_{p \in \mathcal{N}} \int_{w_p^l} \sum_{e_h^l \subset \bar{w}_p^l} \mathbf{L}^2_{e_h^l}(u_h^l) \varphi_p^l \ \mathrm{dA} \right)^{1/2} \|z\|_{H^1(\Gamma)} \\
&+ C\sqrt{2} \left(\sum_{p \in \mathcal{N}} \|\mathbf{R}_h\|_{l^2, L^\infty(w_p)} \|\delta_h\|_{L^\infty(w_p)} \int_{w_p^l} \sum_{e_h^l \subset \bar{w}_p^l} \mathbf{L}^2_{e_h^l}(u_h^l) \ \mathrm{dA} \right)^{1/2} \|z\|_{H^1(\Gamma)}.
\end{aligned}$$

Using again Remark 5.4.3 and the DG lift estimate in Lemma 5.4.4, we have that

$$\sum_{p\in\mathcal{N}}\int_{w_p^l}\sum_{e_h^l\subset\bar{w}_p^l}\mathbf{L}^2_{e_h^l}(u_h^l)\varphi_p^l\ \mathrm{dA}\leq\sum_{e_h^l\in\mathcal{E}_h^l}\int_\Gamma\mathbf{L}^2_{e_h^l}(u_h^l)\ \mathrm{dA}$$
$$\leq C_L\sum_{e_h\in\mathcal{E}_h}\|\mathbf{F}_h\|^2_{L^\infty(w^\partial_{e_h})}\|\mathbf{P}_h(\mathbf{I}-d\mathbf{H})\mathbf{P}\|^2_{L^\infty(w_{e_h})}\|\delta_{e_h}\|^2_{L^\infty(e_h)}\|\sqrt{\beta_{e_h}}[u_h]\|^2_{L^2(e_h)}.$$

Similarly, we have that

$$\sum_{p\in\mathcal{N}}\int_{w_p^l}\sum_{e_h^l\subset\bar{w}_p^l}\mathbf{L}^2_{e_h^l}(u_h^l)\ \mathrm{dA}\leq C\sum_{K_h^l\in\mathcal{T}_h^l}\int_{K_h^l}\sum_{e_h^l\subset\partial K_h^l}\mathbf{L}^2_{e_h^l}(u_h^l)\ \mathrm{dA}$$
$$\leq C\sum_{K_h^l\in\mathcal{T}_h^l}\sum_{e_h^l\subset\partial K_h^l}\int_\Gamma\mathbf{L}^2_{e_h^l}(u_h^l)\ \mathrm{dA}$$
$$\leq CC_L\sum_{K_h\in\mathcal{T}_h}\sum_{e_h\subset\partial K_h}\|\mathbf{F}_h\|^2_{L^\infty(w^\partial_{e_h})}\|\mathbf{P}_h(\mathbf{I}-d\mathbf{H})\mathbf{P}\|^2_{L^\infty(w_{e_h})}\|\delta_{e_h}\|^2_{L^\infty(e_h)}\|\sqrt{\beta_{e_h}}[u_h]\|^2_{L^2(e_h)}.$$

For term VI we have the following,

$$VI=\sum_{e_h\in\mathcal{E}_h}\int_{e_h}[u_h]\left(\left\{\mathbf{F}_h\nabla_{\Gamma_h}z_h;(\delta_{e_h}n^{-l}-\mathbf{P}^{-l}n_h)\right\}+d\left\{\mathbf{F}_h\nabla_{\Gamma_h}z_h;\mathbf{H}n_h\right\}\right)\ \mathrm{ds_h}$$
$$=\sum_{p\in\mathcal{N}}\sum_{\bar{e}_h\ni p}\int_{e_h}z_p^{-l}[u_h]\left\{\mathbf{F}_h\nabla_{\Gamma_h}\varphi_p;(\delta_{e_h}n^{-l}-\mathbf{P}^{-l}n_h)\right\}+z_p^{-l}[u_h]d\left\{\mathbf{F}_h\nabla_{\Gamma_h}\varphi_p;\mathbf{H}n_h\right\}\ \mathrm{ds_h}.$$

Multiplying by $\beta_{e_h}\beta_{e_h}^{-1}$, applying Cauchy-Schwartz and an inverse estimate, making use of (5.9) and recalling that $\nabla_{\Gamma_h}\varphi_p=\mathbf{P}_h\nabla\varphi_p$, the first term of VI is bounded above by

$$\sum_{p\in\mathcal{N}}\sum_{\bar{e}_h\ni p}\|\sqrt{\beta_{e_h}}[u_h]\left\{\mathbf{F}_h\nabla_{\Gamma_h}\varphi_p;(\delta_{e_h}n^{-l}-\mathbf{P}^{-l}n_h)\right\}\|_{L^2(e_h)}\|\beta_{e_h}^{-\frac{1}{2}}z_p^{-l}\|_{L^2(e_h)}$$
$$\leq C\sum_{p\in\mathcal{N}}\|\sqrt{\delta_h}\|_{L^\infty(w_p)}\sum_{\bar{e}_h\ni p}\|\sqrt{\beta_{e_h}}[u_h]\left\{\nabla\varphi_p;\left(\mathbf{F}_h\mathbf{P}_h\right)^T(\delta_{e_h}n^{-l}-\mathbf{P}^{-l}n_h)\right\}\|_{L^2(e_h)}\|z\|_{L^2(w_p^l)}$$
$$\leq C\sum_{p\in\mathcal{N}}\|\sqrt{\delta_h}\|_{L^\infty(w_p)}\sum_{\bar{e}_h\ni p}h_{e_h}^{-1}\|\sqrt{\beta_{e_h}}[u_h]\left\{|\left(\mathbf{F}_h\mathbf{P}_h\right)^T(\delta_{e_h}n^{-l}-\mathbf{P}^{-l}n_h)|\right\}\|_{L^2(e_h)}\|z\|_{L^2(w_p^l)}$$
$$\leq C\left(\sum_{p\in\mathcal{N}}\|\delta_h\|_{L^\infty(w_p)}\sum_{\bar{e}_h\ni p}h_{e_h}^{-2}\|\sqrt{\beta_{e_h}}[u_h]\left\{|\left(\mathbf{F}_h\mathbf{P}_h\right)^T(\delta_{e_h}n^{-l}-\mathbf{P}^{-l}n_h)|\right\}\|^2_{L^2(e_h)}\right)^{\frac{1}{2}}\|z\|_{H^1(\Gamma)}.$$

Similarly, for the second term of VI, we get the upper bound

$$C\left(\sum_{p\in\mathcal{N}}\|\delta_h\|_{L^\infty(w_p)}\sum_{\bar{e}_h\ni p}h_{e_h}^{-2}\|d\sqrt{\beta_{e_h}}[u_h]\left\{|\left(\mathbf{F}_h\mathbf{P}_h\right)^T\mathbf{H}n_h|\right\}\|^2_{L^2(e_h)}\right)^{1/2}\|z\|_{H^1(\Gamma)}.$$

To bound the final term VII in our residual equation, we first prescribe the

functional J as follows:

$$J(v) = \|\mathrm{e}_h\|_{DG}^{-1} \left(\sum_{K_h^l \in \mathcal{T}_h^l} (\mathrm{e}_h, v)_{H^1(K_h^l)} + \sum_{e_h^l \in \mathcal{E}_h^l} \delta_{e_h}^{-1} \beta_{e_h} ([\mathrm{e}_h], [v])_{L^2(e_h^l)} \right)$$

which is in fact a functional on $H^1(\Gamma) + S_h^l$. Note that $J(\mathrm{e}_h) = \|\mathrm{e}_h\|_{DG}$. For such a functional, the solution z of the dual problem (5.14) satisfies

$$\|z\|_{H^1(\Gamma)}^2 \leq J(z) \leq \|z\|_{DG} = \|z\|_{H^1(\Gamma)},$$

where we have used that $\mathbf{L}(z) = 0$ and $[z] = 0$ since $z \in H^1(\Gamma)$. Hence $\|z\|_{H^1(\Gamma)} \leq 1$. Making use of this stability estimate, the DG lifting estimate given in Lemma 5.4.4 and the approximation result in Lemma 5.5.3 (for which we use that $u_h^\perp = u_h - u_h^c$ with u_h^c given as in the proof of Lemma 5.5.3), we have that

$$\begin{aligned} VII := \mathcal{A}^{IP}(u_h^{\perp,l}, z) - J(u_h^{\perp,l}) \leq C \Bigg(& \sum_{K_h \in \mathcal{T}_h} \|\sqrt{\beta_{e_h}}[u_h]\|_{L^2(\partial K_h)}^2 \\ & + \|\mathbf{F}_h\|_{L^\infty(w_{\partial K_h}^\partial)}^2 \|\mathbf{P}_h(\mathbf{I} - d\mathbf{H})\mathbf{P}\|_{L^\infty(w_{\partial K_h})}^2 \|\delta_{e_h}\|_{L^\infty(\partial K_h)}^2 \|\sqrt{\beta_{e_h}}[u_h]\|_{L^2(\partial K_h)}^2 \Bigg)^{1/2}. \end{aligned} \tag{5.24}$$

Combining all of the estimates in this section and writing them in terms of element-wise computations completes the proof of Theorem 5.5.1.

5.6 A posteriori lower bound (efficiency)

We now show that the estimator in Theorem 5.5.1 is efficient up to higher-order terms.

Theorem 5.6.1. *Suppose that $\mathcal{T}_h$ is shape-regular. As before, let $R := f_h\delta_h + \Delta_{\Gamma_h} u_h - u_h\delta_h$ and $r := [\nabla_{\Gamma_h} u_h; n_h]$. Then, for each $K_h \in \mathcal{T}_h$, we have that*

$$\begin{aligned} & \eta_{K_h} + \|\sqrt{\beta_{e_h}}[u_h]\|_{L^2(\partial K_h)} \\ & \leq C \max\left\{1, \|\mathbf{R}_h\|_{l^2, L^\infty(w_{K_h})}^{1/2}\right\} \left(\|u - u_h^l\|_{DG} + \|\mathbf{B}_h \nabla_{\Gamma_h} u_h\|_{L^2(w_{K_h})} \right) \\ & \quad + C h_{K_h} \|R - \bar{R}\|_{L^2(w_{K_h})} + C h_{K_h}^{1/2} \|r - \bar{r}\|_{L^2(\partial K_h)}. \end{aligned}$$

where η_{K_h} is given in Theorem 5.5.1. Here C depends on the number of elements in w_{K_h}, the minimum angle of the elements in w_{K_h} and on the penalty parameter α.

$\bar{R}$ and $\bar{r}$ are respectively piecewise linear approximations of R and r and assumed to yield optimal error estimates.

Proof. The proof will follow the bubble function approach considered in Verfürth [1989], which was then straightforwardly applied to the DG framework in Karakashian and Pascal [2003] and Schötzau and Zhu [2009]. First we bound the element residual $\|R\|_{L^2(K_h)}$. Let $p \in \mathcal{N}$ and $K_h \subset w_p$. Letting p_i, $1 \leq i \leq 3$ be the nodes of K_h, we define the bubble function $\phi_{K_h} = \prod_{i=1}^{3} \varphi_{p_i}$. Integrating by parts on K_h, lifting the resulting integral onto K_h^l, making use of the fact that the exact solution satisfies $(f + \Delta_\Gamma u - u)|_{K_h^l} = 0$ and integrating by parts on K_h^l, we get

$$\begin{aligned}
\int_{K_h} R\bar{R}\phi_{K_h} \, \mathrm{dA_h} &= \int_{K_h} f_h \delta_h \bar{R}\phi_{K_h} + \nabla_{\Gamma_h} u_h \cdot \nabla_{\Gamma_h}(\bar{R}\phi_{K_h}) - u_h \delta_h \bar{R}\phi_{K_h} \, \mathrm{dA_h} \\
&= \int_{K_h^l} f\bar{R}^l\phi_{K_h}^l + \mathbf{R}_h^l \nabla_\Gamma u_h^l \cdot \nabla_\Gamma(\bar{R}^l\phi_{K_h}^l) - u_h^l \bar{R}^l \phi_{K_h}^l \, \mathrm{dA} \\
&= \int_{K_h^l} \nabla_\Gamma(u - u_h^l) \cdot \nabla_\Gamma(\bar{R}^l\phi_{K_h}^l) \, \mathrm{dA} + \int_{K_h^l} (u - u_h^l)\bar{R}^l\phi_{K_h}^l \, \mathrm{dA} \\
&+ \int_{K_h^l} (\mathbf{P} - \mathbf{R}_h^l)\nabla_\Gamma u_h^l \cdot \nabla_\Gamma(\bar{R}^l\phi_{K_h}^l) \, \mathrm{dA}.
\end{aligned}$$

Note that we have used the fact that $\phi_{K_h} = 0$ on ∂K_h so that all boundary terms resulting from the integration by parts vanish. We then have that

$$\begin{aligned}
&\int_{K_h} R\bar{R}\phi_{K_h} \, \mathrm{dA_h} \leq C \left(\|u - u_h^l\|_{DG} + \|(\mathbf{P} - \mathbf{R}_h^l)\nabla_\Gamma u_h^l\|_{L^2(K_h^l)} \right) \|\nabla_\Gamma(\bar{R}^l\phi_{K_h}^l)\|_{L^2(K_h^l)} \\
&\leq C \left(\|u - u_h^l\|_{DG} + \|\mathbf{B}_h \nabla_\Gamma u_h\|_{L^2(K_h)} \right) \|\mathbf{R}_h\|_{L^\infty(K_h)}^{1/2} \|\nabla_{\Gamma_h}(\bar{R}\phi_{K_h})\|_{L^2(K_h)}
\end{aligned}$$

where we have used Poincare's inequality. Since $\bar{R}\phi_{K_h}$ is a polynomial, it satisfies the inverse inequality

$$\|\nabla_{\Gamma_h}(\bar{R}\phi_{K_h})\|_{L^2(K_h)} \leq C h_{K_h}^{-1} \|\bar{R}\|_{L^2(K_h)}$$

where C depends only on the shape-regularity of K_h. Applying this inverse inequality, we get

$$\int_{K_h} R\bar{R}\phi_{K_h} \, \mathrm{dA_h} \leq C h_{K_h}^{-1} \|\mathbf{R}_h\|_{L^\infty(K_h)}^{1/2} \left(\|u - u_h^l\|_{DG} + \|\mathbf{B}_h \nabla_\Gamma u_h\|_{L^2(K_h)} \right) \|\bar{R}\|_{L^2(K_h)}.$$

Applying Theorem 2.2 in Ainsworth and Oden [2011], we have that

$$\begin{aligned}\|\bar{R}\|^2_{L^2(K_h)} &\leq C\|\sqrt{\phi_{K_h}}\bar{R}\|^2_{L^2(K_h)} \\ &\leq C\left(\int_{K_h} R\bar{R}\phi_{K_h}\ \mathrm{dA_h} + \int_{K_h}\bar{R}(\bar{R}-R)\phi_{K_h}\ \mathrm{dA_h}\right) \\ &\leq C\left(\int_{K_h} R\bar{R}\phi_{K_h}\ \mathrm{dA_h} + \|R-\bar{R}\|_{L^2(K_h)}\|\bar{R}\phi_{K_h}\|_{L^2(K_h)}\right) \\ &\leq C\left(\int_{K_h} R\bar{R}\phi_{K_h}\ \mathrm{dA_h} + \|R-\bar{R}\|_{L^2(K_h)}\|\bar{R}\|_{L^2(K_h)}\right).\end{aligned}$$

Combining this with the previous inequality, we get

$$\begin{aligned}\|\bar{R}\|^2_{L^2(K_h)} \leq \Big(&\|R-\bar{R}\|_{L^2(K_h)} \\ &+ Ch^{-1}_{K_h}\|\mathbf{R}_h\|^{1/2}_{L^\infty(K_h)}\big(\|u-u^l_h\|_{DG} + \|\mathbf{B}_h\nabla_\Gamma u_h\|_{L^2(K_h)}\big)\Big)\|\bar{R}\|_{L^2(K_h)}.\end{aligned}$$

Dividing both sides by $\|\bar{R}\|_{L^2(K_h)}$ and making use of the triangle inequality, we obtain

$$\begin{aligned}h_{K_h}\|R\|_{L^2(K_h)} \leq C\Big(&\|\mathbf{R}_h\|^{1/2}_{L^\infty(K_h)}\big(\|u-u^l_h\|_{DG} + \|\mathbf{B}_h\nabla_\Gamma u_h\|_{L^2(K_h)}\big) \\ &+ h_{K_h}\|R-\bar{R}\|_{L^2(K_h)}\Big).\end{aligned}$$

Next we bound the jump residual $\|r\|_{L^2(\partial K_h)}$. Let e_h be an edge which is shared by elements $K^1_h = K_h$ and K^2_h and whose closure contains the nodes p_1 and p_2. Let $\lambda_{i,j}$, $i,j=1,2$, be the barycentric coordinate on triangle i corresponding to vertex p_j, and define $\phi_{e_h}|_{K^i_h} = \lambda_{i,1}\lambda_{i,2}$. Thus $\phi_{e_h} \in H^1_0(K^1_h \cup K^2_h)$, and $\phi_{e_h} > 0$ on e_h. Finally let $w_{e_h} = K^1_h \cup K^2_h$. Applying similar arguments as for the element residual $\|R\|_{L^2(K_h)}$, we have that

$$\begin{aligned}&\int_{e_h} r\bar{r}\phi_{e_h}\ \mathrm{ds_h} = \int_{w_{e_h}} \Delta_{\Gamma_h}u_h\bar{r}\phi_{e_h} + \nabla_{\Gamma_h}u_h\cdot\nabla_{\Gamma_h}(\bar{r}\phi_{e_h})\ \mathrm{dA_h} \\ &= \int_{w_{e_h}} R\bar{r}\phi_{e_h}\ \mathrm{dA_h} + \int_{w^l_{e_h}} \mathbf{R}^l_h\nabla_\Gamma u^l_h\cdot\nabla_\Gamma(\bar{r}^l\phi^l_{e_h})\ \mathrm{dA} + \int_{w^l_{e_h}}(u^l_h - f)\bar{r}^l\phi^l_{e_h}\ \mathrm{dA} \\ &= \int_{w_{e_h}} R\bar{r}\phi_{e_h}\ \mathrm{dA_h} + \int_{w^l_{e_h}} \nabla_\Gamma(u^l_h - u)\cdot\nabla_\Gamma(\bar{r}^l\phi^l_{e_h})\ \mathrm{dA} + \int_{w^l_{e_h}}(u^l_h - u)\bar{r}^l\phi^l_{e_h}\ \mathrm{dA} \\ &+ \int_{w^l_{e_h}} (\mathbf{R}^l_h - \mathbf{P})\nabla_\Gamma u^l_h\cdot\nabla_\Gamma(\bar{r}^l\phi^l_{e_h})\ \mathrm{dA}\end{aligned}$$

where again we have used the fact that $\phi_{e_h} = 0$ on ∂w_{e_h} so that all boundary terms resulting from the integration by parts vanish. We now proceed to bounding the

terms as done previously to obtain

$$\int_{e_h} r\bar{r}\phi_{e_h}\ \mathrm{ds_h} \leq C\Bigg(\|R\|_{L^2(w_{e_h})}\|\bar{r}\phi_{e_h}\|_{L^2(w_{e_h})} \\ + \left(\|u-u_h^l\|_{DG} + \|\mathbf{B}_h\nabla_{\Gamma_h}u_h\|_{L^2(w_{e_h})}\right)\|\mathbf{R}_h\|^{1/2}_{L^\infty(w_{e_h})}\|\nabla_{\Gamma_h}(\bar{r}\phi_{e_h})\|_{L^2(w_{e_h})}\Bigg)$$

where again the constant C depends only on the shape regularity of the grid. Since $\bar{r}\phi_{e_h}$ is a polynomial, it satisfies the inverse inequalities

$$\|\bar{r}\phi_{e_h}\|_{L^2(w_{e_h})} \leq Ch_{K_h}^{1/2}\|\bar{r}\|_{L^2(e_h)} \quad , \quad \|\nabla_{\Gamma_h}(\bar{r}\phi_{e_h})\|_{L^2(w_{e_h})} \leq Ch_{K_h}^{-1/2}\|\bar{r}\|_{L^2(e_h)}.$$

Applying these inverse inequalities, we get

$$\int_{e_h} r\bar{r}\phi_{e_h}\ \mathrm{ds_h} \leq C\Bigg(h_{K_h}^{-1/2}\|\mathbf{R}_h\|^{1/2}_{L^\infty(w_{e_h})}\left(\|u-u_h^l\|_{DG} + \|\mathbf{B}_h\nabla_\Gamma u_h\|_{L^2(w_{e_h})}\right) \\ + h_{K_h}^{1/2}\|R\|_{L^2(w_{e_h})}\Bigg)\|\bar{r}\|_{L^2(e_h)}.$$

Applying Theorem 2.4 in Ainsworth and Oden [2011], we have that

$$\begin{aligned}\|\bar{r}\|^2_{L^2(e_h)} &\leq C\|\sqrt{\phi_{e_h}}\bar{r}\|^2_{L^2(e_h)} \\ &\leq C\left(\int_{e_h} r\bar{r}\phi_{e_h}\ \mathrm{dA_h} + \|r-\bar{r}\|_{L^2(e_h)}\|\bar{r}\phi_{e_h}\|_{L^2(e_h)}\right) \\ &\leq C\left(\int_{e_h} r\bar{r}\phi_{e_h}\ \mathrm{dA_h} + \|r-\bar{r}\|_{L^2(e_h)}\|\bar{r}\|_{L^2(e_h)}\right).\end{aligned}$$

Combining this with the previous inequality, we get

$$\|\bar{r}\|^2_{L^2(e_h)} \leq C\Big(\|r-\bar{r}\|_{L^2(e_h)} + h_{K_h}^{-1/2}\|\mathbf{R}_h\|^{1/2}_{L^\infty(w_{e_h})}\big(\|u-u_h^l\|_{DG} \\ + \|\mathbf{B}_h\nabla_\Gamma u_h\|_{L^2(w_{e_h})}\big) + h_{K_h}^{1/2}\|R\|_{L^2(w_{e_h})}\Big)\|\bar{r}\|_{L^2(e_h)}.$$

Dividing both sides by $\|\bar{r}\|_{L^2(e_h)}$ and making use of the triangle inequality, we obtain

$$h_{K_h}^{1/2}\|r\|_{L^2(e_h)} \leq C\Big(\|\mathbf{R}_h\|^{1/2}_{L^\infty(w_{e_h})}\left(\|u-u_h^l\|_{DG} + \|\mathbf{B}_h\nabla_\Gamma u_h\|_{L^2(w_{e_h})}\right) \\ + h_{K_h}\|R\|_{L^2(w_{e_h})} + h_{K_h}^{1/2}\|r-\bar{r}\|_{L^2(e_h)}\Big).$$

For the jump term in our estimator, we note that since $[u] = 0$ we have that

$$\left\| \sqrt{\beta_{e_h}}[u_h] \right\|_{L^2(\partial K_h)} = \left\| \sqrt{\delta_{e_h}^{-1}\beta_{e_h}}[u_h^l] \right\|_{L^2(\partial K_h^l)} = \left\| \sqrt{\delta_{e_h}^{-1}\beta_{e_h}}[u - u_h^l] \right\|_{L^2(\partial K_h^l)}$$
$$\leq C\|u - u_h^l\|_{DG}.$$

□

5.7 Numerical tests

In this section we present some numerical tests which verify the reliability and efficiency of the a posteriori estimator given in Theorem 5.5.1.

5.7.1 Implementation aspects

In all our numerical tests we choose the polynomial order on each element $K_h \in \mathcal{T}_h$ to be 1, the penalty parameter α to be equal to 10 and the constant C appearing in the estimator given in Theorem 5.5.1 to be equal to 1. In addition, given that the signed-distance function d is rarely available in practice but appears explicitely in our estimator, we have to approximate it using the level-set function ϕ via (4.56). Further implementational details can be found in the relevant section in Chapter 4 as well as in Demlow and Dziuk [2008].

5.7.2 Test problem on Dziuk surface

The first test problem will consider

$$-\Delta_\Gamma u + u = f \tag{5.25}$$

on the Dziuk surface

$$\Gamma = \{x \in \mathbb{R}^3 \ : \ (x_1 - x_3^2)^2 + x_2^2 + x_3^2 = 1\}.$$

As a test solution, we took the function

$$u(x, y, z) = e^{\frac{1}{1.85-(x-0.2)^2}} \sin y$$

which has sharp gradient changes, as shown in Figure 5.1(a). In Figure 5.2(a) we plot each of the contributions of our error estimator against the number of degrees of freedom when performing global refinement for the Dziuk surface. Note that we plot the

standard residual with its geometric scaling term i.e. $\left(\sum_{K_h\in\mathcal{T}_h} \|\mathbf{R}_h\|_{l^2,L^\infty(w_{K_h})}\eta^2_{K_h}\right)^{\frac{1}{2}}$. Notice how both the geometric residual $\left(\sum_{K_h\in\mathcal{T}_h} \mathcal{G}^2_{K_h}\right)^{1/2}$ and the DG geometric residual $\left(\sum_{K_h\in\mathcal{T}_h} \mathcal{G}^2_{DG_{K_h}}\right)^{1/2}$ converge with higher order as noted in Remark 5.5.2. Figure 5.2(b) confirms that our estimator is efficient, with an efficiency index of about 5.6.

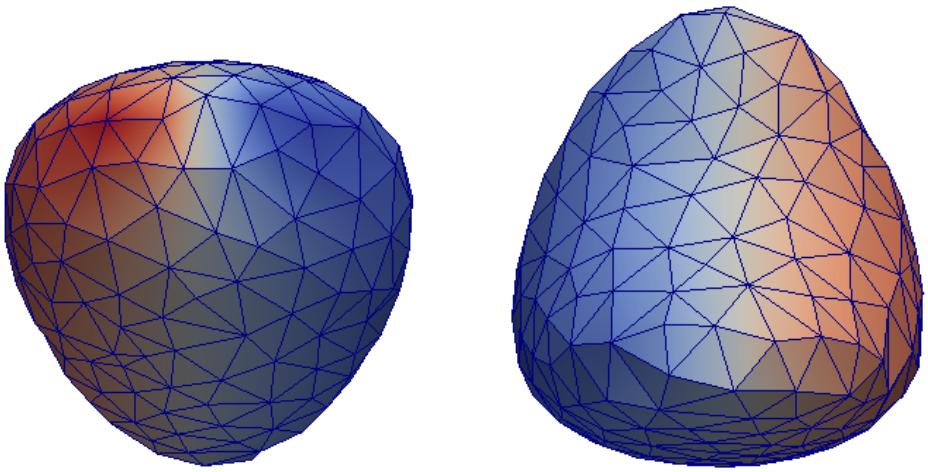

(a) (b)

Figure 5.1: Front and rear view of the initial grid for the Dziuk surface.

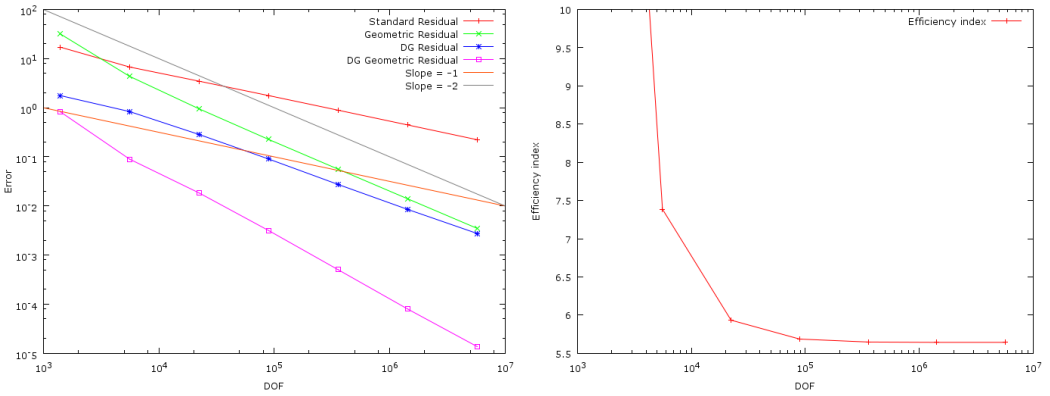

(a) (b)

Figure 5.2: Residual components (left) and efficiency index (right) for the Dziuk surface.

5.7.3 Test problem on Enzensberger-Stern surface

Our second test problem considers (5.25) on the Enzensberger-Stern surface given by

$$\Gamma = \{x \in \mathbb{R}^3 \ : \ 400(x^2y^2 + y^2z^2 + x^2z^2) - (1 - x^2 - y^2 - z^2)^3 - c = 0\}$$

where $c = 40$ and whose exact solution is chosen to be given by $u(x) = x_1x_2$. In Figure 5.3(a) we plot each of the contributions of our error estimator against the number of degrees of freedom when performing global refinement for the Enzensberger-Stern surface. Figure 5.4(b) again confirms that our estimator is efficient, with an efficiency index of about 5.9. It is worth noticing that the geometric residual term remains the dominant source of error all the way through our computations despite converging with higher order. This issue will be considered in more detail in Chapter 7.

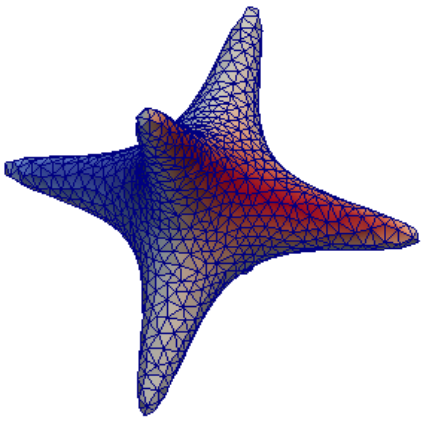

(a)

Figure 5.3: Initial grid for the Enzensberger-Stern surface.

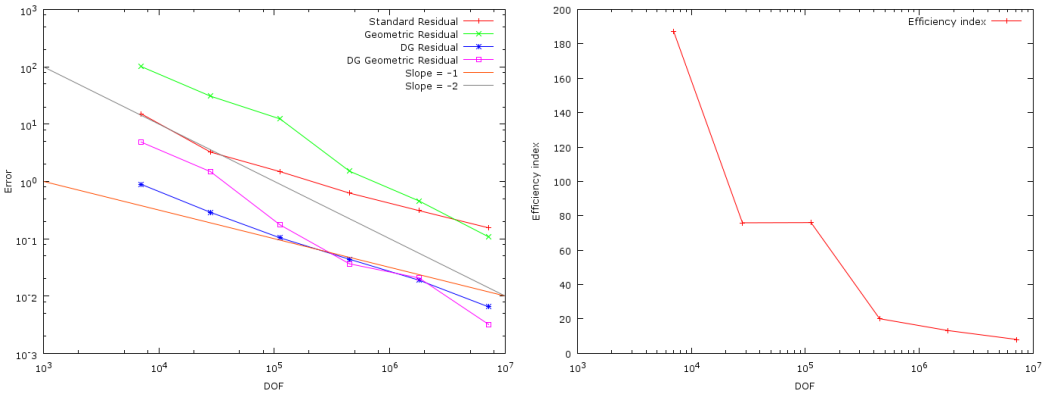

(a) (b)

Figure 5.4: Residual components (left) and efficiency index (right) for the Enzensberger-Stern surface.

Chapter 6

DG Methods for Advection-Diffusion Problems on Surfaces

In this chapter, we extend the surface DG framework considered in Chapter 4 to advection-diffusion problems posed on surfaces. Before reading this chapter, it is worth having a look at Section 3.7 which outlines some key issues arising in the planar setting for first-order hyperbolic problems.

6.1 Problem formulation

We consider the model problem

$$-\Delta_\Gamma u + u + w \cdot \nabla_\Gamma u = f \quad \text{on } \Gamma \tag{6.1}$$

where the velocity field $w \in [W^{2,\infty}(\Gamma)]^3$ can be assumed to be purely *tangential* to the surface, i.e. $w \cdot \nu = 0$ everywhere, since any normal contribution would vanish when multiplied with $\nabla_\Gamma u$. We will also assume, for simplicity, that the velocity field is divergence-free which, together with $w \cdot \nu = 0$, implies that $\nabla_\Gamma \cdot w = 0$. The analysis that follows can be straightforwardly extended to non divergence-free velocity fields.

The weak formulation resulting from (6.1) is given as follows: find $u \in H^1(\Gamma)$ such that

$$\int_\Gamma \nabla_\Gamma u \cdot \nabla_\Gamma v + uv - uw \cdot \nabla_\Gamma v \, \mathrm{dA} = \int_\Gamma fv \, \mathrm{dA} \quad \forall v \in H^1(\Gamma). \tag{6.2}$$

Existence and uniqueness of a solution $u \in H^2(\Gamma)$ follow again from standard arguments and we refer to Aubin [1982] and Wloka [1987] for more details on elliptic regularity on surfaces.

6.1.1 Motivation

Besides the fact that one would naturally be interested in extending the DG framework to advection-diffusion problems posed on surfaces (which arise as models for various physical and biological phenomena as discussed in Chapter 1), extending the analysis from the previous chapters to the model problem (6.1) is surprisingly non-trivial.

To see this, consider the following surface DG version of the discrete scheme (3.23) for first order hyperbolic problems given in Section 3.7 i.e.

$$\begin{aligned}\mathcal{B}_h^k(u_h, v_h) := &\sum_{\widehat{K}_h \in \widehat{\mathcal{T}}_h} \int_{\widehat{K}_h} -u_h w_h \cdot \nabla_{\Gamma_h^k} v_h + \gamma_h u_h v_h \ \mathrm{dA_{hk}} \\ &+ \sum_{\widehat{e}_h \in \widehat{\mathcal{E}}_h} \int_{\widehat{e}_h} \widehat{w_h u_h}[v_h] \ \mathrm{ds_{hk}} \end{aligned} \tag{6.3}$$

where $\widehat{w_h u_h}$ is some numerical flux. For this subsection and this subsection only, we choose $\gamma_h = c$ for some $c \geq c_0 > 0$ and $w_h = w^{-l}$ i.e. the scheme simply lifts the velocity field w downwards onto the discrete surface Γ_h^k. If we simply chose the discrete velocity field to be the true velocity field surface lifted downwards, the matrix resulting from such a scheme may not be positive-definite independently of h.This can be seen by integrating by parts (using Lemma 4.2.3) in a similar fashion to (3.24), choosing $u_h \equiv 0$ for every $\widehat{K}_h \in \widehat{\mathcal{T}}_h$ except for the two elements $\widehat{K}_h^+$ and $\widehat{K}_h^-$ for which $\widehat{e}_h = \widehat{K}_h^+ \bigcap \widehat{K}_h^-$. Furthermore, we choose $\widehat{n}_h^+ = (-1, 0, 0)$, $\widehat{n}_h^- = (\cos(q), \sin(q), 0)$ with $q \in (0, 2\pi)$. Note that unless $q = 0, 2\pi$, we have that $\widehat{n}_h^+ \neq -\widehat{n}_h^-$. The velocity w^{-l} at $\widehat{e}_h$ is assumed to be $(-1, 0, 0)$, so that $w^{-l} \cdot \widehat{n}_h^+ = 1 > 0$ and $w^{-l} \cdot \widehat{n}_h^- = -\cos(q) < 0$. Finally, we assume that $u_h^+ = u_h^- = 1$ so that $[u_h] = 0$ on $\widehat{e}_h$. With these conditions, it is clear from (3.24) that the stability of (6.3) boils down to showing that

$$-\frac{1}{2} \sum_{\widehat{K}_h \in \widehat{\mathcal{T}}_h} \int_{\partial \widehat{K}_h} \left(w^{-l} \cdot n_{\widehat{K}_h} \right) u_h^2 \ \mathrm{ds_{hk}} \geq 0$$

which, from Lemma 4.2.3 and the above conditions, is equivalent to showing that

$$-\frac{1}{2}\int_{\widehat{e}_h}[w^{-l}u_h^2;\widehat{n}_h]\ \mathrm{ds_{hk}} \geq 0.$$

Notice that the numerical flux does not appear given that it is scaled with $[u_h]=0$, and thus cannot influence the sign of the above quantity. Expanding the expression, we have that

$$\begin{aligned}-\frac{1}{2}\int_{\widehat{e}_h}[w^{-l}u_h^2;\widehat{n}_h]\ \mathrm{ds_{hk}} &= -\frac{1}{2}\int_{\widehat{e}_h} w^{-l}u_h^{2+}\cdot\widehat{n}_h^{+} + w^{-l}u_h^{2-}\cdot\widehat{n}_h^{-}\ \mathrm{ds_{hk}}\\ &= \frac{1}{2}|\widehat{e}_h|\,(\cos(q)-1) < 0.\end{aligned}$$

Hence, in general, whenever $\widehat{n}_h^{+} \neq -\widehat{n}_h^{-}$, h-independent positive-definiteness of the matrix resulting from the scheme may not hold, regardless of the choice of the modified upwind flux.

6.2 Discrete scheme, properties and convergence

6.2.1 Surface DG/UP discretisation

We can now define a discrete DG formulation on Γ_h^k based on the unified surface DG discretisation of the diffusion term discussed in Chapter 4 and a surface upwind flux (UP) discretisation of the advection term. We will refer to it as the surface DG/UP method. The problem reads: find $u_h \in \widehat{S}_{hk}$ such that

$$\mathcal{C}_h^k(u_h,v_h) = \sum_{\widehat{K}_h\in\widehat{\mathcal{T}}_h}\int_{\widehat{K}_h} f_h v_h\ \mathrm{dA_{hk}}\ \forall v_h \in \widehat{S}_{hk} \tag{6.4}$$

with

$$\mathcal{C}_h^k(u_h,v_h) := \mathcal{A}_h^k(u_h,v_h) + \mathcal{B}_h^k(u_h,v_h) \tag{6.5}$$

where $\mathcal{A}_h^k(u_h,v_h)$ corresponds to any of the surface DG methods given in Table 4.1 and $\mathcal{B}_h^k(u_h,v_h)$ is defined in (6.3). Note that the discrete velocity field w_h present in $\mathcal{B}_h^k(u_h,v_h)$ is now at our disposal and will be related to w in Section 6.3. For reasons that will be clear later on, the discrete mass perturbation coefficient γ_h is given by

$$\gamma_h = \begin{cases} 0 & \text{if } 1+\nabla_{\Gamma_h^k}\cdot w_h > 0;\\ -\frac{1}{2}\nabla_{\Gamma_h^k}\cdot w_h & \text{if } 1+\nabla_{\Gamma_h^k}\cdot w_h \leq 0.\end{cases} \tag{6.6}$$

Finally, with the convention that $\widehat{n}_h^+$ is the conormal to $\widehat{e}_h \subset \partial \widehat{K}_h$, we define the surface upwind flux $\widehat{w_h u_h}$ present in $\mathcal{B}_h^k(u_h, v_h)$ by

$$\widehat{w_h u_h} = \{w_h u_h; \widehat{n}_h\} + \rho_{\widehat{e}_h}[u_h]$$

where $\rho_{\widehat{e}_h} := \frac{1}{2}|w_h^+ \cdot \widehat{n}_h^+|$.

After stating a number of assumptions we make on the discrete velocity field w_h, we shall prove stability and convergence in the DG norm given in (4.34) with (4.33a) but with the scaling $\beta_{\widehat{e}_h}$ present in $\|\cdot\|_{*,h}$ norm replaced by $\beta_{\widehat{e}_h} + \rho_{\widehat{e}_h}$.

6.2.2 Assumptions

We now state several assumptions which will allow the analysis to follow through straightforwardly. These assumptions will then be justified in Section 6.3 for the simpler setting of piecewise linear surface approximations. We will assume that the discrete velocity field w_h is tangential to Γ_h^k and satisfies

$$w_h^+ \cdot \widehat{n}_h^+ = -w_h^- \cdot \widehat{n}_h^- \tag{6.7}$$

on each edge $\widehat{e}_h \in \widehat{\mathcal{E}}_h$ and, if the data velocity field $w \in [W^{m+1,\infty}(\Gamma_h^k)]^3$, we have that, for all $\widehat{K}_h \in \widehat{\mathcal{T}}_h$,

$$\|\mathbf{P}_{hk} w^{-l} - w_h\|_{L^\infty(\widehat{K}_h)} \lesssim h^{m+1}, \tag{6.8}$$

$$\left\|(\mathbf{P}_{hk} w^{-l} - w_h) \cdot \widehat{n}_h^+\right\|_{L^\infty(\partial \widehat{K}_h)} \lesssim h^{m+1}, \tag{6.9}$$

$$\|\nabla_{\Gamma_h^k} \cdot w_h\|_{L^\infty(\widehat{K}_h)} \lesssim h^l \tag{6.10}$$

where $0 \leq m \leq k$ and $l > 0$. Note that assumption (6.10) implies that

$$\gamma_h \equiv 0 \quad \text{for } h \text{ small enough.} \tag{6.11}$$

Remark 6.2.1. From assumption (6.7), we have that

$$\widehat{w_h u_h} = \begin{cases} w_h^+ \cdot \widehat{n}_h^+ u_h^+ & \text{if } w_h^+ \cdot \widehat{n}_h^+ > 0; \\ w_h^+ \cdot \widehat{n}_h^+ u_h^- & \text{if } w_h^+ \cdot \widehat{n}_h^+ < 0; \\ 0 & \text{if } w_h^+ \cdot \widehat{n}_h^+ = 0, \end{cases}$$

and it can thus be seen that this flux works in exactly the same way as the classical (planar) upwind flux when scaled with the jump term $[v_h]$.

6.2.3 Boundedness and stability

Lemma 6.2.2. *The surface DG/UP bilinear form $\mathcal{C}_h^k$ is bounded and stable in the DG norm, i.e.,*

$$\mathcal{C}_h^k(u_h, v_h) \lesssim \|u_h\|_{DG}\|v_h\|_{DG}, \quad \mathcal{C}_h^k(u_h, u_h) \gtrsim \|u_h\|_{DG}^2,$$

for every $u_h, v_h \in \widehat{S}_{hk}$, provided that the discrete velocity field w_h satisfies (6.7) and the penalty parameter α is chosen sufficiently large.

Proof. Boundedness of $\mathcal{C}_h^k$ follows from similar arguments to that of $\mathcal{A}_h^k$, given in the proof of Lemma 4.3.5. To show stability, we proceed in a similar fashion to the planar case setting detailed in Section 3.7 by testing (6.5) with $v_h = u_h$ and integrating by parts on each $K_h \in \mathcal{T}_h$. By doing so, we obtain

$$\begin{aligned}\mathcal{C}_h^k(u_h, u_h) = \mathcal{A}_h^k(u_h, u_h) &+ \sum_{\widehat{K}_h \in \widehat{\mathcal{T}}_h} \int_{\widehat{K}_h} \left(\gamma_h + \frac{1}{2}\nabla_{\Gamma_h^k} \cdot w_h\right) u_h^2 \, \mathrm{dA_{hk}} \\ &+ \sum_{\widehat{e}_h \in \widehat{\mathcal{E}}_h} \int_{\widehat{e}_h} \{w_h u_h; \widehat{n}_h\}[u_h] + \rho_{\widehat{e}_h}|[u_h]|^2 \, \mathrm{ds_{hk}} \\ &- \frac{1}{2} \sum_{\widehat{K}_h \in \widehat{\mathcal{T}}_h} \int_{\partial \widehat{K}_h} \left(w_h \cdot n_{\widehat{K}_h}\right) u_h^2 \, \mathrm{ds_{hk}}. \end{aligned} \tag{6.12}$$

Applying Lemma 4.2.3, we then have that

$$\begin{aligned}\sum_{\widehat{K}_h \in \widehat{\mathcal{T}}_h} \int_{\partial \widehat{K}_h} \left(w_h \cdot n_{\widehat{K}_h}\right) u_h^2 \, \mathrm{ds_{hk}} &= \sum_{\widehat{e}_h \in \widehat{\mathcal{E}}_h} \int_{\widehat{e}_h} [w_h u_h^2; \widehat{n}_h] \, \mathrm{ds_{hk}} \\ &= \sum_{\widehat{e}_h \in \widehat{\mathcal{E}}_h} \int_{\widehat{e}_h} \{w_h; \widehat{n}_h\}[u_h^2] + [w_h; \widehat{n}_h]\{u_h^2\} \, \mathrm{ds_{hk}}.\end{aligned}$$

Now, making use of assumption (6.7), we have that $[w_h; \widehat{n}_h] = 0$ and, in addition,

$$\begin{aligned}\{w_h u_h; \widehat{n}_h\}[u_h] &= \left(\frac{1}{2} w_h^+ u_h^+ \cdot \widehat{n}_h^+ - \frac{1}{2} w_h^- u_h^- \cdot \widehat{n}_h^-\right)\left(u_h^+ - u_h^-\right) \\ &= \left(\frac{1}{2} w_h^+ u_h^+ \cdot \widehat{n}_h^+ + \frac{1}{2} w_h^+ u_h^- \cdot \widehat{n}_h^+\right)\left(u_h^+ - u_h^-\right) \\ &= \frac{1}{2} w_h^+ \cdot \widehat{n}_h^+ \left(u_h^+ + u_h^-\right)\left(u_h^+ - u_h^-\right) \\ &= \frac{1}{2}\{w_h; \widehat{n}_h\}[u_h^2].\end{aligned}$$

Plugging this equality back into (6.12) and cancelling the resulting terms yields

$$\mathcal{C}_h^k(u_h, u_h) = \mathcal{A}_h^k(u_h, u_h) + \sum_{\widehat{K}_h \in \widehat{\mathcal{T}}_h} \int_{\widehat{K}_h} \left(\gamma_h + \frac{1}{2}\nabla_{\Gamma_h^k} \cdot w_h\right) u_h^2 \, \mathrm{dA_{hk}} + \sum_{\widehat{e}_h \in \widehat{\mathcal{E}}_h} \int_{\widehat{e}_h} \rho_{\widehat{e}_h} |[u_h]|^2 \, \mathrm{ds_{hk}}. \tag{6.13}$$

Combining the second and third terms of (6.13) with respectively the mass and jump terms of $\mathcal{A}_h^k(u_h, u_h)$, making use of the expression for γ_h given in (6.6) and proceeding in a similar fashion as for the stability proof of $\mathcal{A}_h^k$ in Lemma 4.3.5, we obtain the desired result independently of h provided that the penalty parameter α is large enough. □

Remark 6.2.3. It is clear from the above proof that assumption (6.7) on the discrete velocity field w_h is key to showing stability of the surface DG/UP bilinear form. If we simply chose the discrete velocity field to be the true velocity field surface lifted downwards i.e. $w_h = w^{-l}$ in (6.5) (in which case assumption (6.7) and all related results would not be satisfied), the matrix resulting from the scheme may not be positive-definite, as discussed in Section 6.1.1.

Lemma 6.2.2 allows us to straightforwardly extend the stability estimate (4.38) to our setting.

As before, for each of the surface DG bilinear forms represented by (6.5), we define a corresponding bilinear form on Γ induced by the surface lifted triangulation $\widehat{\mathcal{T}}_h^\ell$ which is well defined for functions $v_1, v_2 \in H^2(\Gamma) + \widehat{S}_{hk}^\ell$. We define

$$\mathcal{C}(v_1, v_2) := \mathcal{A}(v_1, v_2) + \mathcal{B}(v_1, v_2) \tag{6.14}$$

where $\mathcal{A}$ corresponds to any of the surface lifted DG bilinear forms considered in Chapter 4, and

$$\mathcal{B}(v_1, v_2) = \sum_{\widehat{K}_h^l \in \widehat{\mathcal{T}}_h^l} \int_{\widehat{K}_h^l} -v_1 w \cdot \nabla_\Gamma v_2 \, \mathrm{dA} + \sum_{\widehat{e}_h^l \in \widehat{\mathcal{E}}_h^l} \int_{\widehat{e}_h^l} \left(\{w v_1; n\} + \rho_{\widehat{e}_h} \delta_{\widehat{e}_h}^{-1} [v_1]\right) [v_2] \, \mathrm{ds}.$$

The DG norm on Γ is given as in (4.39) with (4.40a) but with the scaling $\delta_{\widehat{e}_h}^{-1}\beta_{\widehat{e}_h}$ present in $\|\cdot\|_{*,h}$ norm replaced by $\delta_{\widehat{e}_h}^{-1}(\beta_{\widehat{e}_h} + \rho_{\widehat{e}_h})$. Finally, one can easily derive equivalent results of (4.46) and the boundedness/stability estimates given in

Lemma 4.3.8 which hold for the bilinear form $\mathcal{C}$.

6.2.4 Convergence

We now state the main result of this chapter, which is the advection-diffusion analogue of Theorem 4.4.1.

Theorem 6.2.4. *Let $u \in H^{k+1}(\Gamma)$ and $u_h \in \widehat{S}_{hk}$ denote the solutions to (6.2) and (6.4), respectively. Then, under assumptions (6.7), (6.8), (6.9) and (6.10) on the discrete velocity field w_h, with $m \geq k-1$, we have that*

$$\|u - u_h^\ell\|_{DG} \lesssim h^k \left(\|f\|_{L^2(\Gamma)} + \|u\|_{H^{k+1}(\Gamma)} \right),$$

provided the grid size h is small enough and the penalty parameter α is large enough for the surface IP, Bassi et al. and IIPG methods.

Since the key continuity estimate (4.48) can be straightforwardly extended to the bilinear form $\mathcal{C}$, the proof of Theorem 6.2.4 follows the same lines as that of Theorem 4.4.1 as long as the perturbed Galerkin orthogonality result given in Lemma 4.4.5 can be extended to the advection-diffusion setting, which will be the focus of this section. Before doing so, we will require an additional geometric estimate.

Lemma 6.2.5. *Let Γ be a compact smooth and oriented surface in $\mathbb{R}^3$ and let Γ_h^k be its Lagrange interpolant of degree k. Then, for sufficiently small h, we have that*

$$\|\mathbf{P} - \mathbf{P}\mathbf{P}_{hk}\mathbf{P}\|_{L^\infty(\Gamma_h^k)} \lesssim h^{2k}. \tag{6.15}$$

Proof. It is sufficient to show that $(\mathbf{P} - \mathbf{P}\mathbf{P}_{hk}\mathbf{P})\, x$ for $x \in \mathbb{R}^3$ scales appropriately. Setting $\tilde{x} = \mathbf{P}x$ (which is tangential to Γ) and noting that $\mathbf{P}_{hk}\tilde{x} = \tilde{x} - (\tilde{x} \cdot \widehat{\nu}_h)\widehat{\nu}_h$, we have that

$$\begin{aligned}
&(\mathbf{P} - \mathbf{P}\mathbf{P}_{hk}\mathbf{P})\, x = \tilde{x} - \mathbf{P}\mathbf{P}_{hk}\tilde{x} = \tilde{x} - \mathbf{P}\left(\tilde{x} - (\tilde{x} \cdot \widehat{\nu}_h)\widehat{\nu}_h\right) \\
&= \tilde{x} - (\tilde{x} - (\tilde{x} \cdot \nu)\nu - (\tilde{x} \cdot \widehat{\nu}_h)(\widehat{\nu}_h - (\widehat{\nu}_h \cdot \nu)\nu) \\
&= (\tilde{x} \cdot \widehat{\nu}_h)\widehat{\nu}_h - (\tilde{x} \cdot \widehat{\nu}_h)(\widehat{\nu}_h \cdot \nu)\nu \\
&= (\tilde{x} \cdot \widehat{\nu}_h)(\widehat{\nu}_h - \nu) + (\tilde{x} \cdot \widehat{\nu}_h)\nu\,(1 - (\widehat{\nu}_h \cdot \nu)) \\
&= (\tilde{x} \cdot (\widehat{\nu}_h - \nu))(\widehat{\nu}_h - \nu) + (\tilde{x} \cdot (\widehat{\nu}_h - \nu))\nu\,(1 - (\widehat{\nu}_h \cdot \nu)) \\
&\leq |\widehat{\nu}_h - \nu|^2|\tilde{x}| + \frac{1}{2}|\widehat{\nu}_h - \nu|^2|\tilde{x}| \\
&\lesssim h^{2k}|\tilde{x}| \lesssim h^{2k}|x|
\end{aligned}$$

where we have used the equality $1-(\widehat{\nu}_h\cdot\nu)=\frac{1}{2}|\widehat{\nu}_h-\nu|^2$ and the geometric estimate (A.1c). □

Lemma 6.2.6. *Let $u\in H^s(\Gamma)$, $s\geq 2$, and $u_h\in\widehat{S}_{hk}$ denote the solutions to (6.2) and (6.4), respectively. We define the functional $E^{\mathcal{C}}_{hk}$ on $\widehat{S}^{\ell}_{hk}$ by*

$$E^{\mathcal{C}}_{hk}(v^{\ell}_h)=\mathcal{C}(u-u^{\ell}_h,v^{\ell}_h).$$

Then, $E^{\mathcal{C}}_{hk}$ can be written as

$$E^{\mathcal{C}}_{hk}(v^{\ell}_h)=E_{hk}(v^{\ell}_h)+E^{\mathcal{B}}_{hk}(v^{\ell}_h)+E^{data}_{hk}(v^{\ell}_h) \tag{6.16}$$

where E_{hk} is given by (4.50) or (4.51), $E^{\mathcal{B}}_h$ is given by

$$\begin{aligned}E^{\mathcal{B}}_{hk}(v^l_h)=&\sum_{\widehat{K}^l_h\in\widehat{\mathcal{T}}^l_h}\int_{\widehat{K}^l_h}\left(\delta^{-1}_{hk}-1\right)u^l_hv^l_h+\delta^{-1}_{hk}w\cdot(\mathbf{P}-\mathbf{P}_{hk}(\mathbf{I}-d\mathbf{H})\mathbf{P})\,\nabla_\Gamma v^l_hu^l_h\;dA\\&+\sum_{\widehat{e}^l_h\in\widehat{\mathcal{E}}^l_h}\int_{\widehat{e}^l_h}\left(\left\{wu^l_h;\mathbf{P}\widehat{n}^l_h-n\right\}+\left(\delta^{-1}_{\widehat{e}_h}-1\right)\{w^l_hu^l_h;\widehat{n}^l_h\}\right)[v^l_h]\;ds\end{aligned}$$

and finally, the data approximation functional $E^{data}_h(v^{\ell}_h)$ is given by

$$\begin{aligned}E^{data}_{hk}(v^{\ell}_h)=&\sum_{\widehat{K}^l_h\in\widehat{\mathcal{T}}^l_h}\int_{\widehat{K}^l_h}\left(\mathbf{P}_{hk}w-w^l_h\right)\cdot\mathbf{P}_{hk}(\mathbf{I}-d\mathbf{H})\mathbf{P}\nabla_\Gamma v^{\ell}_hu^l_h\;dA\\&+\sum_{\widehat{e}^l_h\in\widehat{\mathcal{E}}^l_h}\int_{\widehat{e}^l_h}\left\{\left(w^l_h-\mathbf{P}_{hk}w\right)u^l_h;\widehat{n}^l_h\right\}\;ds\end{aligned}$$

Furthermore, for h small enough, we have that

$$|E^{\mathcal{B}}_{hk}(v^{\ell}_h)|\lesssim h^{k+1}\|f\|_{L^2(\Gamma)}\|v^{\ell}_h\|_{DG}, \tag{6.17}$$

and, under assumptions (6.7), (6.8), (6.9) and (6.10), we have that

$$|E^{data}_{hk}(v^{\ell}_h)|\lesssim h^{m+1}\|f\|_{L^2(\Gamma)}\|v^{\ell}_h\|_{DG} \tag{6.18}$$

where $0\leq m\leq k$.

Remark 6.2.7. Notice that if $m=k-1$ in (6.18), the data approximation error is suboptimal relative to the geometric error (6.17) but still yields optimal a priori error estimates. If we choose $m=k$, the data approximation error will be of the same (higher) order as the geometric error.

Proof of Lemma 6.2.6. Since the scaling of $E_{hk}(v_h^\ell)$ is known from Lemma 4.4.5, the proof will only focus on the terms which were not dealt with in that lemma. Recall that, for h small enough, (6.11) holds. Using this, it can be easily seen that, for h small enough,

$$\begin{aligned}
&\sum_{\widehat{K}_h^l \in \widehat{\mathcal{T}}_h^l} \int_{\widehat{K}_h^l} u v_h^l \ \mathrm{dA} - \sum_{\widehat{K}_h \in \widehat{\mathcal{T}}_h} \int_{\widehat{K}_h} (1+\gamma_h)\, u_h v_h \ \mathrm{dA_{hk}} \\
&= \sum_{\widehat{K}_h^l \in \widehat{\mathcal{T}}_h^l} \int_{\widehat{K}_h^l} (u - u_h^l) v_h^l \ \mathrm{dA} + \sum_{\widehat{K}_h^l \in \widehat{\mathcal{T}}_h^l} \int_{\widehat{K}_h^l} \left(1 - \delta_{hk}^{-1}\right) u_h^l v_h^l \ \mathrm{dA}.
\end{aligned}$$

Next, we consider terms involving the velocity field in the interior of elements i.e.

$$\begin{aligned}
&- \sum_{\widehat{K}_h^l \in \widehat{\mathcal{T}}_h^l} \int_{\widehat{K}_h^l} w \cdot \nabla_\Gamma v_h^l u \ \mathrm{dA} + \sum_{\widehat{K}_h \in \widehat{\mathcal{T}}_h} \int_{\widehat{K}_h} w_h \cdot \nabla_{\Gamma_h^k} v_h u_h \ \mathrm{dA_{hk}} \\
&= - \sum_{\widehat{K}_h^l \in \widehat{\mathcal{T}}_h^l} \int_{\widehat{K}_h^l} w \cdot \nabla_\Gamma v_h^l (u - u_h^l) + \delta_{hk}^{-1} w \cdot \left(\mathbf{P}_{hk}(\mathbf{I} - d\mathbf{H})\mathbf{P} - \mathbf{P}\right) \nabla_\Gamma v_h^l u_h^l \ \mathrm{dA} \\
&\qquad + \sum_{\widehat{K}_h \in \widehat{\mathcal{T}}_h} \int_{\widehat{K}_h} \left(w_h - w^{-l}\right) \cdot \nabla_{\Gamma_h^k} v_h u_h \ \mathrm{dA_{hk}} \\
&= - \sum_{\widehat{K}_h^l \in \widehat{\mathcal{T}}_h^l} \int_{\widehat{K}_h^l} w \cdot \nabla_\Gamma v_h^l (u - u_h^l) \ \mathrm{dA} + \sum_{\widehat{K}_h^l \in \widehat{\mathcal{T}}_h^l} \int_{\widehat{K}_h^l} \delta_{hk}^{-1} w \cdot \left(\mathbf{P}\mathbf{P}_{hk}\mathbf{P} - \mathbf{P}\right) \nabla_\Gamma v_h^l u_h^l \ \mathrm{dA} \\
&- \sum_{\widehat{K}_h^l \in \widehat{\mathcal{T}}_h^l} \int_{\widehat{K}_h^l} \delta_{hk}^{-1} w \cdot \left(d\mathbf{P}\mathbf{P}_{hk}\mathbf{H}\right) \nabla_\Gamma v_h^l u_h^l \ \mathrm{dA} + \sum_{\widehat{K}_h \in \mathcal{T}_h} \int_{\widehat{K}_h} \left(w_h - \mathbf{P}_{hk} w^{-l}\right) \cdot \nabla_{\Gamma_h^k} v_h u_h \ \mathrm{dA_{hk}}
\end{aligned}$$

where, in the last line, we have made use of the fact that $\nabla_{\Gamma_h^k} v_h = \mathbf{P}_{hk} \nabla_{\Gamma_h^k} v_h$, $w = \mathbf{P} w$ and $\mathbf{P}_{hk} w_h = w_h$. Finally, we consider the terms involving the velocity field on the boundary of elements i.e.

$$\begin{aligned}
&\sum_{\widehat{e}_h^l \in \widehat{\mathcal{E}}_h^l} \int_{\widehat{e}_h^l} \{wu; n\}[v_h^l] \ \mathrm{ds} - \sum_{\widehat{e}_h \in \widehat{\mathcal{E}}_h} \int_{\widehat{e}_h} \{w_h u_h; \widehat{n}_h\}[v_h] \ \mathrm{ds_{hk}} \\
&= \sum_{\widehat{e}_h^l \in \widehat{\mathcal{E}}_h^l} \int_{\widehat{e}_h^l} \{w(u - u_h^l); n\}[v_h^l] \ \mathrm{ds} + \sum_{\widehat{e}_h^l \in \widehat{\mathcal{E}}_h^l} \int_{\widehat{e}_h^l} \left(\{w u_h^l; n\} - \{w_h^l u_h^l; \widehat{n}_h^l\} \delta_{\widehat{e}_h}^{-1}\right) [v_h^l] \ \mathrm{ds}.
\end{aligned}$$

Focusing on one of the terms in the above, using the fact that $w = \mathbf{P} w$ and $\widehat{n}_h^{l+} = \mathbf{P}_{hk}^{l+} \widehat{n}_h^{l+}$, we have that

$$\begin{aligned}
&w u_h^{l+} \cdot n^+ - \delta_{\widehat{e}_h}^{-1} w_h^l u_h^{l+} \cdot \widehat{n}_h^{l+} = w u_h^{l+} \cdot n^+ - w_h^l u_h^{l+} \cdot \widehat{n}_h^{l+} + \left(1 - \delta_{\widehat{e}_h}^{-1}\right) w_h^l u_h^{l+} \cdot \widehat{n}_h^{l+} \\
&= w u_h^{l+} \cdot \left(n^+ - \mathbf{P} \widehat{n}_h^{l+}\right) + \left(\mathbf{P}_{hk}^{l+} w - w_h^l\right) u_h^{l+} \cdot \widehat{n}_h^{l+} + \left(1 - \delta_{\widehat{e}_h}^{-1}\right) w_h^l u_h^{l+} \cdot \widehat{n}_h^{l+}.
\end{aligned}$$

Combining all of the terms, we get that

$$\sum_{\widehat{e}_h^l \in \widehat{\mathcal{E}}_h^l} \int_{\widehat{e}_h^l} \{wu; n\}[v_h^l] \, \mathrm{ds} - \sum_{\widehat{e}_h \in \widehat{\mathcal{E}}_h} \int_{\widehat{e}_h} \{w_h u_h; \widehat{n}_h\}[v_h] \, \mathrm{ds_{hk}}$$
$$= \sum_{\widehat{e}_h^l \in \widehat{\mathcal{E}}_h^l} \int_{\widehat{e}_h^l} \left(\{wu_h^l; n - \mathbf{P}\widehat{n}_h^l\} + \{ (\mathbf{P}_{hk}^l w - w_h^l) \, u_h^l; \widehat{n}_h^l \} + \left(1 - \delta_{\widehat{e}_h}^{-1}\right) \{w_h^l u_h^l; \widehat{n}_h^l\} \right) [v_h^l] \, \mathrm{ds}.$$

This completes the first part of the proof of Lemma 6.2.6. The scaling of the error functional $E_h^{\mathcal{B}}$ follows by applying similar arguments as for the proof of Lemma 4.4.5 in addition to the new geometric estimate given in Lemma 6.2.5. The scaling for the data approximation functional E_h^{data} follows from assumptions (6.8) and (6.9). This completes the proof. □

6.3 Construction of discrete velocity field

We will now attempt to justify the assumptions we have made on w_h by constructing a discrete velocity field which satisfies assumptions (6.7), (6.8), (6.9) and (6.10) in a simpler setting. We only consider a particular direction one could take to construct such a discrete velocity field, and this is by no means the only one. We will restrict ourselves to the piecewise linear surface approximation setting $\Gamma_h := \Gamma_h^1$. As in Chapter 5, we will make use of the notation from the piecewise linear setting (by omitting the hats, e.g. e_h instead of $\widehat{e}_h$) to highlight this.

6.3.1 Surface Raviart-Thomas interpolant

A natural way of constructing a discrete velocity field w_h which satisfies the assumptions we have made is to define it as a *Raviart-Thomas*-type interpolant of w^{-l}, which we will refer to as the surface Raviart-Thomas interpolant.

Let F_{K_h} denote the mapping from the reference element K to K_h. Then we have that $\nabla F_{K_h} = (e_0, e_1) \in \mathbb{R}^{3\times 2}$ where e_0 and e_1 are two edges of K_h intersecting at the vertex x_0. We first define the local spaces

$$\mathbb{P}_{RT}^q(K_h) := \left\{ s_h(x) := \nabla F_{K_h}(F_{K_h}^{-1}(x)) p \left(F_{K_h}^{-1}(x) \right), \; p \in [\mathbb{P}^q(K)]^2 \right\}.$$

We next define the local Raviart-Thomas space of order q on K_h to be given by

$$RT^q(K_h) := \left\{ \bar{w}_h(x) := s_h(x) + (x - x_0) t \left(F_{K_h}^{-1}(x) \right), \; s_h \in \mathbb{P}_{RT}^q(K_h), \; t \in \mathbb{P}^q(K) \right\}.$$

It is clear from the definition of $RT^q(K_h)$ that any function $\bar{w}_h \in RT^q(K_h)$ for every

$K_h \in \mathcal{T}_h$ is tangential to Γ_h. Using the convention that the conormal to $e_h \subset \partial K_h$ is n_h^+, the local degrees of freedom of $\bar{w}_h \in RT^q(K_h)$ are given by

$$\int_{e_h} \bar{w}_h \cdot n_h^+ p_q \ \mathrm{ds_h} \ \forall p_q \in \mathbb{P}^q(e_h), e_h \subset \partial K_h, \tag{6.19}$$

$$\int_{K_h} \bar{w}_h \cdot \mathbf{p}_{q-1} \ \mathrm{ds_h} \ \forall \mathbf{p}_{q-1} \in \mathbb{P}^{q-1}_{RT}(K_h). \tag{6.20}$$

We then define, for $w^{-l} \in [W^{2,\infty}(\Gamma_h)]^3$, the local surface Raviart-Thomas interpolant of order q to be $\Pi^q_{K_h} w^{-l} \in RT^q(K_h)$ satisfying

$$\int_{e_h} \Pi^q_{K_h} w^{-l} \cdot n_h^+ p_q \ \mathrm{ds_h} = \int_{e_h} w^{-l} \cdot n_{e_h}^+ p_q \ \mathrm{ds_h} \ \forall p_q \in \mathbb{P}^q(e_h), e_h \subset \partial K_h, \tag{6.21}$$

$$\int_{K_h} \Pi^q_{K_h} w^{-l} \cdot \mathbf{p}_{q-1} \ \mathrm{ds_h} = \int_{K_h} w^{-l} \cdot \mathbf{p}_{q-1} \ \mathrm{ds_h} \ \forall \mathbf{p}_{q-1} \in \mathbb{P}^{q-1}_{RT}(K_h). \tag{6.22}$$

Here, the "average" conormals $n_{e_h}^{+/-}$ are given by $n_{e_h}^{+/-} := \pm \frac{\frac{1}{2}(n_h^+ - n_h^-)}{|\frac{1}{2}(n_h^+ - n_h^-)|}$.

Remark 6.3.1. Notice that this definition differs from that of the local classical Raviart-Thomas interpolant in the way we have defined the right-hand side of (6.21). We have to use what we call the "average" conormals $n_{e_h}^{+/-}$ instead of the standard conormals $n_h^{+/-}$ because they satisfy $n_{e_h}^+ = -n_{e_h}^-$, which is key for assumption (6.7) to be satisfied. From here on, we will refer to the local classical Raviart-Thomas interpolant by $\widetilde{\Pi}^q_{K_h} w^{-l}$.

Lemma 6.3.2. *Let $\Pi^q_{K_h} w^{-l}$ and $\Pi^q_{K_h^-} w^{-l}$ be the local surface Raviart-Thomas interpolants of $w^{-l} \in [W^{2,\infty}(\Gamma_h)]^3$ (defined as in (6.21)–(6.22)) on respectively the neighbouring elements $K_h, K_h^- \in \mathcal{T}_h$ with conormals n_h^+ and n_h^-. Then we have that*

$$\Pi^q_{K_h} w^{-l} \cdot n_h^+ = -\Pi^q_{K_h^-} w^{-l} \cdot n_h^-$$

on each edge $e_h = \partial K_h \bigcap \partial K_h^-$.

Proof. By (6.21)–(6.22) and using the fact that $n_{e_h}^+ = -n_{e_h}^-$, we have that

$$\begin{aligned}\int_{e_h} \Pi^q_{K_h} w^{-l} \cdot n_h^+ p_q \ \mathrm{ds_h} = \int_{e_h} w^{-l} \cdot n_{e_h}^+ p_q \ \mathrm{ds_h} &= -\int_{e_h} w^{-l} \cdot n_{e_h}^- p_q \ \mathrm{ds_h} \\ &= -\int_{e_h} \Pi^q_{K_h^-} w^{-l} \cdot n_h^- p_q \ \mathrm{ds_h}.\end{aligned}$$

It follows that

$$\int_{e_h} \left(\Pi^q_{K_h} w^{-l} \cdot n_h^+ + \Pi^q_{K_h^-} w^{-l} \cdot n_h^- \right) p_q \, \mathrm{ds_h} = 0$$

for every $p_q \in \mathbb{P}^q(e_h)$. By Proposition 3.2 in Fortin and Brezzi [1991], we have that $\Pi^q_{K_h} w^{-l} \cdot n_h^+, \Pi^q_{K_h^-} w^{-l} \cdot n_h^- \in \mathbb{P}^q(e_h)$ which gives us the pointwise equality

$$\Pi^q_{K_h} w^{-l} \cdot n_h^+ = -\Pi^q_{K_h^-} w^{-l} \cdot n_h^-$$

as required. □

6.3.2 Surface Raviart-Thomas interpolation estimates

Lemma 6.3.3. *Let $\Pi^q_{K_h} w^{-l}$ be the local surface Raviart-Thomas interpolant of $w^{-l} \in [W^{2,\infty}(\Gamma_h)]^3$ defined as in (6.21)–(6.22) and let $\widetilde{\Pi}^q_{K_h} w$ be its local classical Raviart-Thomas interpolant. We then have that*

$$\|\Pi^q_{K_h} w^{-l} - \widetilde{\Pi}^q_{K_h} w^{-l}\|_{L^\infty(K_h)} \lesssim h^2$$

for each $K_h \in \mathcal{T}_h$.

Proof. Denote by $\{N_i^{\partial K_h}\}_{i=1}^{n_{\partial K_h}}$ the set of local degrees of freedom given by (6.19) and $\{\varphi_i^{\partial K_h}\}_{i=1}^{n_{\partial K_h}}$ the associated (vector-valued) basis functions. Similarly, we denote by $\{N_i^{K_h}\}_{i=1}^{n_{K_h}}$ the set of local degrees of freedom given by (6.20) and $\{\varphi_i^{K_h}\}_{i=1}^{n_{K_h}}$ the associated (vector-valued) basis functions. The local degrees of freedom for the local standard Raviart-Thomas interpolant $\{\widetilde{N}_i\}_{i=1}^{n_{\partial K_h}}$ and $\{\widetilde{N}_i\}_{i=1}^{n_{K_h}}$ are defined similarly.

We then have that

$$\Pi^q_{K_h} w^{-l}(x) = \sum_{i=1}^{n_{\partial K_h}} N_i^{\partial K_h}(w^{-l}) \varphi_i^{\partial K_h}(x) + \sum_{i=1}^{n_{K_h}} N_i^{K_h}(w^{-l}) \varphi_i^{K_h}(x),$$

and similarly for $\widetilde{\Pi}^q_{K_h} w^{-l}$. Then by noting that $N_i^{K_h}(w^{-l}) = \widetilde{N}_i^{K_h}(w^{-l})$ and making

use of (6.19) and (6.21), we have that

$$\begin{aligned}
&\|\Pi^q_{K_h} w^{-l} - \widetilde{\Pi}^q_{K_h} w^{-l}\|_{L^\infty(K_h)} = \left\| \sum_{i=1}^{n_{\partial K_h}} \left(N_i^{\partial K_h}(w^{-l}) - \widetilde{N}_i^{\partial K_h}(w^{-l}) \right) \varphi_i^{\partial K_h} \right\|_{L^\infty(K_h)} \\
&\leq \max_{1\leq i\leq n_{\partial K_h}} \left| N_i^{\partial K_h}(w^{-l}) - \widetilde{N}_i^{\partial K_h}(w^{-l}) \right| \sum_{i=1}^{n_{\partial K_h}} \left| \varphi_i^{\partial K_h} \right| \\
&\lesssim \max_{1\leq i\leq n_{\partial K_h}} \left| N_i^{\partial K_h}(w^{-l}) - \widetilde{N}_i^{\partial K_h}(w^{-l}) \right| \\
&= \max_{1\leq i\leq n_{\partial K_h}} \left| \int_{e_h} w^{-l} \cdot n^+_{e_h} \xi_i \, \mathrm{ds_h} - \int_{e_h} w^{-l} \cdot n^+_h \xi_i \, \mathrm{ds_h} \right| \\
&= \max_{1\leq i\leq n_{\partial K_h}} \left| \int_{e_h} w^{-l} \cdot \left(\mathbf{P}^{-l} n^+_{e_h} - \mathbf{P}^{-l} n^+_h \right) \xi_i \, \mathrm{ds_h} \right| \\
&\lesssim \|n - \mathbf{P} n^+_{e_h}\|_{L^\infty(\mathcal{E}_h)} + \|n - \mathbf{P} n^+_h\|_{L^\infty(\mathcal{E}_h)} \lesssim h^2
\end{aligned}$$

where $\{\xi_i\}$ denote the basis functions of $\mathbb{P}^q(e_h)$. The last estimate follows from Lemma A.0.1. □

The following theorem will help justify assumptions (6.8) and (6.9) for the case of the local surface Raviart-Thomas interpolant of zero order ($q = 0$).

Theorem 6.3.4. *Let $w^{-l} \in [W^{2,\infty}(\Gamma_h)]^3$ and $\widetilde{\Pi}^0_{K_h} w^{-l}$ be its local classical Raviart-Thomas interpolant of zero order defined only through condition (6.21) (with $n^+_{e_h}$ replaced by n^+_h). We then have that*

$$\begin{aligned}
\|\mathbf{P}_h w^{-l} - \widetilde{\Pi}^0_{K_h} w^{-l}\|_{L^\infty(K_h)} &\lesssim h \|\nabla_{\Gamma_h} w^{-l}\|_{L^\infty(K_h)}, \\
\left\| \nabla_{\Gamma_h} \cdot \left(\mathbf{P}_h w^{-l} - \widetilde{\Pi}^0_{K_h} w^{-l} \right) \right\|_{L^\infty(K_h)} &\lesssim h |\nabla_{\Gamma_h} w^{-l}|_{W^{1,\infty}(K_h)}
\end{aligned}$$

for each $K_h \in \mathcal{T}_h$.

Proof. The proof of the first estimate follows similar lines as that of Theorem 6.3 in Acosta et al. [2011]. The second estimate follows similar lines as that of Theorem 1.114 in Ern [2004]. □

The first estimate of Theorem 6.3.4 together with Lemma 6.3.3 guarantees that the local surface Raviart-Thomas interpolant also satisfies Theorem 6.3.4. As such, assumption (6.8) holds when choosing w_h to be the local surface Raviart-Thomas interpolant of zero order.

Assumption (6.9) follows straightforwardly by noting that, from (6.21), $\widetilde{\Pi}^0_{K_h} w^{-l} \cdot n^+_h$ can be thought of as an L^2 projection of $w^{-l} \cdot n^+_h$ onto the space of piecewise constant functions living on $e_h \subset \partial K_h$. Coupling this fact with Lemma 6.3.3

validates (6.9) when choosing w_h to be the local surface Raviart-Thomas interpolant of zero order.

We finally show that assumption (6.10) holds for local surface Raviart-Thomas interpolants of zero order.

Lemma 6.3.5. *Let $w^{-l} \in [W^{2,\infty}(\Gamma_h)]^3$ and $\Pi^0_{K_h} w^{-l}$ be its local surface Raviart-Thomas interpolant of zero order defined only through condition (6.21). We then have that*

$$\left\| \nabla_{\Gamma_h} \cdot \Pi^0_{K_h} w^{-l} \right\|_{L^\infty(K_h)} \lesssim h.$$

Proof. We have that

$$\begin{aligned} \left\| \nabla_{\Gamma_h} \cdot \Pi^0_{K_h} w^{-l} \right\|_{L^\infty(K_h)} \leq & \left\| \nabla_{\Gamma_h} \cdot \left(\Pi^0_{K_h} w^{-l} - \mathbf{P}_h w^{-l} \right) \right\|_{L^\infty(K_h)} \\ & + \| \nabla_{\Gamma_h} \cdot \mathbf{P}_h w^{-l} \|_{L^\infty(K_h)}. \end{aligned}$$

Making use of Lemma 3.2 in Olshanskii et al. [2013], we have that the second term scales like h. For the first term, we have that

$$\begin{aligned} \left\| \nabla_{\Gamma_h} \cdot \left(\Pi^0_{K_h} w^{-l} - \mathbf{P}_h w^{-l} \right) \right\|_{L^\infty(K_h)} \leq & \left\| \nabla_{\Gamma_h} \cdot \left(\Pi^0_{K_h} w^{-l} - \widetilde{\Pi}^0_{K_h} w^{-l} \right) \right\|_{L^\infty(K_h)} \\ & + \left\| \nabla_{\Gamma_h} \cdot \left(\widetilde{\Pi}^0_{K_h} w^{-l} - \mathbf{P}_h w^{-l} \right) \right\|_{L^\infty(K_h)}. \end{aligned}$$

The second term in the above scales appropriately by the second estimate of Theorem 6.3.4. For the first term we proceed as in the proof of Lemma 6.3.3 to get that

$$\begin{aligned} & \left\| \nabla_{\Gamma_h} \cdot \left(\Pi^0_{K_h} w^{-l} - \widetilde{\Pi}^0_{K_h} w^{-l} \right) \right\|_{L^\infty(K_h)} \\ & \leq \max_{1 \leq i \leq n_{\partial K_h}} \left| N_i^{\partial K_h}(w^{-l}) - \widetilde{N}_i^{\partial K_h}(w^{-l}) \right| \sum_{1 \leq i \leq n_{\partial K_h}} \left| \nabla_{\Gamma_h} \cdot \varphi_i^{\partial K_h} \right| \\ & \lesssim \max_{1 \leq i \leq n_{\partial K_h}} \left| N_i^{\partial K_h}(w^{-l}) - \widetilde{N}_i^{\partial K_h}(w^{-l}) \right| h^{-1} \lesssim h \end{aligned}$$

as required. □

Remark 6.3.6. Proving corresponding results for higher-order Raviart-Thomas interpolants is not a trivial extension of the proofs given in this section. This is due to the fact that, on higher order surface approximations, the conormals $\widehat{n}_h^{+/-}$ are no longer constant along each edge $\widehat{e}_h \in \widehat{\mathcal{E}}_h$ but, instead, vary pointwise.

6.4 Numerical tests

In the following test problems, we will go slightly beyond the theory dealt with in this chapter by considering advection-diffusion problems of the form

$$-\epsilon\Delta_\Gamma u + w \cdot \nabla_\Gamma u + u = f \text{ on } \Gamma \tag{6.23}$$

where $0 < \epsilon \ll \|w\|_{L^\infty(\Gamma)}|\Gamma|^{\frac{1}{2}}$, which corresponds to the advection-dominated regime. For the test problems discussed below, we will focus on a surface IP discretisation of the diffusion term and call the resulting approximation the surface IP/UP approximation. Furthermore, the discrete velocity field w_h is chosen to be the zero order surface Raviart-Thomas interpolant of w^{-l} i.e. $w_h|_{K_h} = \Pi^0_{K_h} w^{-l}$. We will also briefly discuss the case when we choose $w_h = w^{-l}$ in the numerics. Further implementational aspects can be found in Section 4.5.1.

6.4.1 Test problem on torus

Our first test problem, considered in Olshanskii et al. [2013], involves solving (6.23) on the torus

$$\Gamma = \left\{ (x_1, x_2, x_3) \mid \left(\sqrt{x_1^2 + x_2^2} - 1 \right)^2 + x_3^2 = \frac{1}{16} \right\}$$

with velocity field

$$w(x) = \frac{1}{\sqrt{x_1^2 + x_2^2}} (-x_2, x_1, 0)^T .$$

Note that the velocity field w is tangential to the torus and divergence-free. We set $\epsilon = 10^{-6}$ and construct the right-hand side f such that the solution u of (6.23) is given by

$$u(x) = \frac{x_1 x_2}{\pi} \arctan\left(\frac{x_3}{\sqrt{\epsilon}} \right).$$

Note that u has a sharp internal layer as shown in Figure 6.1.

Figure 6.1 shows the exact solution and both the unstabilised surface FEM approximation and the surface IP/UP approximation of (6.23). Notice how, as in the planar case, the unstabilised surface FEM approximation exhibits global spurious oscillations whilst the surface IP/UP approximation is completely free of such oscillations. We obtain similar results for the case when we choose $w_h = w^{-l}$ in the surface IP/UP method, although L^∞ errors tend to be slightly larger for such a choice.

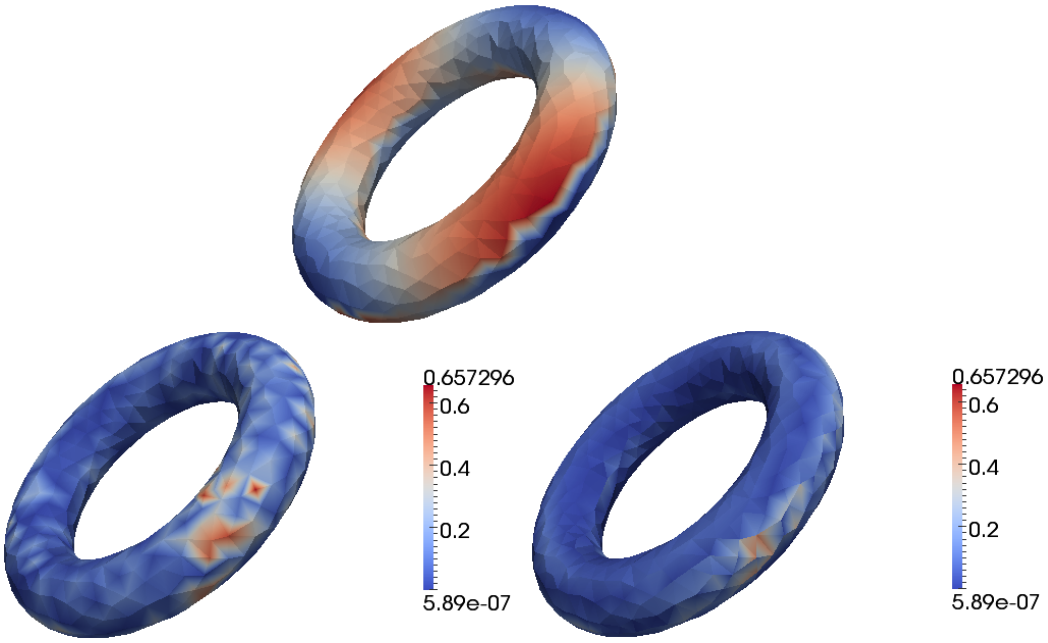

Figure 6.1: Exact solution of (6.1) (top) and pointwise errors for respectively the (unstabilised) surface FEM approximation (bottom left) and the surface IP/UP approximation (bottom right) on the torus (1410 elements).

6.4.2 Test problem on sphere

Next, we consider (6.1) on the unit sphere

$$\Gamma = \{x \in \mathbb{R}^3 \ : \ |x| = 1\}$$

with velocity field

$$w(x) = \left(-x_2\sqrt{1-x_3^2}, x_1\sqrt{1-x_3^2}, 0\right)^T.$$

Notice again that w is tangential to the sphere and divergence-free. We perform siulations for $\epsilon = 1, 10^{-3}, 10^{-6}$ and construct the right-hand side f such that the solution u of (6.23) is given by the expression given in the previous test problem. Tables 6.1, 6.2 and 6.3 show the L^2 and H^1 norm errors/EOCs outside the sharp internal layer, given by $D = \{x \in \Gamma \ : \ |x_3| > 0.3\}$, for the (unstabilised) surface FEM approximation with $\epsilon = 1, 10^{-3}, 10^{-6}$. Similarly, Tables 6.4, 6.5 and 6.6 show the resulting errors for the surface IP/UP approximation.

As expected, the results indicate that the surface IP/UP method performs

Elements	h	$L_2(D)$-error	$L_2(D)$-eoc	$H^1(D)$-error	$H^1(D)$-eoc
632	0.223929	0.00405438		0.0515491	
2528	0.112141	0.00105686	1.94	0.0262205	0.98
10112	0.0560925	0.000267298	1.98	0.0132106	0.99
40448	0.028049	6.70853e-05	1.99	0.00662013	1.00
161792	0.0140249	1.67875e-05	2.00	0.00331284	1.00

Table 6.1: Errors and convergence orders for the (unstabilised) surface FEM approximation of (6.1) on the subdomain D of the unit sphere for $\epsilon = 1$.

Elements	h	$L_2(D)$-error	$L_2(D)$-eoc	$H^1(D)$-error	$H^1(D)$-eoc
632	0.223929	0.023718		0.460813	
2528	0.112141	0.00377738	2.65	0.147209	1.65
10112	0.0560925	0.000367357	3.36	0.0358393	2.03
40448	0.028049	5.18992e-05	2.82	0.0144664	1.31
161792	0.0140249	1.25028e-05	2.05	0.00716878	1.01

Table 6.2: Errors and convergence orders for the (unstabilised) surface FEM approximation of (6.1) on the subdomain D of the unit sphere for $\epsilon = 10^{-3}$.

Elements	h	$L_2(D)$-error	$L_2(D)$-eoc	$H^1(D)$-error	$H^1(D)$-eoc
632	0.223929	0.0446193		0.865006	
2528	0.112141	0.0173573	1.36	0.6525	0.40
10112	0.0560925	0.00936689	0.89	0.727195	-0.16
40448	0.028049	0.00604055	0.63	0.93466	-0.36
161792	0.0140249	0.00356562	0.76	1.09546	-0.23
647168	0.00701247	0.00169426	1.07	1.038	0.08

Table 6.3: Errors and convergence orders for the (unstabilised) surface FEM approximation of (6.1) on the subdomain D of the unit sphere for $\epsilon = 10^{-6}$.

Elements	h	$L_2(D)$-error	$L_2(D)$-eoc	$DG(D)$-error	$DG(D)$-eoc
632	0.223929	0.00375621		0.0496429	
2528	0.112141	0.000978274	1.94	0.025178	0.98
10112	0.0560925	0.000247591	1.98	0.0126658	0.99
40448	0.028049	6.21797e-05	1.99	0.00634436	1.00
161792	0.0140249	1.55661e-05	2.00	0.00317464	1.00

Table 6.4: Errors and convergence orders for the IP/UP approximation of (6.23) on the subdomain D of the unit sphere for $\epsilon = 1$.

Elements	h	$L_2(D)$-error	$L_2(D)$-eoc	$DG(D)$-error	$DG(D)$-eoc
632	0.223929	0.00567022		0.129852	
2528	0.112141	0.00119357	2.25	0.0611303	1.09
10112	0.0560925	0.000268463	2.15	0.0285963	1.10
40448	0.028049	6.32703e-05	2.08	0.0138836	1.04
161792	0.0140249	1.53156e-05	2.05	0.00683969	1.02

Table 6.5: Errors and convergence orders for the IP/UP approximation of (6.23) on the subdomain D of the unit sphere for $\epsilon = 10^{-3}$.

Elements	h	$L_2(D)$-error	$L_2(D)$-eoc	$DG(D)$-error	$DG(D)$-eoc
632	0.223929	0.00732565		0.159321	
2528	0.112141	0.00217458	1.75	0.0889267	0.84
10112	0.0560925	0.00064893	1.75	0.0501573	0.83
40448	0.028049	0.000191337	1.76	0.0282022	0.83
161792	0.0140249	5.39969e-05	1.83	0.0153762	0.88
647168	0.00701247	1.39351e-05	1.95	0.00778131	0.98

Table 6.6: Errors and convergence orders for the IP/UP approximation of (6.23) on the subdomain D of the unit sphere for $\epsilon = 10^{-6}$.

better than the unstabilised surface FEM, namely regarding its robustness with respect to the ϵ parameter. The results for the surface IP/UP method indicate a $O(h^2)$ convergence in the $L^2(D)$-norm and $O(h)$ in the $DG(D)$-norm independently of ϵ. The unstabilised surface FEM, on the other hand, shows a much more erratic behaviour for smaller ϵ and does not appear to attain its asymptotic convergence rates within our computational domain for $\epsilon = 10^{-6}$.

Elements	h	$L_2(D)$-error	$L_2(D)$-eoc	$DG(D)$-error	$DG(D)$-eoc
632	0.223929	0.00408458		0.112754	
2528	0.112141	0.00104637	1.96	0.0570778	0.98
10112	0.0560925	0.000265394	1.98	0.0286707	0.99
40448	0.028049	6.67961e-05	1.99	0.014371	1.00
161792	0.0140249	1.67035e-05	2.00	0.00718674	1.00
647168	0.00701247	4.16052e-06	2.00	0.00359164	1.00

Table 6.7: Errors and convergence orders for the IP/UP approximation of (6.23) with $w_h = w^{-l}$ on the subdomain D of the unit sphere for $\epsilon = 10^{-6}$.

Table 6.7 show the relevant errors when using $w_h = w^{-l}$ in the surface IP/UP approximation for $\epsilon = 10^{-6}$. The errors appear to be smaller by a fact of about

0.5 compared to those shown in Table 6.6 for which we chose $w_h|_{K_h} = \Pi^0_{K_h} w^{-l}$. This can be explained by the fact that triangulations for simple surfaces such as the unit sphere can be constructed to be very "smooth" (in the sense that the relation $n_h^+ = -n_h^-$ pratically holds for each $e_h \in \mathcal{E}_h$) and that the zero order Raviart-Thomas approximation error is relatively large.

Chapter 7

Extensions

In this chapter, we will look into a variety of interesting topics which fall beyond the theory discussed in Chapters 4, 5 and 6. The first topic will numerically investigate alternative conormal choices for the surface IP method. The second topic will consider issues arising when applying the surface DG analysis considered in Chapters 4, 5 and 6 to nonconforming grids. The last topic will deal with adaptive refinement strategies for PDEs posed on complicated surfaces, following on from Chapter 5.

7.1 Alternative conormal choices

In this section, we will look at alternative choices for the conormals $\widehat{n}_h^+$ and $\widehat{n}_h^-$ which have been appearing thus far, which is a feature that appears exclusively for the case of problems posed on discrete surfaces. For the sake of simplicity, we will restrict ourselves to considering the surface IP method and piecewise linear surface approximations/ansatz functions i.e. $k = 1$, and make use of the notation specific to the piecewise linear surface approximation setting (see Chapter 5).

7.1.1 Approximation of surface conormals

Consider a generalisation of the surface IP bilinear form (4.10) which, when written out explicitely, is given by

$$\begin{aligned}\tilde{\mathcal{A}_h^{IP}}(u_h, v_h) := &\sum_{K_h \in \mathcal{T}_h} \int_{K_h} \nabla_{\Gamma_h} u_h \cdot \nabla_{\Gamma_h} v_h + u_h v_h \, \mathrm{dA_h} \\ &- \sum_{e_h \in \mathcal{E}_h} \int_{e_h} (u_h^+ - u_h^-) \frac{1}{2} (\nabla_{\Gamma_h} v_h^+ \cdot n_{e_h}^+ - \nabla_{\Gamma_h} v_h^- \cdot n_{e_h}^-) \\ &\qquad + (v_h^+ - v_h^-) \frac{1}{2} (\nabla_{\Gamma_h} u_h^+ \cdot n_{e_h}^+ - \nabla_{\Gamma_h} u_h^- \cdot n_{e_h}^-) \, \mathrm{ds}_h \\ &+ \sum_{e_h \in \mathcal{E}_h} \int_{e_h} \beta_{e_h} (u_h^+ - u_h^-)(v_h^+ - v_h^-) \, \mathrm{ds}_h \end{aligned} \tag{7.1}$$

where $n_{e_h}^+$ and $n_{e_h}^-$ are simply vectors which lie on the intersection $e_h \in \mathcal{E}_h$ of neighbouring elements K_h^+ and K_h^-. Now suppose that we want to assemble the system matrix on an element K_h and we assume that $K_h = K_h^-$ for all $e_h \subset \partial K_h$. To this end, we fix $v_h = \varphi^-$ with $\mathrm{supp}(\varphi^-) = K_h$ which leads to

$$\begin{aligned}\tilde{\mathcal{A}_h^{IP}}(u_h, \varphi^-) := &\int_{K_h} \nabla_{\Gamma_h} u_h \cdot \nabla_{\Gamma_h} \varphi^- + u_h \varphi^- \, \mathrm{dA_h} \\ &+ \sum_{e_h \subset \partial K_h} \int_{e_h} (u_h^+ - u_h^-) \frac{1}{2} \nabla_{\Gamma_h} \varphi^- \cdot n_{e_h}^- + \varphi^- \frac{1}{2} (\nabla_{\Gamma_h} u_h^+ \cdot n_{e_h}^+ - \nabla_{\Gamma_h} u_h^- \cdot n_{e_h}^-) \, \mathrm{ds}_h \\ &- \sum_{e_h \subset \partial K_h} \int_{e_h} \beta_{e_h} (u_h^+ - u_h^-) \varphi^- \, \mathrm{ds}_h. \end{aligned}$$

To assemble the block on the diagonal of the matrix we need to take $u_h = \psi^-$ with $\mathrm{supp}(\psi^-) = K_h$. For the off-diagonal block we take $u_h = \psi^+$ with $\mathrm{supp}(\psi^+) = K_h^+$ for one neighbour K_h^+ of K_h. We will then discuss different choices for $n_{e_h}^{+/-}$ which are linked to several intuitive ways of approximating respectively the surface conormals $n^{+/-}$ of e_h^l. We use one choice for $n_{e_h}^+$ in both cases. To cover all of the choices we want to consider, it is necessary to use different choices for $n_{e_h}^-$, i.e., the vector belonging to the element K_h on which we are assembling the matrix. For the diagonal block we will denote our choice for this vector with n_D^- and use the original notation $n_{e_h}^-$ for the choice used to assemble the off-diagonal block. Note that $n_D^- = n_h^-$ for all of the choices discussed below except for Choice 3.

Now consider $u_h = \psi^-$ with $\operatorname{supp}(\psi^-) = K_h$ in (7.1) using n_D^- instead of $n_{e_h}^-$:

$$\tilde{\mathcal{A}}_h^{IP}(\psi^-, \varphi^-) := \int_{K_h} \nabla_{\Gamma_h}\psi^- \cdot \nabla_{\Gamma_h}\varphi^- + \psi^-\varphi^- \, \mathrm{dA_h}$$
$$- \sum_{e_h \subset \partial K_h} \int_{e_h} \frac{1}{2}\psi^- \nabla_{\Gamma_h}\varphi^- \cdot n_D^- + \varphi^- \frac{1}{2}\nabla_{\Gamma_h}\psi^- \cdot n_D^- - \beta_{e_h}\psi^-\varphi^- \, \mathrm{ds}_h.$$

Next we take $u_h = \psi^+$ with $\operatorname{supp}(\psi^+) = K_h^+$ for one neighbour K_h^+ of K_h, we now have

$$\tilde{\mathcal{A}}_h^{IP}(\psi^+, \varphi^-) := \sum_{e_h \subset \partial K_h} \int_{e_h} \frac{1}{2}\psi^+ \nabla_{\Gamma_h}\varphi^- \cdot n_{e_h}^- \, \mathrm{ds}_h + \varphi^- \frac{1}{2}\nabla_{\Gamma_h}\psi^+ \cdot n_{e_h}^+ - \beta_{e_h}\psi^+\varphi^- \, \mathrm{ds}_h.$$

We can now prescribe choices for the vectors n_D^-, $n_{e_h}^-$, $n_{e_h}^+$ and will later investigate the behaviour of the numerical scheme (7.1) for different choices of these three vectors.

Choice 1

$$n_D^- = n_h^- \quad , \quad n_{e_h}^- = n_h^- \quad , \quad n_{e_h}^+ = -n_h^-.$$

Such a choice corresponds to using the IP method in a planar setting, for which $n_h^+ = -n_h^-$, and is the simplest scheme to implement.

Choice 2

$$n_D^- = n_h^- \quad , \quad n_{e_h}^- = n_h^- \quad , \quad n_{e_h}^+ = n_h^+.$$

This choice yields the surface IP method (4.10) whose error analysis has been discussed in detail in Chapters 4.

Choice 3

$$n_D^- = \frac{\frac{1}{2}(n_h^- - n_h^+)}{|\frac{1}{2}(n_h^- - n_h^+)|} \quad , \quad n_{e_h}^- = \frac{\frac{1}{2}(n_h^- - n_h^+)}{|\frac{1}{2}(n_h^- - n_h^+)|} \quad , \quad n_{e_h}^+ = \frac{\frac{1}{2}(n_h^+ - n_h^-)}{|\frac{1}{2}(n_h^+ - n_h^-)|}.$$

This choice corresponds to prescribing the vectors to be the average of the two conormals and yields additional symmetry in the resulting matrix due to the fact that the vectors are now independent of the element on which they are computed.

Choice 4

$$n_D^- = n_h^- \quad , \quad n_{e_h}^- = -n_h^+ \quad , \quad n_{e_h}^+ = -n_h^-.$$

This particular choice corresponds to using the formulation of the planar IP method (3.15) on the discrete surface Γ_h, but with a *modified* penalty term that does not

depend on the conormals i.e.

$$\tilde{\mathcal{A}}_h^{IP}(u_h, v_h) = \sum_{K_h \in \mathcal{T}_h} \int_{K_h} \nabla_{\Gamma_h} u_h \cdot \nabla_{\Gamma_h} v_h + u_h v_h \, \mathrm{dA_h}$$
$$- \sum_{e_h \subset \partial K_h} \int_{e_h} (u_h^+ n_h^+ + u_h^- n_h^-) \cdot \frac{1}{2}(\nabla_{\Gamma_h} v_h^+ + \nabla_{\Gamma_h} v_h^-)$$
$$+ \frac{1}{2}(\nabla_{\Gamma_h} u_h^+ + \nabla_{\Gamma_h} u_h^-) \cdot (v_h^+ n_h^+ + v_h^- n_h^-) \, \mathrm{ds}_h$$
$$+ \sum_{e_h \subset \partial K_h} \int_{e_h} \beta_{e_h} (u_h^+ - u_h^-)(v_h^+ - v_h^-) \, \mathrm{ds}_h \quad \text{(modified penalty term)}.$$

We summarise the choices in Table 7.1.

Choice	n_D^-	$n_{e_h}^-$	$n_{e_h}^+$	Description
1	n_h^-	n_h^-	$-n_h^-$	Planar (non-sym)
2	n_h^-	n_h^-	n_h^+	Analysis (sym pos-def)
3	$\frac{\frac{1}{2}(n_h^- - n_h^+)}{\lvert\frac{1}{2}(n_h^- - n_h^+)\rvert}$	$\frac{\frac{1}{2}(n_h^- - n_h^+)}{\lvert\frac{1}{2}(n_h^- - n_h^+)\rvert}$	$\frac{\frac{1}{2}(n_h^+ - n_h^-)}{\lvert\frac{1}{2}(n_h^+ - n_h^-)\rvert}$	Average (sym pos-def)
4	n_h^-	$-n_h^+$	$-n_h^-$	Arnold et al. [2002] (sym pos-def)

Table 7.1: Choices of n_D^-, $n_{e_h}^+$ and $n_{e_h}^-$, description of the numerical schemes they respectively lead to and properties of resulting matrix.

We also consider the planar IP method (3.15) on the discrete surface Γ_h with its true penalty term, given by

$$\sum_{e_h \subset \partial K_h} \int_{e_h} \beta_{e_h} (u_h^+ n_h^+ + u_h^- n_h^-) \cdot (v_h^+ n_h^+ + v_h^- n_h^-) \, \mathrm{ds}_h \quad \text{(true penalty term)}.$$

Choosing $v_h = \varphi^-$ and $u_h = \psi^-$ as before yields

$$\sum_{e_h \subset \partial K_h} \int_{e_h} \beta_{e_h} \psi^- \varphi^- \, \mathrm{ds}_h.$$

For $u_h = \psi^+$ we now have,

$$\sum_{e_h \subset \partial K_h} \int_{e_h} \beta_{e_h} \psi^+ \varphi^- (n_h^+ \cdot n_h^-) \, \mathrm{ds}_h.$$

The matrices arising from Choices 2-4 are symmetric positive definite, so the Conjugate Gradient (CG) method is particularly well suited for such matrix problems. Choice 1 however yields a non-symmetric matrix, for which we use the Biconjugate Gradient Stabilized (BICGSTAB) method. All of these solvers make

use of the algebraic multigrid algorithm (AMG) preconditioner coupled with the incomplete-LU factorisation preconditioner to speed up the solvers. Information on the implementation of these solvers and preconditioners in DUNE can be found in Blatt and Bastian [2007] and on their parallelisation in Blatt and Bastian [2008].

7.1.2 Conormal choices for sphere

We consider the DG approximation of (4.59) for different choices of n_D^-, $n_{e_h}^+$ and $n_{e_h}^-$. Figure 7.1(a,b) shows respectively the ratios of the L^2 and DG errors $\frac{\text{Err}_i}{\text{Err}_2}$ with $i = 1, 3, 4$ where Err_i denotes the error in the corresponding norm when using Choice i. For this simple test problem, the different choices do not appear to give significantly different results.

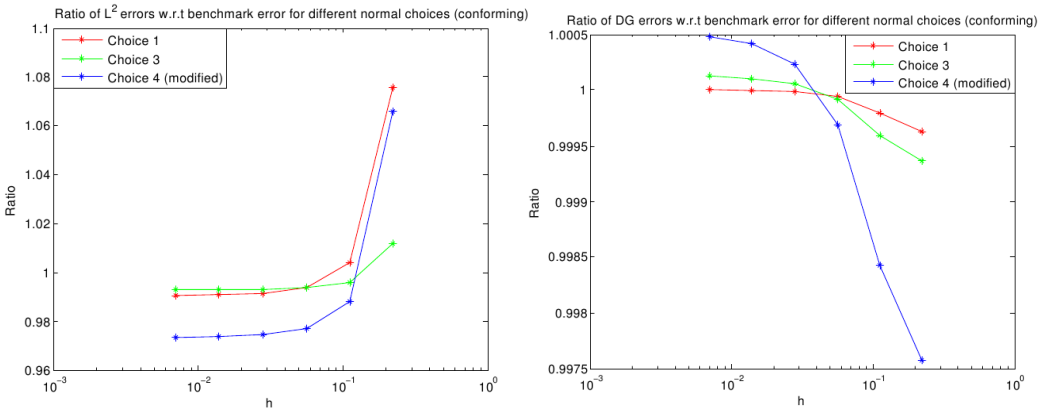

(a) (b)

Figure 7.1: Ratio of respectively L^2 and DG errors for (4.59) on the unit sphere with respect to the analysis error (Choice 2) for Choices 1, 3 and 4.

A few remarks on Choice 4 with the *true* penalty term which, as mentioned before, would correspond to the planar IP method (3.15) on Γ_h: interestingly, the scheme fails to converge for such a choice. The convergence of the numerical scheme appears to be particularly sensitive to small perturbations in the off-diagonal entries of the resulting matrix, namely the ones caused by the product of the conormals $n_h^+ \cdot n_h^-$ when using the true penalty term for Choice 4. Such a sensitivity seems counter-intuitive considering that $n_h^+ \cdot n_h^- = -1 + \frac{1}{2}|n_h^+ + n_h^-|^2 \to -1$ as $h \to 0$, especially considering that we did not observe convergence even for very small h. Note that, in the flat case, $n_h^+ \cdot n_h^-$ is equal to -1. We tried to reproduce this problem in the flat case, taking two different values for the penalty parameter on e_h depending on whether we are assembling the diagonal or the off-diagonal block. A difference as small as 10^{-5} leads to similar problems. We do not have an explanation

for such a behaviour (and we do not exclude the possibility that this could be an implementation issue rather than a mathematical one), and so further investigation of this sensitivity would be useful. Table 7.2 shows the L^2 and DG errors/EOCs when using Choice 4 with the true penalty term, which shows the loss of convergence discussed above. In addition, we show in Table 7.3 that the conormals $n_h^{+/-}$ behave as expected for this test problem.

Elements	h	L_2-error	L_2-eoc	DG-error	DG-eoc
632	0.223929	0.594031		6.1414	
2528	0.112141	0.480233	0.30	3.92988	0.64
10112	0.0560925	0.451843	0.09	2.97823	0.40
40448	0.028049	0.444274	0.02	2.66527	0.16
161792	0.0140249	0.442029	0.01	2.57612	0.05
647168	0.00701247	0.441281	0.00	2.55134	0.01

Table 7.2: Errors and convergence orders for (4.59) on the unit sphere for Choice 4 with *true* penalty term.

Elements	h	$\|1 + n_h^+ \cdot n_h^-\|_{L^\infty(\mathcal{E}_h)}$	eoc	$\|n_h^+ + n_h^-\|_{L^\infty(\mathcal{E}_h)}$	eoc
632	0.223929	0.025248		0.224715	
2528	0.112141	0.00721	1.81	0.120084	0.90
10112	0.0560925	0.001823	1.98	0.0603874	0.99
40448	0.028049	0.000457	1.99	0.0302372	1.00
161792	0.0140249	0.000114	2.00	0.0151241	1.00
647168	0.00701247	0.000029	1.98	0.00756271	1.00

Table 7.3: Conormal estimates and convergence orders on the unit sphere.

7.1.3 Conormal choices for Dziuk surface

We again consider the DG approximation of (4.59) for different choices of n_D^-, $n_{e_h}^+$ and $n_{e_h}^-$. Figure 7.2(a,b) show respectively the ratios of the L^2 and DG errors for the Dziuk surface test problem. Choices 2 (analysis) and 3 (average) appear to give the best results in both the L^2 and DG norms. In particular, the additional symmetry induced by using Choice 3 which we mentioned previously makes it the preferable choice. Since Choice 4 with or without the true penalty term appears to be consistently less accurate than the other choices, we omit this choice in our next test problem.

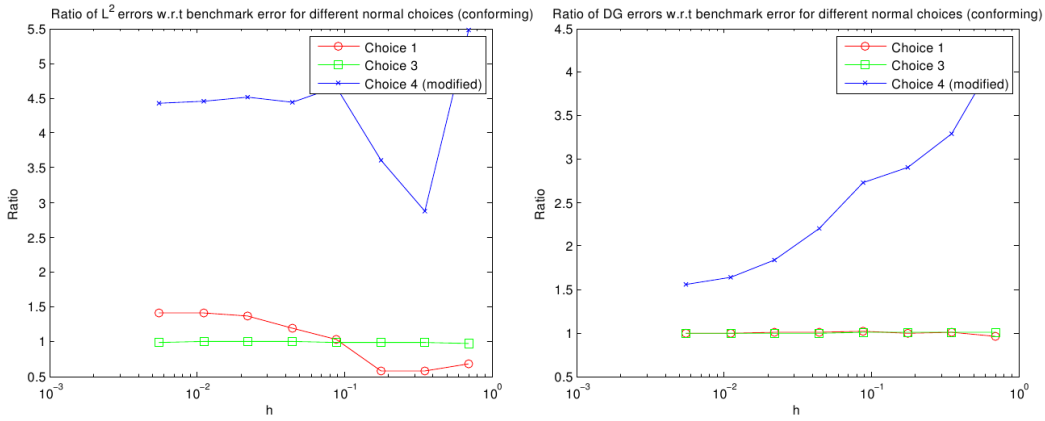

(a) (b)

Figure 7.2: Ratio of respectively L^2 and DG errors for (4.59) on the Dziuk surface with respect to the analysis error (Choice 2) for Choices 1, 3 and 4.

7.1.4 Conormal choices for Enzensberger-Stern surface

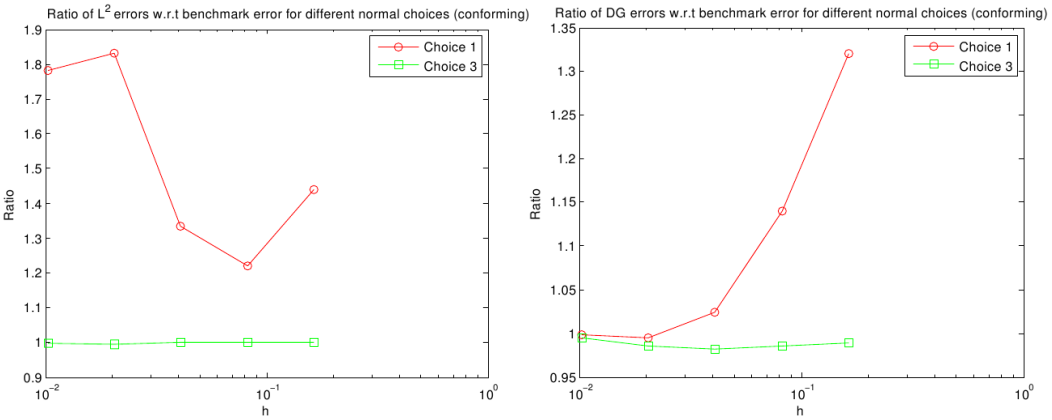

(a) (b)

Figure 7.3: Ratio of respectively L^2 and DG errors for (4.59) on the Enzensberger-Stern surface with respect to the analysis error (Choice 2) for Choices 1 and 3.

The results of our final test problem are shown in Figure 7.3(a,b), which show respectively the ratios of the L^2 and DG errors for the Enzensberger-Stern surface test problem. These results confirm that Choices 2 and 3 are the preferable ones to use for DG schemes on surfaces.

7.2 Nonconforming grids

The analysis discussed in Chapters 4, 5 and 6 would be a bit different if we were to replicate it on nonconforming grids. In such a situation, newly created (hanging) nodes created during the refinement process would get lifted to the smooth surface Γ, as shown in Figure 7.4. An interesting point to note is that neighbouring elements may not necessarily share a common edge due to this. Furthermore, if we denote the lift of the edge e_h shown in Figure 7.4 to be e_h^l then it is not necessarily the case that the lift of $\tilde{e}_h$ coincides with that of e_h.

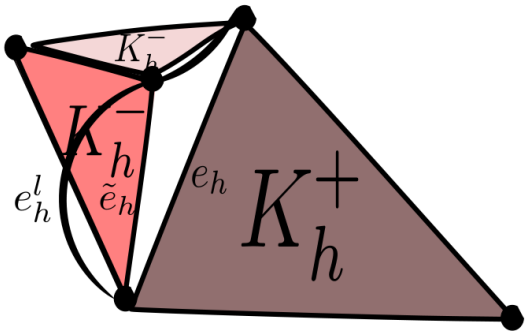

Figure 7.4: Instance of a nonconforming grid resulting from the discretisation of a problem posed on a surface.

In order to deal with these issues in the analysis, one would first have to redefine the surface DG bilinear forms in such a way that it does not involve terms that are defined on the skeleton $\mathcal{E}_h$ of the grid, as such terms no longer make sense in this setting. This is easily done by replacing any terms of the form $\sum_{e_h \in \mathcal{E}_h} \int_{e_h} \dots$ by $\frac{1}{2} \sum_{K_h \in \mathcal{T}_h} \int_{\partial K_h} \dots$.

Secondly, one could perform the error analysis by considering a conforming triangulation $\mathcal{T}_h^c$ of $\mathcal{T}_h$ and posing a discrete solution u_h^c on $\mathcal{T}_h^c$. The conforming triangulation $\mathcal{T}_h^c$ can be constructed by bisecting the element K_h^+ shown in Figure 7.4 and lifting the resulting hanging node onto the surface (which coincides with the hanging node of the neighbouring element). The standard error analysis can then be applied for u_h^c, but in addition one would have to derive and evaluate a new error functional $\tilde{E}_h$, which stems from the fact that u_h^c does not satisfy the original problem.

7.2.1 Numerical tests

Although our analysis was restricted to conforming grids, our numerical tests suggest that the estimates of Theorem 4.4.1 also hold for nonconforming grids in the piecewise linear setting, as shown in Tables 7.4, 7.5 and 7.6 for respectively the unit sphere, the Dziuk surface and the Enzensberger-Stern surface. The resulting DG approximations are shown in respectively Figures 7.5, 7.7 and 7.9.

Elements	h	L_2-error	L_2-eoc	DG-error	DG-eoc
1580	0.112141	0.146369		4.24728	
6320	0.0560925	0.0402358	1.86	2.11183	1.01
25280	0.028049	0.0104518	1.94	1.04316	1.02
101120	0.0140249	0.0026346	1.99	0.516816	1.01
404480	0.00701247	0.000658561	2.00	0.25718	1.01

Table 7.4: Errors and convergence orders for (4.59) on the unit sphere for nonconforming grids.

Elements	h	L_2-error	L_2-eoc	DG-error	DG-eoc
230	0.353599	0.21889		0.777436	
920	0.176993	0.0530078	2.05	0.413817	0.91
3680	0.0885231	0.0281113	0.92	0.223119	0.89
14720	0.0442651	0.00442299	2.67	0.111518	1.00
58880	0.022133	0.00104207	2.08	0.0562128	0.99
235520	0.0110666	0.00026444	1.99	0.0281247	1.00
942080	0.00553329	6.60383e-05	2.00	0.0140544	1.00

Table 7.5: Errors and convergence orders for (4.59) on the Dziuk surface for nonconforming grids.

Elements	h	L_2-error	L_2-eoc	DG-error	DG-eoc
5895	0.0817973	0.43854		0.931253	
23580	0.040885	0.104653	2.06	0.308369	1.59
94320	0.0204411	0.0161014	2.70	0.11975	1.36
377280	0.0102204	0.00109894	3.87	0.0552095	1.12

Table 7.6: Errors and convergence orders for (4.59) on the Enzensberger-Stern surface for nonconforming grids.

In addition, and in a similar fashion to what was done in Section 7.1, we numerically investigate alternative conormal choices for nonconforming grids. Re-

sults are shown in Figures 7.6(a,b), 7.8(a,b) and 7.10(a,b) for respectively the unit sphere, the Dziuk surface and the Enzensberger-Stern surface.

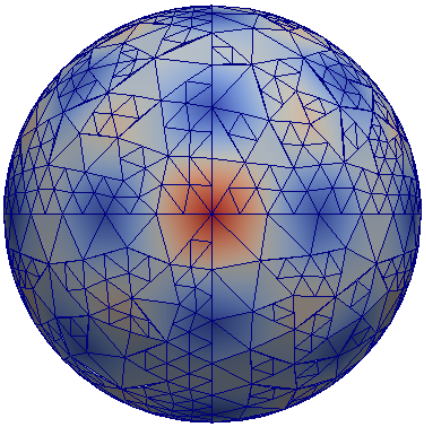

(a)

Figure 7.5: DG approximation of (4.59) on the unit sphere using a nonconforming grid.

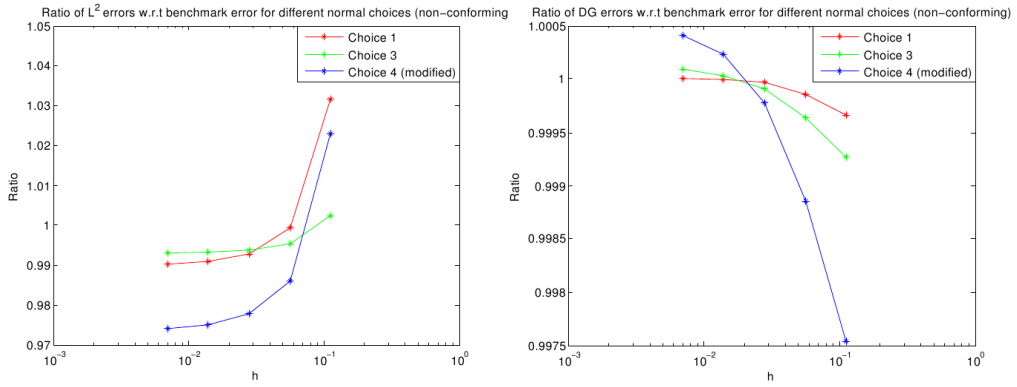

(a) (b)

Figure 7.6: Ratio of respectively L^2 and DG errors for (4.59) on the unit sphere with respect to the analysis error (Choice 2) for Choices 1, 3 and 4 on nonconforming grids.

7.3 Adaptive refinement on surfaces

In this section, we look at the benefits of using adaptive refinement for PDEs posed on surfaces, following on from the surface DG a posteriori error analysis discussed in Chapter 5, and present our own adaptive strategy based on the geometric residual of the estimator.

Despite the geometric residual being asymptotically of higher order, it is

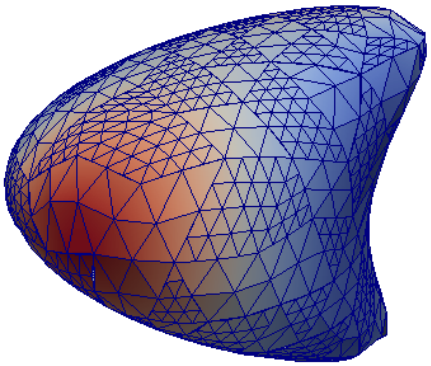

(a)

Figure 7.7: DG approximation of (4.59) on the Dziuk surface using a nonconforming grid.

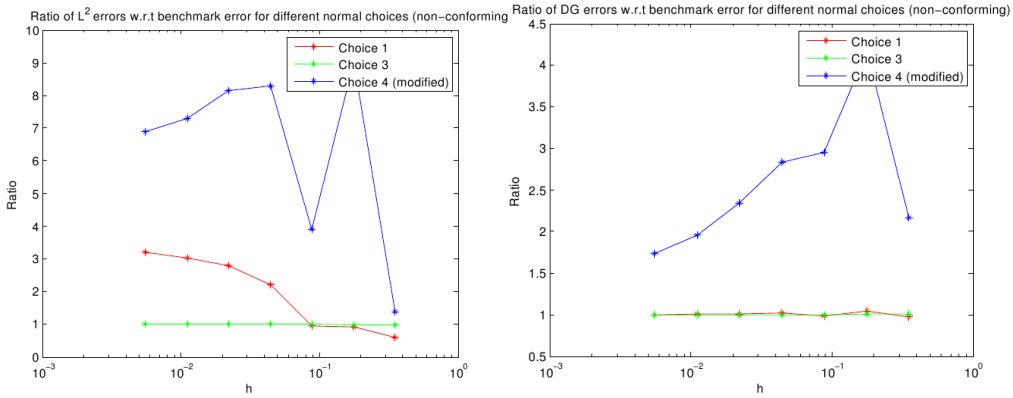

(a) (b)

Figure 7.8: Ratio of respectively L^2 and DG errors for (4.59) on the Dziuk surface with respect to the analysis error (Choice 2) for Choices 1, 3 and 4 on nonconforming grids.

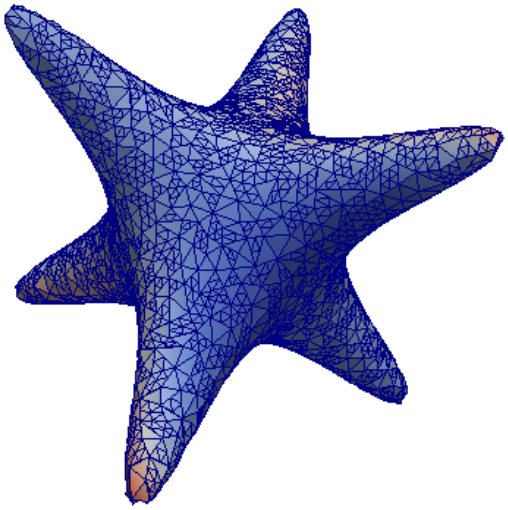

(a)

Figure 7.9: DG approximation of (4.59) on the Enzensberger-Stern surface using a nonconforming grid.

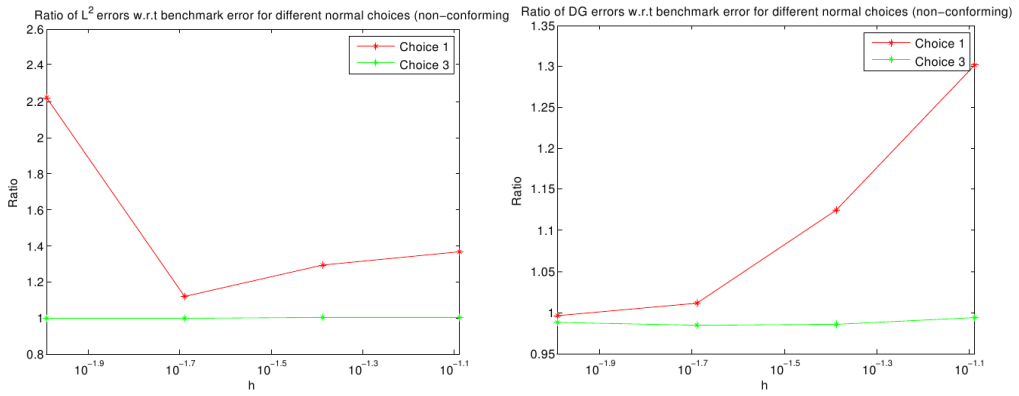

(a) (b)

Figure 7.10: Ratio of respectively L^2 and DG errors for (4.59) on the Enzensberger-Stern surface with respect to the analysis error (Choice 2) for Choices 1 and 3 on nonconforming grids.

often the case that initial grids poorly resolve areas of high curvature. This is in fact the case with our initial grid of the Dziuk surface as can be seen in Figure 5.1(b). Hence, in practice, the geometric residual can be very large for coarser grids and even remain dominant after multiple global refinements. What we now aim to show is that adaptive refinement strategies based on our estimator are not only useful for problems with sharp changes in the solution, but are also a way of rapidly decreasing the geometric residual for grids with poorly resolved high curvature areas compared to global refinement.

7.3.1 Adaptive refinement on Dziuk surface

Figure 7.11(a) shows the plots of the estimator and the true error when performing global and adaptive refinement against the number of degrees of freedom for the Dziuk surface. The adaptive refinement strategy used here is the so-called fixed fraction strategy, detailed for example in Section 3.2 of Rannacher and Suttmeier [1999], with rate $\theta = 0.3$. We give a schematic description of the adaptive refinement below.

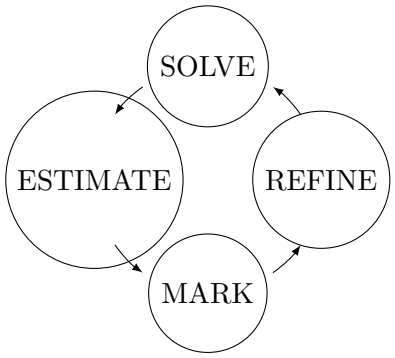

Start with an intitial grid $\mathcal{T}_h^0$. Then for $n \geq 0$:

- SOLVE: compute a finite element approximation u_h of u.
- ESTIMATE: use u_h to compute local indicators $\{\eta_{K_h}\}_{K_h \in \mathcal{T}_h}$. If $\sum_{K_h \in \mathcal{T}_h} \eta_{K_h} <$ TOL, break.
- MARK: depending on value of local indicator η_{K_h}, mark corresponding element K_h for refinement or not.
- REFINE: Refine marked elements $K_h \in \mathcal{T}_h^n$ to construct new grid $\mathcal{T}_h^{n+1}$.

Notice how, in Figure 7.11(a), the estimator and the true error decrease at a faster rate for coarser grids when using adaptive refinement, which is due to it rapidly reducing the initially dominant geometric residual. In addition, our estimator appears to attain a given error with approximately a third of the number of degrees of freedom required by global refinement. Figure 7.11(b) shows an adaptively refined grid for the Dziuk surface colour coded by element size. Notice how our estimator captures both the region with exponential peaks (right) and the regions with high

curvature (left).

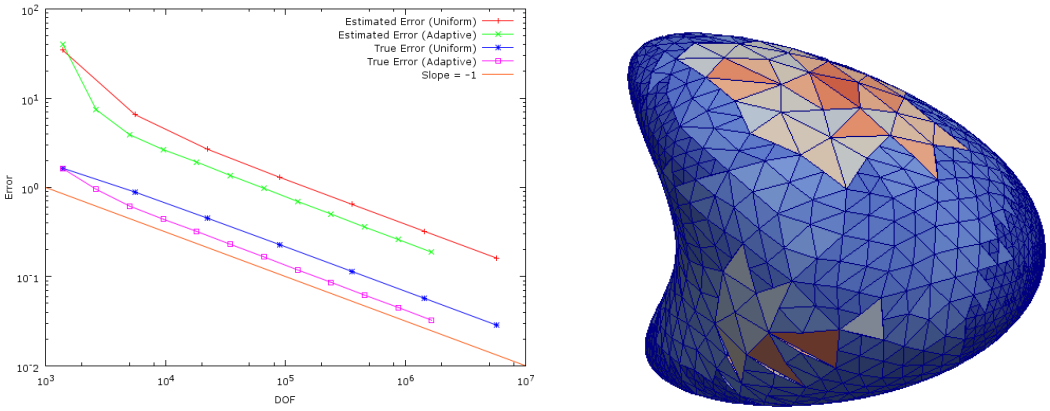

(a) (b)

Figure 7.11: Estimated/true errors for uniform and adaptive refinement (left) and an adaptively refined
grid (right) for the Dziuk surface colour coded by element size.

7.3.2 Adaptive refinement on Enzensberger-Stern surface

This is a more extreme example of a surface with high curvature areas whose initial grid poorly resolves them, as shown in Figure 5.3(a). In fact, it is worth noting that as $c \to 0$ the width δ_U of the open subset U required for the one-to-one property of (2.1) to hold locally tends to zero.

Figure 7.12(a) shows the plots of the estimator and the true error when performing global and adaptive refinement against the number of degrees of freedom for the Enzensberger-Stern surface. The estimator decreases at a much faster rate for coarser grids when using adaptive refinement by rapidly reducing the geometric residual. Figure 7.12(b) shows the efficiency of the estimator when performing respectively uniform and adaptive refinement, the latter converging significantly faster to an efficiency index of 5.9. Figure 7.12(c) shows an adaptively refined grid for the Enzensberger-Stern surface colour coded by element size. Again, our estimator manages to capture the regions of high curvature which were the cause of the dominant geometric residual occuring for global refinement.

Geometric adaptive refinement

We also consider an adaptive refinement strategy based on the geometric residual, as numerics have suggested that it is the dominant contribution for grids that poorly resolve the underlying surface. This strategy only computes the DG approximation

u_h if the geometric residual statisfies

$$\frac{\left(\sum_{K_h\in\mathcal{T}_h}\mathcal{G}^2_{K_h}\right)^{1/2}}{\left(\sum_{K_h\in\mathcal{T}_h}\mathcal{R}^2_{K_h}+\mathcal{R}^2_{DG_{K_h}}+\mathcal{G}^2_{K_h}+\mathcal{G}^2_{DG_{K_h}}\right)^{1/2}}\leq tol_{\text{geometric}}$$

where $tol_{\text{geometric}}\in(0,1)$ is some user-defined tolerance which prescribes how small the geometric residual should be relative to the full estimator. Otherwise, we recompute the estimator and adaptively refine the grid until the criteria is satisfied. We give a schematic description of the new geometric adaptive refinement below.

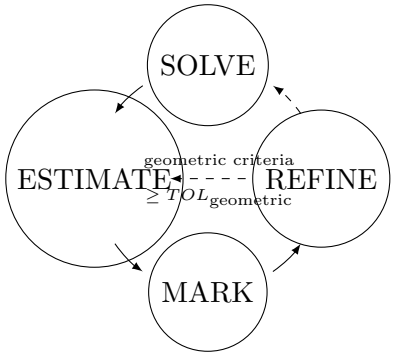

Start with an intitial grid $\mathcal{T}_h^0$.

- SOLVE: compute a finite element approximation u_h of u.

Then for $n\geq 0$:

- ESTIMATE: use u_h to compute local indicators $\{\eta_{K_h}\}_{K_h\in\mathcal{T}_h}$. If $\sum_{K_h\in\mathcal{T}_h}\eta_{K_h}<\text{TOL}$, break.
- MARK: depending on value of local indicator η_{K_h}, mark corresponding element K_h for refinement or not.
- REFINE: Refine marked elements $K_h\in\mathcal{T}_h^n$ to construct new grid $\mathcal{T}_h^{n+1}$.
- While

$$\frac{\sum_{K_h\in\mathcal{T}_h}\mathcal{G}_{K_h}}{\sum_{K_h\in\mathcal{T}_h}\eta_{K_h}}\geq TOL_{\text{geometric}}$$

go to ESTIMATE else SOLVE.

In Figures 7.12(a) and 7.12(b) we also show respectively the plots of the estimator/true error and the efficiency index when performing our geometric adaptive refinement strategy. Highlighted are the iterations at which the DG approximation is recomputed; the true error is only plotted for those iterations. Our estimator reaches a similar error as the standard adaptive strategy as we increase the number

of degrees of freedom but requires far less recomputations of the DG approximation (11 for the standard adaptive strategy compared to 5 for the geometric adaptive strategy), hence significantly more computationally efficient. It is also worth mentioning that although we do not have a rigorous proof that the stopping criteria for our geometric adaptive refinement strategy would be satisfied, it appears that this is in fact the case for all of our test problems, with the number of iterations required to satisfy the stopping criteria decreasing as expected. Note also that after a number of refinement steps the curves for both refinement strategies seem to collapse but that we are in fact reaching the same error with slightly fewer elements in addition to requiring far fewer computations of u_h.

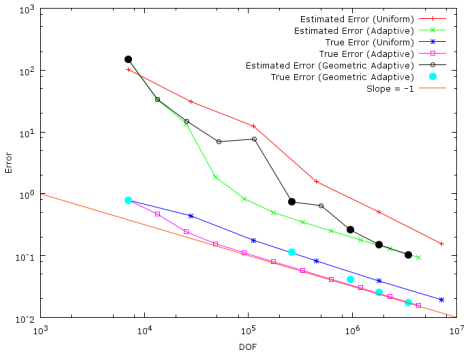

(a)

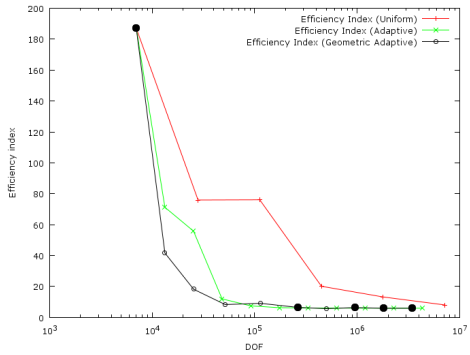

(b)

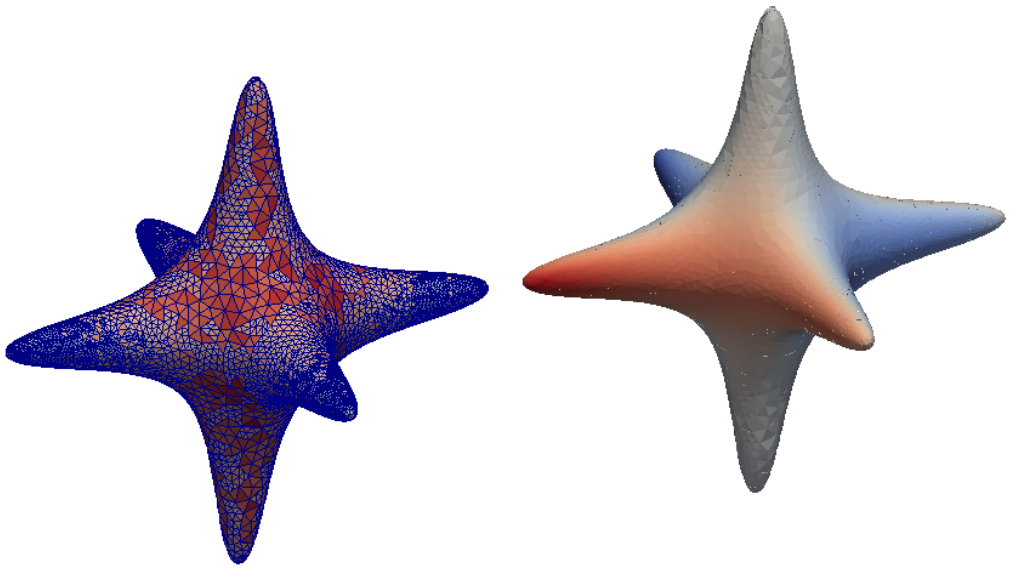

(c)

Figure 7.12: Estimated/true errors (top right) and efficiency indices (top left) for uniform and adaptive refinement. Results for both standard and geometric adaptation strategies are shown. The solution and a colour coding of the adaptive grid are shown in the bottom row.

Chapter 8

Conclusions and Further Research

In this PhD thesis, we have been the first to extend the discontinuous Galerkin framework to surface partial differential equations and investigate issues arising when doing so. This was done by deriving both (optimal) a priori and (reliable/efficient) a posteriori error estimates for surface DG approximations of elliptic PDEs posed on compact smooth oriented surfaces in $\mathbb{R}^3$ without boundary. We verified all of the estimates numerically for a number of complicated test problems, a number of which went beyond the results covered by the theory.

One of the key aspects in enabling a natural treatment of DG methods on surfaces was to follow the original formulation of DG methods, given in say Arnold [1982], rather than the modern approach considered in Arnold et al. [2002]. Using an original formulation than the modern one allows us to derive boundedness and stability bounds which are independent of h, as detailed in Remark 4.3.6.

In order to obtain a priori error estimates for the resulting surface DG methods, one requires additional geometric estimates compared to surface FEM to estimate the error functional arising from the variational crime caused by approximating the surface. These involve estimating the change of measure between discrete and lifted edges $\delta_{\widehat{e}_h}$ as well as the (pointwise) difference between surface conormals and *projected* discrete conormals $n - \mathbf{P}\widehat{n}_h^l$. Introducing projected discrete conormals $\mathbf{P}\widehat{n}_h^l$ in the analysis rather than simply discrete conormals $\widehat{n}_h^l$ is crucial for obtaining optimal error estimates.

Our extension of the surface DG analysis to advection-diffusion problems on surfaces required the introduction of a discrete velocity field w_h which satisfied a

number of assumptions. In particular, we required that $w_h \cdot \widehat{n}_h^+ = -w_h \widehat{n}_h^-$ in order to derive h-independent positive-definiteness of the matrix resulting from the numerical scheme. The introduction of such a discrete velocity field was justified by considering a situation where one may not necessarily obtain h-independent positive-definiteness by simply lifting the original velocity downwards. We then explicitely constructed w_h by taking it to be a surface Raviart-Thomas interpolant of w^{-l}. Such a choice (which is by no means the only possible one) naturally satisfies the assumption required for h-independent positive-definiteness and allows us to derive optimal error estimates for the resulting scheme in the DG norm.

There are a number of areas one may choose to pursue further research in. A particularly interesting one would be to extend the a posteriori error analysis discussed in Chapter 5 to surface DG methods other than the surface IP method, nonconforming grids and $hp-$adaptive refinement, where both the polynomial order of the approximation and that of the surface approximation can differ across elements. As discussed in Chapter 1, one of the advantages of DG methods lies in their ability to deal with adaptive refinement so this is a natural path to consider.

Having detailed the a priori analysis of surface DG methods for a simple advection-diffusion problem, it would also be natural to rigorously look into both a priori and a posteriori analysis of advection dominated problems of the form (6.23) and look into how the small ϵ parameter affects the estimates. Extending the analysis for the purely hyperbolic case ($\epsilon = 0$) is another interesting path to take: preliminary results have suggested that one obtains suboptimal estimates for the error functional arising from the surface approximation, with a convergence order of h instead of h^2 in the piecewise linear setting, and thus suboptimal estimates for the scheme. This appears to be caused by the application of inverse estimates, required to eliminate gradient terms, which results in a loss of a full h power.

The presence of a reaction term in our advection-diffusion equation plays a crucial part in getting the analysis to follows through: it is used for both the stability of the scheme and in the convergence proof when we assumed that the mass perturbation coefficient $\gamma_h \equiv 0$ for h small enough. Given that in many applications no such term is present, it would be natural to extend the analysis for the case when no reaction term is present.

We hope that much of the work discussed in this thesis (and in the publications that have resulted from it) will provide a stepping stone for further research in this exciting new field.

Appendix A

Geometric Estimates

Lemma A.0.1. *Let Γ be a compact smooth and oriented surface in $\mathbb{R}^3$ and let Γ_h^k be its Lagrange interpolant of degree k. Furthermore, we denote by $n^{+/-}$ the unit (surface) conormals to respectively $\widehat{e}_h^{l+/-}$. Then, omitting the surface lift symbols, we have that*

$$\|d\|_{L^\infty(\Gamma_h^k)} \lesssim h^{k+1}, \tag{A.1a}$$

$$\|1-\delta_{hk}\|_{L^\infty(\Gamma_h^k)} \lesssim h^{k+1}, \tag{A.1b}$$

$$\|\nu-\widehat{\nu}_h\|_{L^\infty(\Gamma_h^k)} \lesssim h^{k}, \tag{A.1c}$$

$$\|\mathbf{P}-\mathbf{R}_{hk}\|_{L^\infty(\Gamma_h^k)} \lesssim h^{k+1}, \tag{A.1d}$$

$$\|1-\delta_{\widehat{e}_h}\|_{L^\infty(\widehat{\mathcal{E}}_h)} \lesssim h^{k+1}, \tag{A.1e}$$

$$\sup_{\widehat{K}\in\widehat{\mathcal{T}}_h} \|\mathbf{P}-\mathbf{R}_{\widehat{e}_h}\|_{L^\infty(\partial\widehat{K}_h)} \lesssim h^{k+1}, \tag{A.1f}$$

$$\|n^{+/-}-\mathbf{P}\widehat{n}_h^{+/-}\|_{L^\infty(\widehat{\mathcal{E}}_h)} \lesssim h^{k+1}, \tag{A.1g}$$

for sufficiently small h, where $\mathbf{R}_{\widehat{e}_h}=\delta_{\widehat{e}_h}^{-1}\mathbf{P}(\mathbf{I}-d\mathbf{H})\mathbf{P}_{hk}(\mathbf{I}-d\mathbf{H})$.

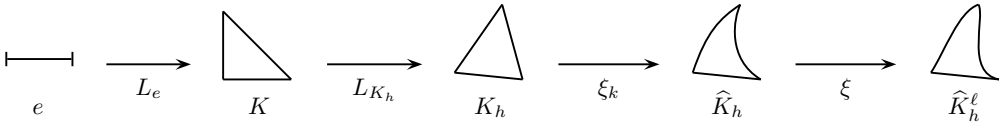

Figure A.1: Diagram of mappings.

Bibliography

G. Acosta, T. Apel, R. Durán, and A. Lombardi. Error estimates for Raviart-Thomas interpolation of any order on anisotropic tetrahedra. *Mathematics of Computation*, 80(273):141–163, 2011.

M. Ainsworth and J.T. Oden. *A posteriori error estimation in finite element analysis*, volume 37. John Wiley & Sons, 2011.

D.P. Amarasinghe, A. Aylwin, P. Madhavan, and C. Pettitt. Biomembranes report. *arXiv preprint arXiv:1212.1641*, 2012.

P. Antonietti and P. Houston. A class of domain decomposition preconditioners for h-discontinuous Galerkin finite element methods. *J Sci Comput*, 2011.

P. Antonietti, A. Dedner, P. Madhavan, S. Stangalino, B. Stinner, and M. Verani. High order discontinuous Galerkin methods on surfaces. *arXiv preprint arXiv:1402.3428*, 2014.

D.N. Arnold. An interior penalty finite element method with discontinuous elements. *SIAM Journal on Numerical Analysis*, pages 742–760, 1982.

D.N. Arnold, F. Brezzi, B. Cockburn, and L.D. Marini. Unified analysis of discontinuous Galerkin methods for elliptic problems. *SIAM journal on numerical analysis*, pages 1749–1779, 2002.

T. Aubin. *Nonlinear analysis on manifolds, Monge-Ampere equations*, volume 252. Springer, 1982.

G.A. Baker. Finite element methods for elliptic equations using nonconforming elements. *Mathematics of Computation*, 31(137):45–59, 1977.

F. Bassi and S. Rebay. A high-order accurate discontinuous finite element method for the numerical solution of the compressible Navier–Stokes equations. *Journal of computational physics*, 131(2):267–279, 1997.

F. Bassi, S. Rebay, G. Mariotti, S. Pedinotti, and M. Savini. A high-order accurate discontinuous finite element method for inviscid and viscous turbomachinery flows. In *Proceedings of 2nd European Conference on Turbomachinery, Fluid Dynamics and Thermodynamics*, pages 99–108. Technologisch Instituut, Antwerpen, Belgium, 1997.

P. Bastian, M. Blatt, A. Dedner, C. Engwer, R. Klöfkorn, R. Kornhuber, M. Ohlberger, and O. Sander. A Generic Grid Interface for Parallel and Adaptive Scientific Computing. Part II: Implementation and Tests in DUNE. *Computing*, 82(2–3):121–138, 2008a. doi: http://www.springerlink.com/content/gn177r643q2168g7/.

P. Bastian, M. Blatt, A. Dedner, C. Engwer, R. Klöfkorn, M. Ohlberger, and O. Sander. A Generic Grid Interface for Parallel and Adaptive Scientific Computing. Part I: Abstract Framework. *Computing*, 82(2–3):103–119, 2008b. doi: http://www.springerlink.com/content/4v77662363u41534/.

P. Bastian, M. Blatt, A. Dedner, C. Engwer, J. Fahlke, C. Gräser, R. Klöfkorn, M. Nolte, M. Ohlberger, and O. Sander. DUNE Web page, 2012. http://www.dune-project.org.

C.E. Baumann and J.T. Oden. A discontinuous hp finite element method for the Navier-Stokes equations, 10th. In *International Conference on Finite Element in Fluids*, 1998.

M. Blatt and P. Bastian. The iterative solver template library. In B. Kågström, E. Elmroth, J. Dongarra, and J. Waśniewski, editors, *Applied Parallel Computing. State of the Art in Scientific Computing*, volume 4699 of *Lecture Notes in Computer Science*, pages 666–675. Springer, 2007. URL http://elib.uni-stuttgart.de/opus/volltexte/2006/2839/pdf/TR_2006_08.pdf.

M. Blatt and P. Bastian. On the generic parallelisation of iterative solvers for the finite element method. *Int. J. Comput. Sci. Engrg.*, 4(1):56–69, 2008. doi: 10.1504/IJCSE.2008.021112. URL http://portal.acm.org/citation.cfm?id=1457168.1457174.

D. Braess. *Finite elements: Theory, fast solvers, and applications in solid mechanics*. Cambridge University Press, 2001.

S. Brdar, A. Dedner, and R. Klöfkorn. Compact and stable discontinuous Galerkin methods for convection-diffusion problems. *J. Sci. Comp.*, 34(1):263–282, 2012.

F. Brezzi, G. Manzini, D. Marini, P. Pietra, and A. Russo. Discontinuous finite elements for diffusion problems. *Atti Convegno in onore di F. Brioschi (Milano 1997), Istituto Lombardo, Accademia di Scienze e Lettere*, pages 197–217, 1999.

F. Brezzi, L.D. Marini, and E. Süli. Discontinuous Galerkin methods for first-order hyperbolic problems. *Mathematical models and methods in applied sciences*, 14 (12):1893–1903, 2004.

B. Cockburn. Discontinuous Galerkin methods. *ZAMM-Journal of Applied Mathematics and Mechanics/Zeitschrift für Angewandte Mathematik und Mechanik*, 83 (11):731–754, 2003.

B. Cockburn and C.-W. Shu. The local discontinuous Galerkin method for time-dependent convection-diffusion systems. *SIAM Journal on Numerical Analysis*, 35(6):2440–2463, 1998.

B. Cockburn, G.E. Karniadakis, and C.W. Shu. The development of discontinuous Galerkin methods. *UMSI research report/University of Minnesota (Minneapolis, Mn). Supercomputer institute*, 99:220, 2000.

C. Dawson, S. Sun, and M.F. Wheeler. Compatible algorithms for coupled flow and transport. *Comput. Methods Appl. Mech. Engrg.*, 193(23-26):2565–2580, 2004. ISSN 0045-7825. doi: 10.1016/j.cma.2003.12.059. URL http://dx.doi.org/10.1016/j.cma.2003.12.059.

K. Deckelnick, C.M. Elliott, and V. Styles. Numerical diffusion-induced grain boundary motion. *Interfaces Free Bound.*, 3(4):393–414, 2001.

K. Deckelnick, G. Dziuk, and C.M. Elliott. Computation of geometric partial differential equations and mean curvature flow. *Acta Numerica*, 14:139–232, 2005.

A. Dedner and P. Madhavan. Adaptive discontinuous Galerkin methods on surfaces. *arXiv preprint arXiv:1402.2117*, 2014a.

A. Dedner and P. Madhavan. Discontinuous Galerkin methods for advection-dominated problems on surfaces. *In preparation*, 2014b.

A. Dedner, R. Klöfkorn, M. Nolte, and M. Ohlberger. A Generic Interface for Parallel and Adaptive Scientific Computing: Abstraction Principles and the DUNE-FEM Module. *Computing*, 90(3–4):165–196, 2010. doi: http://www.springerlink.com/content/vj103u6079861001/.

A. Dedner, R. Klöfkorn, M. Nolte, and M. Ohlberger. DUNE-FEM Web page, 2012. http://dune.mathematik.uni-freiburg.de.

A. Dedner, P. Madhavan, and B. Stinner. Analysis of the discontinuous Galerkin method for elliptic problems on surfaces. *IMA Journal of Numerical Analysis*, 2013. doi: 10.1093/imanum/drs033. URL http://imajna.oxfordjournals.org/content/early/2013/01/23/imanum.drs033.abstract.

A. Demlow. Higher-order finite element methods and pointwise error estimates for elliptic problems on surfaces. *SIAM J. Numer. Anal*, 47(2):805–827, 2009.

A. Demlow and G. Dziuk. An adaptive finite element method for the Laplace-Beltrami operator on implicitly defined surfaces. *SIAM Journal on Numerical Analysis*, 45(1):421–442, 2008.

J. Douglas, Jr. and T. Dupont. Interior penalty procedures for elliptic and parabolic Galerkin methods. In *Computing methods in applied sciences (Second Internat. Sympos., Versailles, 1975)*, pages 207–216. Lecture Notes in Phys., Vol. 58. Springer, Berlin, 1976.

G. Dziuk. Finite elements for the Beltrami operator on arbitrary surfaces. *Partial differential equations and calculus of variations*, pages 142–155, 1988.

G. Dziuk and C.M. Elliott. Finite elements on evolving surfaces. *IMA journal of numerical analysis*, 27(2):262, 2007a.

G. Dziuk and C.M. Elliott. Surface finite elements for parabolic equations. *J. Comput. Math*, 25(4):385–407, 2007b.

G. Dziuk and C.M. Elliott. Finite element methods for surface PDEs. *Acta Numerica*, 22:289–396, 2013.

C.M. Elliott and B. Stinner. Modeling and computation of two phase geometric biomembranes using surface finite elements. *J. Comp. Phys.*, 229:6585–6612, 2010.

C.M. Elliott, B. Stinner, and C. Venkataraman. Modelling cell motility and chemotaxis with evolving surface finite elements. *Journal of The Royal Society Interface*, page rsif20120276, 2012.

A. Ern. *Theory and practice of finite elements*, volume 159. Springer, 2004.

M. Fortin and F. Brezzi. *Mixed and hybrid finite element methods*. Springer, 1991.

H. Garcke, K.F. Lam, and B. Stinner. Diffuse interface modelling of soluble surfactants in two-phase flow. *Communications in mathematical science*, 12(8):1475–1522, 2014.

E.H. Georgoulis, E. Hall, and P. Houston. Discontinuous Galerkin methods for advection-diffusion-reaction problems on anisotropically refined meshes. *SIAM Journal on Scientific Computing*, 30(1):246–271, 2007.

E.H. Georgoulis, E. Hall, and P. Houston. Discontinuous galerkin methods on hp-anisotropic meshes ii: a posteriori error analysis and adaptivity. *Applied Numerical Mathematics*, 59(9):2179–2194, 2009.

J. Giesselmann and T. Müller. Geometric error of finite volume schemes for conservation laws on evolving surfaces. *Numerische Mathematik*, pages 1–28, 2014.

P. Houston, D. Schötzau, T.P. Wihler, and C. Schwab. Energy norm a posteriori error estimation of hp-adaptive discontinuous Galerkin methods for elliptic problems. *Mathematical Models and Methods in Applied Sciences*, 17(1):33–62, 2007.

A.J. James and J. Lowengrub. A surfactant-conserving volume-of-fluid method for interfacial flows with insoluble surfactant. *J. Comp. Phys.*, 201(2):685–722, 2004.

L. Ju and Q. Du. A finite volume method on general surfaces and its error estimates. *Journal of Mathematical Analysis and Applications*, 352(2):645–668, 2009.

L. Ju, L. Tian, and D. Wang. A posteriori error estimates for finite volume approximations of elliptic equations on general surfaces. *Computer Methods in Applied Mechanics and Engineering*, 198(5-8):716–726, 2009.

O.A. Karakashian and F. Pascal. A posteriori error estimates for a discontinuous Galerkin approximation of second-order elliptic problems. *SIAM Journal on Numerical Analysis*, 41(6):2374–2399, 2003.

U. Langer and S.E. Moore. Discontinuous Galerkin isogeometric analysis of elliptic PDEs on surfaces. *arXiv preprint arXiv:1402.1185*, 2014.

K. Larsson and M.G. Larson. A continuous/discontinuous Galerkin method and a priori error estimates for the biharmonic problem on surfaces. *arXiv preprint arXiv:1305.2740*, 2013.

M. Lenz, S.F. Nemadjieu, and M. Rumpf. A convergent finite volume scheme for diffusion on evolving surfaces. *SIAM Journal on Numerical Analysis*, 49(1):15–37, 2011.

K. Mekchay, P. Morin, and R. Nochetto. Afem for the laplace-beltrami operator on graphs: design and conditional contraction property. *Mathematics of Computation*, 80(274):625–648, 2011.

M.P. Neilson, J. Mackenzie, S. Webb, and R.H. Insall. Modelling cell movement and chemotaxis pseudopod based feedback. *SIAM Journal on Scientific Computing*, 33(3), 2011.

M.A. Olshanskii, A. Reusken, and X. Xu. A stabilized finite element method for advection–diffusion equations on surfaces. *IMA Journal of Numerical Analysis*, page drt016, 2013.

C. Ortner and E. Süli. Discontinuous Galerkin finite element approximation of nonlinear second-order elliptic and hyperbolic systems. *SIAM Journal on Numerical Analysis*, 45(4):1370–1397, 2007.

R. Rannacher and F.-T. Suttmeier. A posteriori error estimation and mesh adaptation for finite element models in elasto-plasticity. *Computer methods in applied mechanics and engineering*, 176(1):333–361, 1999.

L. Rineau and M. Yvinec. 3d surface mesh generation. *CGAL Editorial Board, editor, CGAL User and Reference Manual*, 3:53, 2009.

B. Rivière, M.F. Wheeler, and V. Girault. Improved energy estimates for interior penalty, constrained and discontinuous Galerkin methods for elliptic problems. part i. *Computational Geosciences*, 3(3-4):337–360, 1999.

D. Schötzau and L. Zhu. A robust a-posteriori error estimator for discontinuous Galerkin methods for convection–diffusion equations. *Applied numerical mathematics*, 59(9):2236–2255, 2009.

D. Schötzau, C. Schwab, and A. Toselli. Mixed hp-dgfem for incompressible flows. *SIAM Journal on Numerical Analysis*, pages 2171–2194, 2003.

A. Sokolov, R. Strehl, and S. Turek. Numerical simulation of chemotaxis models on stationary surfaces. Technical report, Fakultät für Mathematik, TU Dortmund, November 2012. Ergebnisberichte des Instituts für Angewandte Mathematik, Nummer 463.

R. Verfürth. A posteriori error estimators for the Stokes equations. *Numerische Mathematik*, 55(3):309–325, 1989.

J. Wloka. Partial differential equations. *Cambridge University*, 1987.